



**Monitoring of gully
erosion at ERA Ranger
Uranium Mine
Northern Territory,
Australia**

JRW Bell
GR Willgoose

January 1998



Monitoring of gully erosion at ERA Ranger Uranium Mine Northern Territory, Australia.

by

Justin R.W. Bell and Garry R. Willgoose

Department of Civil, Surveying and Environmental Engineering,
The University of Newcastle
Callaghan NSW 2308

January 1998

File Reference: JR-05-210

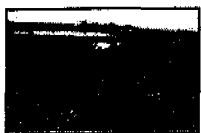


ENVIRONMENTAL RESEARCH INSTITUTE OF THE SUPERVISING SCIENTIST



Table of Contents

<i>Executive Summary</i>	<i>i</i>
<i>Table of Contents</i>	<i>ii</i>
1.0 Introduction	1
1.1 Background	1
1.2 Objectives	5
1.3 Field Trial	6
1.3.1 Hydrology Model	6
1.3.2 SIBERIA evolution model	9
2.0 Experimental	11
Cap Site	11
Gully Catchment	13
Batter Slope	15
3.0 Field Trial Results	20
3.1 Hydrology	20
3.2 Gully Development	24
4.0 Model Calibration and Predictions	47
4.1 Theory	47
4.2 Initial Surface and Determination of Parameters	54
4.3 Simulations	61
Standard	61
Increased Width	61
Upper Section	62
Random Erodibility	62
Differential Erodibility with Depth	65
5.0 Assessment of Batter Slope Landforms	73
5.1 Standard	73
5.2 Slope Dependence	82
5.3 Increased Width	89
5.4 Randomised Erodibility	95
5.5 Differential Erodibility with Depth	106
5.6 Slope Final	132
6.0 Discussion	139
7.0 References	146
Acknowledgements	147
Appendices	148



Monitoring Gully Formation

Executive Summary

As part of the proposed rehabilitation at Ranger Uranium Mine, ERARM, investigation into the long term erosional stability of the final design landforms is currently being conducted.

The steep batter slopes of the proposed landform are considered highly susceptible to erosion, with previous investigations highlighting possible problems caused by the development of gullies through the containment structure.

This project constitutes one aspect of this assessment process.

The aims of this project were to:

- Firstly, initiate a gully on the steep batter slopes of the Northern Waste Rock Dump.
- Secondly, to monitor the development of the gully, and hydrology of the gully catchment.

These two components constituted the field trial and were conducted with the assistance of the Office of the Supervising Scientist, *eriss* and ERA Ranger Mine.

- The third objective, was assessment of the capability of the landform evolution model SIBERIA to predict the extent, depth and width of gullies formed on the steep waste rock slopes,
- and finally, by comparison between observed and predicted landforms, ascertain dominant erosional processes, and assess implications of additional erosion modules on these predictions.

SIBERIA was adapted to represent the batter - gully catchment study site, and validated through direct comparison between predicted and observed landforms.

Modification of the homogenous initial landform to incorporate heterogeneity, increased catchment outlet width, and implementation of rudimentary armouring module, have encapsulated the dynamism of the development process observed on site.

Depths of erosion are comparable to those observed, and behaviour of gully development is mimicked by model simulations shown here.



Monitoring Gully Formation

1.0 Introduction

1.1 Background

Ranger Uranium Mine (ERARM) is located about 270km east of Darwin, surrounded by the Kakadu National Park, Northern Territory.

As part of the mine rehabilitation strategy, storage of mine tailings, a by-product of the uranium processing system, in existing facilities may be involved. Containment and isolation of this material will be required, with structural integrity of the containment structure of at least 1000 years.

The overall strategy employs engineered landforms designed to avert such potential hazards, with this investigation forming part of the assessment of the erosional stability of these landforms.

The above ground rehabilitation option involves a landform about 4 km² area, and rises to a height of 17m above the surrounding area, Figure 1.1.2.

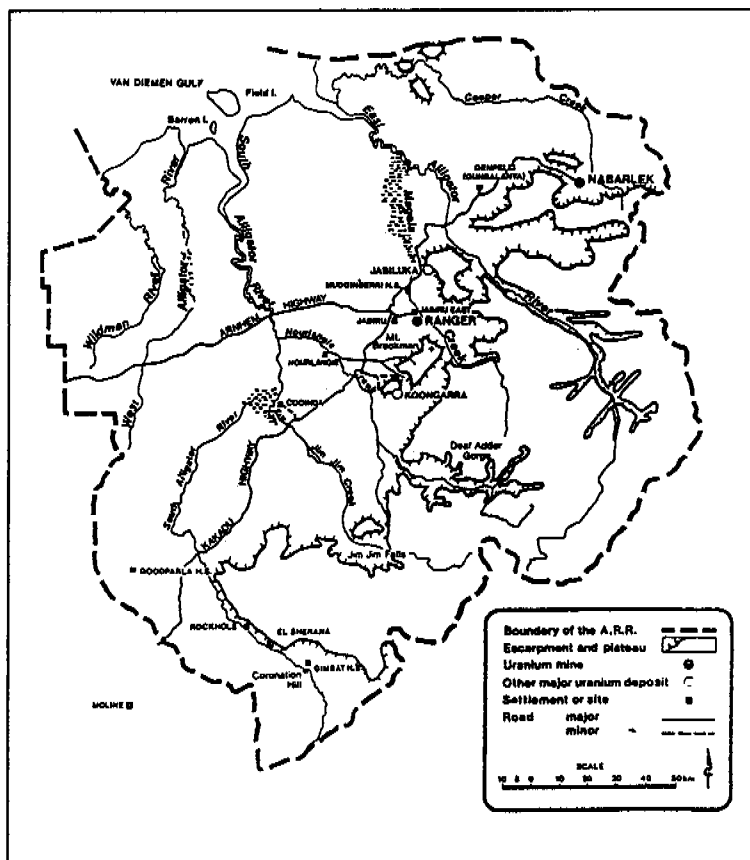
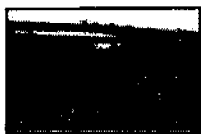


Figure 1.1.1: ERARM is located within the sensitive Kakadu National Park, Northern Territory.



Monitoring Gully Formation

The validation of predictions from the landform evolution model SIBERIA, used to assess the long term stability of these landforms, with a gully erosion study constitutes the major aims of this report.

Regions likely to suffer degradation are highlighted in Figure 1.1.2, where gullies are predicted to form along the batter slopes surrounding the proposed landform. Incision at the transition point between the long cap sites, and the steep batter slopes extenuate back into the structure under some simulation conditions investigated previously.

This project was conducted on the Northern Waste Rock Dump. These waste rock slopes have been exposed for several years, and were considered ideal for the relatively straightforward experimental component of this study.

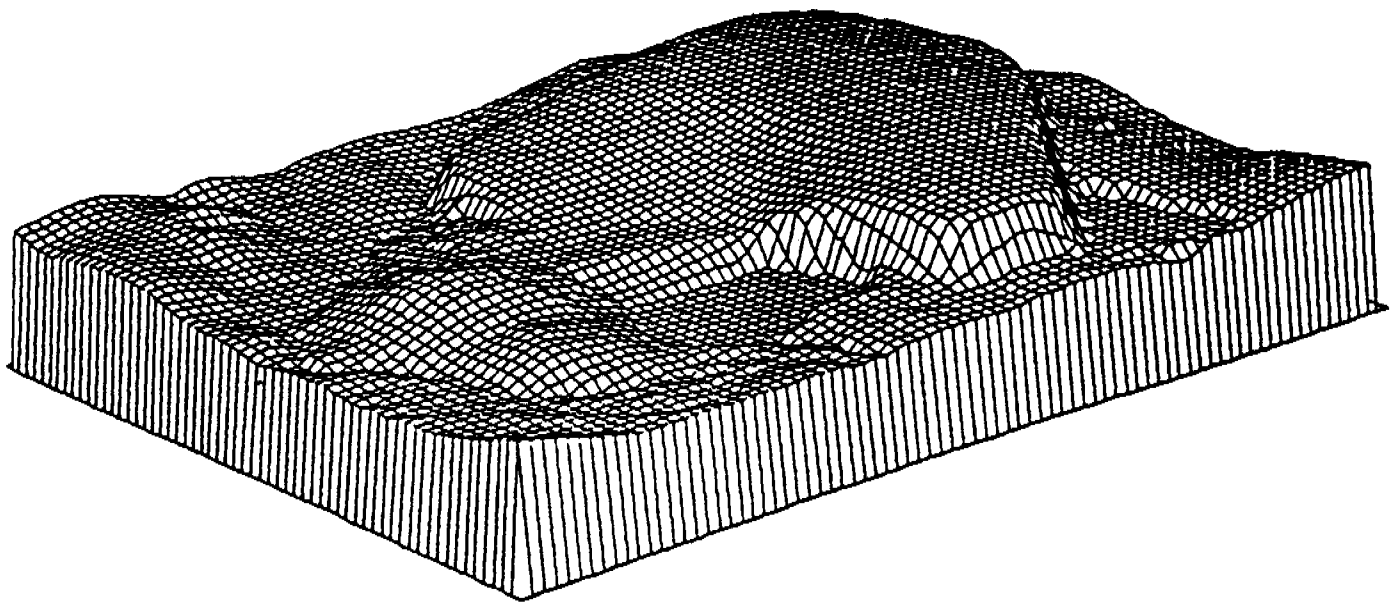
The overall design for the landform is constrained by objectives not considered here, and the reader is directed to Willgoose and Riley, 1992 for further discussion.

This study concentrates on the development of an experimental regime, and modelling simulations conducted on a small section of this batter slope, with adaptation of the landform evolution model SIBERIA to validate predictions through direct comparison with observed development.

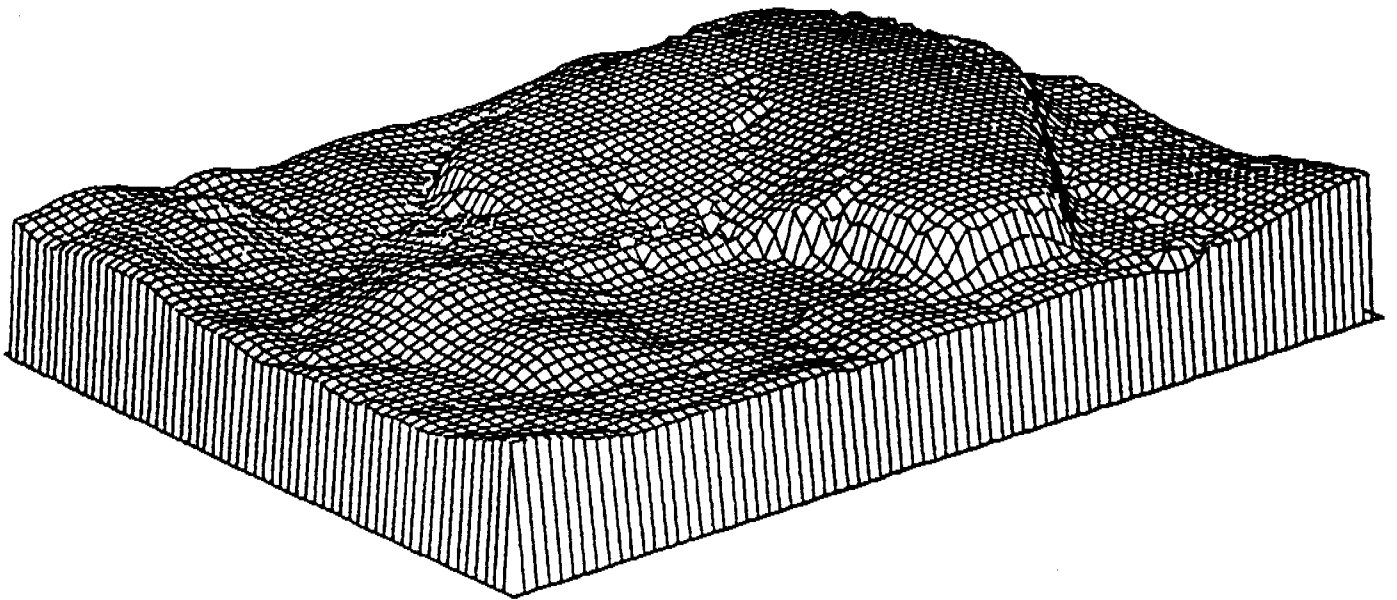
The section of batter slope chosen for this investigation has been exposed for several years, with Figure 1.1.3, and 1.1.4 offering a comparison between relatively freshly exposed material, and remnant fine material found on the study site.

The surrounding National Park is pictured in Figure 1.1.4, with monsoonal rains coming to the region between December and February. The intensity of the climate in the region has been well documented, with exposure to large temperature differentials, high humidity, and large monsoonal rainstorms providing idyllic conditions for rapid degradation of soil surface material by geochemical weathering mechanisms.

During the 96-97 Wet Season, many storm events were monitored with only a relatively few leading to significant alteration of the gully formation once it had been initiated.



As constructed.



1000 years after construction.

Figure 1.1.2: Regions likely to suffer from erosion are highlighted in this simulation of one of the proposed landforms. Gullies are predicted to form on the steep batter slopes surrounding the structure (Willgoose and Riley, 1993 Figure 4).



Monitoring Gully Formation



Figure 1.1.3: The Southern waste rock dump located about 2km east of the study site, with relatively recently exposed material being deposited.



Figure 1.1.4: The batter slopes of the Northern waste rock dump has been exposed for a period of several years. Some natural re-vegetation had occurred, which was not considered to have any impact on the erosion study. It was also noted that relatively fine material has accumulated in the upper surface layers of the study site.



Monitoring Gully Formation

1.2 Objectives

The project constitutes one part of the continuing calibration and validation of the landform evolution model SIBERIA, used to predict erosional development of proposed rehabilitated landforms.

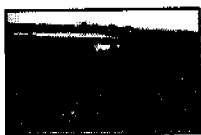
Amongst the objectives of this work, the implementation of a field trial involved the following:

- Construction a catchment on top of the WRD at ERARM, and establishment of monitoring regime necessary to monitor the hydrology of the constructed catchment, and the development of the gully on the waste rock slopes, once it had been instigated.
- Monitoring and recording the formation of the gullies on this slope, once initiated, and advise on the suitability of different measurement techniques, as well as the monitoring of hydrology of the gully catchment throughout the numerous storm events experienced during the 96-97 Wet Season.

Establishment of the field trial was conducted with the assistance of the geomorphology team at the Office of the Supervising Scientist *eriss*, and ERA Ranger Mine. Development of monitoring regime to record hydrological and sediment loss estimation was conducted during the Wet Season, late November to March.

The next component of the project involved computational work conducted at the University of Newcastle as part of a final year environmental engineering project by the author, with the assistance of Dr G.R. Willgoose, author of the SIBERIA model. This work involved the following objectives:

- Adaptation of the landform evolution model SIBERIA to be representative of the gully catchment - batter slope study site,
- Assessment of different erosional mechanisms, by comparison between model simulations, through systematic implementation of an array of erosion modules,
- and, By comparison between predictions generated by the model and development observed on site, assess the capability of the model to predict the size and extent of gullies formed on the steep waste rock slopes.



Monitoring Gully Formation

1.3 Field Trial

Amongst the aims of this project, the construction of a catchment and the instigation of a gully on the batter slopes of the NWRD included the implementation of event monitoring equipment. Recommissioning of a previously established sheet flow erosion plot, with associated equipment and expertise supplied by *eriss*, and earth moving equipment and labor supplied by ERA Ranger Mine to construct the catchment, constituted establishment of the field site.

Hydrology of numerous storm events encountered during the experimental period was devised using discharge-head relationship devised from hydraulic control structure attached to the small erosion plot, with rainfall tipping bucket gauge and water level sensor attached to electronic logging equipment for continuous monitoring.

The results from previous work conducted by *eriss* was used to determine on-site erosional characteristics and were incorporated into an estimate for the total sediment loss relationship, which constitutes one part of the input requirements for the landform evolution model SIBERIA, together with results from the rainfall-runoff hydrology model calibration.

Figure 1.3.1 outlines the relationship between the fundamental components of the gully erosion study with discharge-runoff entrained within the constructed catchment funnelled over the side of the steep batter slopes.

These two major components summarise the calibration and input requirements of the SIBERIA model, with the relationship between catchment runoff and total sediment loss following typically adopted forms.

1.3.1 Hydrology Model

Runoff is the most important determinant in estimates of soil erosion, and consequently in the initiation and continuing development of gully erosion. (Willgoose *et al*, 1992). The hydrology model used to fit natural rainfall data from plots on top of the NWRD was based on kinematic wave flooding routing model DISTFW, incorporated within the non-linear regression fitting package NLFIT.

Experimental Methodology

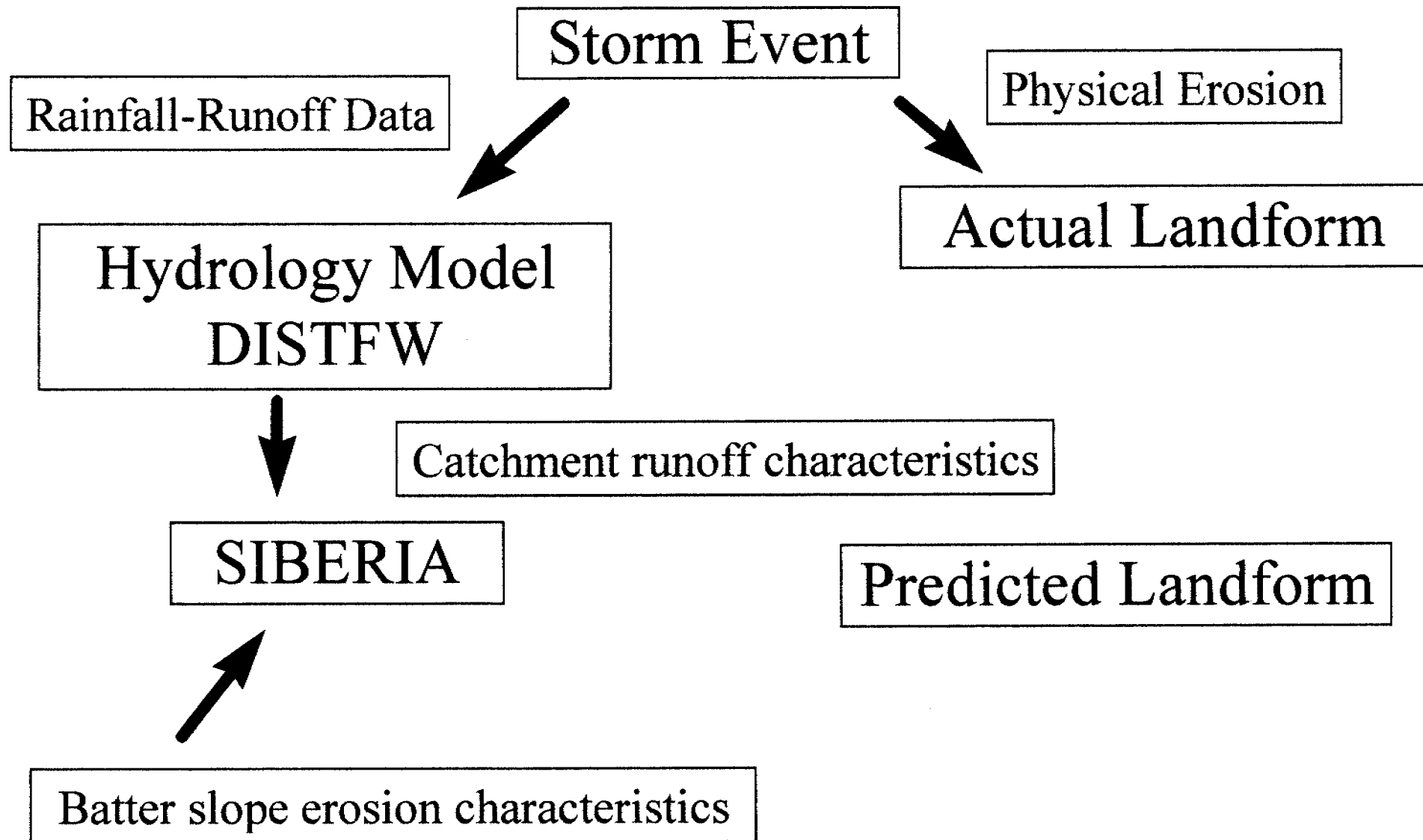


Figure 1.3.1: The gully catchment with the small scale monitoring plot supplied water for from an area of 7213m² to the steep batter slopes of the NWRD. The combination of hydrology and estimates of total sediment loss from the catchment, are used to calibrate the landform model SIBERIA, with direct comparison between observed and predicted landforms validating these inherent assumptions.



Monitoring Gully Formation

The kinematic wave flood routing model, DISTFW is a distributed parameter generalised kinematic model (Willgoose, Kuczera, and Williams, 1995).

This model discretised the catchment into a number of sub-catchments connected together with a channel network, and was calibrated using natural rainfall-runoff data obtained from the cap site during the monitoring period.

The model simulates Hortonian runoff with Philips infiltration, with kinematic wave component influencing properties of the predicted runoff hydrograph from the gully catchment, whilst infiltration rates mainly influence of runoff volume.

The two kinematic wave parameters are C_r , and e_m that are defined by flow geometry and surface roughness respectively. The infiltration rate (Hortonian runoff with Philips infiltration) is a function of the cumulative infiltration and the two parameters in this case are S_ϕ and ϕ , Sorptivity and Long term infiltration respectively. Further detail of assumptions, conclusions and description of model basis are found in Evans, in prep., and Willgoose *et al*, 1995.

As outlined below, values adopted for calibration of user defined runoff module used in SIBERIA landform model reflect accumulated data from work conducted at ERARM.

The calibration procedure used for fitting of parameters using the non-linear regression package NLFIT involved the following procedure:

- Fit C_r and ϕ (approximate fitting of timing, and volume of hydrograph)
- Fit S_ϕ and ϕ (more exact fitting of volume)
- Fit C_r and e_m (routing behaviour)
- Fit all 4 parameters (for exactness)

Although Kuczera notes that this sheetflow assumption is widely discredited, except under ideal conditions, parameters for infiltration and conveyance characterise the hydrological behaviour of each of these storm events, with these issues considered in Evans, in prep.



Monitoring Gully Formation

1.3.2 SIBERIA evolution model

Computer models used to simulate the changes of landforms over time provide a link between the study of process, and the study of landforms.

A landform evolution model using runoff and erosion physics to simulate the changing form of a catchment with time has been developed. Such aspects of computer modelling for the longer term timescale, that operate in geomorphology, can rarely be substantiated with short term measurements. The combination of time and space, usually physically based of continuity of mass, provide a predictive tool with forecast capability as well as a tool for improved understanding, (Kirkby, 1996).

The simplicity of any simulation model is an important characteristic, with field observation consistent with the theoretical explanation of landscape processes.

The computer model SIBERIA (Willgoose, Bras, and Rodriguez-Iturbe, 1991a-d) is amongst these simulation models capable of prediction of landscape forms in the longer term, and is used to study the erosional development of catchments and their channel networks.

Elevation changes within the catchment are simulated using a mass transport continuity equation applied over geologic time (Willgoose *et al*, 1993). If more material enters a region than leaves then elevations rise and vice versa, with the model averaging the mass transport process over time. The mass continuity equation used consists of two major component, fluvial sediment transport and diffusive mass movement mechanisms such as soil creep, rainsplash, and landslide.

Other significant aspects of the erosional development of the catchment include the differentiation between processes occurring on hillslopes and those occurring in channels.

Channelisation is simulated using another governing equation, once a channel initiation threshold is exceeded (a value beyond which a channel is initiated). This threshold represents a transition in the dominant erosion mechanism, with this second component of the model not being considered in this study (Willgoose *et al*, 1991a-d).



Monitoring Gully Formation

The governing equation of elevations within the catchment model is expressed as:

$$\frac{\partial z}{\partial t} = C_o + \frac{\nabla q_s}{\rho_s(1-n)} + D \left(\frac{\partial^2 z}{\partial x^2} + \frac{\partial^2 z}{\partial y^2} \right) \quad (\text{Willgoose } et al, 1992) \quad (1.3.1)$$

where

z = elevation

C_o = tectonic uplift (this term neglected over short term)

q_s = sediment transport per unit width,

$\rho_s(1-n)$ = bulk density of sediment

Validation of the evolution model SIBERIA, is presently being conducted with experimental laboratory analysis and field trials such as this one.

The characteristic of the natural catchment once formed, is substantially different to that proposed in the rehabilitation, with long hillslopes contributing flow to the tops of the batter slopes considered likely to trigger erosional degradation of these slopes.

The validation of predictions from the landform model is at the heart of this investigation, with preliminary field trial estimate the physical characteristics of a gully formed on the batter slopes.

By assessing the outcomes of this modelling analysis insight can be gained into the other factors contributing to the formation of gullies on the batter slopes, that are not presently not fully implemented in the model.

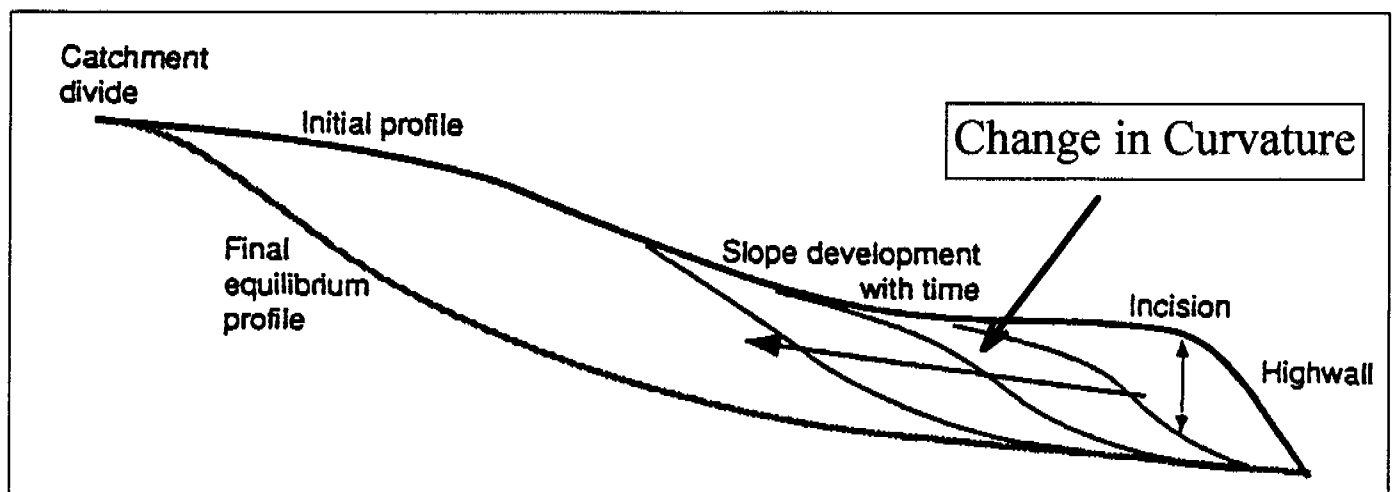
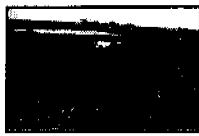


Figure 1.3.2: The schematic diagram of initial landform is considered far from equilibrium profile (Willgoose *et al*, 1992 Figure 6.1)



Monitoring Gully Formation

2.0 Experimental

The field trial involved monitoring hydrologic behaviour of the gully catchment (using the small scale erosion plot), and intensive measurement of the dimensions, size and extent of the gully once formed on the steep waste rock slopes.

Cap Site

From previous work conducted by *eriss* at ERARM, a small scale erosion plot remained centrally located on top of the NWRD.

The plot consisted of an isolated area bounded by damp coarse bituminised aluminium, with a 250mm diameter PVC sewer pipe located at the downstream end. This plot was of standard size to those used previously, at 20m by 30m (591m²), constructed on relatively flat ground of 1-2% slope, consisting of relatively undisturbed, unvegetated waste rock surface material.

The downstream sewer half pipe was set into the ground at surface level. Sediment-laden overland flow could deposit larger sized particles along this pipe referred to as bed load, whilst suspended material was transported through the hydraulic control structure, although these devices were only used to measure rainfall and runoff for the cap site within this study.

A standard 150mm RBC flume was recommissioned, with a discharge-head relationship assumed from previously constructed devices:

$$Q(L/s) = 18.4 * H + 940H^2 \quad (2.1.1)$$

where

H = height of water or head, m

Q = flow discharge, L/s

The stilling basin served dual purposes; reduction of surging of flow discharge leading to erroneous results, and to provide a collection point for bed load material, for continuous monitoring.



Monitoring Gully Formation



Figure 2.1: A standard 150mm flume was re-commissioned and used for monitoring hydrological data for the study site. Discharge recorded from the cap site area 591m^2 , together with cumulative rainfall was used to calibrate the hydrology model DIST-FW, and hence characterise each of the storm events.

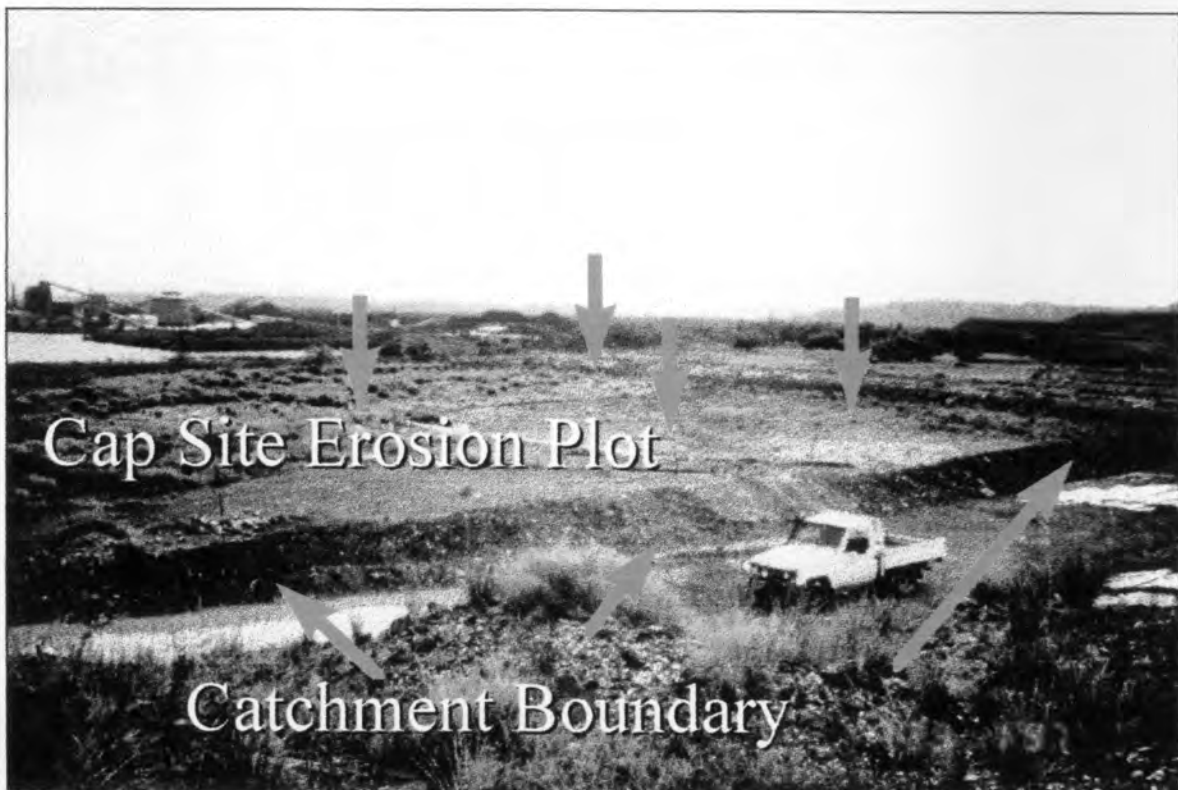


Figure 2.2: Monitoring equipment was attached to the recommissioned erosion plot located centrally in this figure, within the constructed gully catchment of area 7213m^2 .



Monitoring Gully Formation

A drainage channel was also constructed downstream from the cap site to dissipate flow discharge and prevent backing up of the monitoring site during large storm events. This experimental design has been in previous site investigations, and reference is made to other studies for construction details (Moliere, Evans, Riley and Willgoose, 1997).

The DISTFW rainfall-runoff hydrology model was then used to evaluate each of the significant storm events, with the catchment discretisation described Figure 2.3, with model catchment description detailed in Appendix A.

Gully Catchment

ERARM constructed a catchment with large earth moving equipment to create an irregularly shaped soft earthen bund wall, which was used to generate a large water supply for the study site.

The surface material disturbed by the construction of this catchment appeared as red-brown sediment during the preliminary storm events, however this material tended to subside in concentration over time, although was still evident at the conclusion of the monitoring period.

The bund wall reached a height of 1m and effectively captured all rain falling within the gully catchment, and directed it through a notch at the downstream end to the batter slope, illustrated in Figure 2.2. The site was relatively flat, with slope ranging between 1 and 2%, slope length of 110m, with an area of 7213m². Although a relatively uniform surface, some sections were depressed, leading to regions pooling during large storm events.

During the construction of the gully catchment, a small reservoir was inadvertently created along the upstream side of the entrance to the batter slope. This reservoir effectively shielded the batter slope from high surface flow velocities, and buffered the impact of all but large events on the slope, once the gully was initiated. Runoff collected during a rainfall event was subsequently released slowly, well after the end of storm activity.



Monitoring Gully Formation

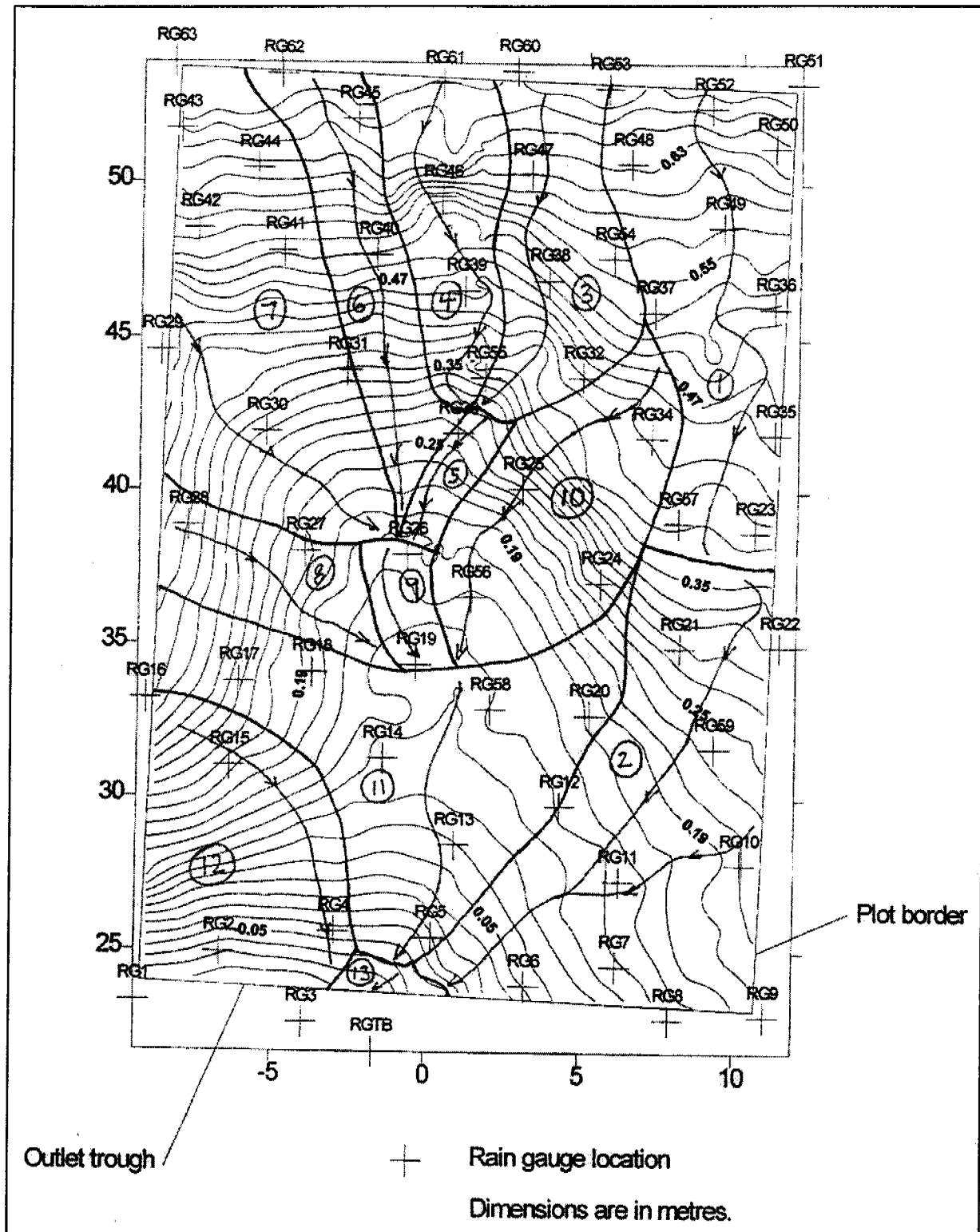
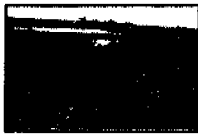


Figure 2.3: Cap site subcatchment discretisation, noting that kinematic wave routing model evaluates each of this subcatchment using Hortonian overland flow with Philips infiltration, Evans *et al*, in prep.



Monitoring Gully Formation

Intensive investigation of the response of the gully catchment may be conducted in the future, although the reservoir was neglected given the method of implementation of the hydrology model into the landform model SIBERIA, with Figure 2.4 illustrating the subcatchment discretisation for this site.

Calibration of the DIST-FW hydrology model to include these storage effects was neglected, as pooling did not seem to significantly affect the passage of large storm events, where reservoir water level exceeded the weir height and rapid moving water cascaded directly into the gully network.

These measurements together with the catchment analysis outlined in Figure 2.3, and Figure 2.4 below, constitute the input requirements for the hydrology model. Appendix A contains estimates of slope length, and area, as well as with for each of the elements incorporated in the catchment description file *.fw.

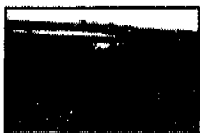
For the purposes of modelling discharge-runoff-sediment transport relationship, such factors as discrepancies between small and large scale catchment response have been neglected, with assumption that behaviour of cap site could be scaled up to represent the whole catchment. Of the many components in operation on site, large pooling leading to excessive infiltration, ponding in reservoir behind leading edge of bund wall leading to filling of this storage area before commencement of flow in the gully, have been neglected considering the magnitude of erosional development of the batter slope.

The model was calibrated using hydrology data extracted from the cap site using 3 separate storm events. These events were considered significantly large and were noteworthy because of changes in the size and dimension of the gully.

Once calibrated comparison between small scale erosion plot and gully catchment could be made using area-discharge scaling factor of $\sim 12.204 (7213\text{m}^2 / 591\text{m}^2)$.

Batter Slope

The batter slope regions of the proposed landform are considered highly susceptible to erosion. The study site is located adjacent to a previously eroded surface which had been triggered during intense monsoonal activity 95-96 Wet Season.



Monitoring Gully Formation

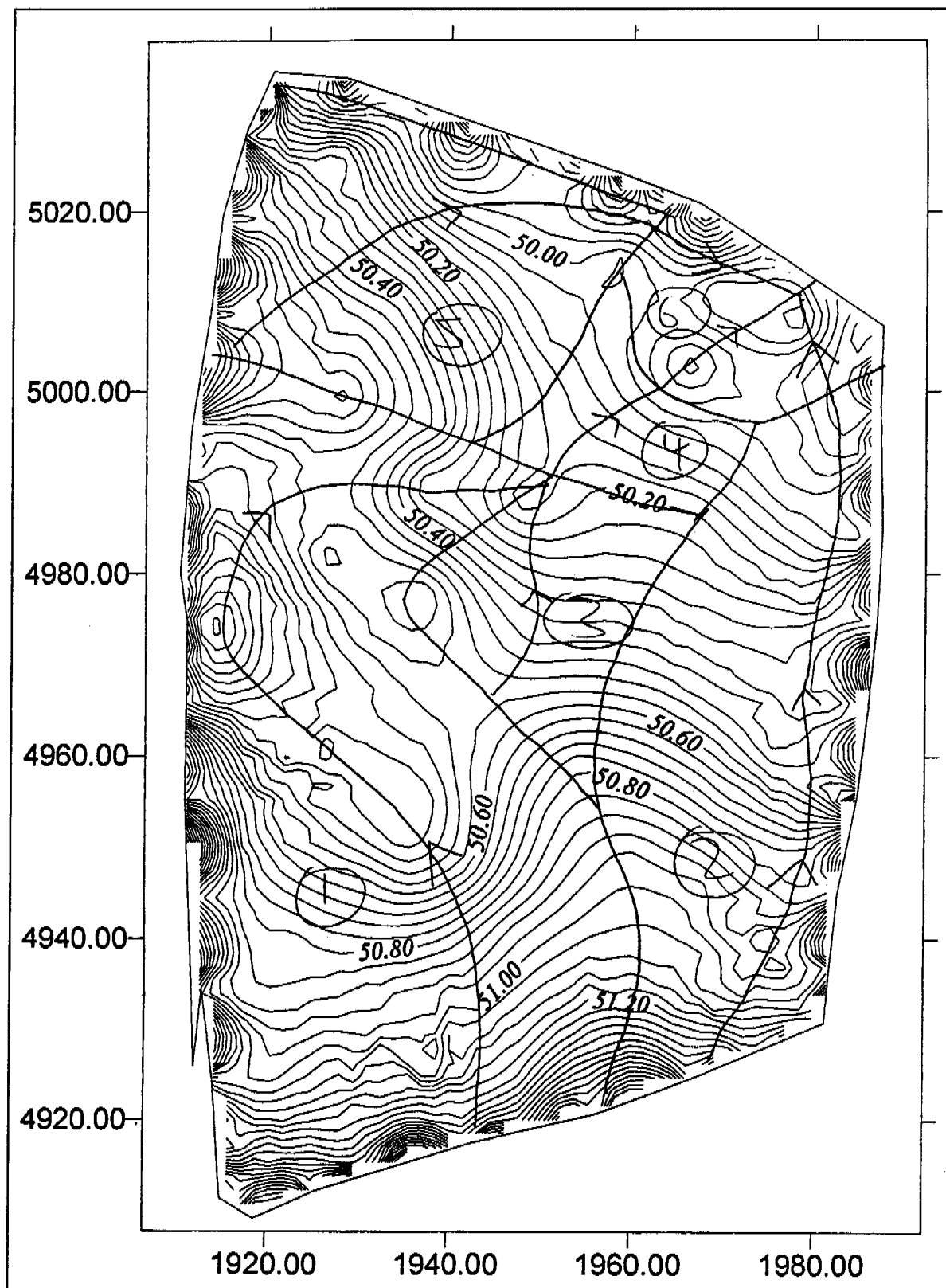


Figure 2.4: Gully Catchment was discretised into a number of subcatchment for implementation into the DISTFW hydrology model. Although some areas of the site were depressed leading to pooling, and the existence of the buffering reservoir, these were neglected given the method of implementation into the modelling package SIBERIA outlined below.



Monitoring Gully Formation

The slope is complex, changing profile from 1:3 through to 1:8, concave in upper sections and convex in lower sections. From previous work conducted by eriss, a large scale concrete apron and flume remained at the base of this slope. Extensive survey details were undertaken prior to the commencement of monitoring, as well as mid-way through the Wet Season, and after the completion of monitoring. Figure 2.6 highlights the complex nature of the slope profile, with measurement transects taken at a series of 10 points along the slope. Erosion pins were also utilised in an attempt to monitor changes in surface profile following each storm event.

Measurements were taken from within the gully, once it had formed, with fluorescent lead-pigment paint used to delineate active sections of the slope, Figure 2.5. Intensive analysis of gully formation has been determined to be relatively futile, with overall behaviour and erosion depths considered to be the most important findings from this study. The purpose of transect measurements were initially to determine the cross-sectional area of the gully at various points down slope. Conversion of these measurements to surface elevations involved estimation of height of string elevation, assumed to be horizontal across slope, and subtracting the recorded vertical height between string and surface. The volumetric difference between each of the 3 significant storm events could then be determined using a numerical mapping package.

Erosion pins were 50cm long, and sunk about 25cm to 35cm into the batter slope surface. An extensive measurement regime is included in Appendix B, although it is noted that measurements taken involved large discrepancies due to the nature of waste rock material. Detailed measurements taken for each of the cross-sectional areas, as well as widths of gully at different locations are also summarised in Appendix B.

Reference is made to the use of survey equipment for future analysis on site, given the medium time scale expected for erosional development. According to the experimental method, the movement of material out of transect lines constituted a significantly eroded section, even though only one or two boulders may have been dislodged. This is evident in Figure 2.5, where removal of fine material has left large rock fragments exposed.

The geological characteristic of the layers of the batter slope were considered important, as pictured in Figure 2.7, with variability in erosion behaviour, particle grain size, resistance to scouring adding complexity to the overall behaviour of the material. Implementation of an approximate armouring erosion module to the landform model involved conservative estimation of the erodibility of this material based on mean particle diameter, d_{50} .

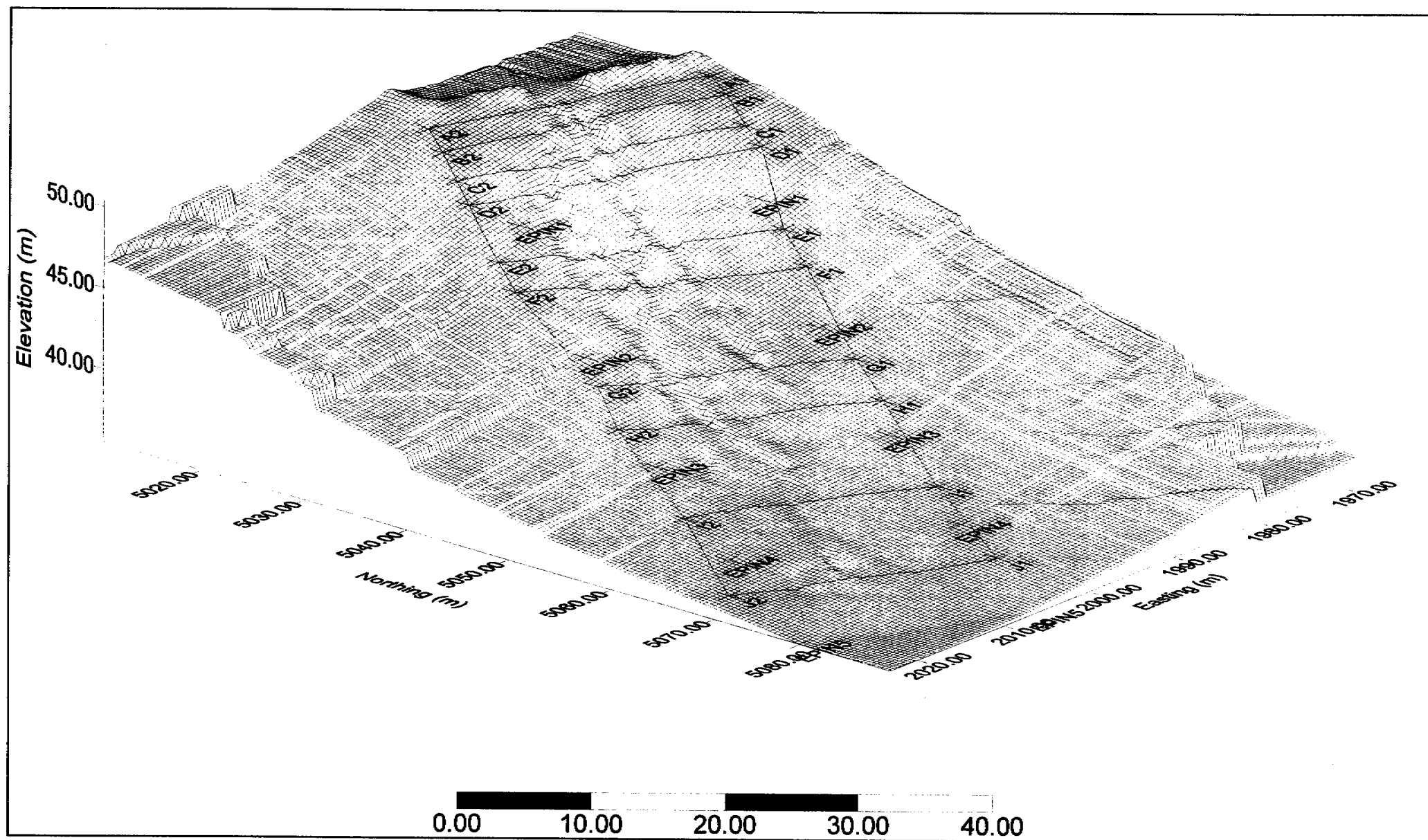


Figure 2.6: The batter slope study site was examined using a series of measurement transects located at 10 positions along the slope, with residual series of erosion pins from previous studies also used, but found to be unsuitable in this application.



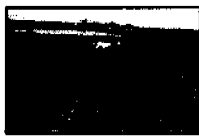
Monitoring Gully Formation



Figure 2.5: Measurements were taken using twine strung across two starposts at 10 positions along the hillslope. Although considered a crude method of measurement, the inherent variability of rock material dictated that approximations could only suffice.



Figure 2.7: The erodibility of the waste rock material was dependent on the mean grain size, relative weathering and overall rock consistency. Erosion pins used, were considered ineffective, with excavation of gully reaching 50 to 60cm in places removing these devices.



3.0 Field Trial Results

3.1 Hydrology

Rainfall-runoff data from the cap site, for the three storm events occurring on 261296, 010197, and 230197 were used to calibrate the DISTFW model using the non-linear regression package NLFIT. The parameters C_r and ϕ , S_ϕ and ϕ , and C_r and e_m were fitted firstly, with Sorptivity found to be effectively zero for all calibration runs, and was set to be zero for subsequent investigations. Hydrographs, and cumulative rainfall for each of these 3 significant events are presented in Figure 3.1.1.

The parameters were calibrated using individual storm events, whilst the next stage incorporated calibration of multiple storm events (using all three of these storms together). The purpose of multiple regression analysis was to characterise an average hydrologic behaviour for the cap site, and consequently the gully catchment.

The data appears well fitted with error in the estimation of C_r ranging between 17 and 27%, whilst e_m ranged between 3.8 to 4.9%, and ϕ between 5.6 and 15% appear to be within acceptable ranges.

Prospective errors in estimation of C_r , e_m and ϕ are: 15.2%, 3.5%, and 6.8% respectively, suggesting additional two storm events provide marginal improvement in estimating parameter values.

Table 3.1.1: Calibration results for cap site for individually fitted storm events: 261296, 010197, and 230197. Calibrated value and standard deviation is expressed.

Event	C_r (mm/hr ^{0.5})	e_m	ϕ (mm/hr)
261296	25.59 ± 6.92	2.52 ± 0.12	7.27 ± 1.05
010197	5.61 ± 0.95	1.55 ± 0.06	16.34 ± 0.92
230197	5.44 ± 0.70	1.27 ± 0.05	6.57 ± 0.99

Table 3.1.2: Joint calibration results for the cap site for the three designated storm events (mean ± s.d.).

Event	C_r (mm/hr ^{0.5})	e_m	ϕ (mm/hr)
average	7.90 ± 1.20	1.72 ± 0.06	11.74 ± 0.80

Monitoring Gully Formation

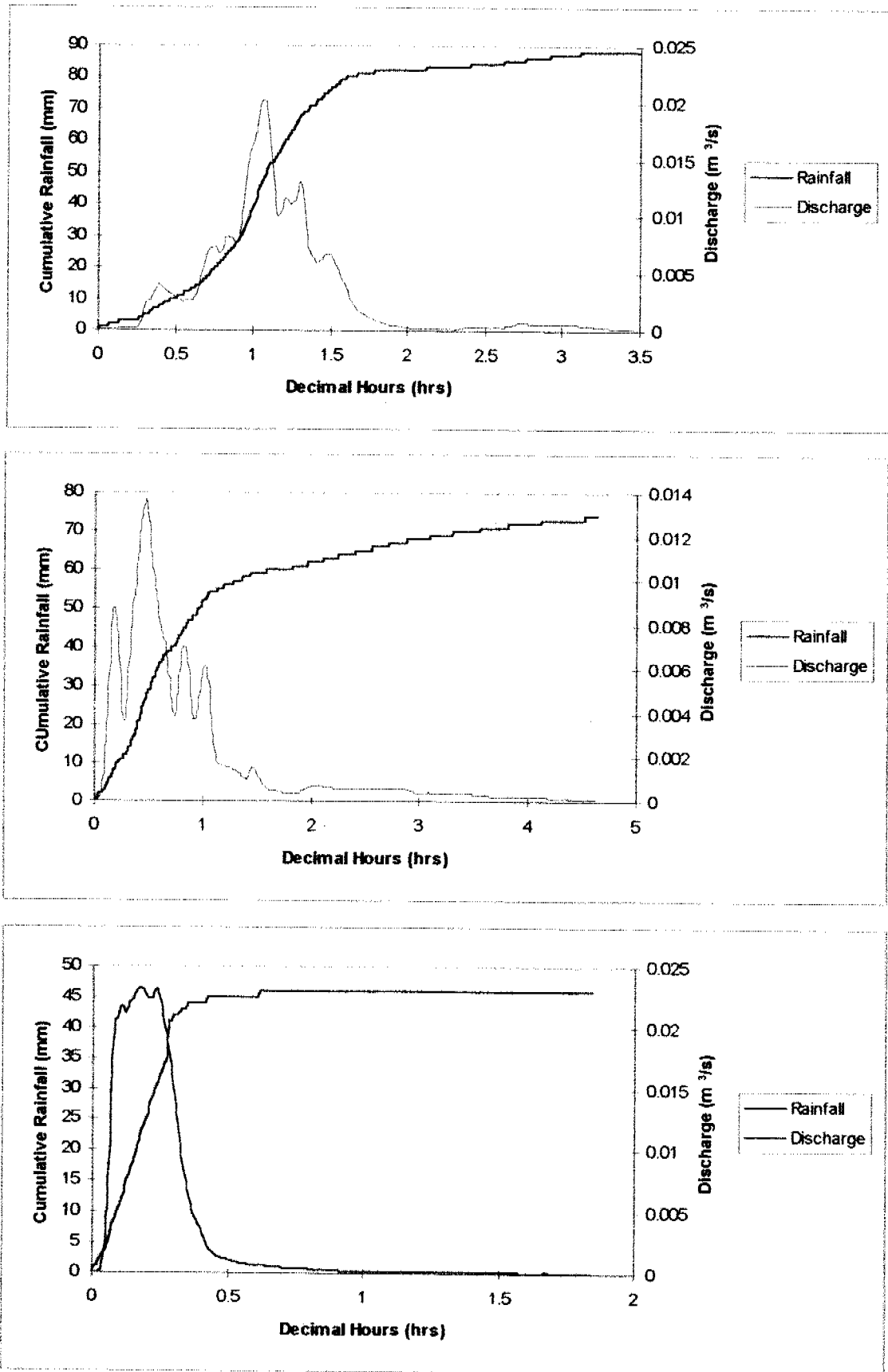
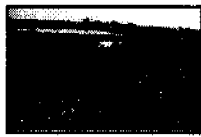


Figure 3.1.1: Observed runoff hydrographs and cumulative rainfall plots for cap site storm events monitored on: a) 261296, b) 010197, and c) 230197.



Monitoring Gully Formation

Table 3.1.3: Calibration results for gully catchment using individual storm events (mean \pm s.d.).

Event	Cr (mm/hr ^{0.5})	e_m	ϕ (mm/hr)
261296	35.29 \pm 3.33	2.67 \pm 0.12	6.59 \pm 1.09
010197	67.45 \pm 7.15	1.78 \pm 0.08	29.64 \pm 1.00
230197	82.42 \pm 5.19	1.36 \pm 0.06	5.18 \pm 1.18

Table 3.1.4: Calibration results for the catchment, for runoff events fitted simultaneously (mean \pm s.d.).

Event	Cr (mm/hr ^{0.5})	e_m	ϕ (mm/hr)
average	85.87 \pm 6.55	1.84 \pm 0.06	24.74 \pm 0.79

The next stage of the rainfall-runoff calibration involved approximating the discharge from the gully catchment itself. As outlined above, an approximate scaling was employed, as installation of monitoring equipment at the head of the gully network would have disturbed water flow. Adjustments were made to the catchment description file *.fw, and a multiplier factor of 12.204 was used for each of the runoff (*.ro) files. The model parameters Cr, e_m and ϕ were fitted once again, with Sorptivity S_ϕ again found to be effectively zero. From Table 3.1.3, the error in estimate of Cr, e_m and ϕ were (6.3% to 10.6%), (4.4% to 5.5%), and (3% to 22.8%) respectively. These values compare well with Table 3.1.1, noting that error bounds are only exceeded for ϕ , with event 230197. Errors in estimation of Cr, e_m and ϕ are 7.6%, 3.3%, and 3.2% compare favourably with results from Table 3.1.2. Assumptions regarding the effect of scaling up of discharge-runoff data from cap site to be representative of gully catchment seems to have been a reasonable one. The hydrographs and corresponding predictions for gully catchment are illustrated in Figure 3.1.2 below, with these events adopted for calibration of storm events into the SIBERIA landform model, representative if the catchment batter study site.

Further investigation and comparison may be made with results from previous hydrology studies conducted on the cap site, Evans in prep., however these considerations are beyond the focus of this study. It is noted from Table 3.1.1, the variation between values of ϕ , and e_m are replicated in fitting for cap site against the gully catchment. However conveyance (flow geometry, Cr) for the first event seems to remain small, characteristic of the nature of the storm event observed in Figure 3.1.1a. An estimate for e_m of 1.72, and 1.84 for cap site and gully catchment, is consistent with theoretical interpretation of surface roughness of the two sites.

Monitoring Gully Formation

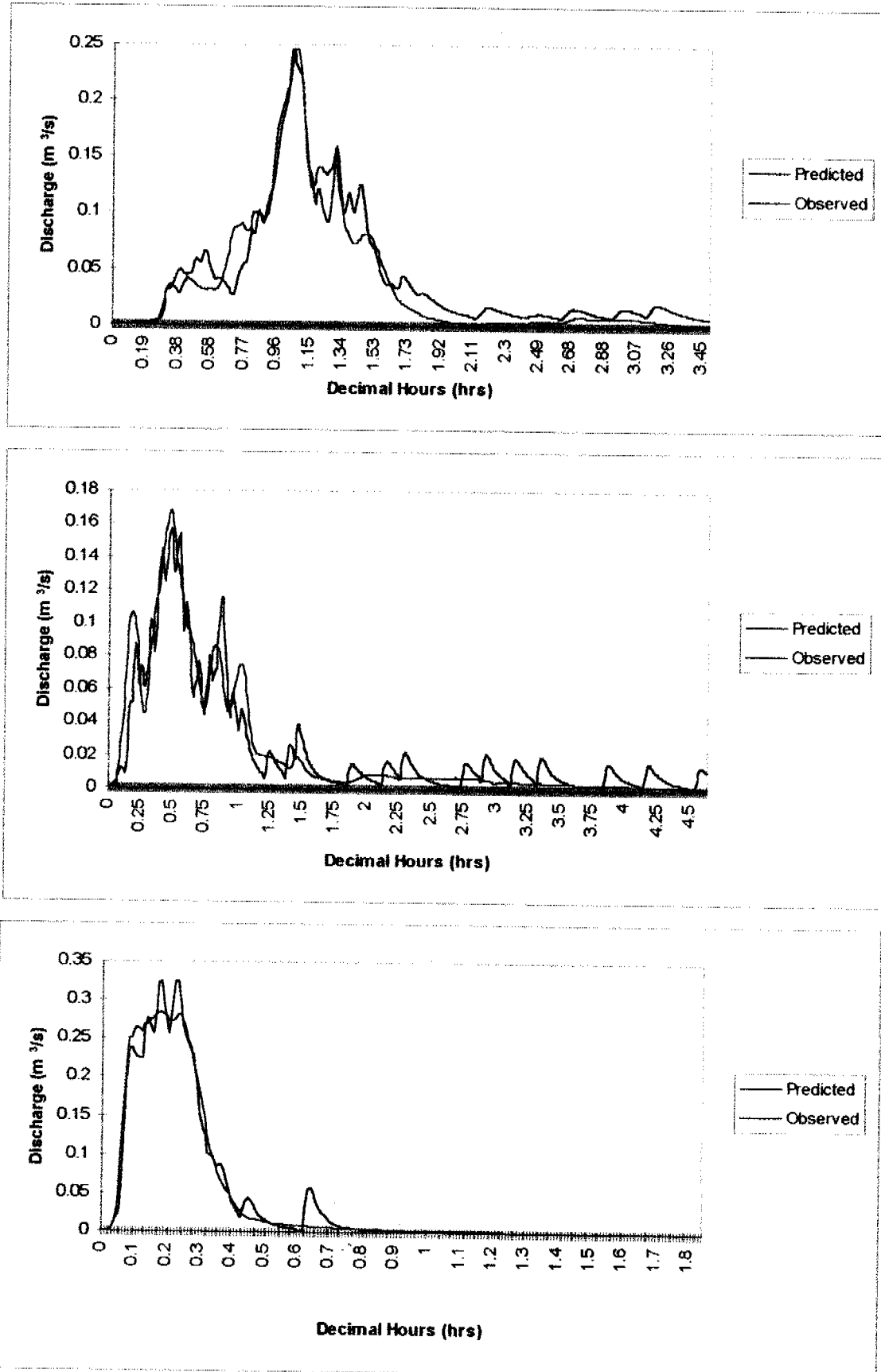
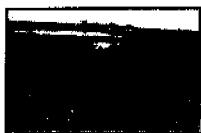


Figure 3.1.2: Gully Catchment hydrographs and predictions from the multiple regression fitting of all three significant storm events; a) 261296, b) 010197, and c) 230197.



Monitoring Gully Formation

3.2 Gully Development

Formation of a gully on the steep batter slopes of the NWRD was monitored during the 96-97 Wet Season. Analysis of the characteristic and nature of the initiation and development of the gully provides a field basis for continuing validation of the SIBERIA model.

The original topography of the site is described in detail above, with an inherent large degree of complexity in both form and constituency. The spatial variability in the waste rock material, illustrated in Figure 2.7 was significant, with the site being exposed and undisturbed for the past several years. Geochemical weathering processes which by their nature, are extremely significant in the region, were considered dominant factors in formation of the soil type material found on the upper surfaces of the slope. The fine particle material on the upper slopes was expected to erode quickly, exposing the coarser grade material below. The upper section of the slope Rows A to C had a very thin layer of fine material compared to between Rows E to F to G, where accumulation of 40cm of fine mulch had occurred. This may have been a product of the construction process of the rock dump, or dependent on the nature of weathering that has occurred.

The erodibility of the waste rock material was expected to be highly differential, with spatial heterogeneity having dramatic consequences on the final shape and form of the instigated gully network. The site characteristics were segregated into the following categories: heterogeneity, differential erodibility with depth and impact of inlet width at the top of the batter slope. The impact of these site characteristics will be the subject of these investigations, with incorporation of these factors into consequent prediction efforts.

The geometry of the batter site is complex with concavo-convex slope. A change in curvature occurs between Row H - Row I, as illustrated in Figure 2.6. Results from field trial observations with excavation on the upper sections and deposition onto lower sections followed expected theoretical behaviour mechanisms. Initial profiles of the batter site also suggested that incision of the top slopes of the highwall



Monitoring Gully Formation

would occur. The degree of erosion at this transition point between the gully catchment and the batter slope was influenced by the relatively thin layer of fine material in this region, and the larger reservoir inadvertently created behind the leading bund wall. This reservoir effectively raised the entry notch about 30cm before runoff from the catchment could enter the gully, with only relatively intense storm events of significant magnitude generating enough runoff for erosion to occur.

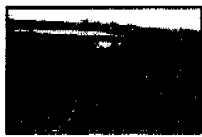
Figure 1.3.2 above outlines the nature of the equilibrium slope formation, far removed from the initial study site characteristics. However the physical attributes of the site are dictated, and hence the location of batter slopes, by the character of the final design solution.

During the monitoring period there were numerous storm events, with many averaging 20 to 30 mm in total. Other studies conducted during the Wet Season, (Bell, 1997) examine these numerous storm events in greater detail.

Three storm events were considered to be significantly large, instigating and directly altering the dimension, depth and length of the gully once formed. As described in Section 3.1 above, these events totalled 89mm, 79mm and 45mm respectively and occurred on 261296, 010197, and 230197 respectively.

The inlet and outlet points of the gully were significant with discharge runoff entering the gully from the 7200 m² catchment area above, and exiting the gully site via a flume located at the base of the slope. Measurements of suspended sediment concentration were taken at the base of the batter slope from the large flume remaining from previous erosion studies, although these samples proved inconsequential to this study. Hydrological data from the cap site, was monitored electronically with average discharge entering the gully estimated and incorporated in calibration of the landform model.

Two measurement techniques were used to ascertain the amount of material shifted proceeding each significant storm event. The intensive monitoring of cross-sectional areas at each of the 10 designated transects was used to generate an approximate picture of the gully form.



Monitoring Gully Formation

An extensive survey regime of the site during the middle of the Wet Season, and a complimentary survey of the site before and after the completion of the monitoring period was used to support findings from the cross-sectional area analysis. From the measurement techniques used on the site, the characteristic of gully formation, with areas of deposition and erosion, was determined.

Inherent difficulty in interpretation of results from this study included erosional development between monitoring rows, and smothering of erosion pins on the lower sections. Problems associated with the use of the erosion pins are highlighted above, with results devised from these dependent on the survey work conducted before the commencement of monitoring period and were not considered of high importance.

Other aspects of the field trial that were not incorporated included the assessment of mean particle diameter as a function of depth as the gully evolved. Estimates of the depth-erodibility relationship coefficients were conservative based on these incomplete estimations from Figure 4.3.7 and alike.

Table 3.2.1 below, summarises the findings from this intensive study, with estimates of the amount of material mobilised from each storm event determined from difference between surface profiles for each of the 3 storm events. Maximum erosion depths and overall profile development are however considered the most important findings in this study. The width of the gully and distance between rows is presented in Table 3.2.2 below, with little development in the upper sections once the gully was initiated. The following figures also attempt to highlight the characteristic of the evolution of the batter slope profile to its' present form.

Figure 3.2.1, 3.2.2, and 3.2.3 illustrate the results of the survey study conducted before the commencement of the Wet Season, during the Wet Season (January 16th) and after the cessation of monitoring period (April 97).

Figures 3.2.4, 3.2.5 and 3.2.6 were derived from the cross-sectional analysis. These surfaces were then used in comparison to original topography, and each consequent event, with the difference between consecutive events indicating regions of deposition

Surface Topography: Pre-Wet Season

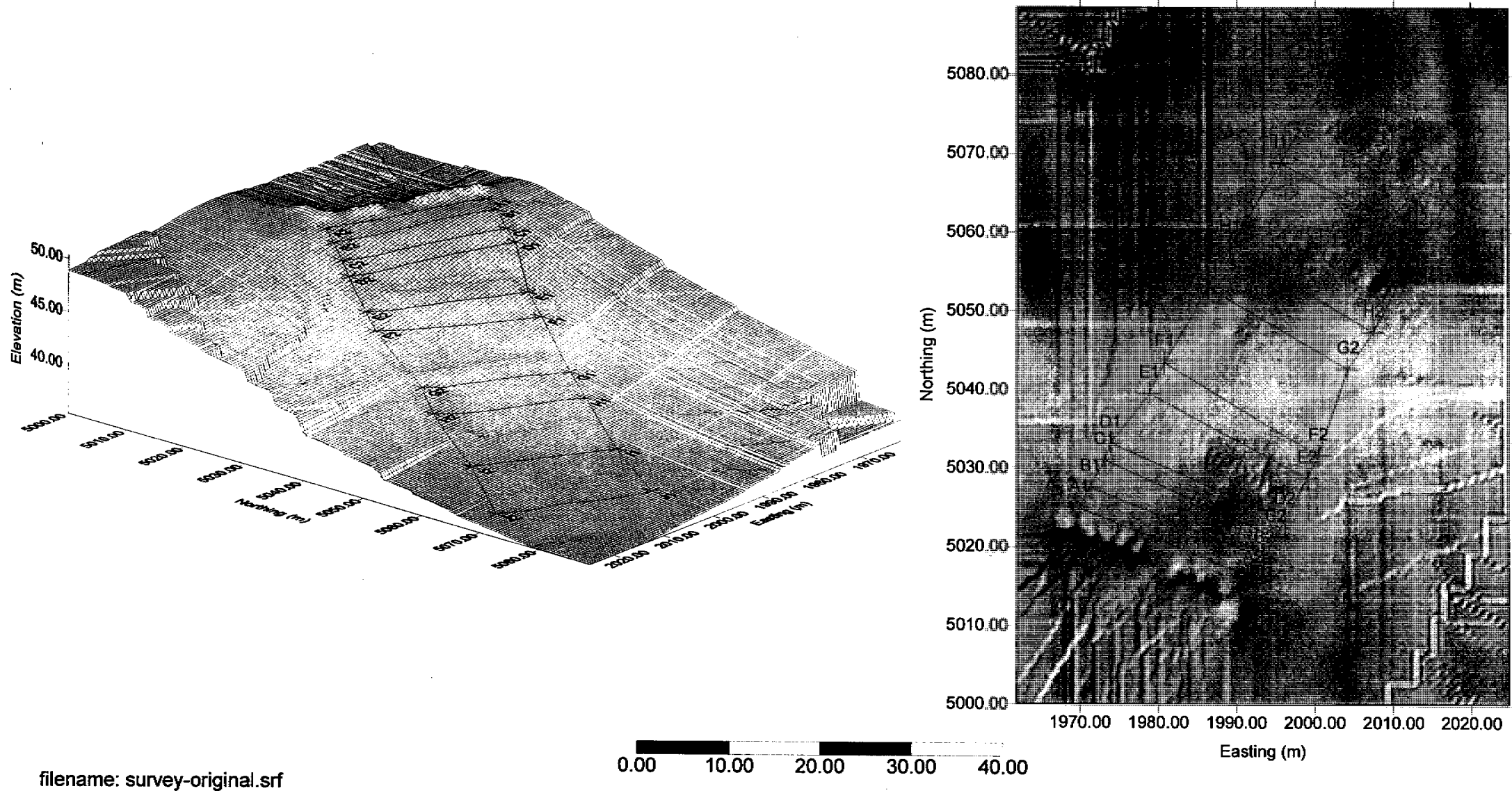


Figure 3.2.1: Three surveys were conducted during the field trial phase of this investigation. The first survey represents the batter slope before the commencement of gulling and was conducted before the start of the Wet Season.

Surface Topography: Mid-Wet Season

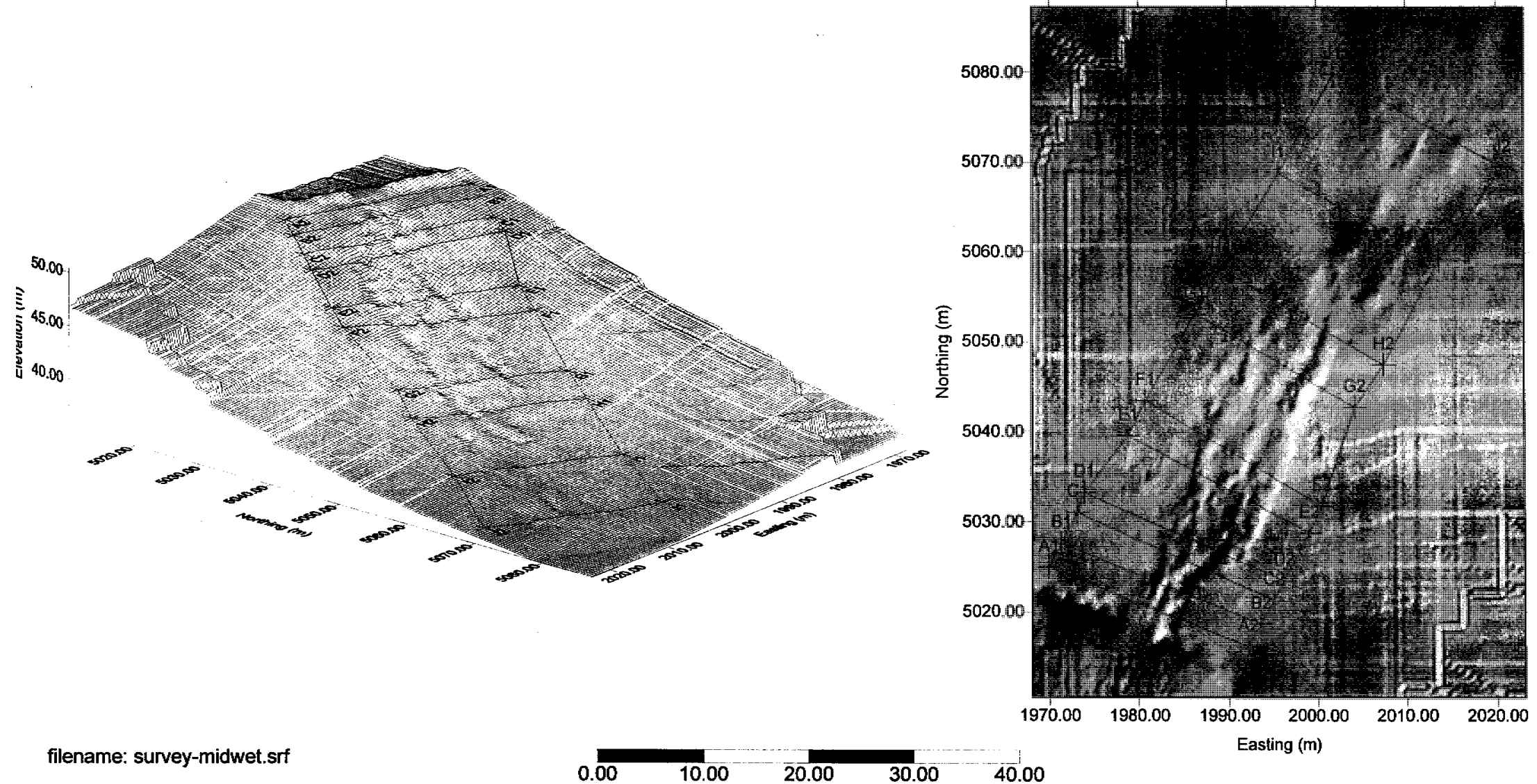


Figure 3.2.2: The next survey was conducted mid-way through the monitoring period on 16th January, where the first two storm events are compared to this landscape.

Surface Topography: Dry Season

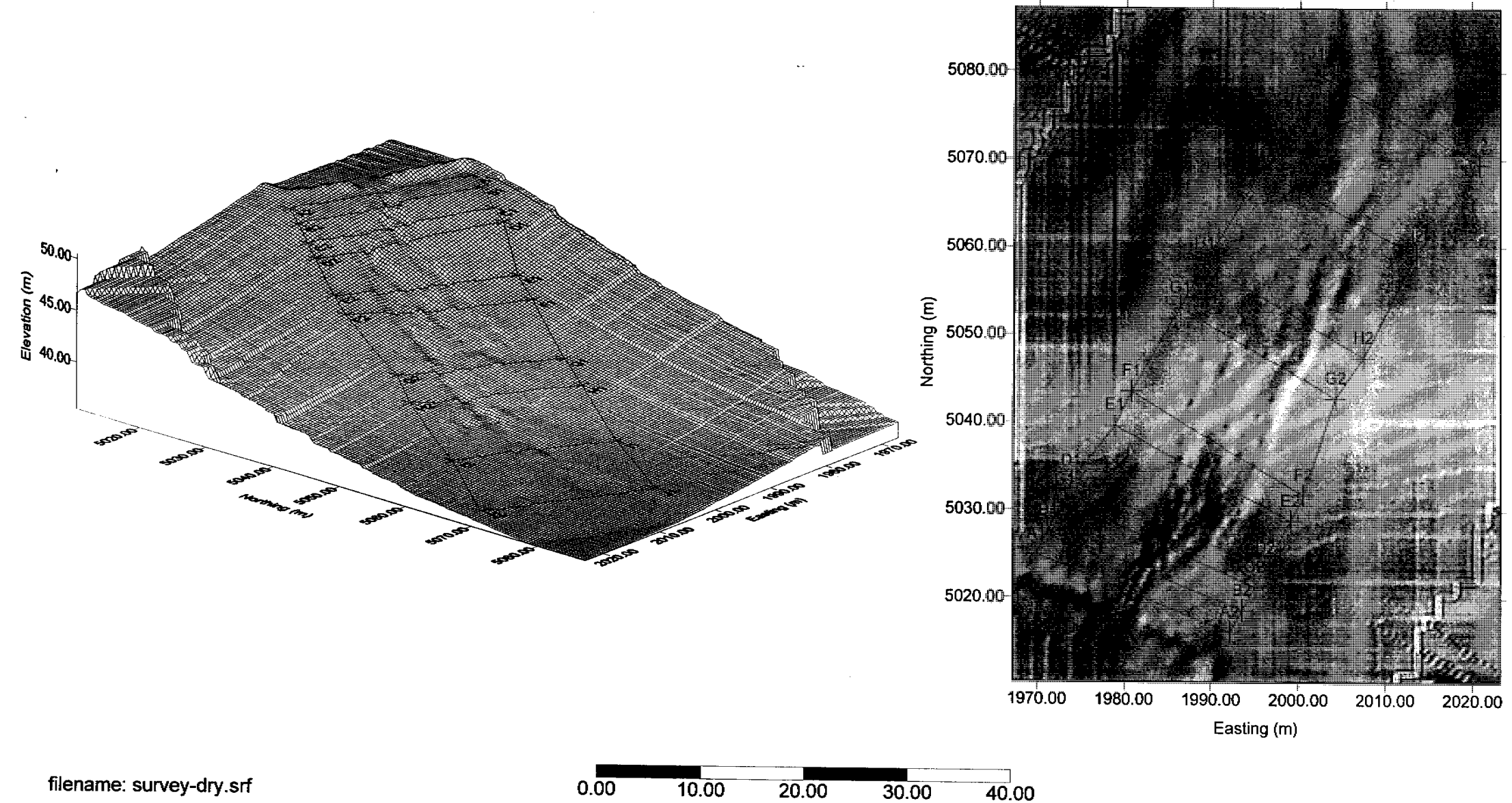


Figure 3.2.3: The final survey was conducted after the cessation of monitoring at the end of the Wet Season, although the detail of this survey was less than that seen in Figure 3.2.2, the continuing development of the gully can be observed to the bottom of the batter slope.

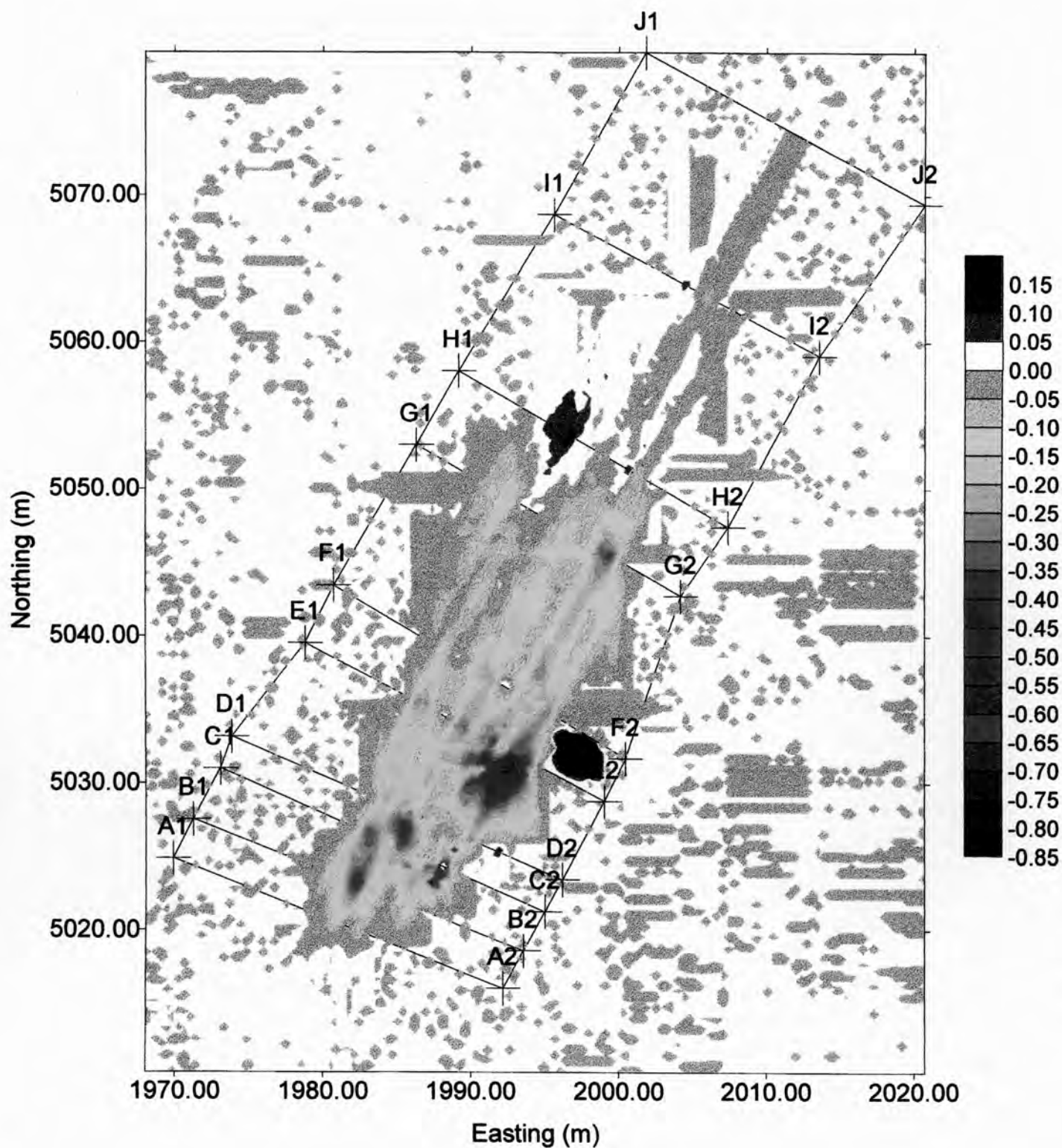


Figure 3.2.4: The results of the intensive cross-sectional analysis based on the 10 transects were translated to elevation data and used to evaluate the difference between measurements taken after each storm event. This figure illustrates the morphology of the batter slope from the initial surface to the storm event 261296, where erosion is represented on negative scale, whilst deposition is positive scale.

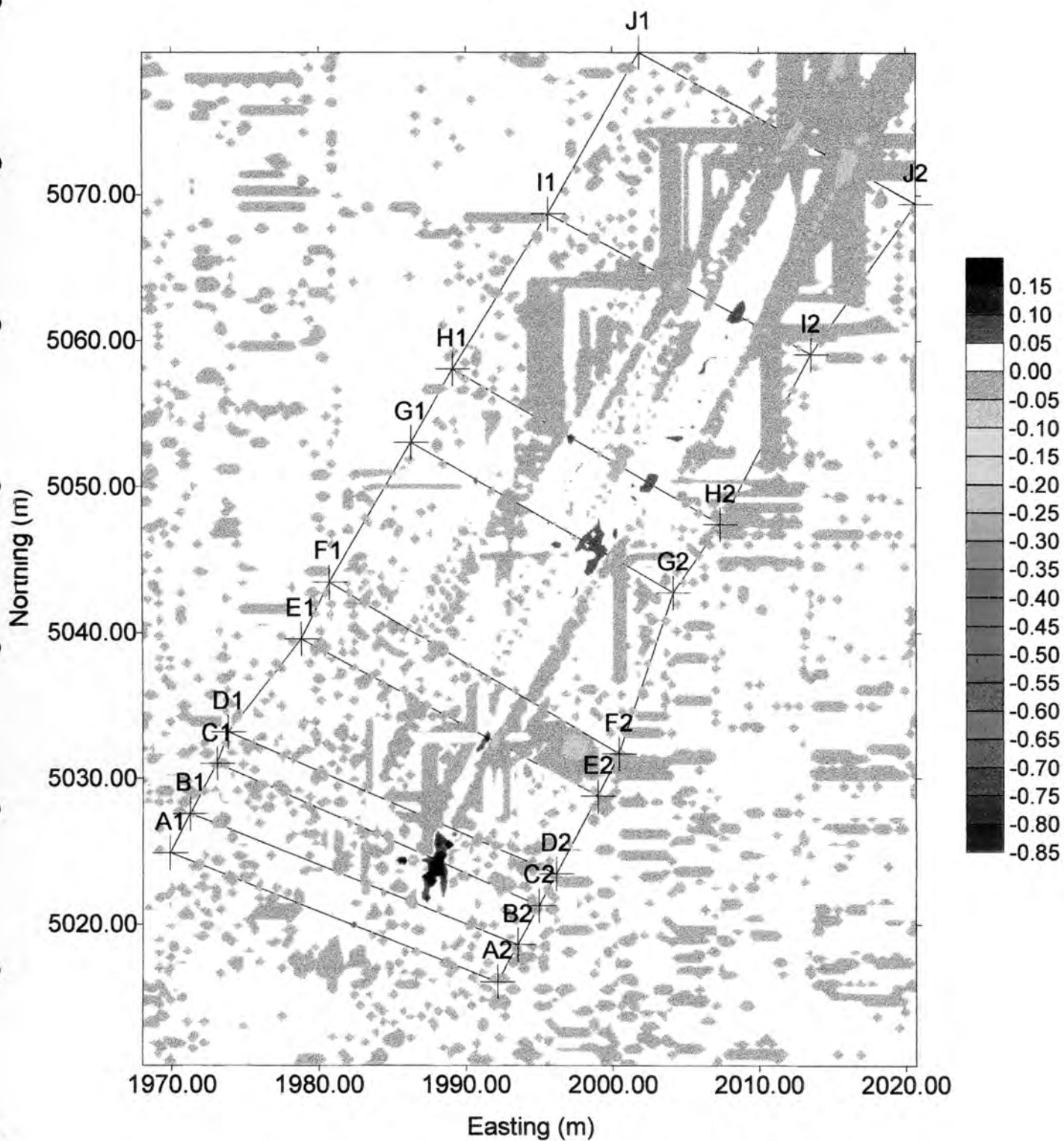


Figure 3.2.5: The difference between the surface profile at 261296, and 010197, where erosion is represented as positive values, and erosion as negative values. There was little alteration in the gully formation was associated with this storm event.

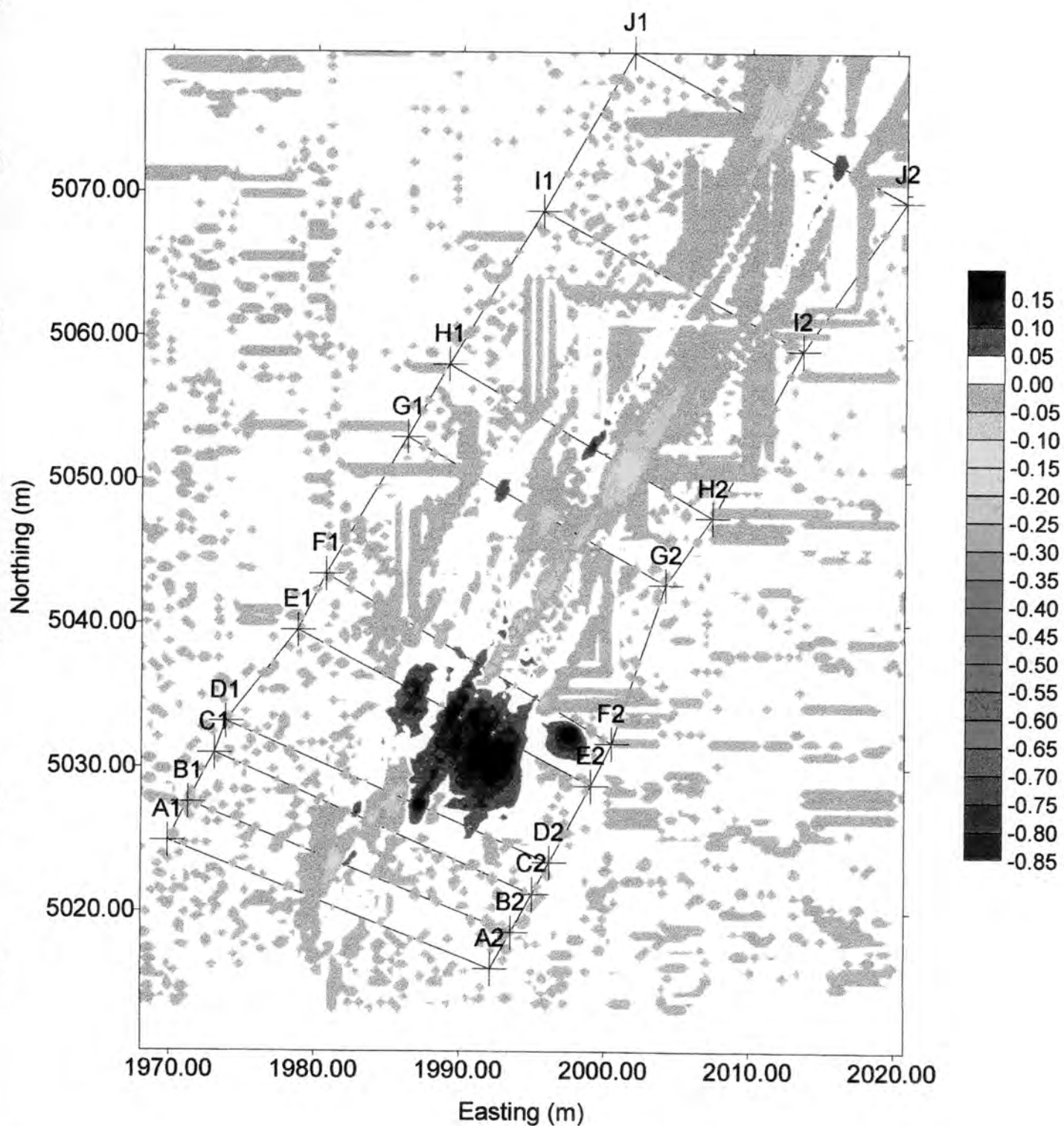
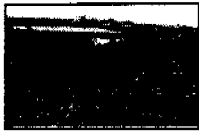


Figure 3.2.6: The difference between surface profile at 010197, and 230197. Erosion is once again represented on negative scale, whilst deposition is represented on positive scale.



Monitoring Gully Formation

Due to the large scale of mechanisms in operation, and as modelling discretisation consisted of a 20m by 60m grid (1m grid space) due to computational limitations, this was not considered beneficial.

Survey positions were taken at numerous random points in an attempt to enhance the findings from this aspect of the study, with a slightly better approximation being obtained in Figure 3.2.2, however it can be seen from the survey results conducted at the conclusion of the study that with approximately half the number of points recorded, a lot of detail was lost.

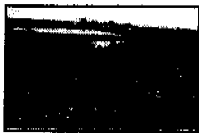
A physical description of the evolution of the gully helps to reaffirm those observations construed from the survey and cross-sectional analysis, with the characteristics of the formation of the gully remaining the most important aspects of the field study. Incorporation of other crucial sediment transport properties such as armouring can be identified readily in the upper sections of the gully after the initial event labelled 010197, with little movement occurring in these sections.

Figure 1.3.2 outlines the likely natural evolution of the steep batter slopes, with predictions based on work by Willgoose *et al*, 1992 suggesting that areas of deposition could be expected within 150 to 200m of the batter slopes, with depths of deposition up to 5m over the 1000 year time period.

From Figure 3.2.1, the initial excavation of the upper sections of the gully from Row A to Row C splits into two major arms, with accompanying deposition onto the divide between these arms, between sections Row D and Row E.

The actual initiation of the gully commenced a few days before the establishment of monitoring methods, with little data obtained and hydrological information about this storm event also being lost.

The first major event occurred on the 261296, with the event illustrated in Figure 3.2.7 occurring on the 191296. This event on 191296 was considered typical of the average storm events encountered during the monitoring period, with relatively even rainfall intensity and total rainfall level reaching 30 to 40mm.



Monitoring Gully Formation

However once the gully was instigated, erosion due to these relatively insignificant storm events was minimal. Although relatively little material was displaced by the preliminary event, the highly erodible upper surface material was quickly reduced about 10 to 20cm in some places. This was noteworthy due to the removal of almost all the finer material from the surface after the formation of the gully following the significant storm event occurring on 26/12/96.

Figure 3.2.7 illustrates cross section located at the point now described as Row D. Although little material was mobilised from the upper surface of the batter slope, the earthworks in development of the catchment boundary wall and the channel linking the cap site to the remainder of the catchment, provided excess sediment during these initial events which was conveyed by the developing gully.

Figure 3.2.7 is compared with Figure 1.1.4, illustrating the batter slope before commencement of monitoring. The layout of the slope was relatively uniform, with little difference in elevation across the traverse. The inherent variability in the erodibility of the waste rock material is also indicated by this figure, material susceptible to geochemical weathering generated the material that was rapidly eroded once gully development commenced.

Other considerations included the nature of the pathway of the gully adopted, defined as the thalweg, minimal elevation point of the gully. This initial event dictated the shape of the formation of the gully during the remainder of the monitoring period. The consequent event, designated as the first major event excavated this cross-section dramatically, with little resemblance between the two surfaces.

Figure 3.2.9 illustrates the divide between each of the two major arms of the gully after the first major storm event, due to nature of inlet point, and armouring encountered within several centimetres of the upper surface.

The establishment of the reservoir above the entrance to the gully network contributed significantly to reducing the velocity of water in the upper sections of the gully. As the water reached the middle sections, the momentum had increased to such an extent that more significant amounts of material could be mobilised.



Monitoring Gully Formation

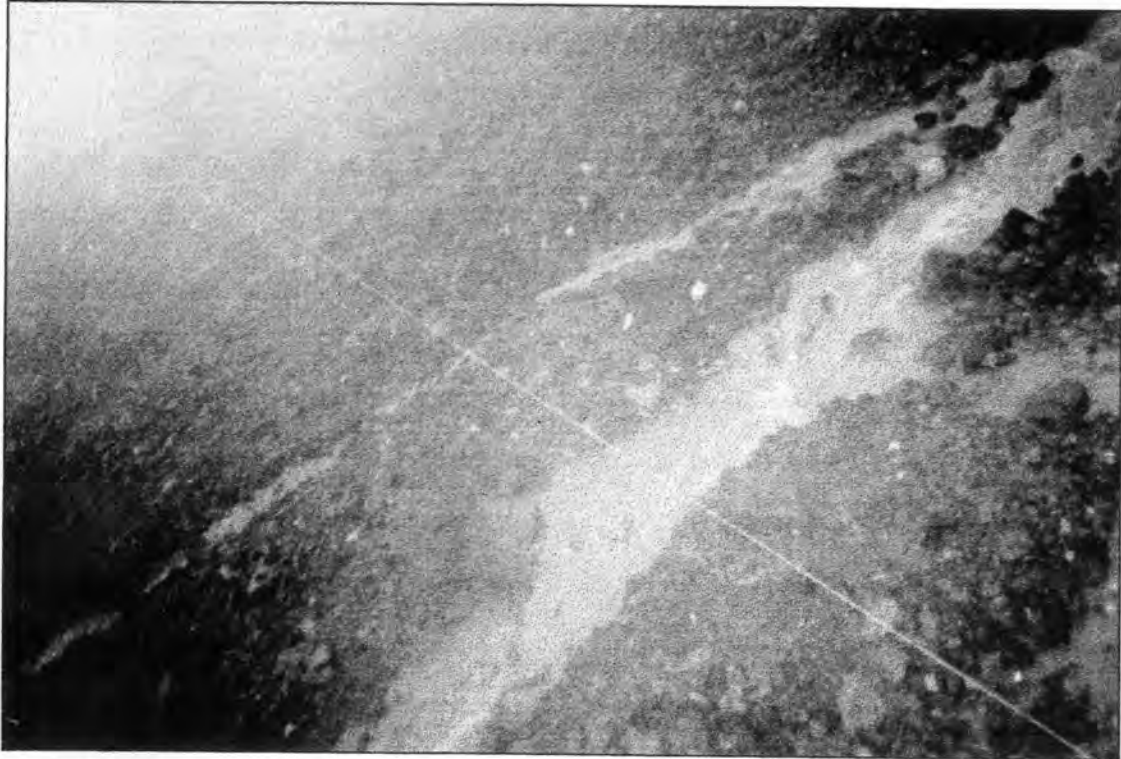


Figure 3.2.7: This cross-section was located at the point now labelled as Row D, with excavation of the loose upper surface material to some 10 to 20cm in depth. At this time little of the monitoring equipment had been established. It is also noted that this profile is not vertical, with the starpost in the upper left corner indicating the degree of elevation.



Figure 3.2.8: The first storm was estimated to be 30 to 40 mm, in total with incomplete installation of monitoring equipment resulting in no hydrological data obtained. However little emphasis was placed on this event, given the magnitude of the first significant event on 261296.



Monitoring Gully Formation

Although the constraint of the artificial reservoir may misrepresent what may happen considering the final design landform, the modelling process does not take into account the initial water velocity regardless, making this discrepancy less significant.

The nature of the waste rock material below the finer grade of material is evident in Figure 3.2.8 and Figure 3.2.9, with the relatively finer material seen centrally. The two arms of the gully were separated at the top of the batter slope due to the very large rock fragments encountered only several centimetres below the surface. The paths of the two arms crossed again below Row D with another tributary to the right of Figure 3.2.10.

Substantial deposition of 10 to 20cm in places at the forefront of the advancing major tributary continued until the end of this event. With large amounts of fine material deposited between Row G and Row H, which was consequently excavated in some degree by the more minor event on the 010197.

The gully extended to Row H during this event and is illustrated in Figure 3.2.11, and Figure 3.2.12, with the pathway becoming indistinct below Row I with deposited material (over erosion pin row 3) relatively easily erodible. It was noted that this event has a peak discharge of 21L/s, with rainfall continuing for approximately 1.5 hours, eroding the material transported initially.

The minor tributary on the right hand side of the slope encountered slightly less erodible material with mean particle diameter approximately twice that of the left hand side. The excavation of the gully halted about Row F to G for the major arm, and Row E to F for the minor arm. It was also noted that the paths of the two thalwegs crossed, and material deposited contributed to the overburden from the excavation of the sections above, as seen in Figure 3.2.11. This was also evident in Figure 3.2.5, with excavation divided between the two major arms, being clearly delineated. Overburden is highlighted in this figure, with minor disturbance of about 10 to 20cm being widespread between Row G and Row H.



Monitoring Gully Formation



Figure 3.2.9: The profile of the upper section was established by the first major storm event. Complete removal of fine material is evident in this figure and comparison is made to Figure 3.2.8 above.



Figure 3.2.10: The two main tributaries were separated between Row A to Row D, with thalwegs crossing below Row D as pictured here. Another tributary developed to the right of this photo, which crossed again below Row E to Row F in consequent events.



Monitoring Gully Formation



Figure 3.2.11: The removal of fine material was more widespread below Row D, as seen by the painted fluorescent lines across the slope. Both channels combined, and the gully pathway was not easily discernible.



Figure 3.2.12: The left tributary also continued down the hillslope with relatively easily erodible material deposited between Row H and Row I making the pathway adopted distinct in the background of this photo.



Monitoring Gully Formation

The diversion of flow into the major gully from the divide pictured in the upper sections of the slope, resulted in significantly more erosion on this side, below Section F2 to Section G2. About one third of the flow was diverted to this path, with this gully ceasing to advance once past the intersection between the concave and convex parts of the batter slope, the point of change in curvature.

The next rainfall event occurred in 010197 with total rainfall of 60mm, and peak discharge entering the gully at 13 L/s, with average 4 L/s. This storm was monitored with a photographic record available. The amount of material moved by this event was considerably less due to the reduced intensity, as well as extensive armouring exhibited in the upper regions from initial activity.

Although the catchment had been constructed for same time, since the first event on 191296, the remnant brown mud sediment is evident in the suspended flow entering the gully in Figure 3.2.12. The buffering effect of the gully is also evident in this figure with flow diverging into the two main arteries. The accumulation of water behind the leading edge of bund wall supplied water to the gully for several hours after the rain had ceased, effectively minimising initial discharge velocity.

The divide between the two main tributaries is still evident in Figure 3.2.13, with coalescing of gully pathways below Row D to Row E pictured in Figure 3.2.14. The fluorescent paint used to delineate the previously eroded sections and was particularly useful in outlining the pathway of the gully as it developed.

The survey results pictured in Figure 3.2.2, were used to derive a directional derivative approximation of the drainage network for the gully, and this appears in Figure 3.2.15.

The third and final significant storm event occurred on 230197, with total rainfall of 45mm, over a period of only 30 mins, with peak discharge 29L/s.

Although Figures 3.2.4, Figure 3.2.5, and Figure 3.2.6 represent a morphology of the landform over a small duration, the inherent lack of detail devised from the cross-sectional analysis allows only generalisations to be made. Extrapolation of the cross-section of the gully at the transects located at both Row F and Row G by the mapping



Monitoring Gully Formation

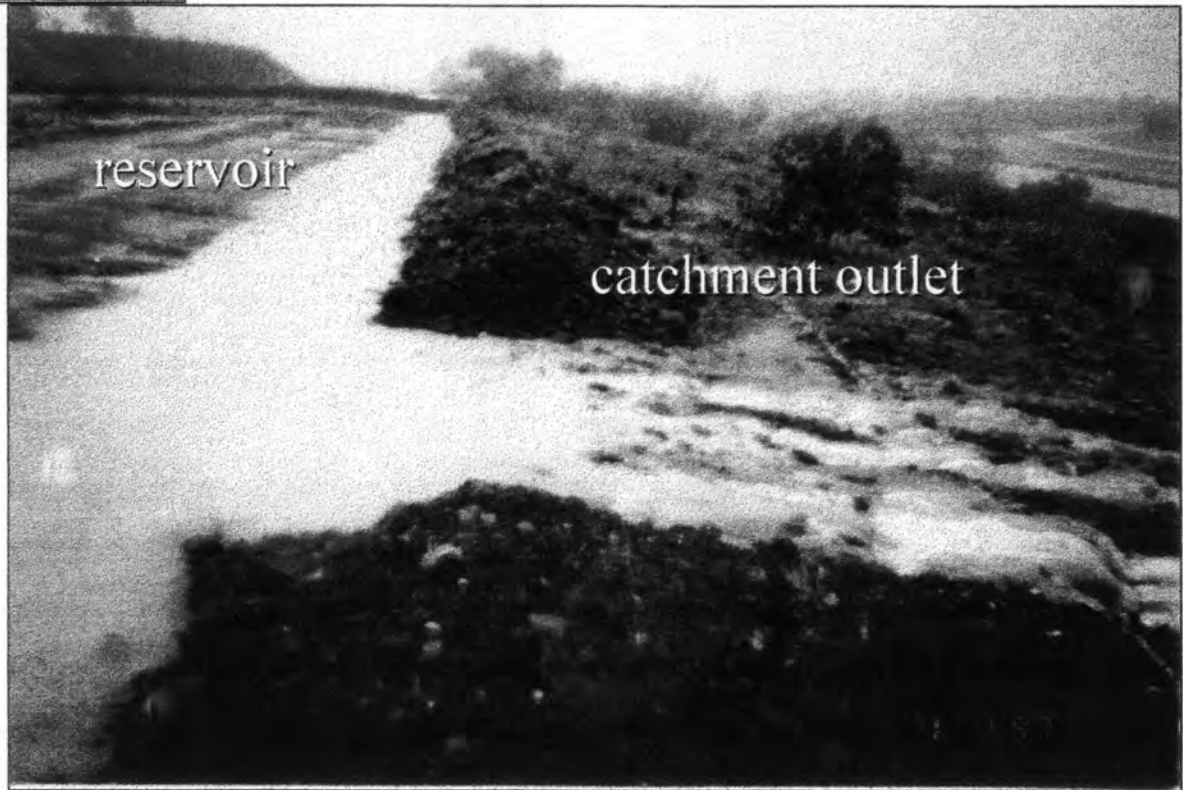


Figure 3.2.13: The inlet point of the catchment extended ~ 3m with approximates of 2m and 4m used during the modelling process.



Figure 3.2.14: The pathway of the gully can be delineated by the fluorescent paint markings, indicating regions that were eroded on deposited between each storm event.

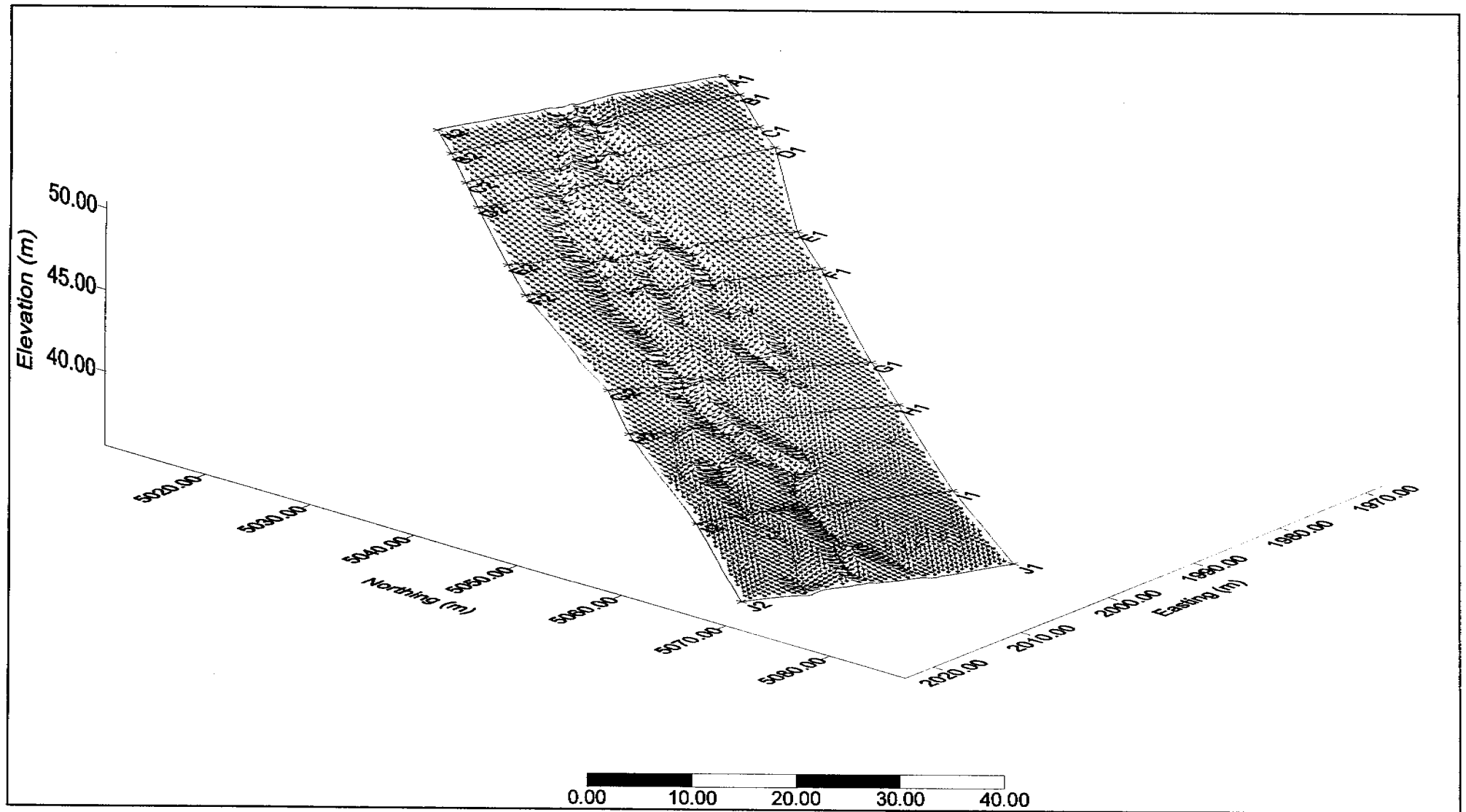


Figure 3.2.15: The survey conducted mid-way through the monitoring period was used to generate a directional derivative schematic of the drainage pattern for the gully.

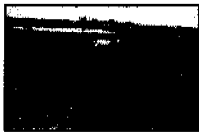
Monitoring Gully Formation

Table 3.2.1: The amount of material excavated or deposited by each event was approximated by the subtraction of the upper surface from the lower surface. Estimates of net deposition can be seen in the events at the end of the monitoring period.

<i>Description</i>	<i>Erosion Volume (m³)</i>	<i>Deposition Volume (m³)</i>	<i>Morphology (m³)</i>
Transect-261296	52.29	5.55	46.74
Transect-010197	5.25	6.94	-1.68
Transect-230197	8.42	13.93	-5.51
Survey-160197	68.90	30.14	38.76

Table 3.2.2: The width of the gully as it developed, is noted not to change significantly due to the extensive armouring experienced at the top of the batter slope, and the low initial velocity due to the artificial reservoir.

<i>ROW : dated 28/12/96.</i>	<i>Width (m)</i>	<i>Location (m..m).</i>
R1-R2 (2.9m)		Using R1
At 1m from R1	2.05m 1.60m	10.55m to 12.60m 13.20m to 14.80m
At 2m from R1	1.95m 1.95m	10.60m to 12.55m 13.15m to 15.10m
R2-R3 (3.4m)		Using R2
At 1m from R2	0.55m 2.37m 1.30m	10.00m to 10.55m 11.35m to 13.72m 15.20m to 17.00m
At 2m from R2	0.35m 2.40m 1.00m 1.80m	10.00m to 10.35m 10.90m to 12.30m 12.70m to 13.70m 15.20m to 17.00m
R3-R4 (2.6m)		Using R3
At 1m from R3	4.45m 1.70m	10.55m to 15.00m 16.10m to 17.80m
R4-EP1 (3m)		Using R4
At 1.5m from R4	1.15m 1.55m 1.75m 2.70m	11.65m to 12.80m 13.70m to 15.25m 15.65m to 17.40m 18.00m to 20.70m
EP1-R5 (3.6m)		Using R5
At 2m from EP1	1.85m 1.80m 3.40m	8.75m to 10.60m 11.20m to 12.00m 13.30m to 16.70m
R5-R6 (3.6m)		Using R5
At 2m from R5	1.10m 1.30m 1.70m 2.20m	8.00m to 9.10m 11.70m to 13.00m 13.30m to 15.00m 15.40m to 17.60m
R6-EP2 (7.9m)		Using R6
At 3m from R6	1.40m 1.70m 1.90m	6.60m to 8.00m 8.30m to 9.00m 10.20m to 12.10m
At 6m from R6	0.75m 1.75m 2.20m 3.20m	6.80m to 7.55m 8.45m to 10.30m 10.80m to 13.00m 14.10m to 17.30m
EP2-R7 (3.8m)		Using R7
At 2m from EP2	1.10m 1.45m 1.10m	5.00m to 6.10m 7.20m to 8.65m 14.10m to 15.20m
R7-R8 (5.7m)		Using R7
At 3m from R7		7.35m to 8.50m 11.60m to 13.00m 14.00m to 16.00m
R8-EP3 (5.2m)		Using R8
At 3m	1.00m 1.70m 3.60m	7.50m to 8.50m 9.20m to 10.90m 11.70m to 14.30m
EP3-R9 (7.8m)		no
R9-EP4 (6.9m)		significant
EP4-R10 (5.7m)		formations
R10-EP5 (9.2m)		here as yet.



Monitoring Gully Formation

package tended to conceal the complex nature of activity in those sections. From Figure 3.2.4, the areas of deposition are less clear, however with comparison with the results presented in Figure 3.2.2 the sections from Row F to Row G allows insight into the nature of this mechanism.

The disturbed sections of the batter slope were cleared of fine particles, resulting in dramatically reduced erodibility. From Figure 3.2.8, the disturbed material could be used to easily identify the path of the minor tributary, with erosion pins dislodged and transported downstream below transect Row D. Below the trees in the middle ground of the photo, a pathway linking the two major arms of the gully crosses. Overburden from this intersection deposited during the end of the initial event, as well as that of the 010197 storm event, with significant scouring observed during the final event.

The layering of fine mulch is of concern in future investigations, with depth in Row G to H about 50 to 60cm, revealed by examination of sidewall of the main gully. The relative heterogeneous nature of fine particles is observed in photographic series in Figure 3.2.16 to Figure 3.2.19, where a 30cm ruler is highlighted in the centre of most of these figures.

Some sections of the gully, once breached eroded quickly with soft earthen material excavated from just above the mined ore, being exposed in Figure 3.2.8. A combination of surface layers has been used to design the batter slope, (pers com. Willgoose, 1997) making excavation to this depth, of some concern.

Further evaluation of the role of rapid geochemical weathering, and impact of diffusive mechanisms on modelling simulations may need to be conducted.



Monitoring Gully Formation



Figure 3.2.16: Excavation of sidewall material slowly increased the width of the gully, with residual layer of fine material about 45cm accumulating at this point.



Figure 3.2.17: The depth of erosion reached 60cm in some places, revealing the heavily armoured rock fragment layer. The differential erodibility of these surfaces is considered with the soft earthen material extracted from above the mined ore seen as brown colour. Depth-erodibility relationships for this slope would therefore be complex, once the protective layer is breached.



Monitoring Gully Formation



Figure 3.2.18: The excavation of material from Row H to Row I, reaches a depth of 60cm with large rock fragments armouring further incised.



Figure 3.2.19: The gully extends to Row I with depth of 20cm to 30cm, whilst almost reaching the concrete apron of the flume pictured in background.



4.0 Model Calibration and Predictions

4.1 Theory

The computer model SIBERIA was developed to study the link between physical process and the development of catchments. The distinction between hillslope and channel based processes is considered some of the most important aspects of this model.

As outlined above, the major components of the model focussed on in this study simulates the evolution of catchment elevations over time by continuity of mass, in this case the batter slope.

Fluvial erosion processes, modelled according to standard forms, is incorporated into influx and outflux of regions within the catchment over time.

Average elevations are therefore determined over monitoring period based on the following governing equation.

$$\frac{\partial z}{\partial t} = \frac{\nabla q_s}{\rho_s(1-n)} + D \cdot \nabla^2 z \quad (\text{adapted from 1.3.1}) \quad (4.1.1)$$

where

z = elevation,

t = time,

q_s = sediment transport per unit width,

$\rho_s(1-n)$ = bulk density of sediment

D = diffusivity of diffusive transport (rainsplash, landslide)

The differential equation is described as a continuity of sediment transport over time, with other components of the governing equation such as tectonic uplift and diffusion terms were neglected for this study. This was considered reasonable since the monitoring period was short, and surface wash erosion was the most commonly observed mechanism. Only the exposed sidewalls of the lower sections of the gully were sufficiently high for landslip mechanisms to occur, and these areas were not considered important for simplification of modelling process.



Monitoring Gully Formation

The more sophisticated methods of diffusion such as soil creep, landslide and rainsplash were considered negligible, as mass transport processes observed were almost entirely dependent on fluvial transport.

The sediment transport process q_s , is modelled by the second term in equation 4.1.1, and can be represented in a number of ways

$$q_s = f(S^n, q_w^m) \quad (4.1.2)$$

where

q_s = sediment flux, g/s
 q_w = discharge, L/s
 m, n = derived exponents
 S = Slope, m/m

with equation 4.1.2 reflecting findings from both field and laboratory observations by soil scientist and geomorphologists. The general form of this model is:

$$q_s = \beta_1 q^{m_1} S^{n_1} (\tau - \tau_c) \quad (4.1.3)$$

where

q = discharge per unit width,
 β_1 = rate constant for sediment transport, function of sediment grain size,
 m_1, n_1 = derived exponents,
 τ = bottom shear stress for the flow,
 τ_c = shear stress threshold (critical shear stress)

However for the material from the waste rock dump the critical shear stress has been attempted to be identified Willgoose *etal*, 1993, and their conclusions were that its value was indistinguishable from zero, with this conclusion adopted in parameter estimation.

Implications as to the nature of the rehabilitation design adopted will incorporate extensive revegetation, in doing so will reduce the erosional force of surface flow significantly. Plants provide protection of the surface by cohesion, and binding of soil particles, increasing the resistance to scouring. Prosser, 1996 suggests that the critical threshold for incision can be several times higher on vegetated surfaces compared to that of bare surfaces, although as stated, this is not considered in this study with minimal vegetation evident on either study site.



Monitoring Gully Formation

Equation 4.1.3 parameterises the total sediment transport, including bed load and suspended sediment loads (as defined above).

Exact values for these parameters has been the focus of previous studies conducted on site such as Willgoose *etal*, 1992, and Evans in prep.

Natural rainfall runoff events and simulated rainfall catchments (largest area ~ 100m²) were used to calibrate the fluvial sediment transport equation (equation 4.3.2) and were shown to be least dominated by diffusion processes (as assumed above). These small scale erosion plots were located on the Northern WRD adjacent to the cap site as described in Section 2.2, with other study sites on the batter slope itself, Willgoose *etal*, 1993.

The parameters fitted to equation 4.1.3 were n_1 , m_1 , and β_1 , where m_1 and β_1 relate directly to estimates of sediment loss for monitored fluvial erosion studies. The exponent n_1 of the slope term S is derived using the following relationship (Evans, Willgoose, and Riley, 1995):

$$q_s \propto \frac{1}{d^{3/2}} \quad (4.1.4)$$

where

d = median sediment grain diameter (mm)

Evans *et al*, 1995 suggests that this function of Einstein-Brown relationship can be adapted to determine a value for the WRD,

$$\left(\frac{S_{Cap}}{S_{Batter}} \right)^{n_1} = \left(\frac{d_{Cap}}{d_{Batter}} \right)^{1.5} \quad (4.1.5)$$

where

S_{Cap} = cap site slope from previous studies ($S_{Cap} = 0.028$),

S_{Batter} = batter site slope ($S_{Batter} = 0.207$),

d_{Cap} = mean diameter size (d_{50} Cap: 0.54mm),

d_{Batter} = mean diameter size (d_{50} Batter: 1.39mm).

Estimate of n_1 based on these values is 0.71 (with 0.69 from Willgoose *etal*, 1993).



Monitoring Gully Formation

This value for n_1 is then adopted and included in the multiple regression analysis used to determine m_1 , and β_1 as described by Evans *et al*, 1995.

$$\log T = \log \beta_1 S^{m_1} + x \cdot \log \int Q^{m_1} dt \text{ (Evans *et al*, 1995 equation 11)} \quad (4.1.6)$$

For this case, the value of n_1 is considered susceptible, since the mean particle diameter, d_{50} varies dramatically once erosion commences.

For sediment transport according to the Einstein-Brown equation in a wide channel, the parameter values for m_1 and n_1 are 1.8 and 2.1 respectively. Investigation into the sensitivity of the estimate of the exponent on the slope component n_1 is conducted below, although a value of 2.1 is initially adopted due to the stability of preliminary modelling results.

From equation 4.1.6 above, the regression analysis is used to determine all the components of the sediment transport equation. By taking S^{m_1} as a known value, the parameter β_1 can be determined, as the $\log K$ term is devised from the analysis process. Thus the estimate of the parameter n_1 influences the erodibility of the material in parameter β_1 as well as the contribution to total sediment loss within the slope component.

Evans *et al*, 1995 noted that regression analysis for total sediment loss of:

$$T_B \text{ (batter)} = 3.34 S^{0.71} w^{-0.8} \int Q^{1.8} dt \text{ (R}^2 = 0.53; \text{ df} = 11; \text{ p} < 0.01), \text{ and} \quad (4.1.7)$$

$$T_C \text{ (cap)} = 13.8 S^{0.71} w^{-0.8} \int Q^{1.8} dt \text{ (R}^2 = 0.53; \text{ df} = 11; \text{ p} < 0.01).$$

with erroneous data points removed, this relationship was analysed again.

$$T_B \text{ (batter)} = 5.05 S^{0.71} w^{-1.8} \int Q^{2.8} dt \text{ (R}^2 = 0.93; \text{ df} = 9; \text{ p} < 0.001), \text{ and} \quad (4.1.8)$$

$$T_C \text{ (cap)} = 20.9 S^{0.71} w^{-1.8} \int Q^{2.8} dt \text{ (R}^2 = 0.93; \text{ df} = 9; \text{ p} < 0.001).$$

where

$$T(g) = \beta_1 \cdot S^{m_1} \cdot w^{(1-m_1)} \cdot \int Q^{m_1} dt$$

with $\int Q^{m_1}$ = Cumulative value of duration of event,
 $T(g)$ = Total sediment loss.



Monitoring Gully Formation

Evans *etal*, 1995 notes that the value suggested for the exponent m_1 at 2.8 does not compare well with previous studies by Willgoose *etal*, 1993 with their estimate of m_1 at 1.68. The estimated value for parameter exponent n_1 from equations 4.1.8 was 0.71 and compares well with previous studies, with a value of 0.69 being determined.

The results of this process, conducted previously by Willgoose *etal*, 1993, is expressed in the following fitted relationship ($r^2 = 0.64$),

$$c = 3.59 q^{0.68} S^{0.69} + \frac{0.178RS}{q} \quad (\text{Willgoose } \textit{etal}, 1993 \text{ equation 5}) \quad (4.1.9)$$

where

c = sediment concentration = q_s / q , (g/L)

q = discharge = $f(q, S, \text{Area})$, (L/s),

q_s = sediment flux, (g/s).

From equation 4.1.9 and above, the fitted parameter values adopted were $\beta_1 = 3.59$, $m_1 = 1.68$, and $n_1 = 0.69$, (and 2.1 for comparison). Rainsplash diffusivity was neglected and these results were considered consisted with other field data accumulated by the geomorphology group at *eriss*.

The next important component of the calibration and adaptation process is the derivation of discharge, q in equation 4.1.9. The discharge relationship is a function of area, slope and surface discharge. In this case the drainage pattern of the catchment is adapted to represent the gully catchment as a series of nodal entry points at the top of the initial batter surface, with the slope of the gully catchment neglected, due to the nature of the constructed reservoir above the head of the gully and the assumption from this that the surface is almost completely flat (slope is 1 to 2% on site).

$$Q = \beta_3 \cdot A^{m_3} \quad (4.1.10)$$

where

Q = average discharge for 1 hour of each of the storm events,

A = area of the gully catchment,

m_3 = exponent on the area in discharge used in sediment transport,

β_3 = coefficient between discharge and area used in sediment transport.

The discharge per unit width term, q was evaluated to be the discharge entering the head of the gully network averaged over the duration of the storm. The average discharge over a 1 hour period, for each of the storm events was used to determine the parameter β_3 , with exponent m_3 representing a non-linear relationship with area, disabled ($m_3 = 1$).



Monitoring Gully Formation

$$\beta_3 = \frac{\text{discharge average in 1 hour}}{\text{area of gully catchment}} \quad (4.1.11)$$

The runoff module within SIBERIA does not directly model runoff, with no continuity of water or runoff routing routine within the model. For this case, a user-specified runoff module was adopted with this representing a series of feed points located at the head of the gully network, at the outlet of the gully catchment. This constituted the discharge-area relationship discussed in equation 4.1.10 above, being applied initially at the 2 or 4 inlet points of the constructed initial landscape.

The parameter β_3 is equivalent to 'mm' of rainfall, and was calibrated for each storm event, whilst it is also noted that β_3 only appears in the discharge-area relationship used in SIBERIA and is representative of the average storm duration of 1 hour.

The coefficient β_1 of the sediment transport equation, represents the erodibility of the waste rock material, and was determined using site specific data and is considered the final component of the calibration process.

The bulk density, ρ_s (1-n) from equation 4.1, for the waste rock material was determined from soil analysis conducted at three locations on the batter slope. The β_1 value, derived from erosion studies and the devised bulk density estimate are combined in the β_1 coefficient used for SIBERIA in equation 4.1.12, with derivation appearing in Appendix D.

From equation 4.1.1, the sediment transport equation was calibrated as follows:

$$\beta_1(siberia) = \frac{\beta_1}{\rho_s(1-n)} \cdot \frac{60s}{\text{min}} \quad (4.1.12)$$

where

$\rho_s(1-n)$ = bulk density,

β_1 = sediment transport coefficient from equation 4.1.9,

time = conversion factor for timestep from 1 hour to 1 minute.

The value of bulk density was used to derive the erodibility coefficient in SIBERIA, with time step reduced from 1 hour duration (derived from the 1 hour duration β_3 discharge relationship) to 1 minute.

It was also noted numerical stability requirements dictated iteration timestep length, within the SIBERIA program, was set to be 0.05 for model simulations presented.

Modelling Methodology

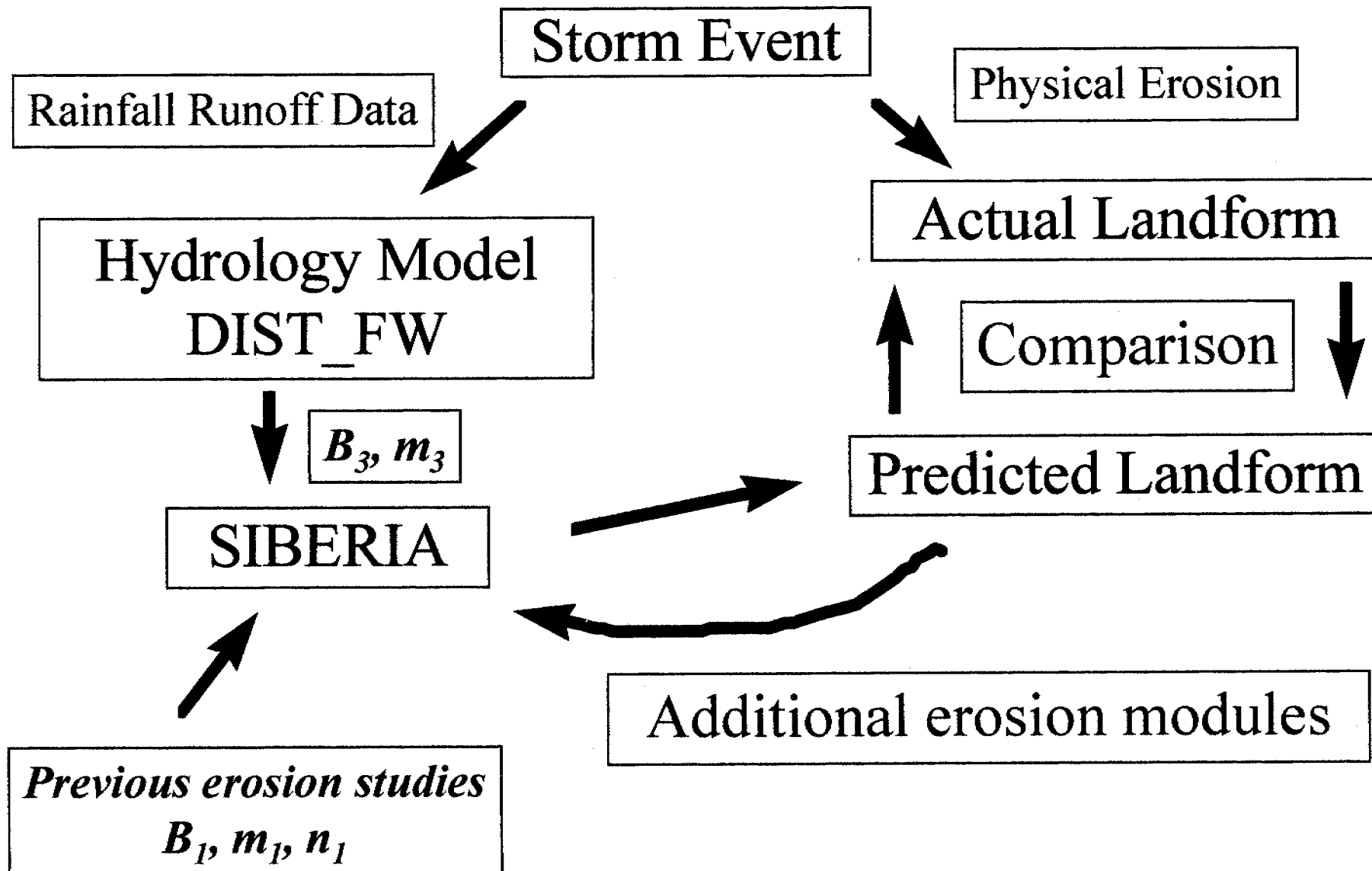


Figure 4.1: The combination of the two major model components, from hydrology and sediment erosion models, allowed the calibration of the landform model SIBERIA to be representative of the batter slope study site. The runoff model was instigated using a series of inlet points across the top of the batter slope, with erosional characteristic (β_1 , m_1 , and n_1) of the site adapted from previous studies.



4.2 Initial Surface and Determination of Parameters

The evolution of the batter slope over the 96-97 Wet Season was intensively monitored. Hydrological data was adapted to represent the three storm events that initiated and altered the gully significantly.

The initial surface was created to approximate the geometry of the batter slope, and gully catchment with runoff from the catchment entering the head of the batter slope from an outlet cut into the bund wall (Section 2.2).

The profile of the batter slope has been described as complex, with 2 approximations being made. The first surface incorporates a small section of the gully catchment, with the top of the surface extending back about 10m into the catchment.

The other alternative did not include the upper section of the catchment, and effectively represented only the study site area. Both of these alternatives are illustrated in Figure 4.2.1 and 4.2.2 respectively.

From Figure 4.2.1, the study area was approximated to a 20m by 60m rectangular grid, closely resembling the transect measurement sections described in Section 2.0. Grid spacing of 1m simplified the calibration of the initial parameters for SIBERIA with each grid representing an area of 1m^2 .

The inlet points were located at points (9,60) and (10,60) for the initial discretisation, with a wide inlet point scenario also considered, with inlet points across points (8,60) to (11,60). The outlet point, as described in Figure 4.2.1, was located at the base of the slope and was assumed to be fixed elevation at points (8,2) to (11,2). The elevations at the entry points to the batter slope were assumed not to be fixed.

Both surfaces were evaluated during the modelling process with theoretical behaviour approaching equilibrium profile of the slope with these surfaces constructed using from results devised from survey conducted during monitoring period. The elevation profile is represented in Figure 4.2.1, and Figure 4.2.2, with nature of slope, rising to elevation of 13m.

The initial profiles were created with another small fortran program named CREATERST2.f and detailed listings of the derivation and implementation are contained in Appendix E.



Monitoring Gully Formation

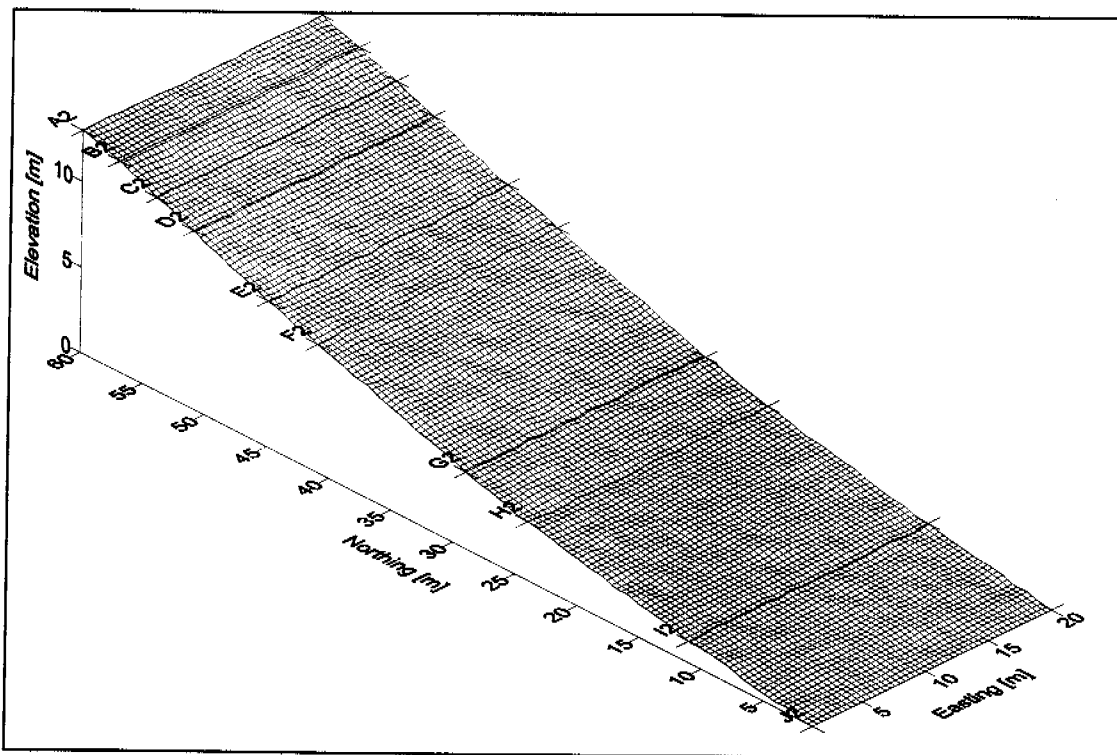


Figure 4.2.1: Initial surface incorporating flat sloping upper section, representative of the catchment outlet point. Feed points for runoff module were set at the extreme left end at the approximate location of the outlet point.

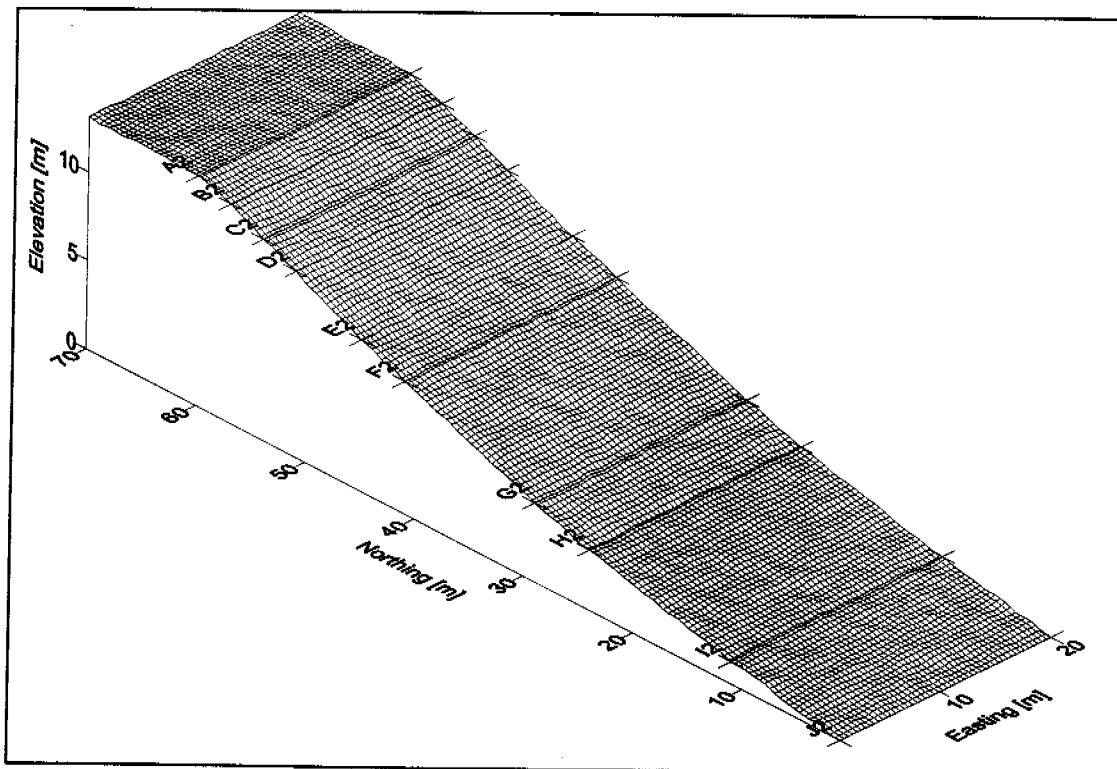


Figure 4.2.2: The other alternative for the initial landform profile did not represent the upper section of the catchment outlet. The inlet feed points of the batter slope appear along the top of the study area.



Monitoring Gully Formation

There are a large number of parameters in SIBERIA, and these control the modes of operation of the model, actual physical parameters, and numerical behaviour of the model. Willgoose, 1992 notes that there are 20 integer parameters and 50 real parameters, with many not presently used but present to allow continuing development of the model. Other input requirements are user defined modules representing the runoff module, and armouring module. Figure 4.2.4 below illustrates the typical format used to present the parameters values adopted for each of the modelling scenarios detailed in Section 4.3.

Many parameters were not altered during the modelling process. Parameters such as β_3 , and the initial surface profiles were altered after each storm event, and other user defined modules were incorporated into investigation of different modelling scenarios. The definition of each of these parameters, illustrating default values if they are not

SIBERIA	8.01								
60	10	20	60	0	0				
5	1	0	1	0	2				
0	0	1	0	0	0				
0	0								
0.000000	1.000000	0.000000	0.000000	1.000000	0.000000				
1.000000	0.000000	1.000000	0.100000	0.000000	0.000000				
0.000000	0.000000	0.000000	0.000000	0.005000	1.680000				
1.000000	1.000000	0.002720	0.112000	0.300000	1.000000				
2.100000	1.930000	0.010000	2.500000	1.000000	0.000000				
10.000000	0.400000	0.100000	2.000000	0.000000	0.000000				
0.000000	1.000000	1.000000	1.000000	0.000000	0.000000				
0.000000	0.000000	0.000000	0.000000	0.000000	0.000000				
0.000000	0.000000	0.000000	0.000000	0.000000	0.000000				
0.000000	0.000000	0.000000	0.000000	0.000000	0.000000				

Integer Parameters

Real Parameters

f.dat

User Defined Modules

Fixed Elevation Points

Random Multiplier Field

Elevation

Drainage Direction

4
8 2
9 2
10 2
11 2
.0000E+00 1.0000 0.0010 0.1414251E+00 0 5 0.0000E+00 0.0000E+00

Figure 4.2.4: Parameters allocated for each of the modelling scenarios are illustrated below using this format. It is noted that parameter value used during each of these scenarios did not alter significantly during the modelling process.



Monitoring Gully Formation

presented below, appears in Willgoose, 1992.

RunT: (#1)

Total time length for duration, set to be 60 minutes, as timestep calibrated to 1 minute periods.

OutT: (#2)

Statistics output duration, set to be 10. This produces a statistical summary of the iteration process, at every 10 timesteps, in this case 10 minutes.

Kx, Ky : (#3 and #4)

Grid coordinates are 20m by 60m, with grid size effectively 1m^2 .

ModeS: (#7)

The mode of solution of the sediment transport equation using explicit or analytic solids. For all cases this was set to be 5.

ModeRn: (#10)

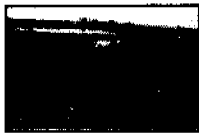
Enabled random perturbations instigated in the initial surface landforms *.rst2 files to be read. For all cases this was enabled, as different surface profiles were used. The multiplier factor is illustrated in Figure 4.2.4 above, with default value of 1.

UserRO: (#12)

This module is activated by UserRO, where the integer parameter refers to either 'f.dat' or 'fwide.dat' representing the two alternative water source entry points. This routine is illustrated in Figure 4.2.5 below, and involves coordinates of the inlet points and amount of area (number of nodes) contributing to each of the points. It was highlighted that the total area was 7200m^2 , with each node equivalent to 3600 nodes for the narrow feed point, and 1800 nodes for wide inlet point. Inlet points incorporating the upper section of the gully catchment into the initial surface were between (8,70) and (11,70) respectively.

UserFT: (#11)

This module is similar to UserRO, with user defined sediment transport rate incorporating the rudimentary armouring component into the model, Figure 4.2.6.



Monitoring Gully Formation

```
SIBERIA RUNOFF
1ST LINE
2ND LINE      ← Narrow Inlet Standard
3RD LINE      Profile: 20 by 60.
2
9 60 3600 1
10 60 3600 1

SIBERIA RUNOFF
1ST LINE
2ND LINE
3RD LINE      ← Wide Inlet with Extended
4             Profile: 20 by 70.
8 70 1800 1
9 70 1800 1
10 70 1800 1
11 70 1800 1
```

Figure 4.2.5: The used defined runoff module replicates the gully catchment behind the 2 or 4 inlet points at the top of the batter slope. Filename 'f.dat' or 'fwide.dat', appears in Figure 4.2.4, with total contributing area of 7200 m² (equivalent to nodes) representing an inflow of 7200/4 or 7200/2 for each inlet point.

The spatially constant mode was adopted for all cases except when considering armouring component. Inclusion of the depth erodibility relationship involved setting this mode to 1 from default value of 0 (Section 4.4).

The exponential relationship between erodibility (measured as function of mean grain size) and depth used to derive these coefficients, are used to multiply the calculated depth of erosion within the SIBERIA model before evaluating new elevations.

This relationship effectively reduces erosion with depth, however cannot distinguish at this stage between previously eroded material, or unsullied hillslope.

```
1ST LINE
2ND LINE
3RD LINE      ← Depth Coefficient, C ~ 15,
15.0 1.0      and exponent, m ~ 1.
```

Figure 4.2.6: The user defined erosion module involved setting the integer parameter, UserFT from 0 to 1. The implementation of this module involves two coefficients used in an exponential relationship between erodibility and depth.

The remainder of the modules (integer parameters) were not considered or altered during the modelling process, and were set at default values.

The next group of parameters were the real parameters, which allocated numerical values to each of the coefficients, and exponents used in the sediment transport model, discharge-area relationship.



Monitoring Gully Formation

$1/a_i$: (#27)

The channel initiation threshold was set to be 0, such that a channel would not be formed, and the channelisation (different sediment transport equation) not implemented.

The differential erosion rate of the hillslope and channel was not considered in this study, with channelisation module disabled for all model simulations.

m_3 : (#37)

The discharge-area relationship is assumed to be linear, with m_3 taken to be unity.

β_3 : (#38)

The coefficient in the discharge-area relationship, equation 4.1.10, was determined from the gully catchment outlet points at the top of the batter slope. For each of the storm events the following values were adopted, with consequent storm events run in series.

Table 4.2.1: The coefficient in the discharge-area relationship was adapted to represent the outlet of the gully catchment. Duration of each storm event were averaged over 1 hour, whilst the event on 230197 was considered to maintain intensity for entire hour, although event only lasted 25 minutes.

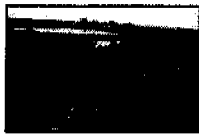
Event	Average Discharge (m ³ /hr)	β_3
261296	19.59	2.72×10^{-3}
010197	14.33	1.99×10^{-3}
230197	22.75	3.16×10^{-3}

β_1 : (#39)

The coefficient in the sediment transport equation, equation 4.1.9, was adapted using the bulk density determined on-site to be 1.93gcm^{-3} in equation 4.1.12 above. The value adopted was 0.112 and represented the erodibility of the surface material within the SIBERIA program.

m_1 : (#40)

The exponent on discharge in sediment transport equation was evaluated using equation 4.1.9 from fitted erosion studies at value of 1.68.



Monitoring Gully Formation

n_t: (#41)

The exponent on slope in sediment transport equation is discussed in Section 4.1 above, where a value of 0.69 from equation 4.1.9, or the default value of 2.1 being adopted during the initial modelling period. Sensitivity analysis of the effect of this parameter will be conducted initially, and using the final simulation scenario comparing all of the implemented modules.

time: (#43)

Iteration time step was set at 0.05 for the majority of simulations conducted, for numerical stability, resulting in computational time lengths of about 25 minutes per storm event.

The modelling process involved the approximation of an initial surface, with the addition of random noise to elevations used to simulate the relatively uniform topography, whilst representing the nature of the waste rock material. This is illustrated in Figure 4.2.1, and Figure 4.2.2 above.



4.3 Simulations

The implementation of parameters into the SIBERIA model was varied to test the capability of the model to predict size and shape, as well as characteristic of the behaviour of gullies formed. By comparison between predictions from SIBERIA to the actual formation, the impact of different mechanisms, and the determination of important parameters could be conducted.

A number of simulation scenarios were investigated to assess the various aspects of erosional mechanisms. These simulations include firstly a standard case, by which the remained of simulations are compared, incorporation of the gully catchment, increase in the width of the inlet points, introduction of random erodibility in the waste rock material, as well as the assessment of the rudimentary armouring model and determination of sensitive parameters such as the slope exponent n_1 .

Standard

The initial surface created to represent the batter slope marks the first stage in assessing model behaviour and predictions. The relationships outlined above, are used to derive the parameters required for the SIBERIA model, with this case specifically representing a standard by which all the other simulation scenarios are compared.

This surface effectively represents a uniform, homogenous material, with fixed outlet point, and the armouring module disabled.

The gully catchment was represented by the user defined runoff module described in Figure 4.2.5 above, with 'f.dat' being adopted for the study site (Figure 4.2.2), and 'fup.dat' being adopted for the extended study site incorporating the gully catchment (Figure 4.2.1).

Increased Width

The impact of increasing the at the top of batter slope was investigated. The total contributing area, representative of the gully catchment was 7200m^2 (equation 4.1.10), with standard runoff module 'f.dat' in Figure 4.2.5 replaced with 'fwide.dat'.



Monitoring Gully Formation

The 'fwide.dat' runoff module distributed the surface flow from the catchment across 4 nodes, instead of 2 nodes for the narrow feed case. Although the total flow is not altered and the erodibility of the surface material remains unchanged, the wide entry point may reduce the extensive erosion observed in preliminary modelling results, with the head of the gully eroding to depths in the order of 2 to 3m. The discretisation of the batter slope into a 20 by 60, 1m² grid, may not be conducive for the development of more than one gully, as the flow-path from the 4 inlet points may concentrate to one within only a few nodal steps.

From Table 4.2.1, the discharge-area coefficient β_3 attempts to characterise the nature of the three storm events. This involved replacing the initial surface for the second storm event with the last generated surface from the first event. i.e. gully-0000060.rst2 is used as the initial surface file for the 010197 storm.

Upper Section

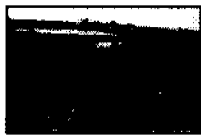
The extension of the batter slope study area to incorporate the 10m of the gully catchment is described in detail above. The expected equilibrium profile for the overall landscape (Figure 1.1.4) tends to indicate that incision of the high wall will extend back into the cap. By extending the profile of the slope to include this additional 10m, with a slope of 2%, this aspect will be investigated.

Alteration of input parameters was restricted to a revised initial surface profile only. However, due to the extensive erosion expected at the head of the gully (at the inlet points), it is possible that a similar landscape to the standard case will be generated, except that erosion will extend a further 10m.

This may indicate the runoff, drainage density being the dominant erosion factor, rather than the slope transition between the catchment and the batter site. Considerable amounts of water are applied to these upper sections, with the development of a gully on these slopes more closely resembling theoretical behaviour.

Random Erodibility

The erodibility of the rock material of the NWRD was approximated from calibration of the sediment transport equation parameter β_1 from previous studies and modified



Monitoring Gully Formation

using the bulk density (Section 4.1) to represent the erosional characteristic of the batter slope.

The entire landform represents a diverse range of erodibility, a function of mean particle diameter, d_{50} and geophysical weathering characteristics of the material, by introducing a random multiplier to the β_1 parameter, a more dynamic and realistic behaviour may be achieved.

As described above, the operational parameter 'ModeRn' has been already implemented, with the coefficient multiplier involving the alteration of the initial surface profile file from a default value of 1.0. By generating a random distribution between 0 and 5, with a mean of 1.0, the overall characteristics of the site is unchanged, but variation in the erodibility of the material has been introduced.

This aspect incorporates a more realistic impression of the gully development observed on site, with pathway dictated primarily by the variability of the material, or the dominant runoff drainage density relationship.

The sediment transport relationship has 2 major components, one of which depends on discharge (relative directly to the amount of water feeding each node) and the other is dependent on slope.

As outlined above, it is expected that for the standard homogenous case the pathway of the gully adopted will not be significantly affected by the random perturbations given to the initial surface elevations. The pathway will more than likely be straight down the slope, depositing material at the change of curvature point between Row G to Row I, before the dominant erosional process changes to be a function of material erodibility. This will be reflected in the comparison between this simulation scenario in the standard batter profile and extended profile cases.

By incorporating random erodibility into this relationship, the pathway adopted will vary, and move across the slope for the standard profile, however once the gully is instigated it is considered unlikely that a new path could be commenced as the drainage density of each node within the gully increases dramatically once it has formed (Figure 4.3.1).

Monitoring Gully Formation

Another interesting consideration may be the effect of deposition on the gully pathway adopted. Although the batter slope was relatively uniform, and the development observed on site was dominated by the initial erodibility of material in the upper sections, deposited sections tended to influence the pathway adopted below the point of curvature change. By changing the behaviour of the simulated gully from a straight line (standard case) to a more realistic random motion, less material was concentrated at these points.

The drainage direction of the nodes surrounding each node point is illustrated in Figure 4.3.1 below, with this indicating which of the 8 adjacent nodes the current node drains into. Once the gully is established, this pathway seems to be determined by dominant drainage direction until the slope component driving the sediment transport equation is reduced in the lower sections.

Once the gully was initiated, the drainage density relationship remains dominant until slope component becomes considerable, observed in transition in lower sections with accumulated material.

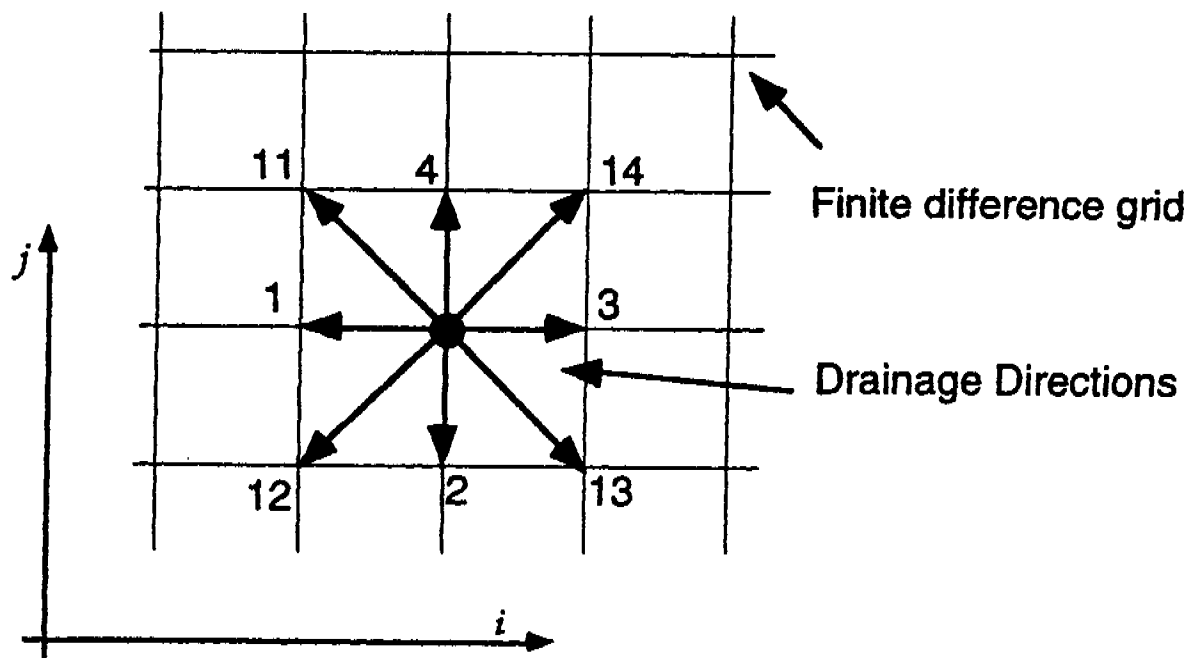


Figure 4.3.2: Drainage direction of the finite difference grid indicates which of the 8 adjacent nodes each node drains into (Willgoose, 1992 Figure 1). The drainage density of the gully once it has been initiated will tend to dictate only one pathway to be adopted. This may be overcome by increasing the grid discretisation of the profile, as well as widening the inlet point or introducing erodibility with depth relationship as described below.

Differential Erodibility with Depth

Armouring was considered to represent the decrease in erodibility with depth of erosion. Conceptually this model is an exponential relationship, a function of mean particle diameter, and represents the risk of erosion of the material at various depths into the batter slope.

The mean particle diameter, d_{50} was used as the measure of the change in the surface characteristic and was incorporated into the following relationship (Figure 4.3.2):

$$\text{erodibility} = \text{initial erodibility} * \frac{1}{C * \text{depth}^{\text{exponent}} + 1} \quad (4.3.1)$$

where

depth = depth of erosion from commencement

exponent = exponent on the depth of erosion (set initially to 1)

C = coefficient reflects the initial and final mean grain size over a given depth eroded.

The implementation of this erosion module involved considerations such as the crude measure of the change in erodibility, no distinction between previous eroded material, and unsullied hillslopes, and conservative estimates of relationship parameters.

Conservative estimate of the erodibility of surface material is based on relationship: $1/d^{3/2}$, with d_{50} initial at 2mm = $1/2^{3/2}$ leading to erodibility $\sim 1/3$, whilst d_{50} final at 20mm at a depth of 2m = $1/20^{3/2} \sim 1/90$ represents a reduction in erodibility by a factor of 1/30.

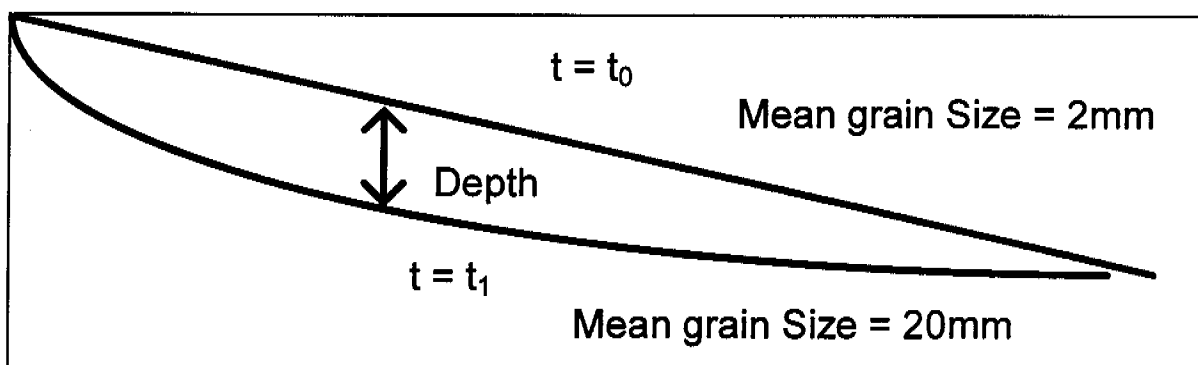


Figure 4.3.2: The effect of the change in d_{50} of surface material with depth represents the next component of the investigation. Although initial and final grain sizes were set to 2mm and 20mm respectively, they represent a conservative approximation.

Monitoring Gully Formation

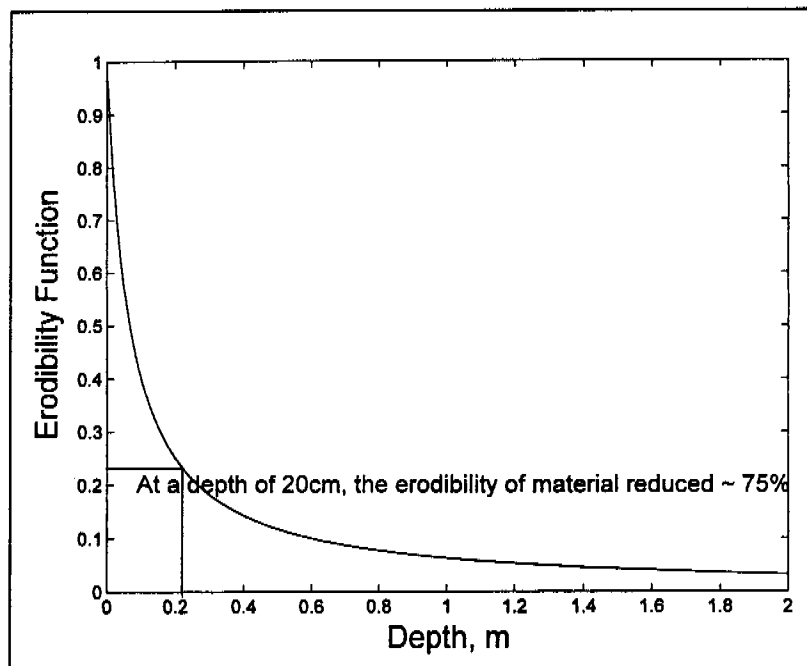


Figure 4.3.3: The change in erodibility function term ($1/\text{coefficient} \times \text{depth}^{\text{exponent}} + 1$) represents an exponential relationship between the depth and erodibility of the surface, determined from the coefficient (relating mean grain size, d_{50}) allocated ($C \sim 2$). i.e. at a depth of 20cm, the erodibility function is ~ 0.25 equating a reduction in erosion of 75%.

The erodibility of the surface, as the gully forms rapidly decreases with parameter values of $C \sim 15$, and $C \sim 2$ being considered. Although this is a relatively crude relationship applied to an extremely complex process, it represents a reasonable estimate or summary of the interaction observed on site, with a dramatic decrease in erodibility of the 'channel bed' once the fine material (d_{50} small) was removed leaving larger boulders exposed, Figure 4.3.4.

Incision in the upper section of the batter slope ranged between 40 and 80cm, with armouring maximised on the very upper sections where water velocity was minimal. Once this characteristic was in place, little further movement or activity occurred.

Further approximations in the erodibility-depth function included the evaluation of sections where deposition had occurred. These sections composed of the fine material from the upper sections represented a highly erodible surface (observed) and implementation of differential erosion between original hillslope and these components represent future research (pers. com. Willgoose, 97).

Numerous modelling scenarios were investigated during the experimental stage, with the impact of various components of the model assessed by progressive inclusion to



Monitoring Gully Formation

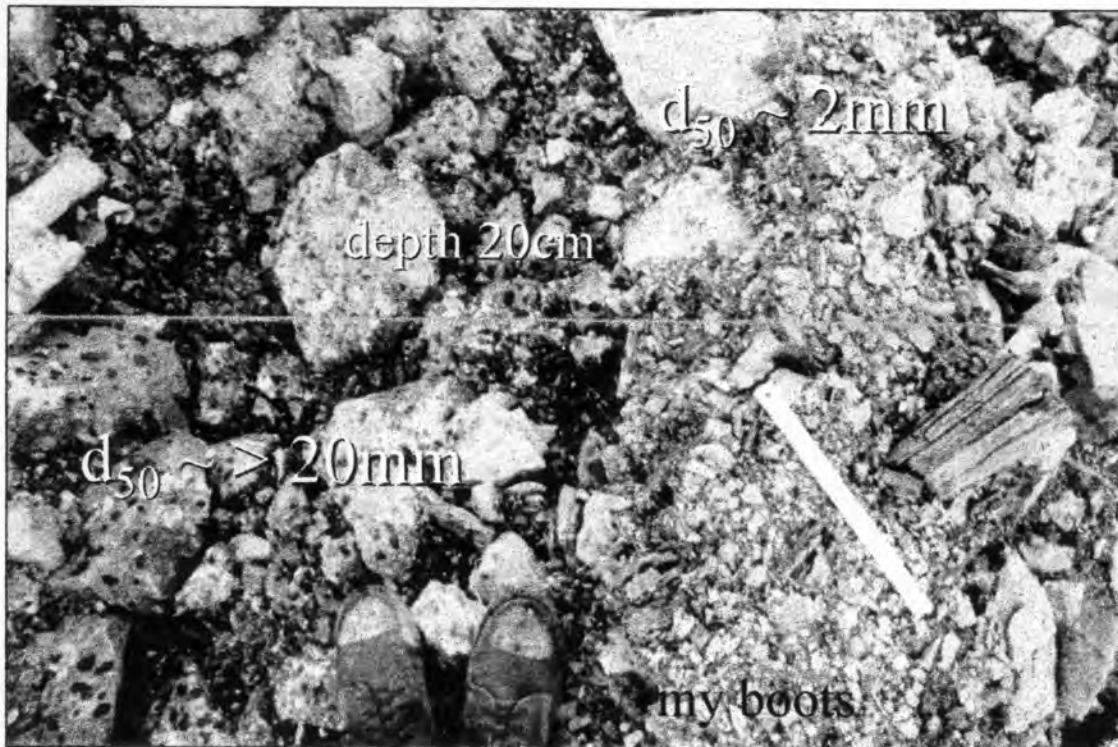


Figure 4.3.4: The difference observed in mean particle diameter, d_{50} between the active (gully) and inactive (hillslope) components of the surface was significant. The fine material observed was quickly eroded leaving large rock fragments exposed which significantly resisted further movement.

an eventual best possible representation. By comparison between the nature of the gully and predictions from the SIBERIA model, an understanding of the soil erosion mechanisms in operation on site can be developed.

Determination of impact of additional components such as heterogeneity, and armouring evolves the prediction to resemble the nature of the actual landform, as closely as possible. Feed back indicated areas of sensitivity, such as the exponent on the slope component in the sediment transport equation, and allowed the evaluation of gullies likely to be formed on the steep batter slopes.

From these regimes, the impact of each component can be assessed, with the final scenario representing the combination of all the erosional mechanisms.

- assessment of the behaviour of the exponent on the slope component n_1 with both the standard and extended profile batter sites.



Figure 4.3.5: Two case scenarios were run; standard refers to the assumption of homogenous material, with armouring module disable, and the inclusion of extended profile in the second file.

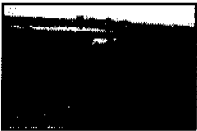
SIBERIA 8.01
 60 10 20 70 0 0
 5 1 0 1 0 2
 0 0 1 0 0 0
 0 0
 0.000000 1.000000 0.000000 0.000000 1.000000
 1.000000 0.000000 1.000000 0.100000 0.000000
 0.000000 0.000000 0.000000 0.000000 0.005000
 1.000000 1.000000 0.002720 0.112000 1.680000
 0.690000 1.930000 0.100000 2.500000 0.300000
 10.000000 0.400000 0.100000 2.000000 1.000000
 0.000000 1.000000 1.000000 1.000000 0.000000
 0.000000 0.000000 0.000000 0.000000 0.000000
 0.000000 0.000000 0.000000 0.000000 0.000000
 0.000000 0.000000 0.000000 0.000000 0.000000
 0.000000 0.000000 0.000000 0.000000 0.000000

Upper Surface with n_1 at 0.69,
 non-armouring, homogenous.

fup.dat \nearrow
 \nwarrow n_1 at 0.69, and upper
 inlet runoff module

4
 8 2
 9 2
 10 2
 11 2
 .0000E+00 1.0000 0.0010 0.1771374E+00 0 5 0.0000E+00 0.0000E+00

Figure 4.3.6: These are the parameter files used to generate the standard and extended profile batters, with exponent on the slope component n_1 changed from 2.1 to 0.69, equation 4.1.9.



Monitoring Gully Formation

- assessment of increasing the inlet width from 2 node points for narrow case, to 4 inlet points for the wide case.

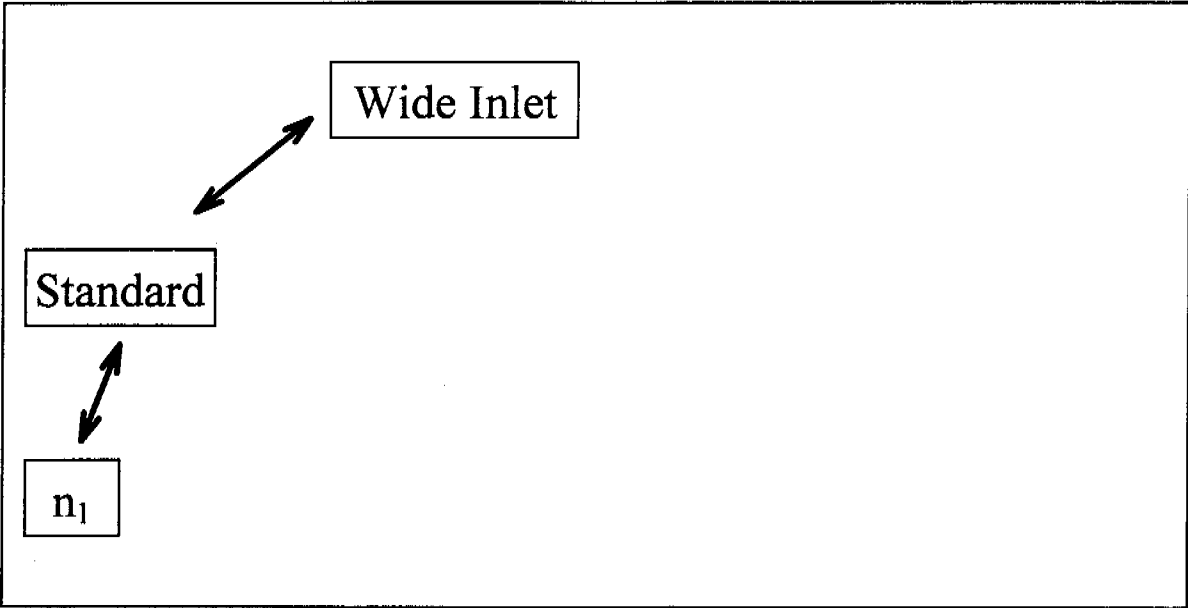


Figure 4.3.7: Parameter files incorporating wide inlet points, and alteration of the user defined runoff module file to describe either the narrow or the wide case.

The parameter files used in these scenario are as follows:

SIBERIA	8.01				
60	10	20	60	0	0
5	1	0	1	0	2
0	0	1	0	0	0
0	0				
0.000000	1.000000	0.000000	0.000000	1.000000	
1.000000	0.000000	1.000000	0.100000	0.000000	
0.000000	0.000000	0.000000	0.000000	0.005000	
1.000000	1.000000	0.002720	0.112000	1.680000	
2.100000	1.930000	0.010000	2.500000	0.300000	
10.000000	0.400000	0.100000	2.000000	1.000000	
0.000000	1.000000	1.000000	1.000000	0.000000	
0.000000	0.000000	0.000000	0.000000	0.000000	
0.000000	0.000000	0.000000	0.000000	0.000000	
0.000000	0.000000	0.000000	0.000000	0.000000	
0.000000	0.000000	0.000000	0.000000	0.000000	

fwide.dat ← wide inlet runoff module

4
8 2
9 2
10 2
11 2
.0000E+00 1.0000 0.0010 0.1150964E+00 0 5 0.0000E+00 0.0000E+00

Figure 4.3.8: The implementation of this simulation involved altering the user defined runoff module to represent a more evenly distributed inlet flow. This file standard profile, with wide inlet point.



Monitoring Gully Formation

- assessment of the alteration of the random field multiplier parameter was used to introduce heterogeneity. Another two scenarios were also used to compare the combined of both the wide inlet feed along with randomised erodibility.

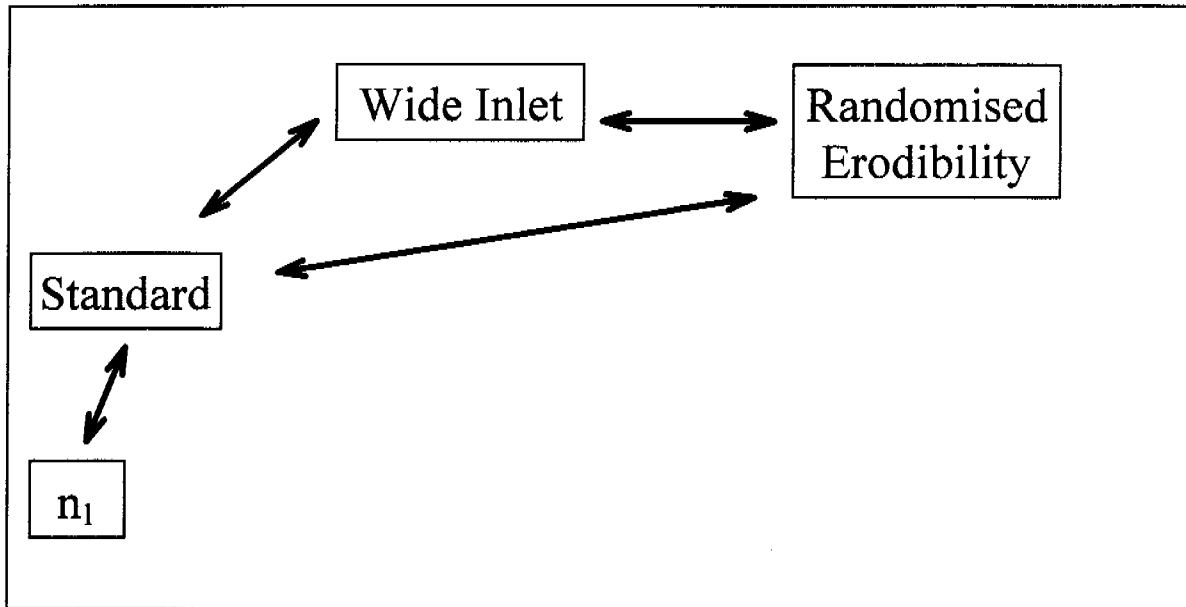


Figure 4.3.9: Methodology flow-paths for the inclusion of wide inlet point, and introduction of randomised erodibility to the batter slope material.

The parameter files used in these scenario are as follows:

SIBERIA					
60	10	20	60	0	0
5	1	0	1	0	2
0	0	1	0	0	0
0	0				
0.000000	1.000000	0.000000	0.000000	1.000000	
1.000000	0.000000	1.000000	0.100000	0.000000	
0.000000	0.000000	0.000000	0.000000	0.005000	
1.000000	1.000000	0.001990	0.112000	1.680000	
2.100000	1.930000	0.010000	2.500000	0.300000	
10.000000	0.400000	0.100000	2.000000	1.000000	
0.000000	1.000000	1.000000	1.000000	0.000000	
0.000000	0.000000	0.000000	0.000000	0.000000	
0.000000	0.000000	0.000000	0.000000	0.000000	
0.000000	0.000000	0.000000	0.000000	0.000000	

f.dat

Second storm event, $\beta_3 = 0.00199$

Change in random field multiplier

4
8 2
9 2
10 2
11 2

.0000E+00 0.1119 0.0010 0.5261294E-01 0 5 0.0000E+00 0.0000E+00

Figure 4.3.10: The implementation of this simulation involved altering integer parameter ModeRn, and adjusting the multiplier coefficients in the initial landscape file, along with increasing inlet width.



Monitoring Gully Formation

- assessment of depth-erodibility relationship, equation 4.3.1 was used to determine the reduction factor that was multiplied by the erosion depth evaluated by SIBERIA before the new elevations for the batter slope catchment were calculated.

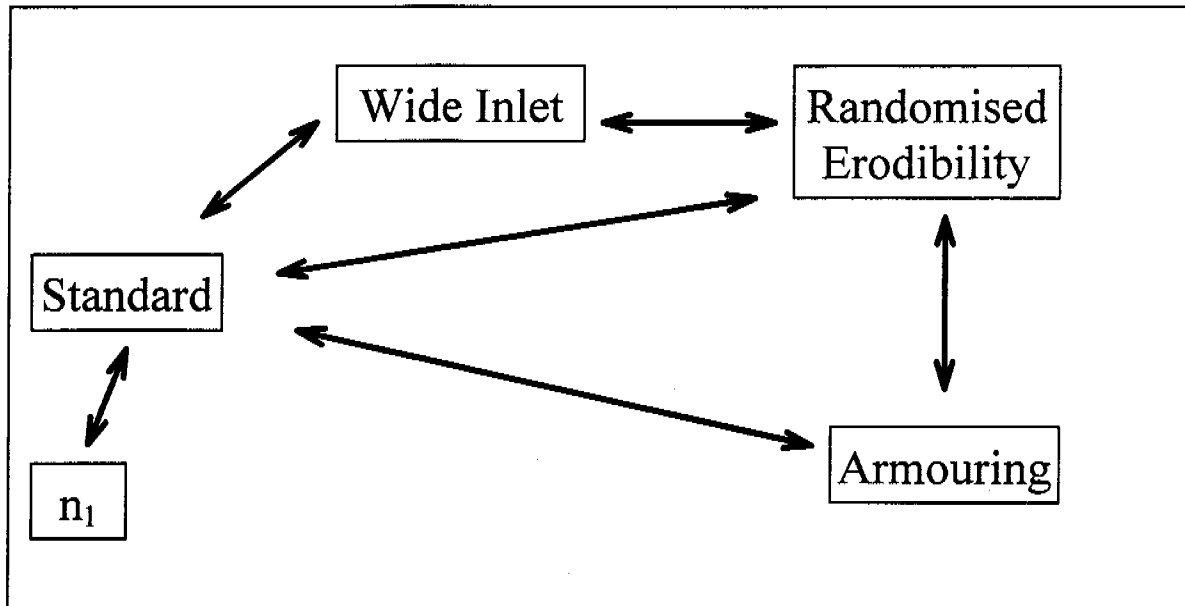


Figure 4.3.11: Methodology flow-paths for these simulations incorporate all of the erosion modules used in this study.

The parameter files used in these scenario are as follows:

SIBERIA 8.01					
60	10	20	70	0	0
5	1	0	1	1	2
0	0	1	0	0	0
0	0				
0.000000	1.000000	0.000000	0.000000	1.000000	
1.000000	0.000000	1.000000	0.100000	0.000000	
0.000000	0.000000	0.000000	0.000000	0.005000	
1.000000	1.000000	0.002720	0.112000	1.680000	
2.100000	1.930000	0.100000	2.500000	0.300000	
10.000000	0.400000	0.100000	2.000000	1.000000	
0.000000	1.000000	1.000000	1.000000	0.000000	
0.000000	0.000000	0.000000	0.000000	0.000000	
0.000000	0.000000	0.000000	0.000000	0.000000	
0.000000	0.000000	0.000000	0.000000	0.000000	

armour.dat
fup.dat

Armouring module

Random multiplier factor not altered between simulations.

4
8 2
9 2
10 2
11 2
.0000E+00 0.0379 0.0010 0.5501554E-01 0 5 0.0000E+00 0.0000E+00

Figure 4.3.12: The implementation of this simulation incorporated the user defined sediment transport rate 'armour.dat'. Incorporates extended profile, randomised erodibility, and differential erode with depth



Monitoring Gully Formation

- investigation into the sensitivity of the exponent on the slope component of the sediment transport equation, n_1 constituted the final step in the modelling analysis.

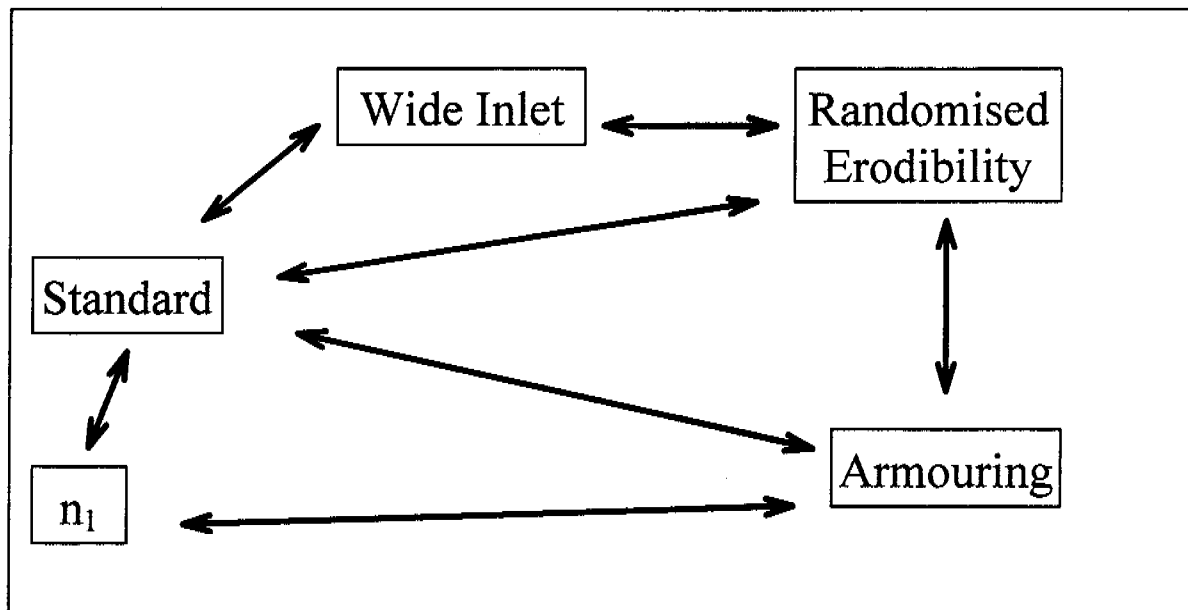


Figure 4.3.12: Methodology flowpaths for these simulations incorporate all of the erosion modules used in this study, combined with a exponent on the slope parameter, $n_1 = 0.69$ in place of 2.1.

The parameter files used in these scenario are as follows:

SIBERIA	8.01					
60	10	20	70	0	0	
5	1	0	1	1	2	
0	0	1	0	0	0	
0	0					
0.000000	1.000000	0.000000	0.000000	0.000000	1.000000	
1.000000	0.000000	1.000000	0.100000	0.000000	0.000000	
0.000000	0.000000	0.000000	0.000000	0.000000	0.005000	
1.000000	1.000000	0.002720	0.112000	1.680000		
2.100000	1.930000	0.100000	2.500000	0.300000		
10.000000	0.400000	0.100000	2.000000	1.000000		
0.000000	1.000000	1.000000	1.000000	0.000000		
0.000000	0.000000	0.000000	0.000000	0.000000		
0.000000	0.000000	0.000000	0.000000	0.000000		
0.000000	0.000000	0.000000	0.000000	0.000000		
0.000000	0.000000	0.000000	0.000000	0.000000		
armour.dat						
fwideup.dat						
4						
8 2						
9 2						
10 2						
11 2						
.0000E+00	0.0379	0.0010	0.5501554E-01	0	5	0.0000E+00 0.0000E+00

Figure 4.3.13: This simulation investigates the sensitivity of the slope exponent n_1 with all of the erosion modules enabled. This file incorporates all of the modelling components of randomised erodibility, armouring, and extended profile with wide inlet field, and $n_1 = 0.69$.



5.0 Assessment of Batter Slope Landforms

The relationships developed in the preceding sections were used to determine the parameters implemented by SIBERIA and to approximate the nature of the batter slope. Initial surface profiles are described, with the effect of each additional component assessed individually, and cumulatively against the standard homogenous scenario.

Evaluation of the impact of these soil mechanisms involves 2 methods: visualisation of areas of erosion and deposition, together with difference between simulation time periods using contour maps. Surface landforms are illustrated below and can be considered representative of predictions from the model produced at a grid size of 0.4m with a numerical mapping package. Interpolation between computational grid points has also led to appearance of erosion 'holes', which were purely an artifact of the modelling simulation process. Contour plots illustrated below are changes that have taken place since the previous time period, and are considered an optimal method for presentation of erosion depths using colour schemes attached to each simulation result.

Initially activity will be concentrated at the top of the batter slope, and over time as the gully develops, the relative sections of erosion and deposition will alter, as the gully extends to the base of the slope.

Erosion is represented as negative numbers on the colour scale, whilst deposition is represented on the positive scale. Areas of deposition can be visualised in the surface landform plots as smoothed areas.

The estimates of differences will highlight aspects observed on site, such as the stabilisation of the gully formation once the gully had initiated, with relatively little activity in the upper sections of the study site.

5.1 Standard

The standard case was run with all of the external erosion modules disabled. This surface is representative of a homogenous material (calibrated to represent the batter slope) and these scenarios were run for equivalent of three hours duration.



Monitoring Gully Formation

At the end of each hour, the average length of storm event, the β_3 parameter was changed to represent the next storm event and the model run again using the last generated surface as the new starting point. Figure 5.1.1 and Figure 5.1.2 give the perspective development of the gully over the monitoring period at 10, 20, 30 and 60 minutes, 1.5, 2, 2.5 and 3 hours respectively. The maximum depth of the gully after 3 hours, at the head of the gully was 5.7m, with deposition between Row G and Row H reaching 0.35m after 1 hour. It is noted that these estimates were obtained using Figure 5.1.3, the contour map of difference between consequent surface profiles.

Significant erosion occurs at the head of the gully, with eroded material from this area deposited at the change of curvature during first hour, whilst deposition between Row H and Row I occurs after 2 and 3 hours. The homogenous nature of the batter slope, combined with the relatively uniform initial surface determine the straight path adopted.

The fixed outlet point is the flume located at the base of the slope, and this can be seen as a boundary condition for the finite difference grid, with transported material surrounding it, at the end of the time period. The material deposited or eroded at each node element within the batter slope catchment influences the drainage direction of nodes, based on altered surface topography. This is apparent as governing equation is directly reliant on the drainage density, as well as the drainage direction and the gully direction changes between 1 and 1.5 hours, as the curvature change is reached, the area of significant deposition.

From Figure 5.1.3 it is apparent that initial activity of the gully on the upper sections of the slope transports considerable amounts of material with the gully developing to between Row F to Row H, within the first storm event. By the end of the first event, the change in direction of the gully is noted in Figure 5.1.3_e and Figure 5.1.4_f. Although maximum erosion occurs at the head of the gully, the section below Row H at 3 hours duration is observed to establish the same nature of erosion as initially observed, with material eroded, deposited in a straight line through Row H and Row I in Figure 5.1.2_d. This is a reflection of the homogenous nature of the material, and indicates that the investigation into the contribution of the slope component in the sediment transport equation is warranted.

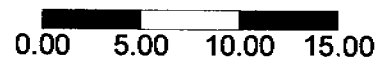
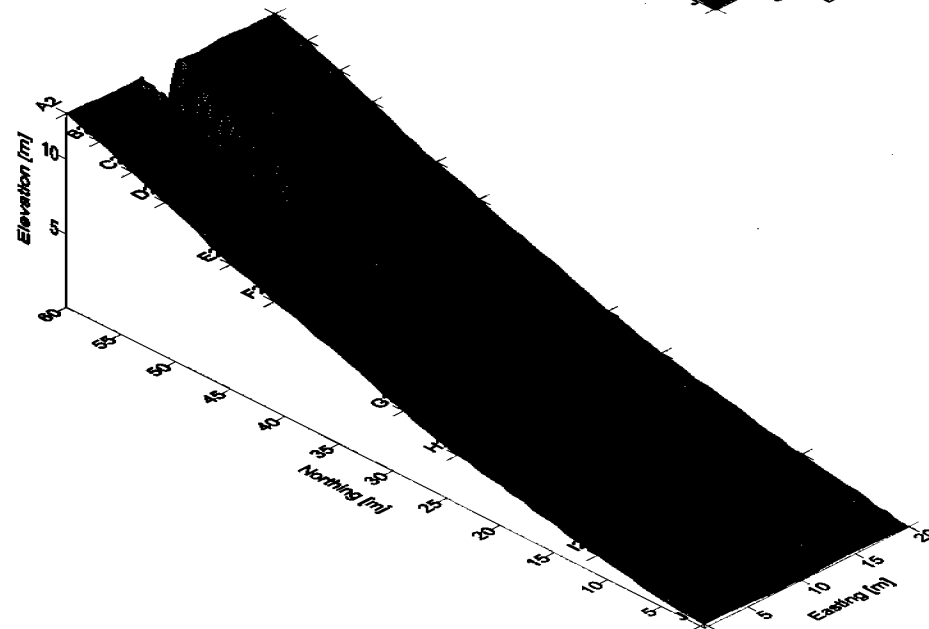
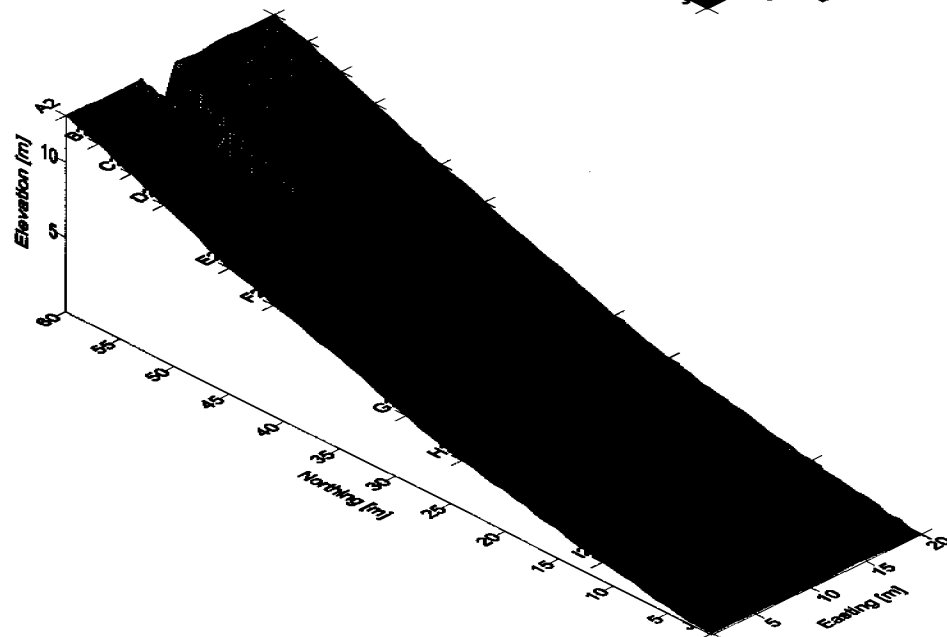
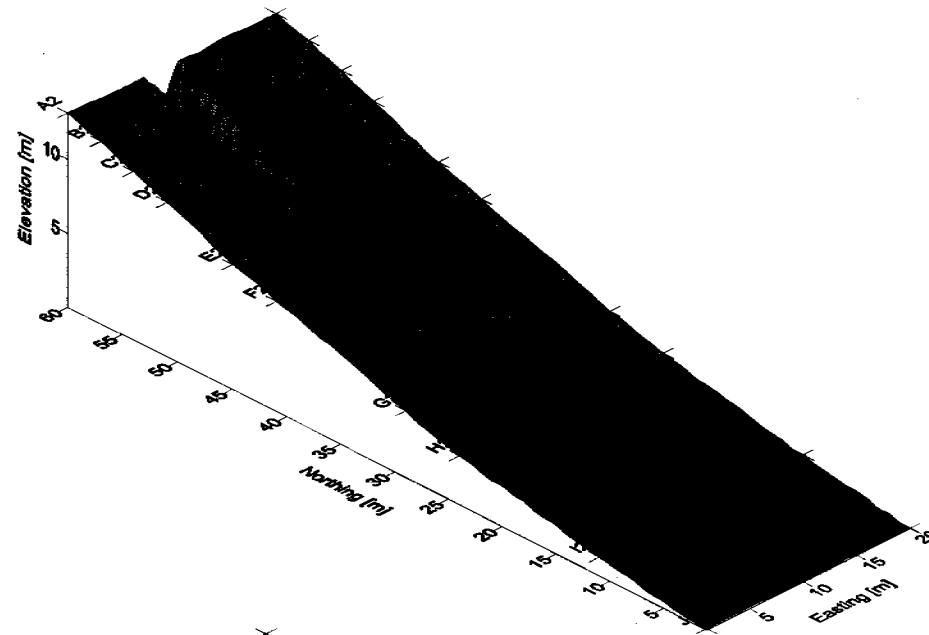
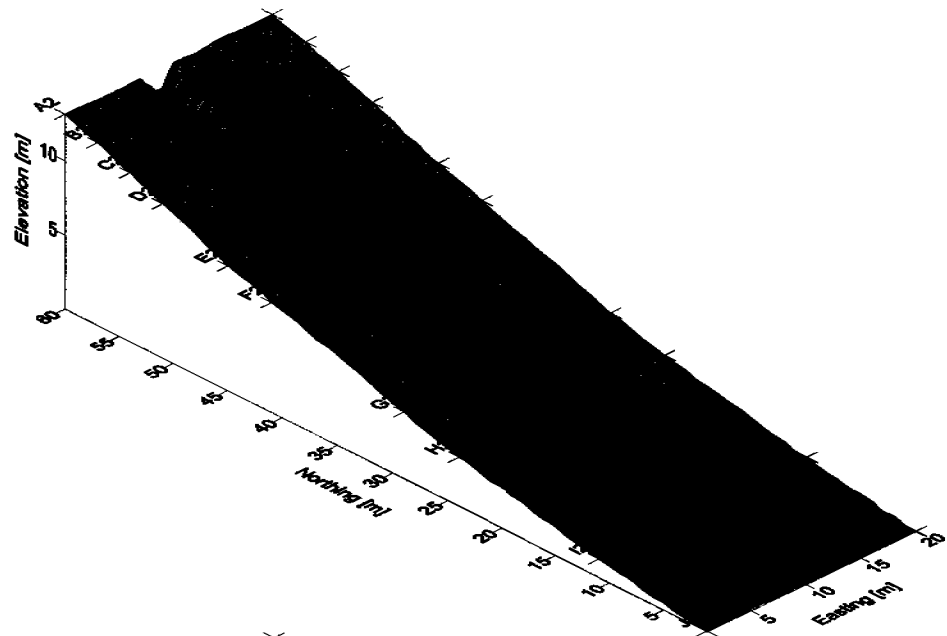


Figure 5.1.1: Simulations for STANDARD scenario at a) 10 minutes, b) 20 minutes, c) 30 minutes, and d) 1 hour.

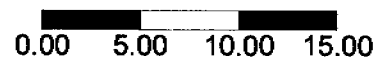
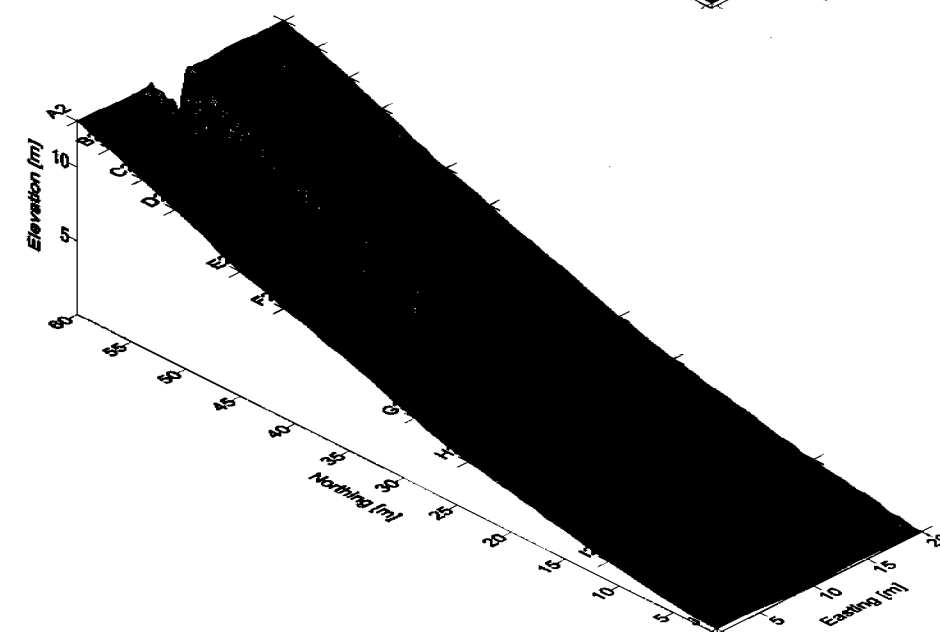
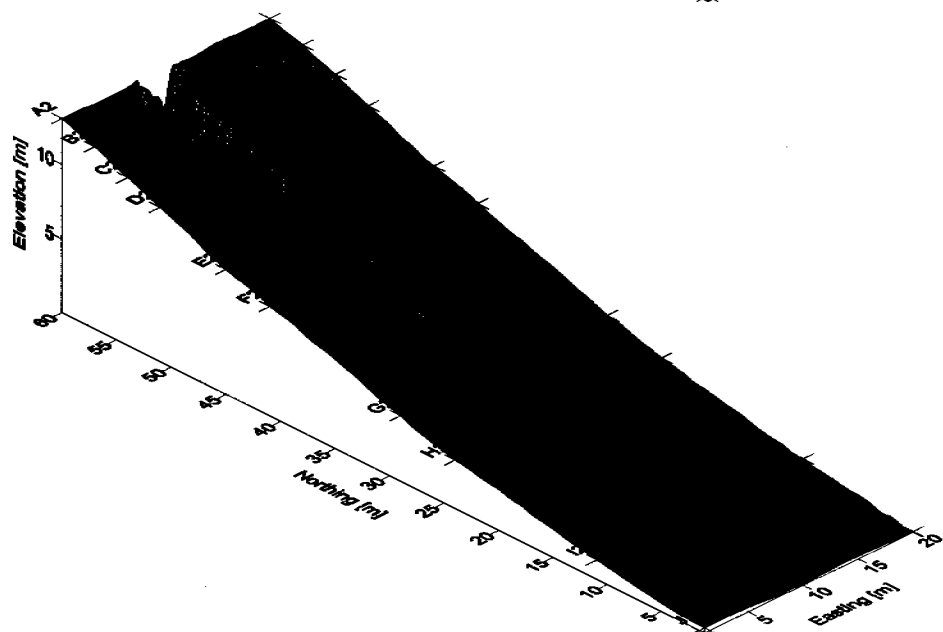
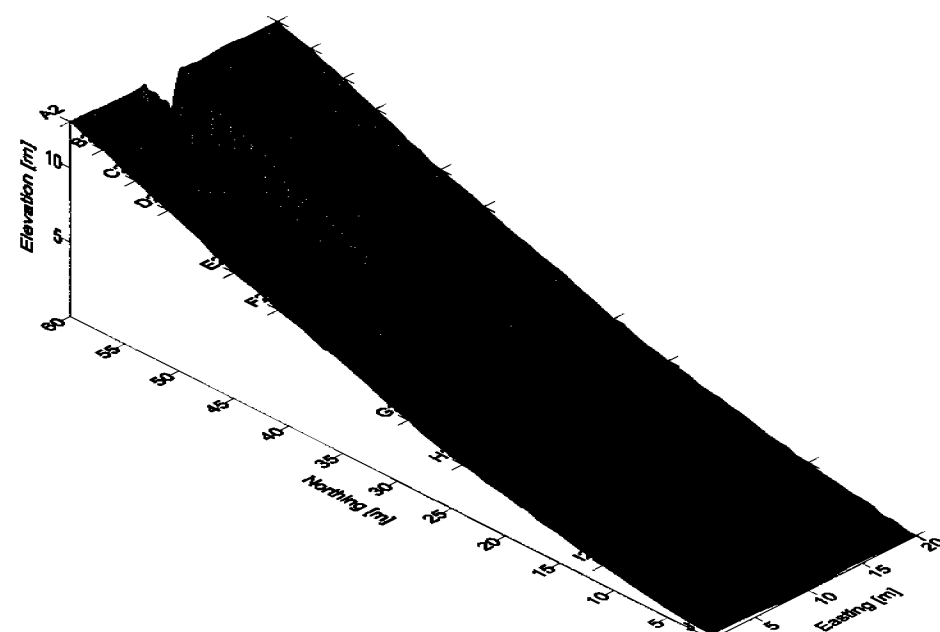
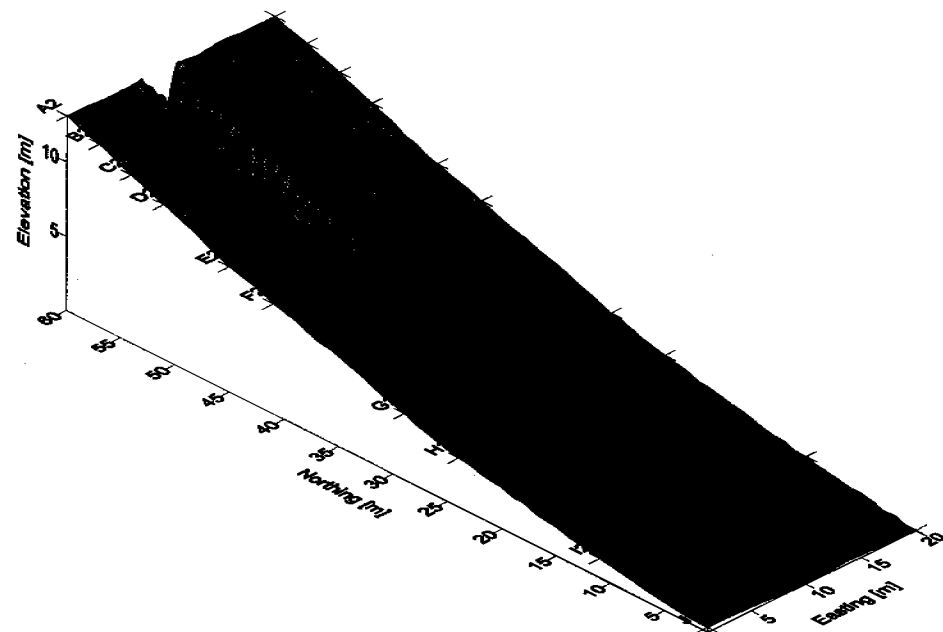


Figure 5.1.2: Simulations for STANDARD scenario at a) 1.5 hours, b) 2 hours this represents the second storm event, and c) 2.5 hours and d) 3 hours representing the final storm event.

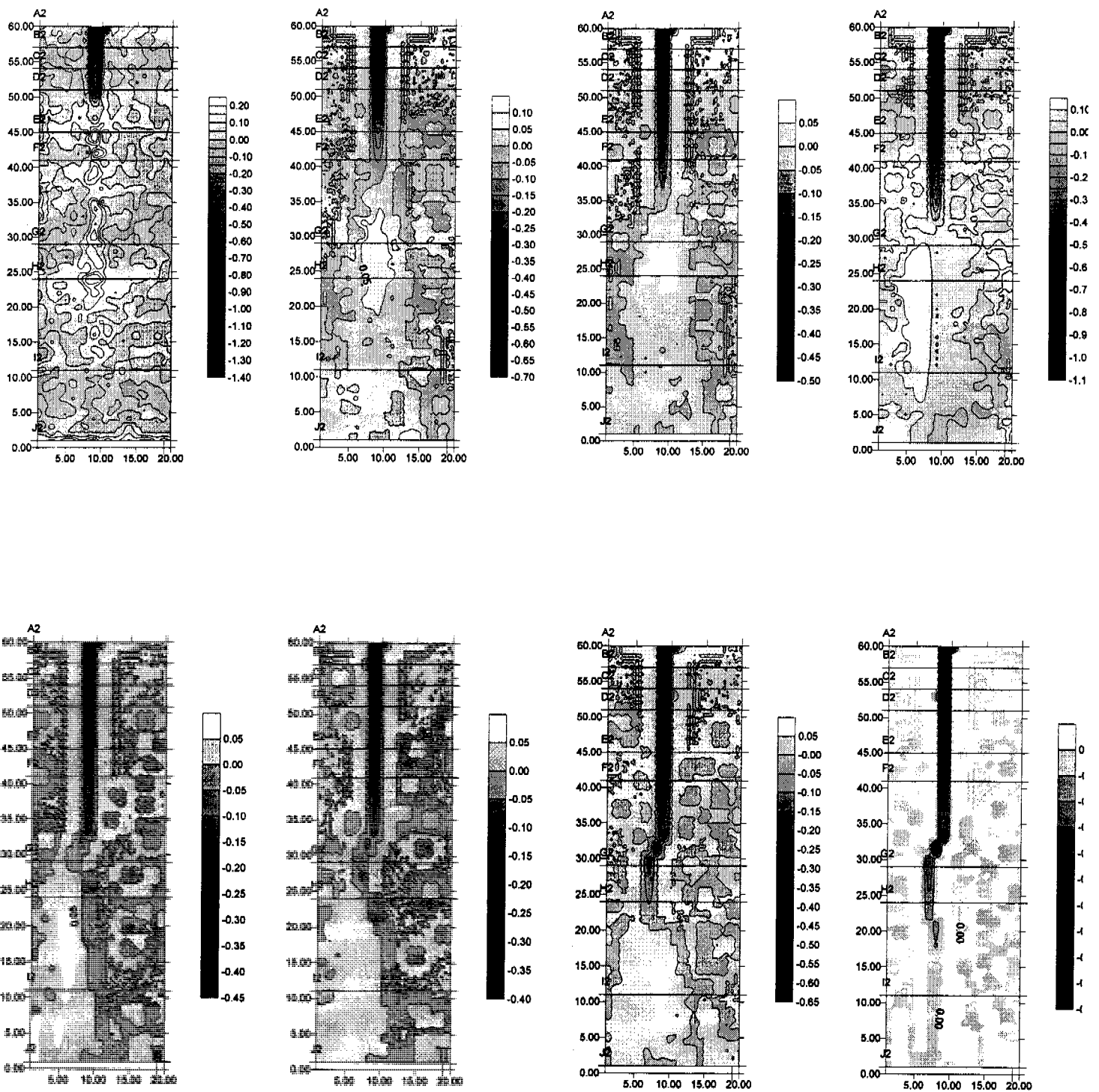


Figure 5.1.3: The initial elevations subtracted from appropriate time period (where erosion is negative, and deposition is positive) such that a) difference between initial surface and prediction at 10 minutes, b) 10 minutes and 20 minutes, c) 20 minutes and 30 minutes, d) 30 minutes and 1 hour. The difference in elevations are also calculated from the remainder of the simulations with e) difference between 1 hours and 1.5 hours, f) 1.5 and 2 hours, g) and 2.5 hours, and h) 2.5 and 3 hours.



Monitoring Gully Formation

The impact of extending the profile of the study area to include a 10m segment of the gully catchment was also investigated. Figure 5.1.4, and Figure 5.1.5 illustrate the simulation surfaces produced by the SIBERIA model for this scenario.

The gully begins to develop after about 30 minutes, with little change occurring at the transition point between the catchment and the batter slope. This point can be identified as Row A between simulations Figure 5.1.4_b, and Figure 5.1.4_c. The surface erodes toward the cap site, with a gully also developing onto the batter slope. Final surfaces were expected to resemble those observed in Figure 5.1.1, and Figure 5.1.2, whereas development process was slower, overall characteristics should be similar.

Once the formation reaches the inlet point of the catchment, the depth of this section increases during the remainder of the 3 hours to a maximum depth of 3 to 4 m. Noting that the depth of the gully at the top of the study area (Row A) reaches 3.4m, approximately half the depth of the previous scenario.

At the change in curvature, the path of the gully changes due to the combination between deposited material, and the contribution of the slope component in the sediment transport equation. Also noted in Figure 5.1.4_c and Figure 5.1.4_d where the path of the gully in the upper section appears to have been dictated by the random perturbations in initial elevations, a function of drainage density due to minimal contribution by slope component.

The behaviour of the gully above this transition point was observed similarly on site, due to the relatively flat nature of the gully catchment (combination of accumulated sediments compacted over time, and the construction of a flat surface initially), and the reservoir at the head of the gully which effectively raised the head of the gully about 30cm.

The initial delay in development observed in these simulations highlights the nature of sediment transport with slope component playing a considerable role. This is highlighted by comparison with previous simulations in Figure 5.1.1 and Figure 5.1.2, where after 60 minutes duration the gully has reached Row E, compared to below Row F, and the final location of the gully was about 5m above that seen for the standard case.

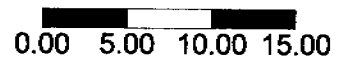
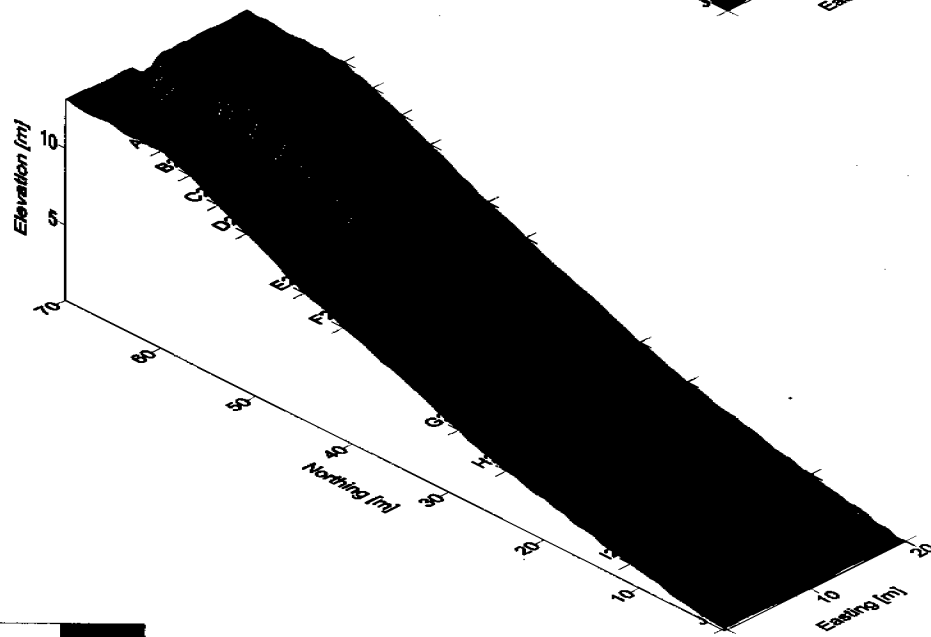
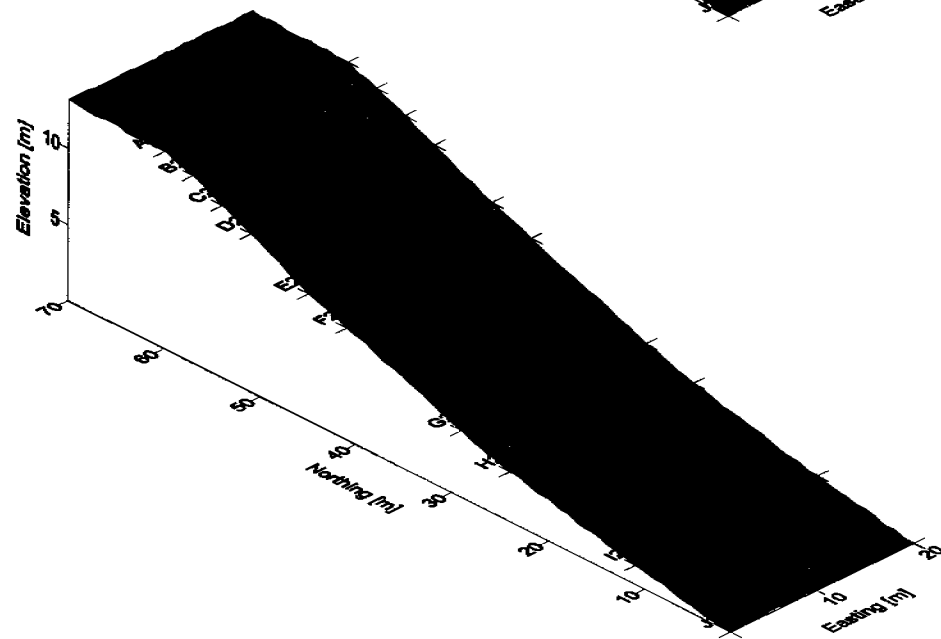
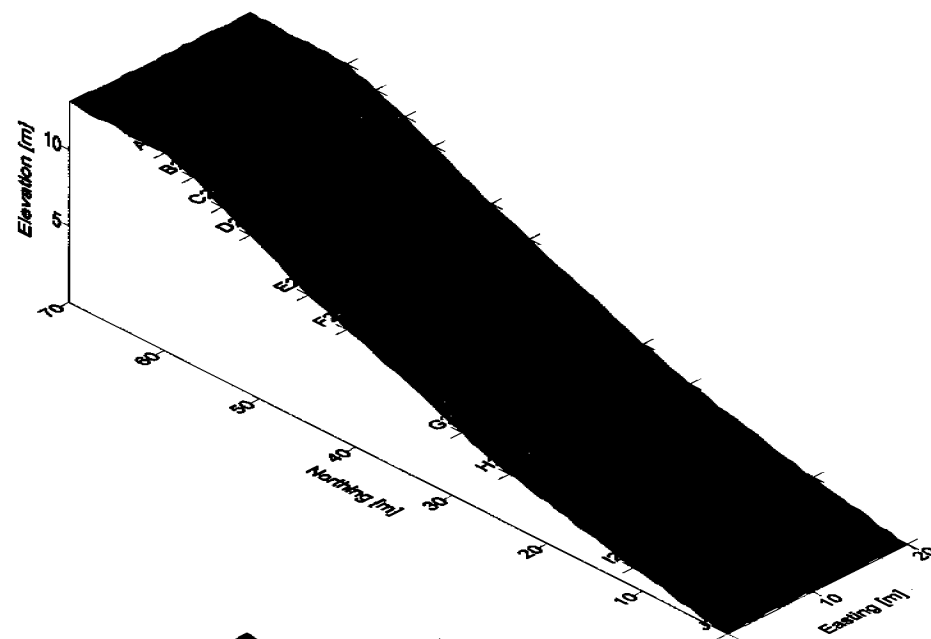
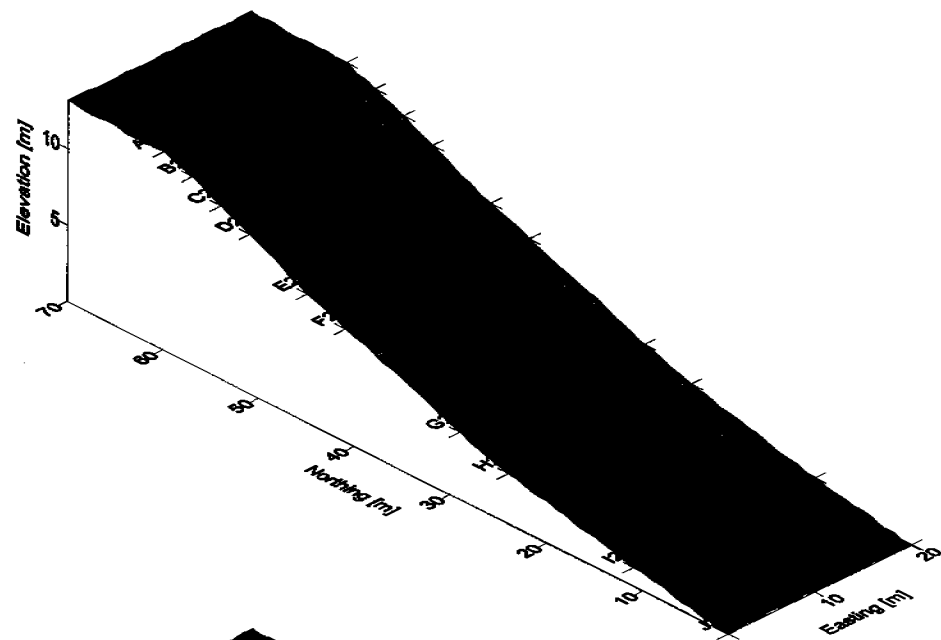
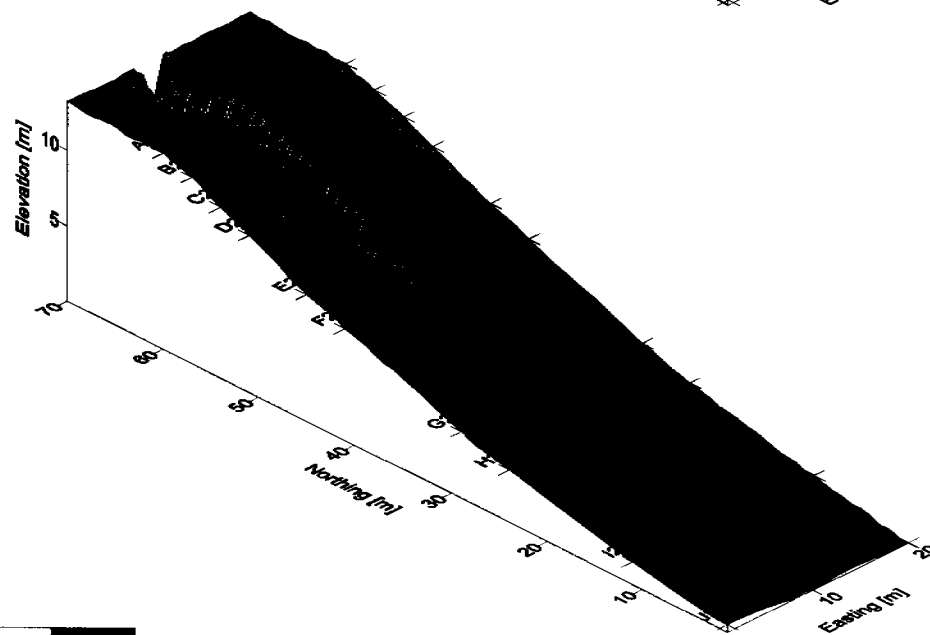
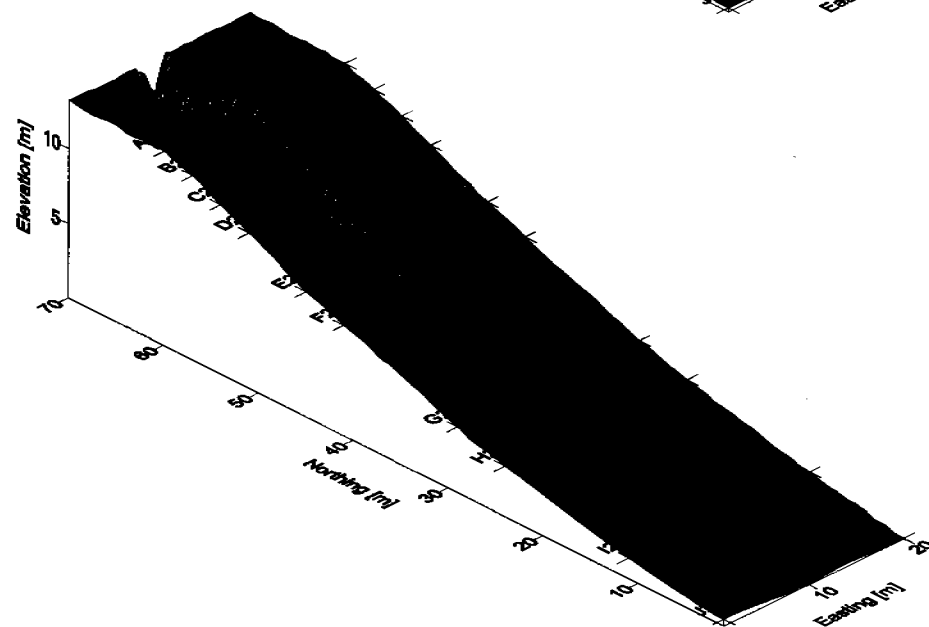
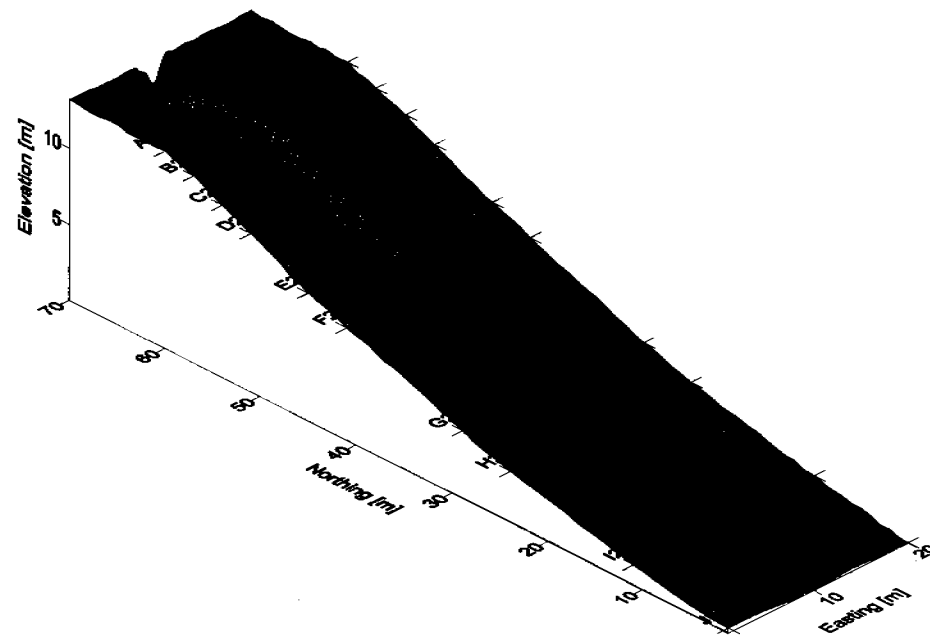
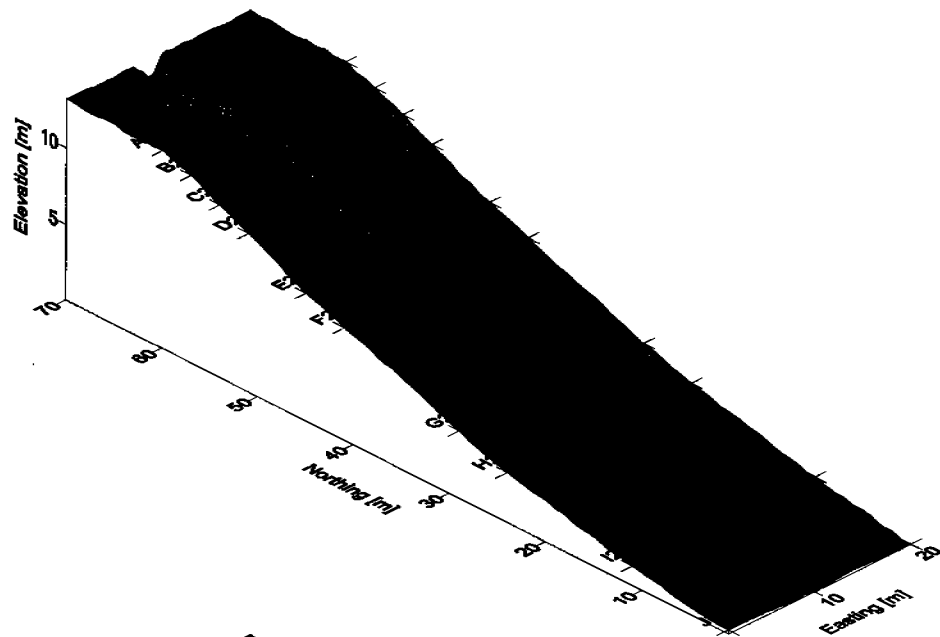


Figure 5.1.4: Simulations for extension of the batter slope to include a portion of the gully catchment, a) 10 minutes, b) 20 minutes, c) 30 minutes, and d) 1 hour.



0.00 5.00 10.00 15.00

Figure 5.1.5: Simulations for extension of the batter slope to include a portion of the gully catchment at a) 1.5 hours, b) 2 hours this represents the second storm event, and c) 2.5 hours and d) 3 hours representing the final storm event.

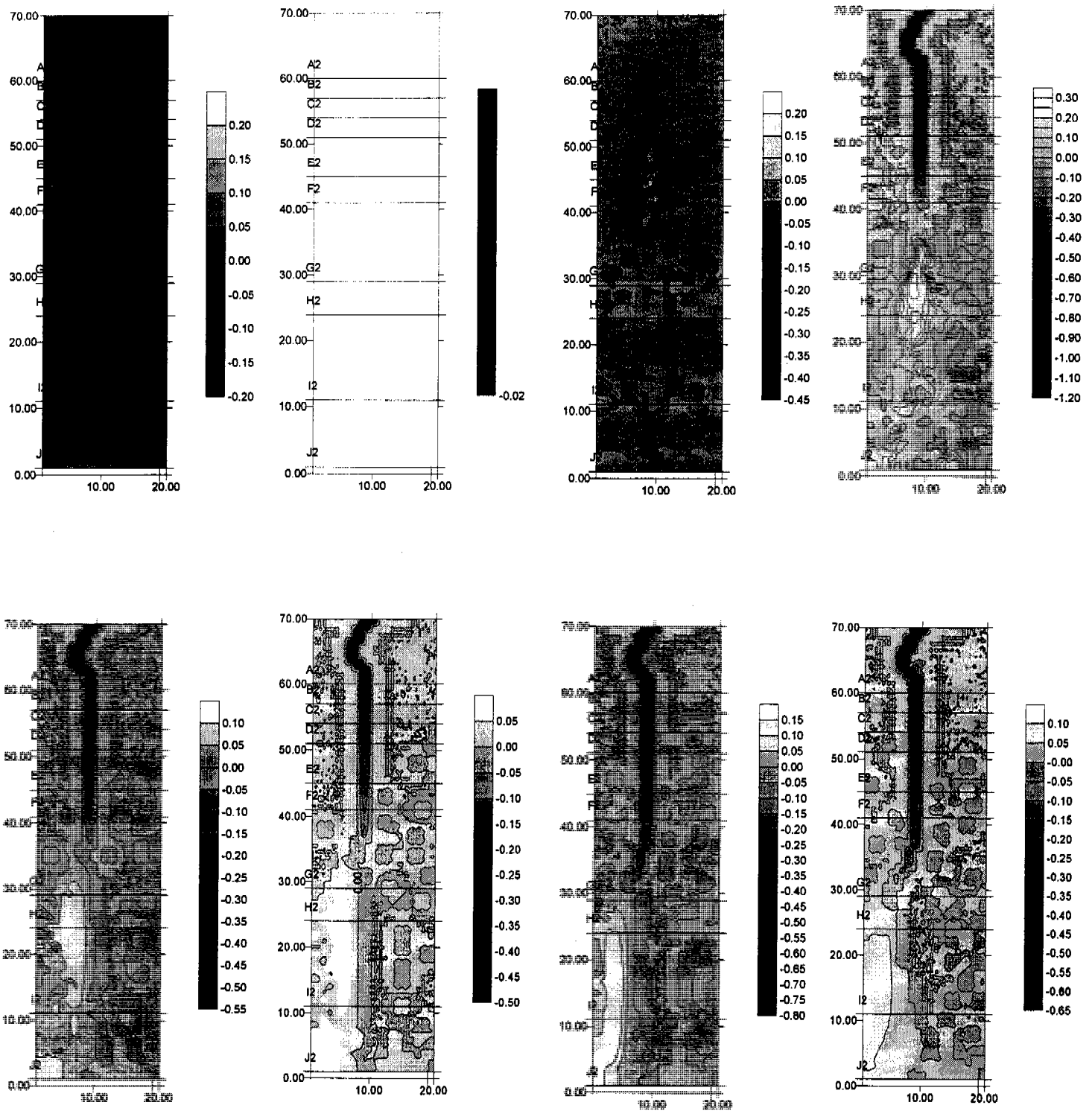


Figure 5.1.6: The initial elevations subtracted from appropriate time period (where erosion is negative, and deposition is positive) such that a) difference between initial surface and prediction at 10 minutes, b) 10 minutes and 20 minutes, c) 20 minutes and 30 minutes, d) 30 minutes and 1 hour. The difference in elevations are also calculated from the remainder of the simulations with e) difference between 1 hours and 1.5 hours, f) 1.5 and 2 hours, g) and 2.5 hours, and h) 2.5 and 3 hours.

5.2 Slope Dependence

The sediment transport equation is dependent on two major components, drainage density and slope dependent component. The exponent on the slope term n_1 has been estimated from field studies to be 0.69 (Section 4.1), however if the sediment transport equation is described according to the Einstein-Brown relationship, a value for n_1 of 2.1 is default.

The impact of the alteration of this exponent was investigated, with n_1 devised from mean particle diameter, equation 4.1.5. The standard batter slope, and the extended profile scenarios were both used to assess the implication of this alteration.

The results of this alteration were expected to be dramatic, with typical slope profiles of the batter site between 20% and 25%, compared to slope profiles of 1.5% to 2% for the gully catchment. The difference in the contribution of the slope component to total sediment transport can be seen with $0.2^{0.69} \sim 0.34$, whilst adopting the same value for the catchment yields $0.2^{2.1} \sim 0.034$, and order of magnitude difference is observed.

Figure 5.2.1, and Figure 5.2.2 illustrates the elevation profiles over the 3 hour duration, with maximum erosion depth at 3 hours reaching 11 to 12m, and erosion at 10 minutes seen to be a level of 4.5m in Figure 5.2.1a.

A similar scenario is observed, with the extension of the batter slope site in Figure 5.2.4, and Figure 5.2.5 respectively. The same behaviour observed in Figure 5.1.4, and Figure 5.1.5 can be seen in this case, where development of the gully is delayed with little activity initially. This can be accounted specifically by consideration of the slope of the catchment, where at 2% slope n_1 at 0.69 yields 0.067, whilst at 2.1 yields 0.00027.

When the gully reaches the inlet point, the excavation of the transition point is considerably greater. Figure 5.2.3, and Figure 5.2.6 illustrate the difference in elevations between modelling simulations using contour plots.

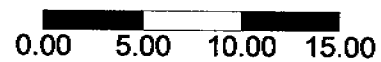
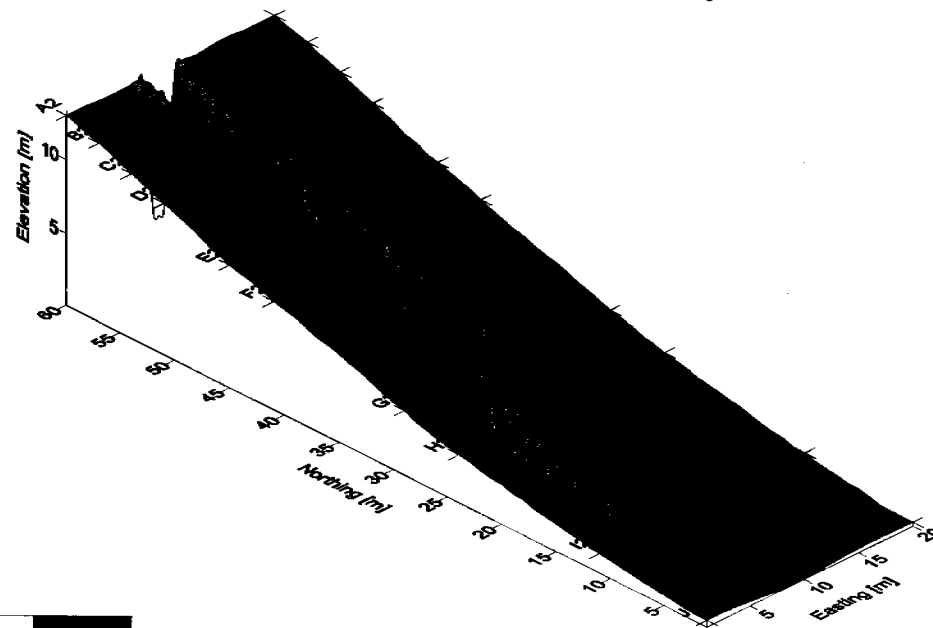
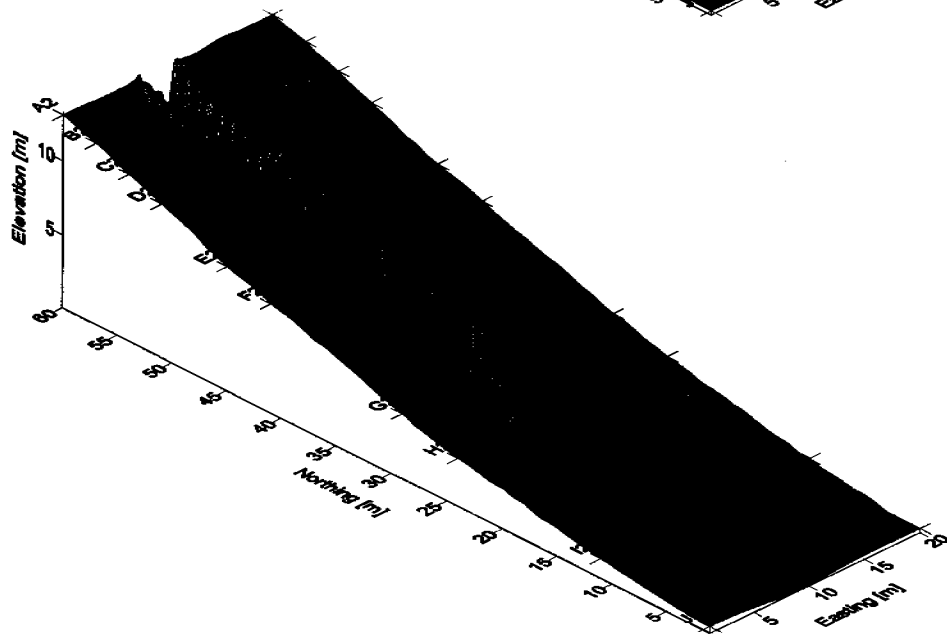
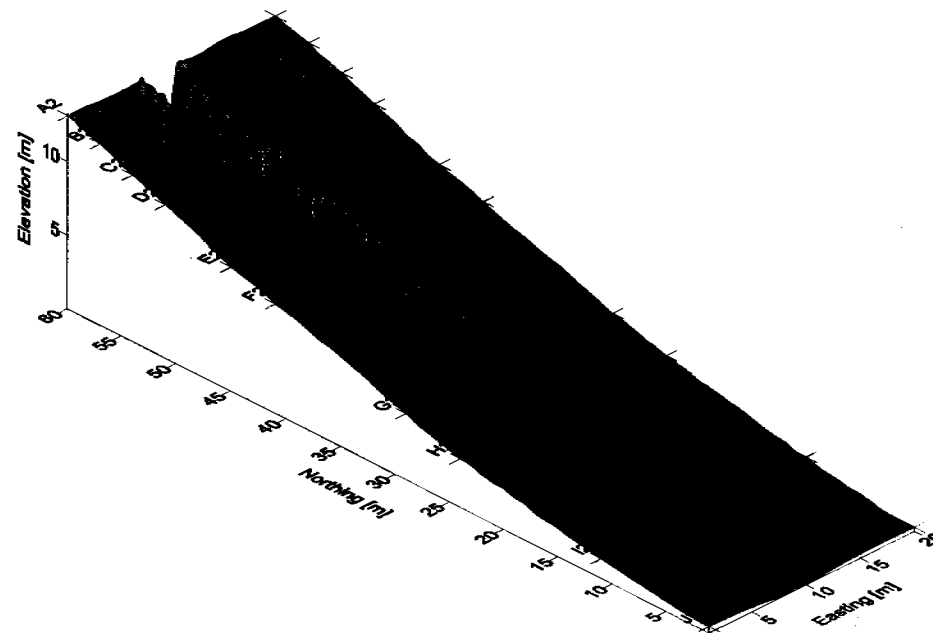
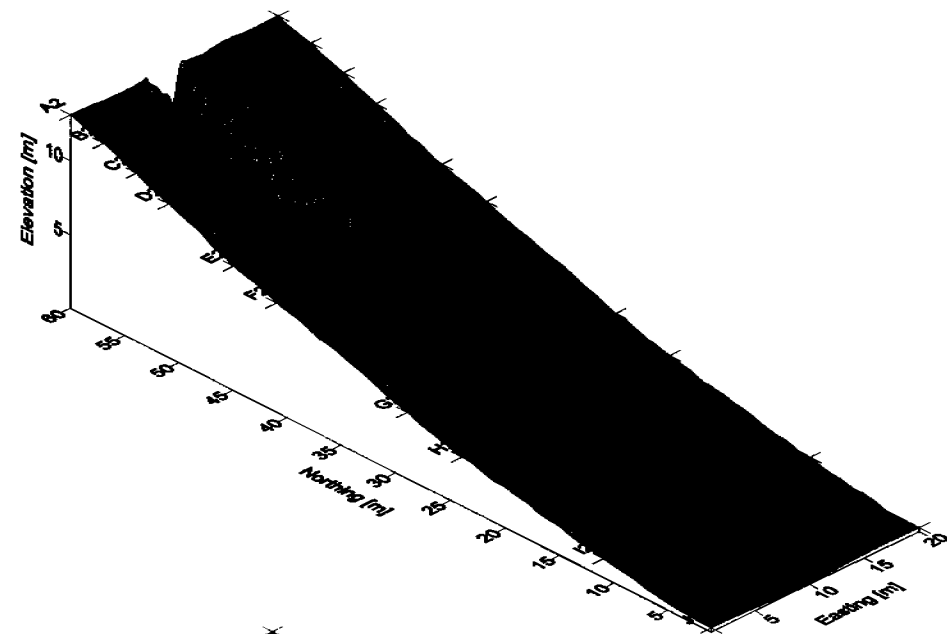


Figure 5.2.1: Simulations for standard batter slope profile with the exponent on the slope term in sediment transport equation set at 0.69, rather than 2.1, a) 10 minutes, b) 20 minutes, c) 30 minutes, and d) 1 hour.

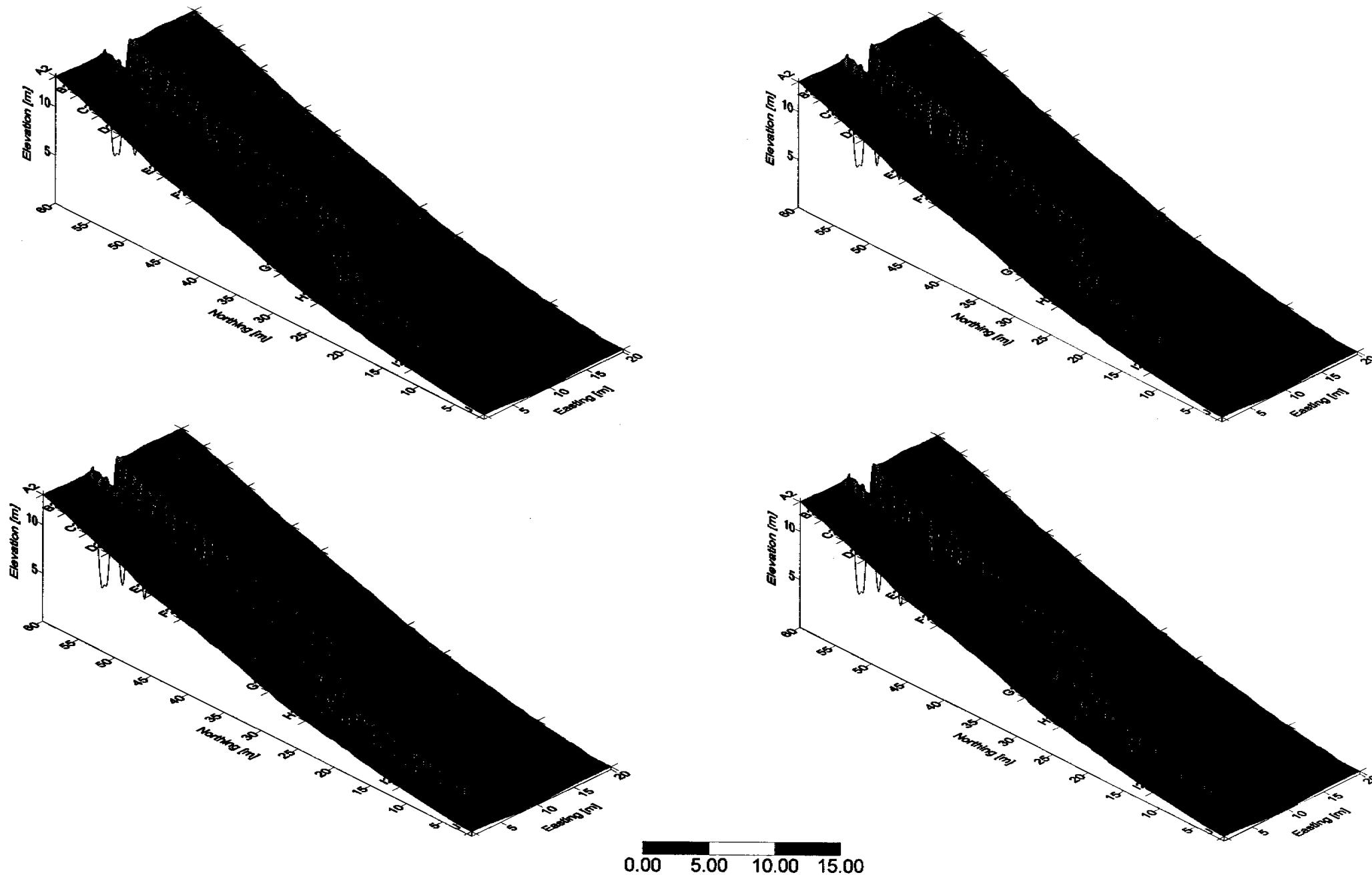


Figure 5.2.2: Simulations for standard batter slope profile with the exponent on the slope term in sediment transport equation set at 0.69, rather than 2.1, at a) 1.5 hours, b) 2 hours this represents the second storm event, and c) 2.5 hours and d) 3 hours representing the final storm event.

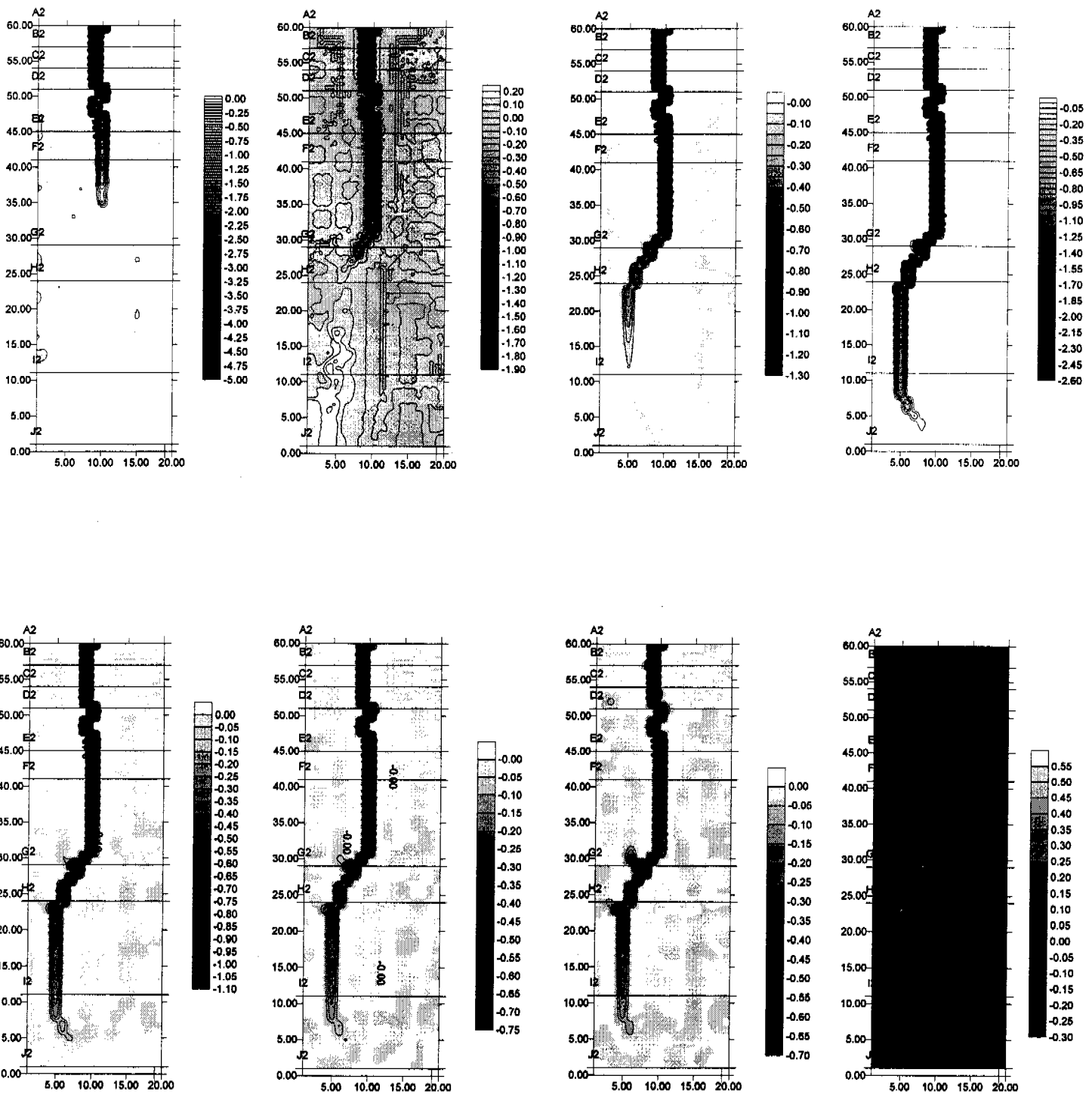


Figure 5.2.3: The initial elevations subtracted from appropriate time period (where erosion is negative, and deposition is positive) such that a) difference between initial surface and prediction at 10 minutes, b) 10 minutes and 20 minutes, c) 20 minutes and 30 minutes, d) 30 minutes and 1 hour. The difference in elevations are also calculated from the remainder of the simulations with e) difference between 1 hours and 1.5 hours, f) 1.5 and 2 hours, g) and 2.5 hours, and h) 2.5 and 3 hours.

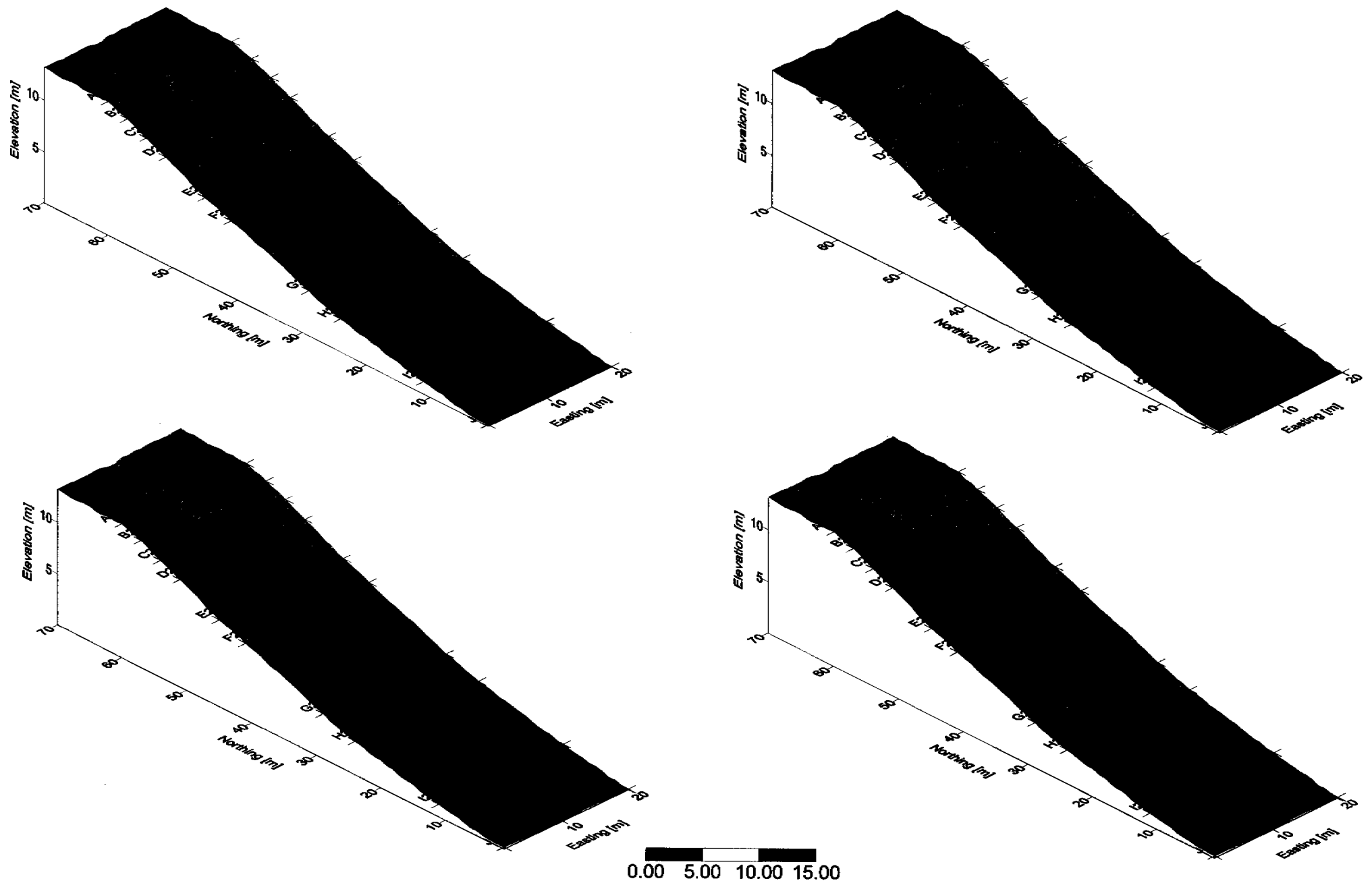


Figure 5.2.4: Simulations for extended batter slope profile with the exponent on the slope term in sediment transport equation set at 0.69, rather than 2.1, a) 10 minutes, b) 20 minutes, c) 30 minutes, and d) 1 hour.

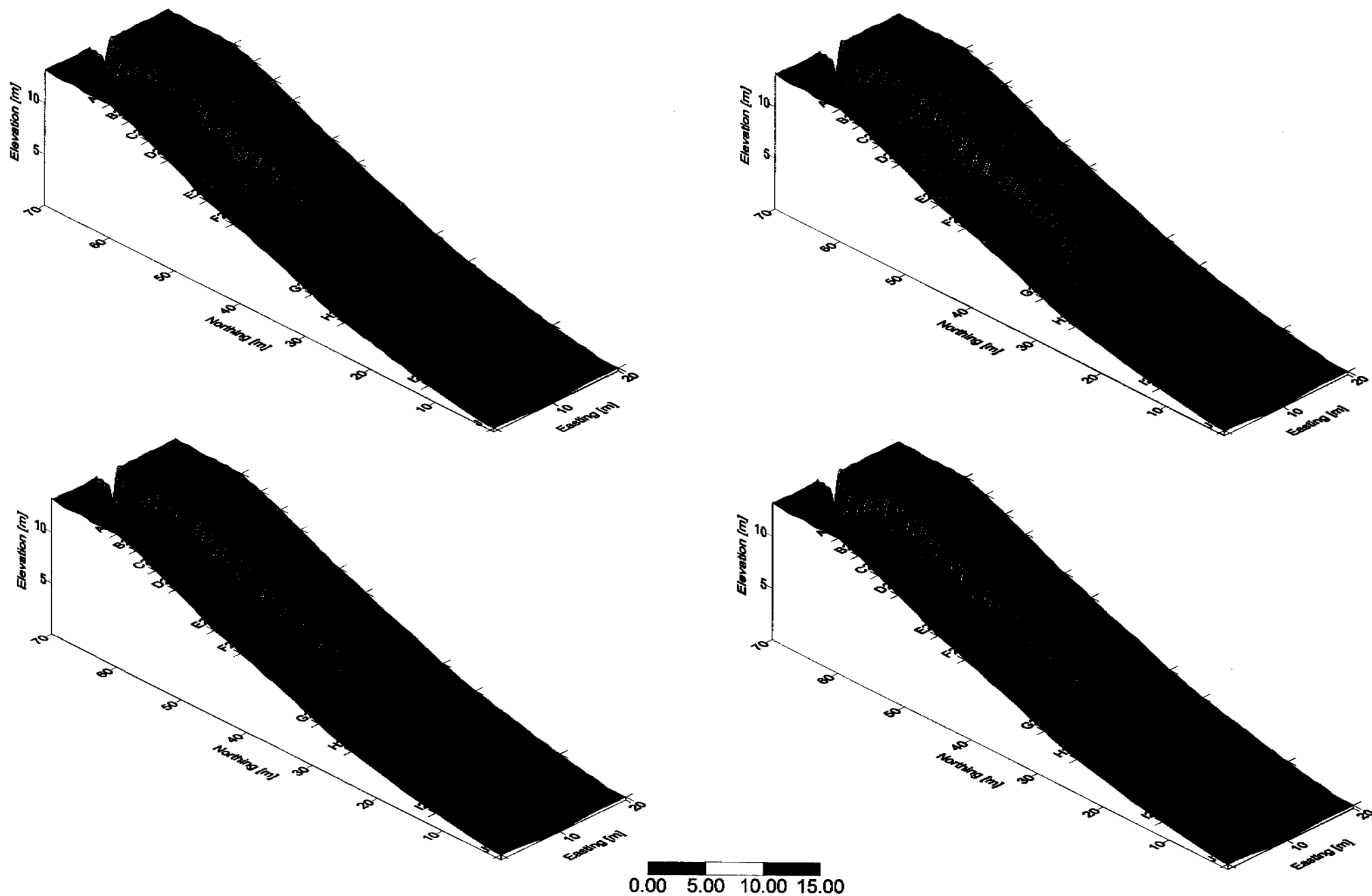


Figure 5.2.5: Simulations for extended batter slope profile with the exponent on the slope term in sediment transport equation set at 0.69, rather than 2.1, at a) 1.5 hours, b) 2 hours this represents the second storm event, and c) 2.5 hours and d) 3 hours representing the final storm event.

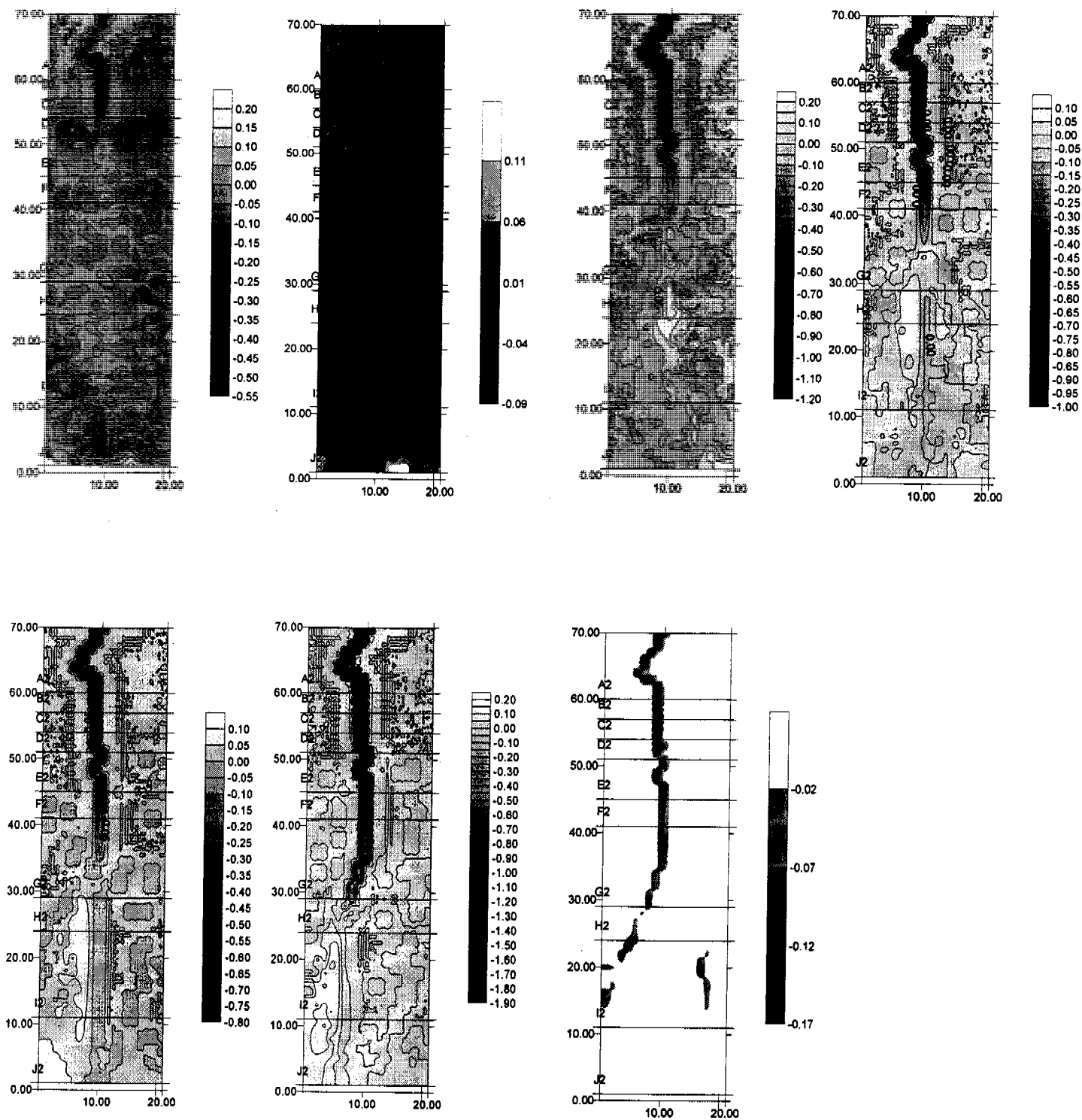


Figure 5.2.6: The morphology contour plots a) initial profile and 10 minutes, b) 10 minutes and 20 minutes, c) 20 minutes and 30 minutes, d) 30 minutes and 1 hour. The difference in elevations are also calculated from the remainder of the simulations with e) difference between 1 hours and 1.5 hours, f) 1.5 and 2 hours, g) 2 and 2.5 hours, and h) 2.5 and 3 hours.



5.3 Increased Width

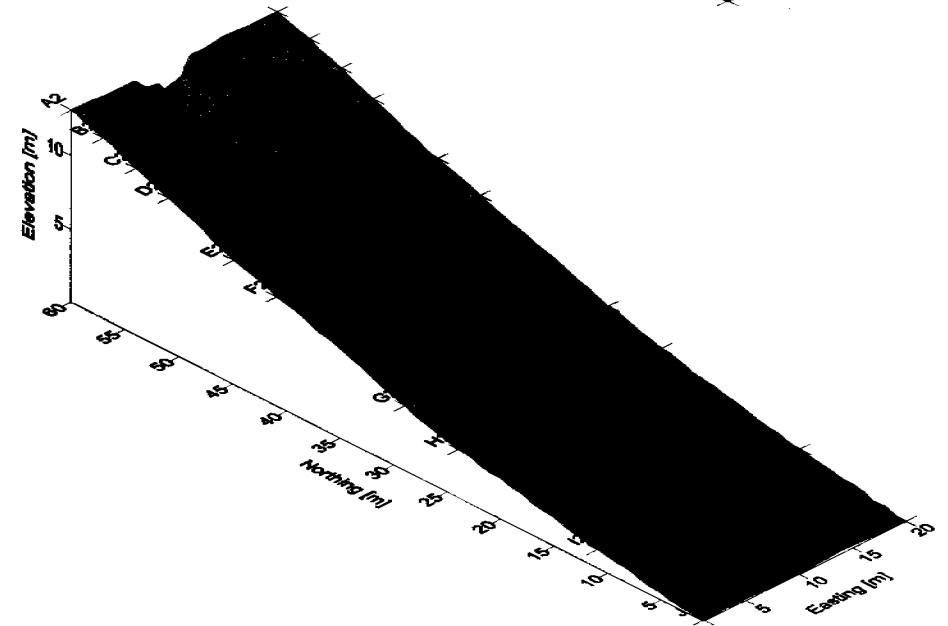
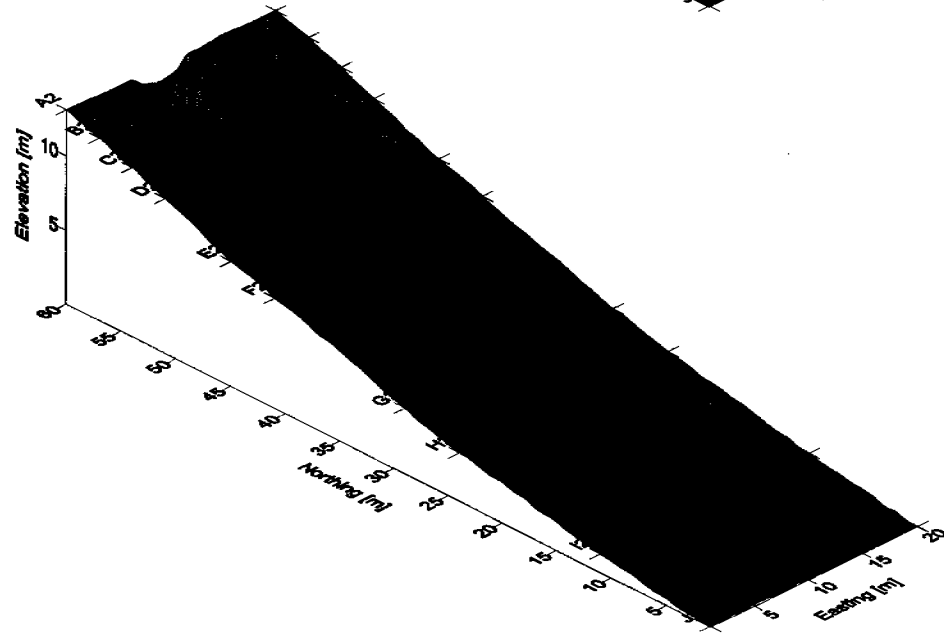
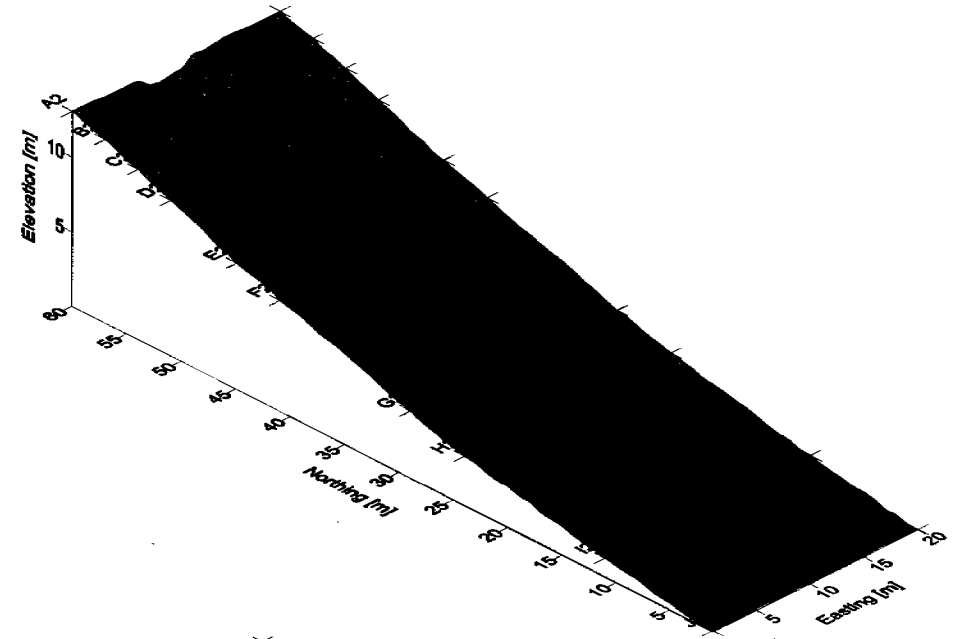
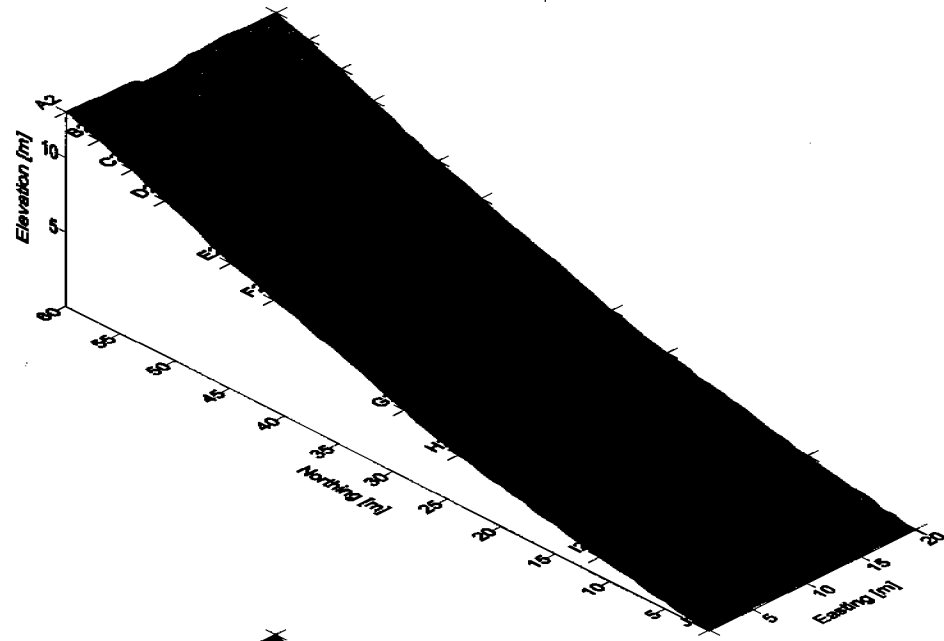
The effect of increasing the number of inlet points was assessed by simulating both the standard batter slope, and also the extended batter profile. The overall discharge was maintained at the same level, with each inlet node, 1800 equivalent nodes instead of 3600 nodes for the standard narrow two feed point scenario.

Gully formation observed in Figure 5.3.1, and Figure 5.3.2, is more widespread at the top of the batter slope with maximum depth of erosion 2.5m for the standard scenario. Whilst in Figure 5.3.4, and Figure 5.3.5 similar behaviour observed in Figure 5.1.4, and Figure 5.1.5, except that the gully does not proceed onto the batter slope.

The rate of development of the gully is considerably slower for the standard profile scenario, with less pronounced regions of deposition, recognised by smoothed areas at the base of the slope (Row G to Row I), with the depth of gully ranging between 0.8 to 1.5m between Row E to Row K.

The erosion depth profiles begin to resemble those observed on site, with excavation of material in some sections to a level of 60cm. Figure 5.3.3 illustrates the spatial distribution of erosion for the wide inlet.

When the same scenario was simulated using the extended profile, considerably different results were predicted. From Figure 5.3.4, and Figure 5.3.5, the development of the gully does not reach the high wall transition point and so the large formations generated above are not predicted to occur. Further investigation including the inclusion of wide inlet point with randomised erodibility of the waste rock material yielded similar behaviour for this extended profile.



0.00 5.00 10.00 15.00

Figure 5.3.1: Simulations for standard batter slope profile with increased width inlet point to four points instead of only two, at a) 10 minutes, b) 20 minutes, c) 30 minutes, and d) 1 hour.

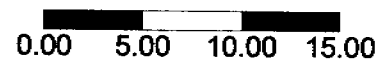
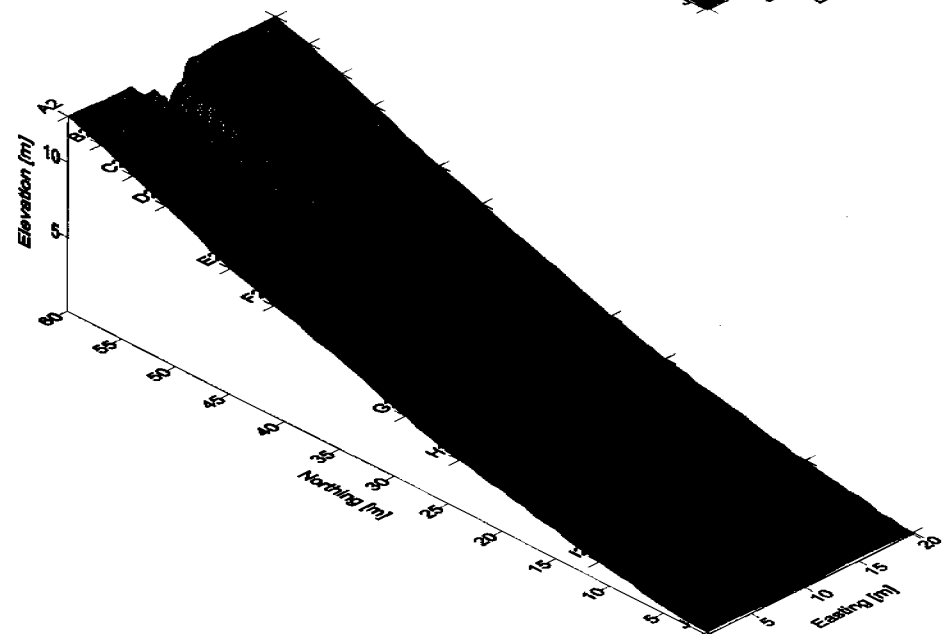
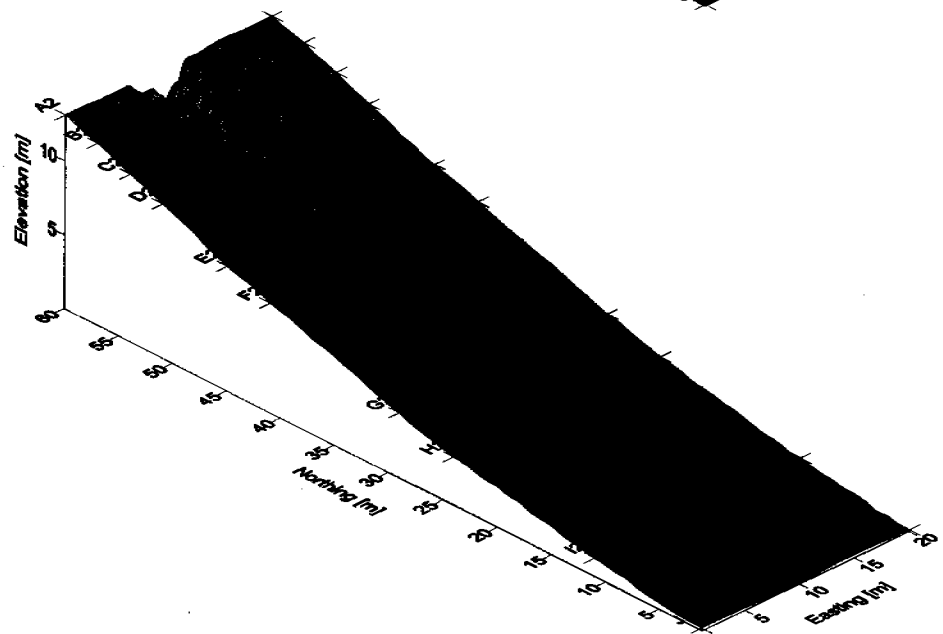
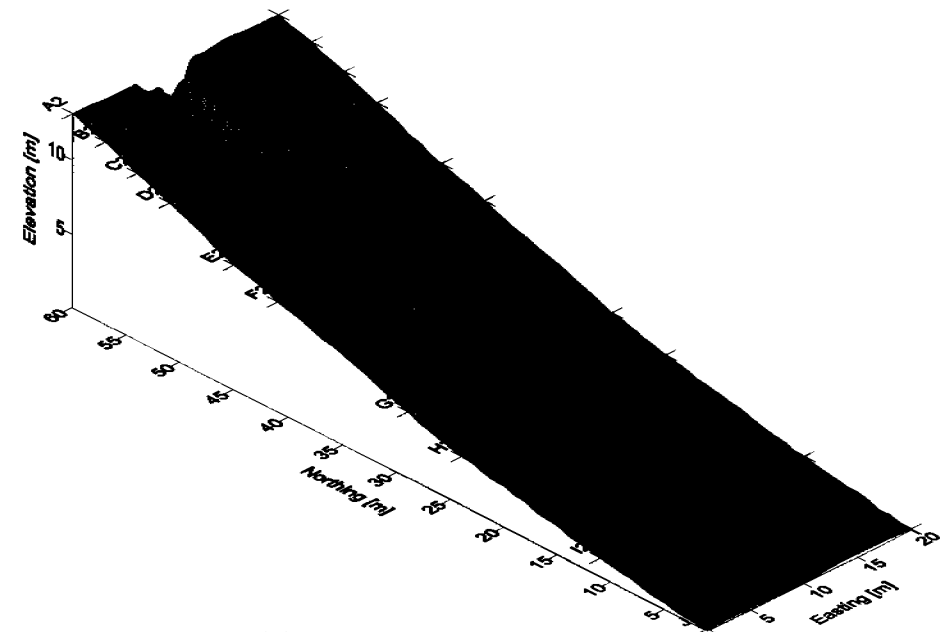
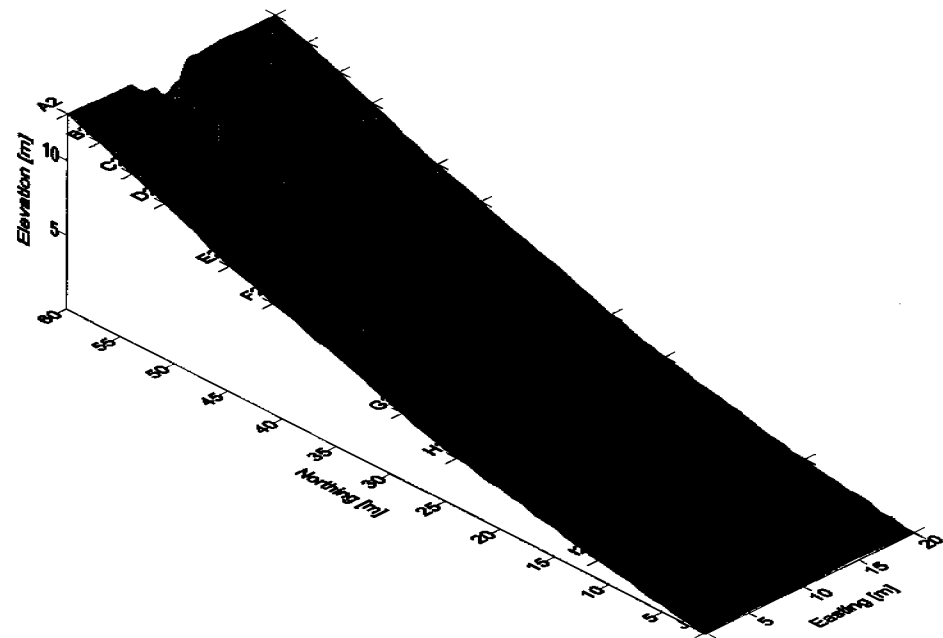


Figure 5.3.2: Simulations for standard batter slope profile with increased width inlet point to four points instead of only two, at a) 1.5 hours, b) 2 hours this represents the second storm event, and c) 2.5 hours and d) 3 hours representing the final storm event.

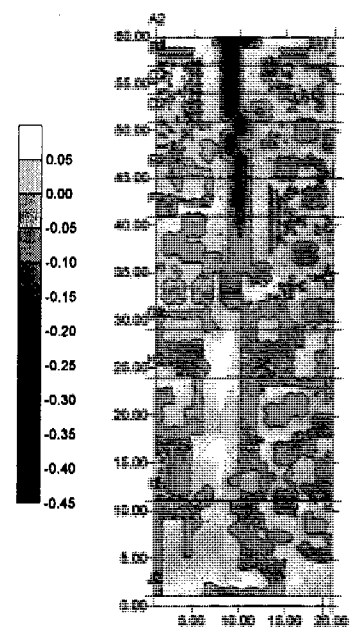
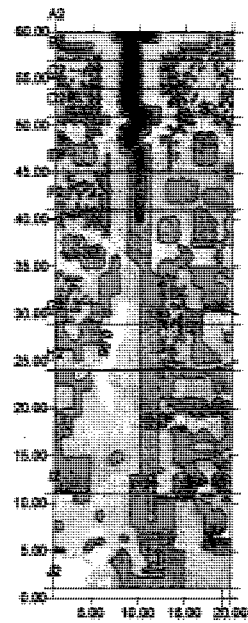
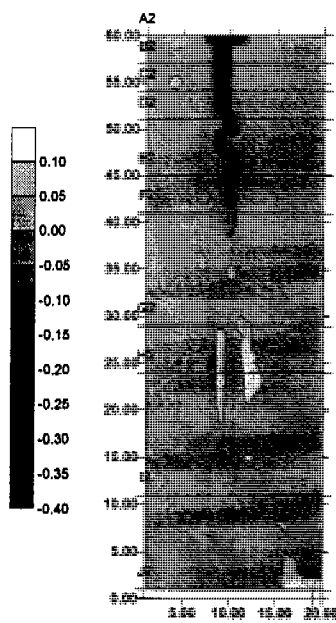
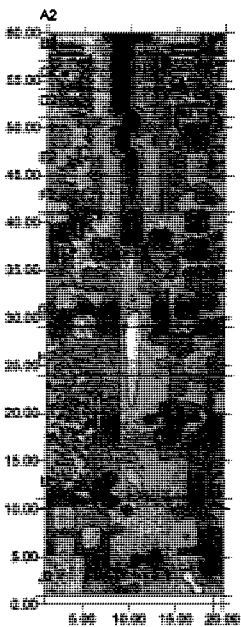
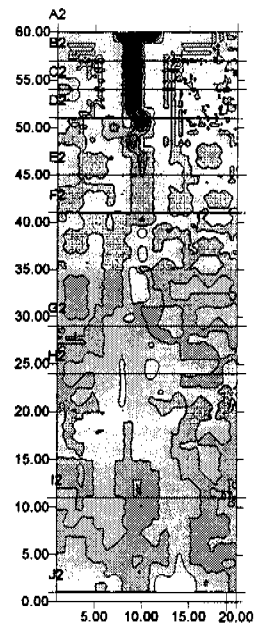
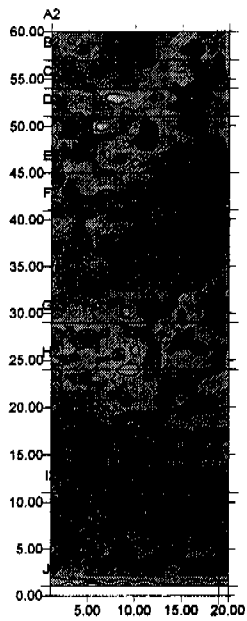


Figure 5.3.3: The morphology contour plots a) initial profile and 10 minutes, b) 10 minutes and 20 minutes, c) 20 minutes and 30 minutes, d) 30 minutes and 1 hour. The difference in elevations are also calculated from the remainder of the simulations with e) difference between 1 hours and 1.5 hours, f) 1.5 and 2 hours, g) 2 and 2.5 hours, and h) 2.5 and 3hours.



Monitoring Gully Formation

5.4 Randomised Erodibility

The erodibility factor β_{e1} was multiplied by a randomly generated number between 0 and 5, with a mean of 1.0 to introduce a random perturbation to the surface erodibility.

By the introduction of some degree of heterogeneity, the formation of the gully was expected to follow those regions more susceptible and the straight line paths characteristic of Sections 5.1 should not be observed.

The sensitivity of the slope to erodibility will have been increased in some sections although the overall erodibility, representative of the actual site, has not been changed, leading to deeper gullies observed where they occur.

This synopsis seems somewhat reasonable, as illustrated in Figure 5.4.1, and Figure 5.4.2 with gully formation across the slope from almost in front of the inlet zone.

The pathway adopted, as discussed above, is dependent on the drainage direction, as well as the surface elevation of the nodes lying around the current node under calculation and ultimately the erodibility of this point, this influences the nature of gully formation with reduced amounts of deposition observed in Figure 5.4.3.

Although the quantity of deposition observed in each of the time periods is reduced, the dynamic nature of the pathway of erosion observed in these simulations is similar to standard scenario in Section 5.1. Inherently the overall erosional characteristic of the slope has not been altered, and predictions indicate similar maximum depths of erosion, although areas of deposition will be more widespread. The maximum depth of erosion at the head of the gully network at 5.5m, indicating that overall nature of gully development has not altered, but merely the pathway adopted. This conforms to the hypothesis that the erodibility of the material had not been significantly changed.

Figure 5.4.4 and Figure 5.4.5 illustrate the same design scenario incorporating the extended profile of the batter slope. Comparison of these simulations with Figures 5.1.4, and 5.1.5 reveal a similar behaviour with initial delay in gully development, until the 30 minute mark, where development initiates at the transition point between



Monitoring Gully Formation

the batter slope and gully catchment. Similarities in the development process also included the maximum depth of erosion at Row A at 4.5m, as can be observed in Figure 5.4.4.

The assessment of the inclusion of wide inlet point with the standard profile combined with randomised erodibility was also conducted, as illustrated in Figure 5.4.7 and Figure 5.4.8. The continuity of transported material in these cases, can be compared to Figure 5.4.4, and 5.4.5 respectively. The depth of erosion ranges between 0.5m and 1.0m for Row E to Row G, whilst more extensive excavation sections between Row B to Row D. It also noted that cross-sectional profile at Row B in Figure 5.4.7_d is almost identical to that observed in Figure 5.3.1_d Row B, with similar observations for all except just below the inlet zone in Row A.

The pathway adopted, mimics that of Figure 5.4.1, and Figure 5.4.2, whilst this is not observed when comparing standard scenario and addition of increased width component (Figure 5.1.1 and 5.1.2 against 5.3.1 and 5.3.2), with a reduction in depths of erosion observed.

A similar comparison can be drawn between the standard extended profile and randomised erodibility scenario, with depth of erosion of similar magnitude, with path dominated by developing process, rather than random perturbations in material characteristic. Once the gully extends past Row D in this figure, the dominant process changes as expected.

Another important observation from Figure 5.4.7, and Figure 5.4.8 where 2 independent erosion paths have developed. By further increasing inlet width, and increasing grid discretisation, modelling simulations can yield predictions similar to the 2 main gully pathways observed on site.

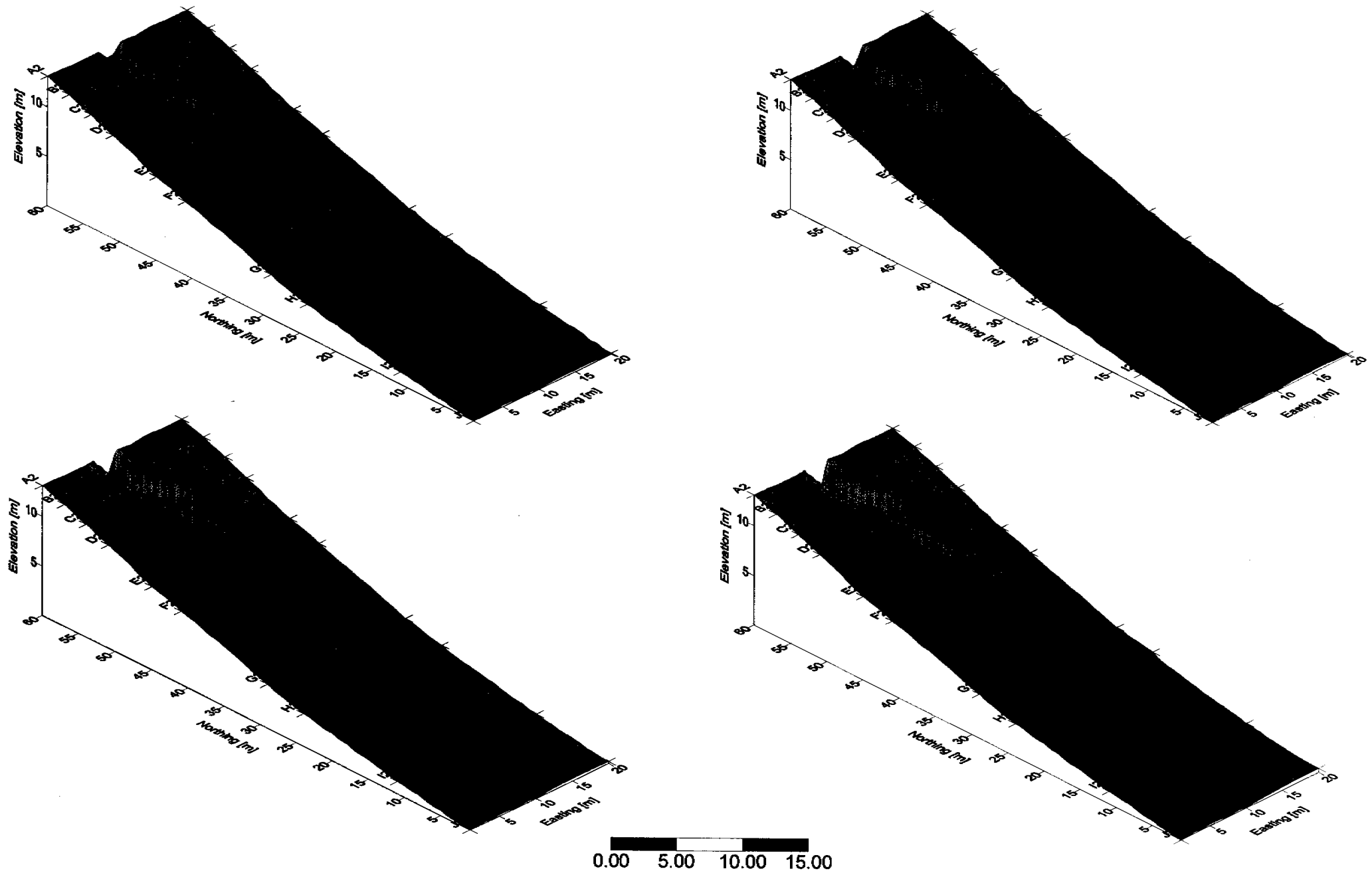
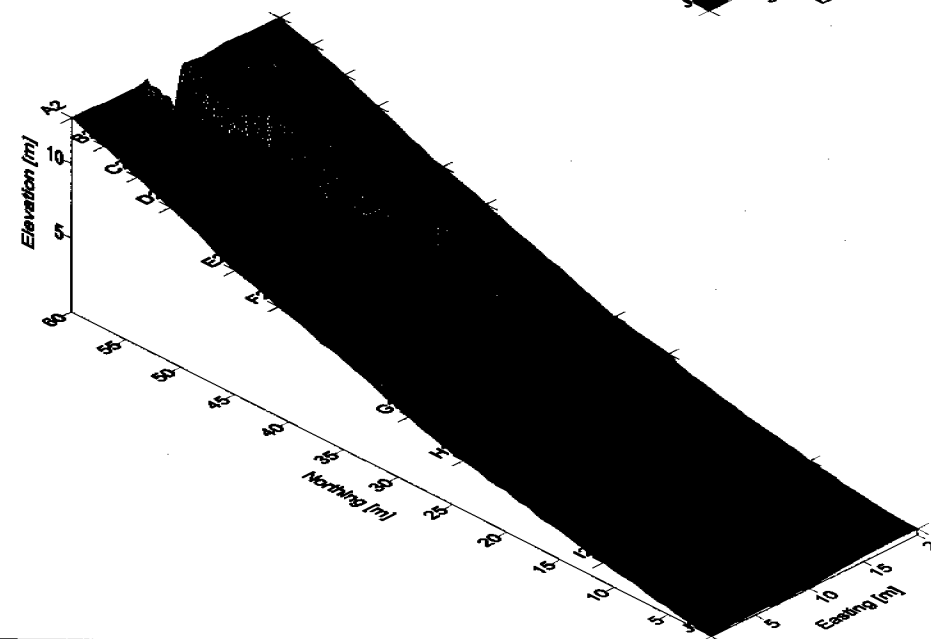
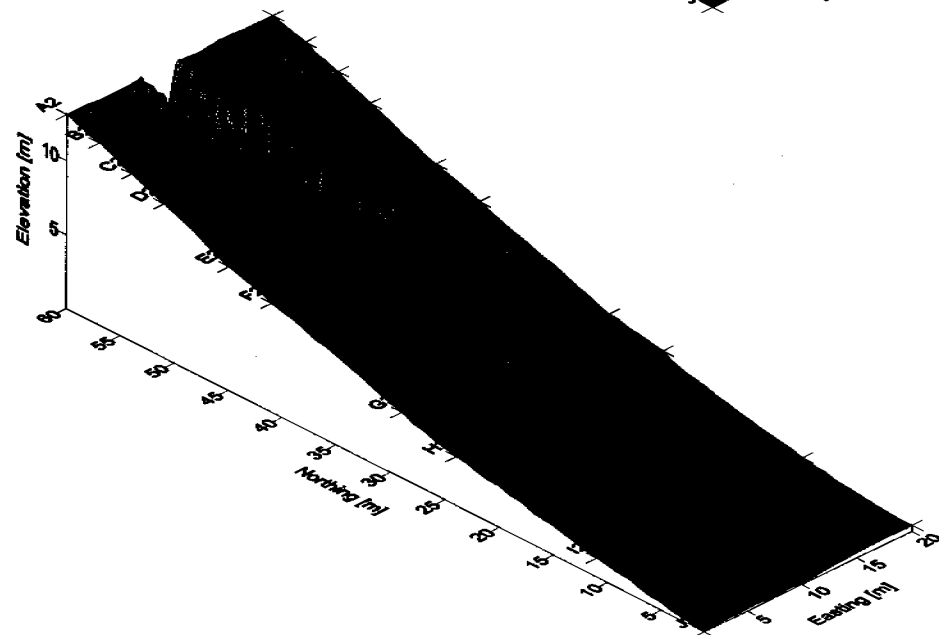
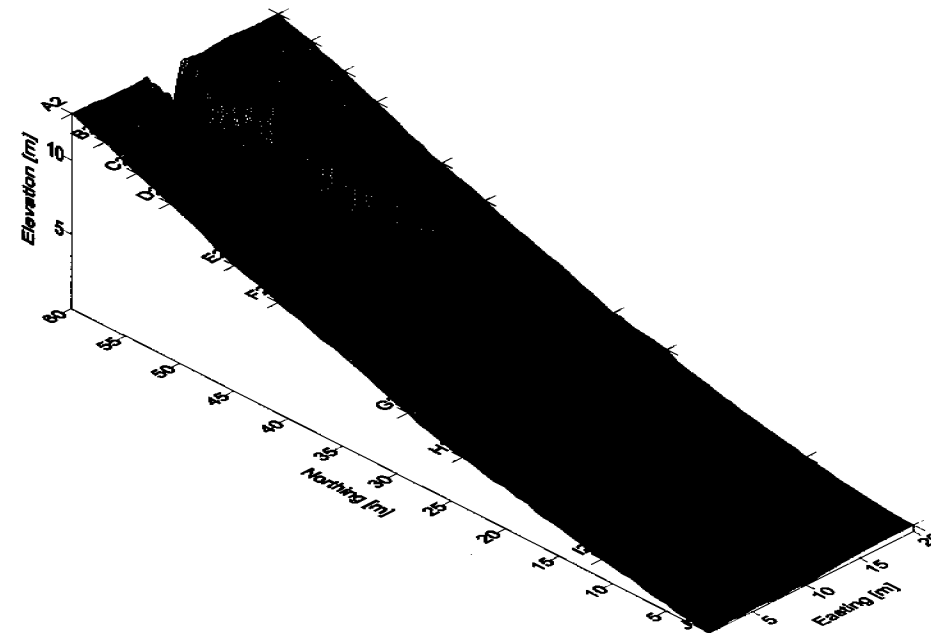
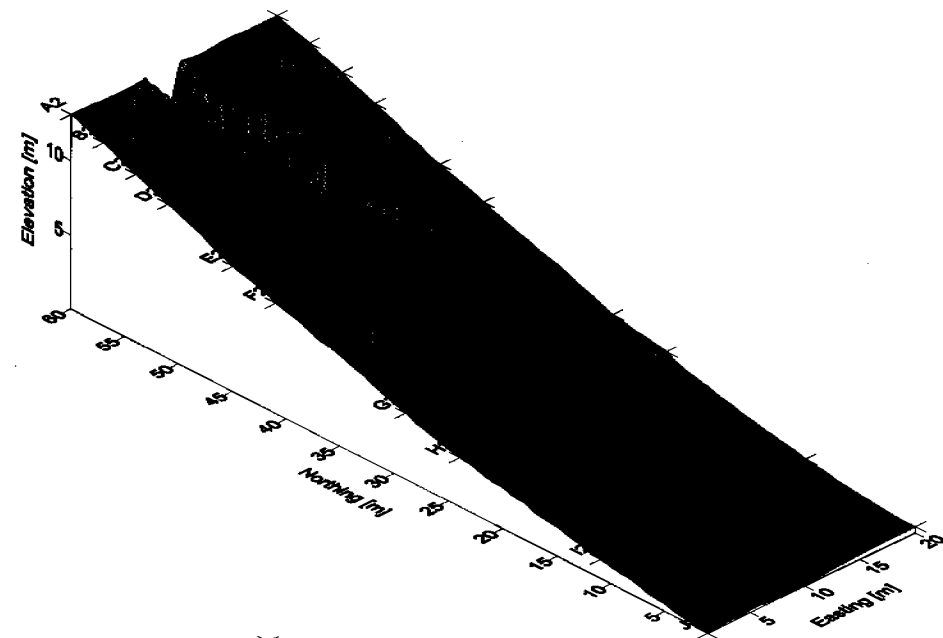


Figure 5.4.1: Simulations for standard batter slope profile with randomised erodibility at a) 10 minutes, b) 20 minutes, c) 30 minutes, and d) 1 hour.



0.00 5.00 10.00 15.00

Figure 5.4.2: Simulations for standard batter slope profile with randomised erodibility, at a) 1.5 hours, b) 2 hours this represents the second storm event, and c) 2.5 hours and d) 3 hours representing the final storm event.

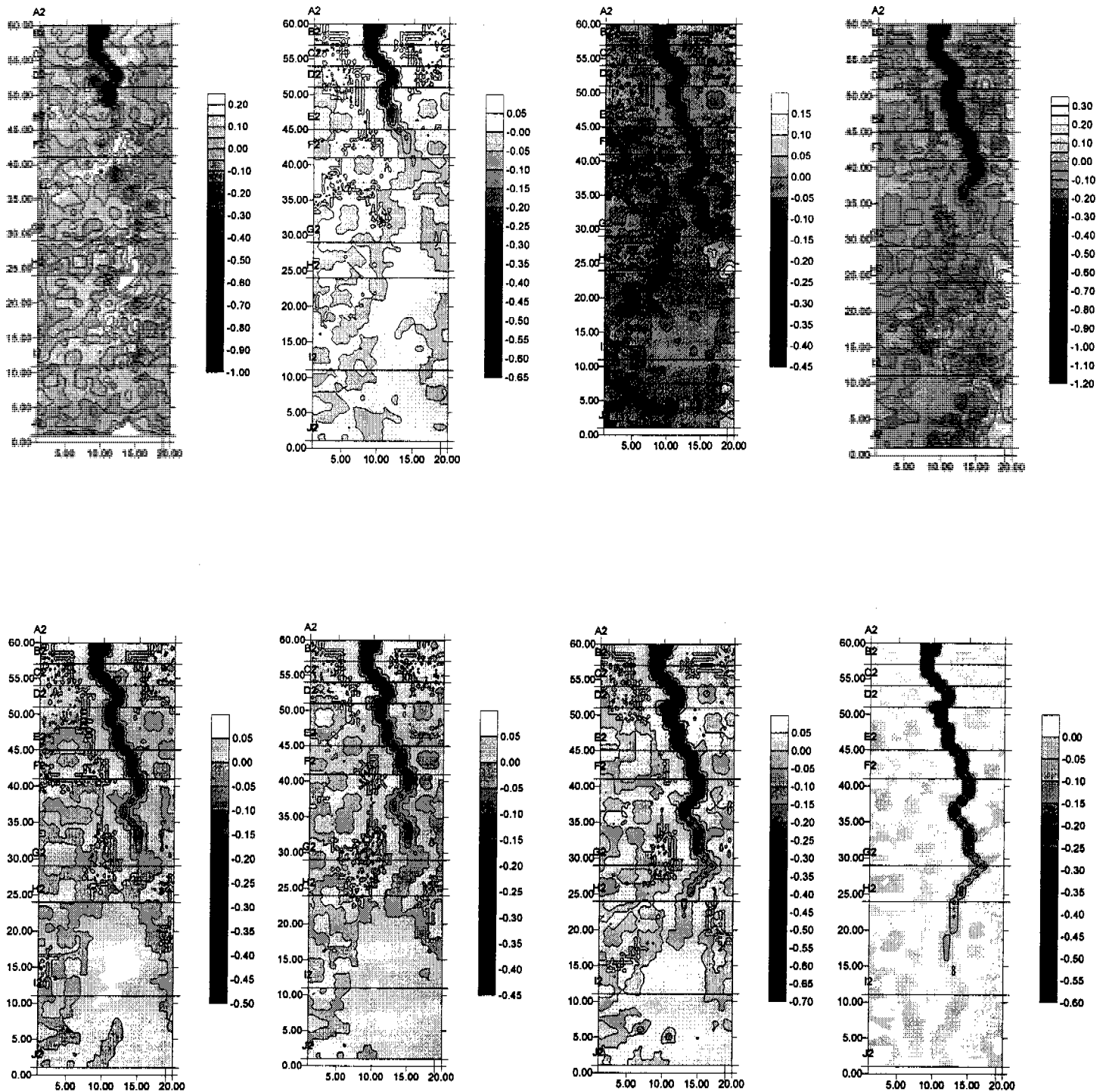
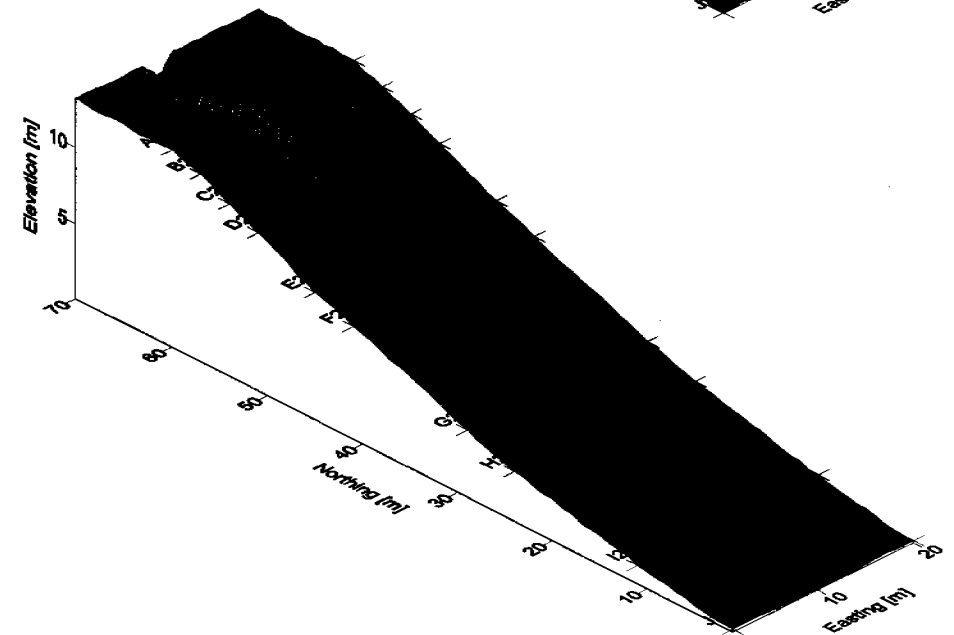
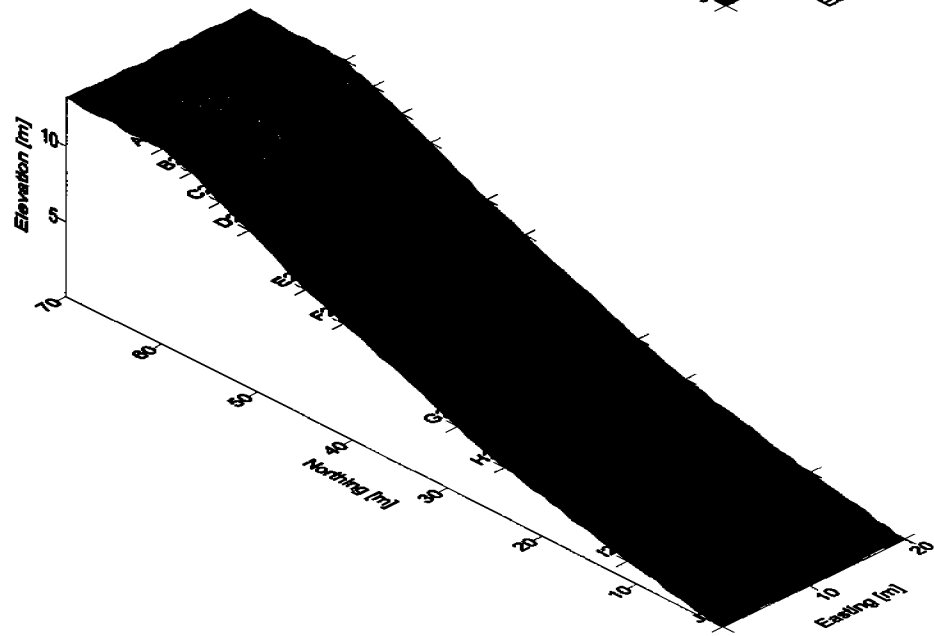
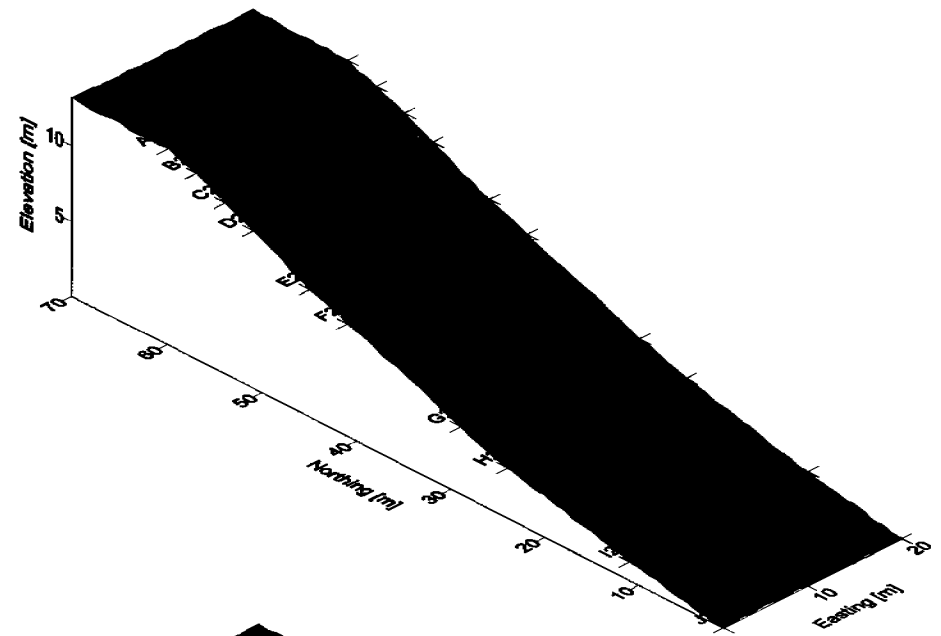
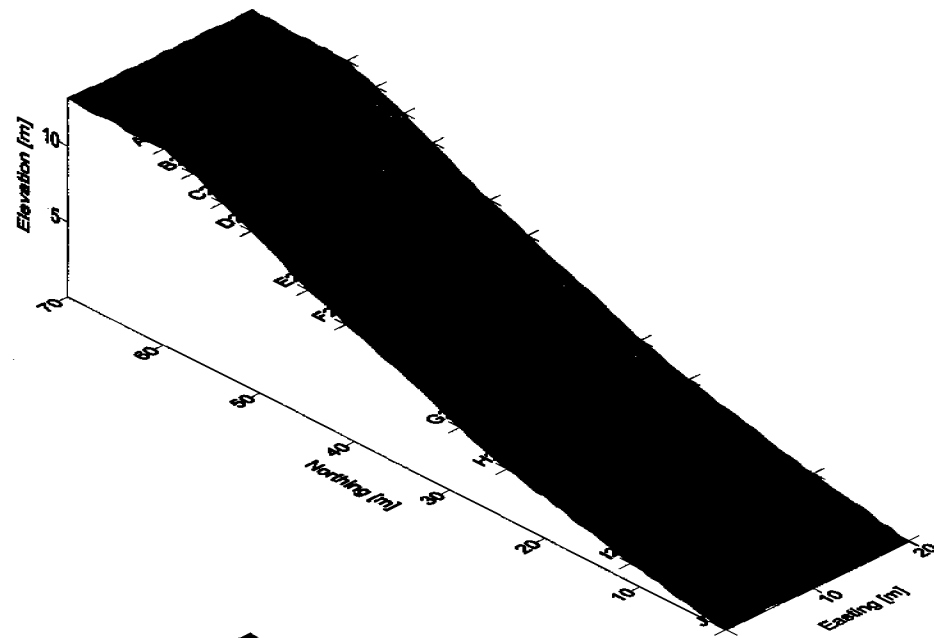
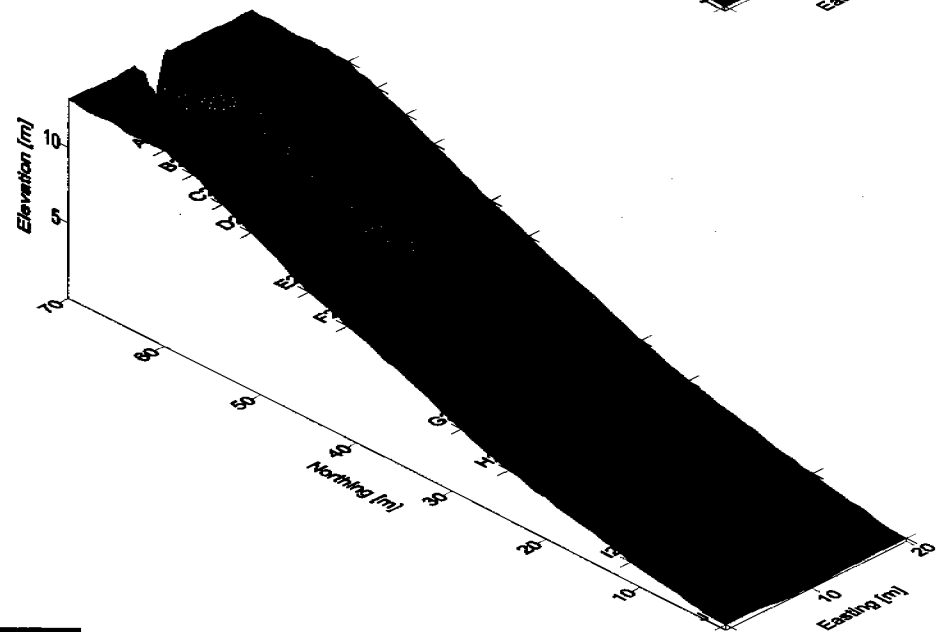
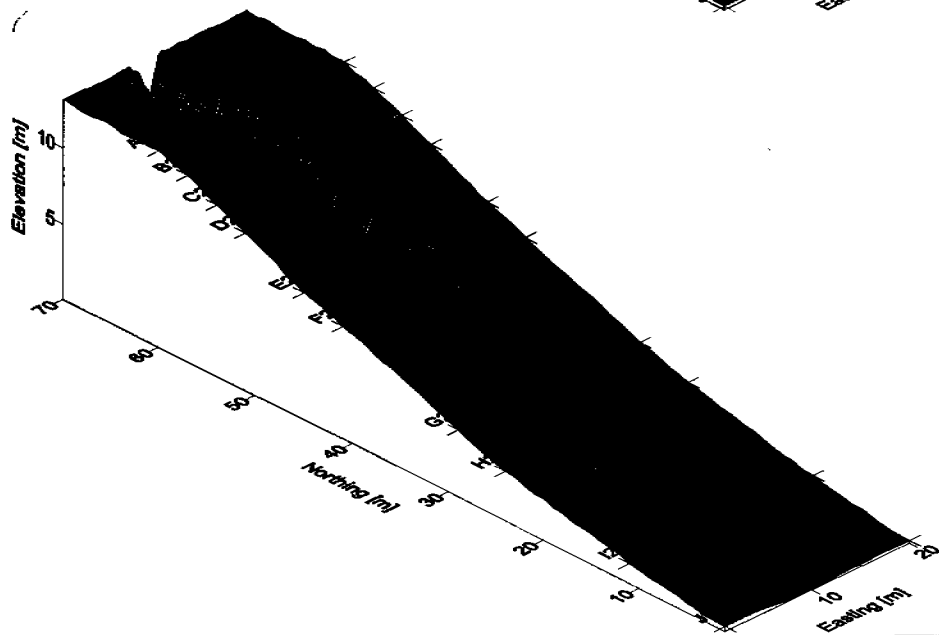
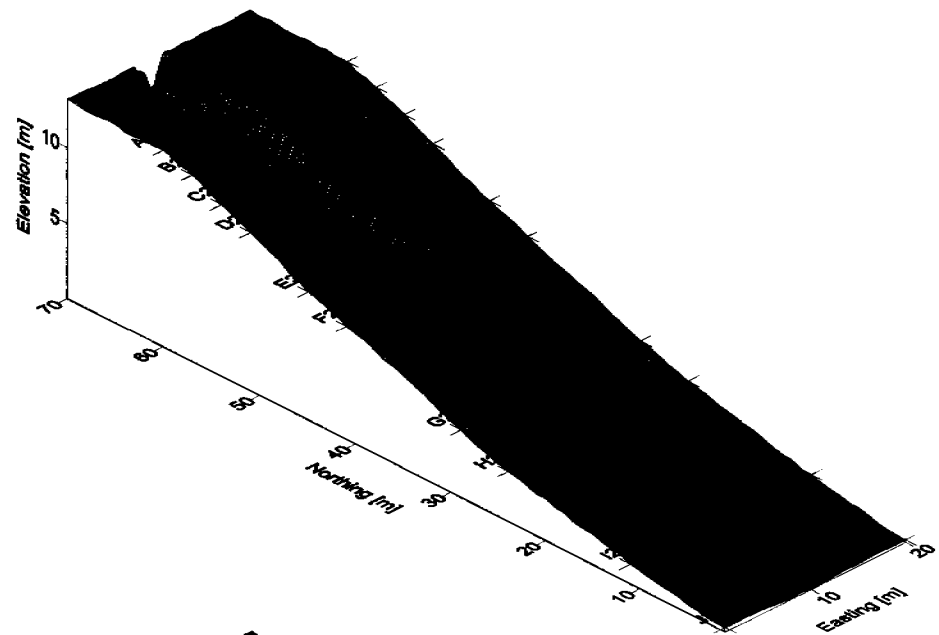
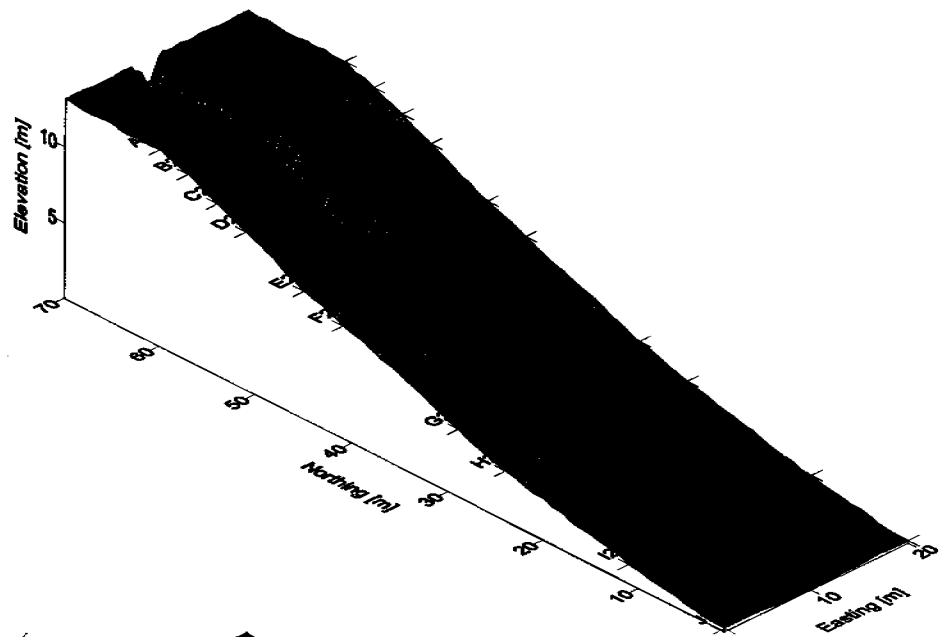


Figure 5.4.3: The morphology contour plots a) initial profile and 10 minutes, b) 10 minutes and 20 minutes, c) 20 minutes and 30 minutes, d) 30 minutes and 1 hour. The difference in elevations are also calculated from the remainder of the simulations with e) difference between 1 hours and 1.5 hours, f) 1.5 and 2 hours, g) 2 and 2.5 hours, and h) 2.5 and 3 hours.



0.00 5.00 10.00 15.00

Figure 5.4.4 ^{Extended} Simulations for standard batter slope profile with randomised erodibility at a) 10 minutes, b) 20 minutes, c) 30 minutes, and d) 1 hour.



0.00 5.00 10.00 15.00

extended
 Figure 5.4.8: Simulations for standard batter slope profile with randomised erodibility, at a) 1.5 hours, b) 2 hours this represents the second storm event, and c) 2.5 hours and d) 3 hours representing the final storm event.

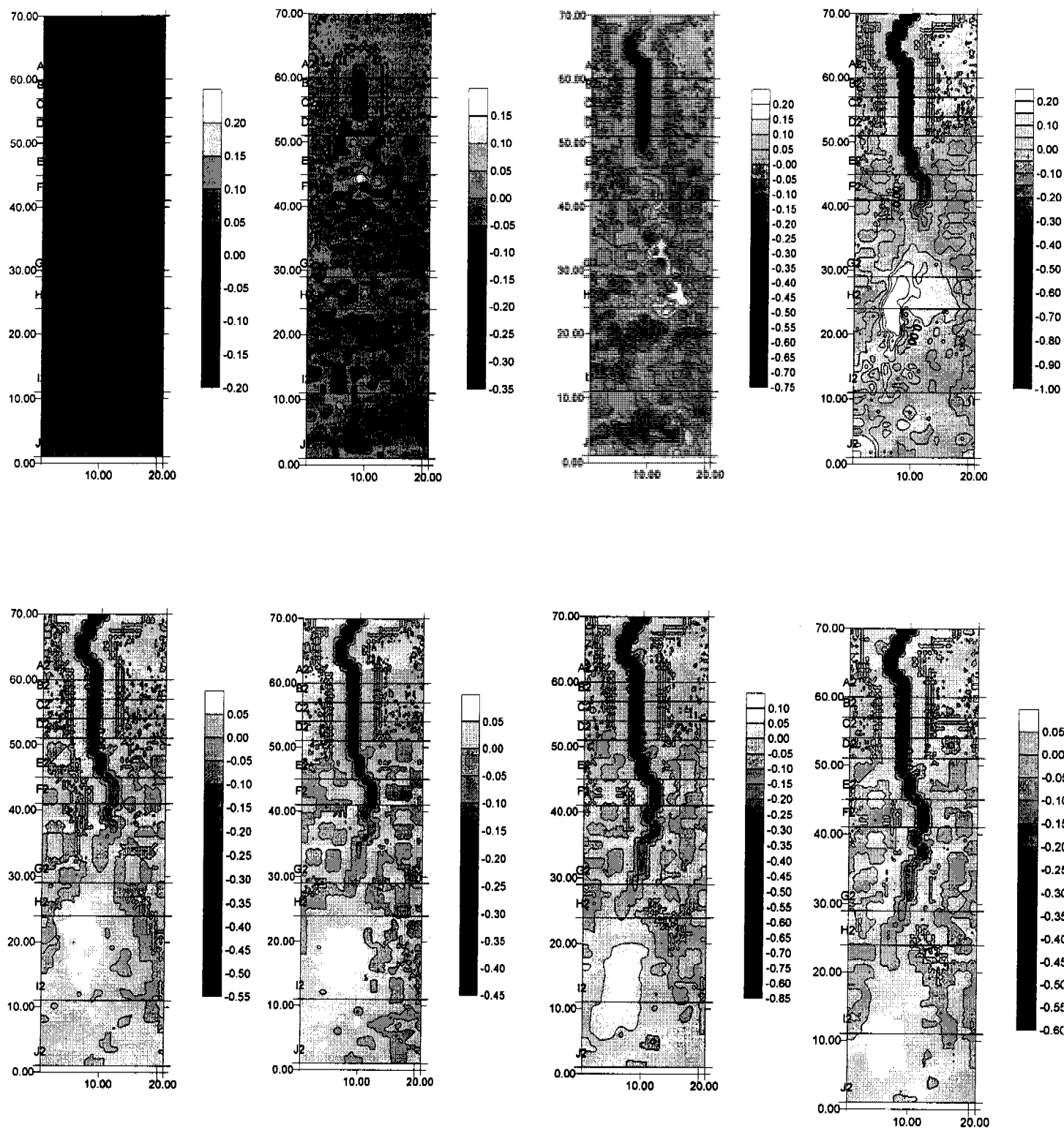


Figure 5.4.6: The morphology contour plots a) initial profile and 10 minutes, b) 10 minutes and 20 minutes, c) 20 minutes and 30 minutes, d) 30 minutes and 1 hour. The difference in elevations are also calculated from the remainder of the simulations with e) difference between 1 hours and 1.5 hours, f) 1.5 and 2 hours, g) 2 and 2.5 hours, and h) 2.5 and 3 hours.

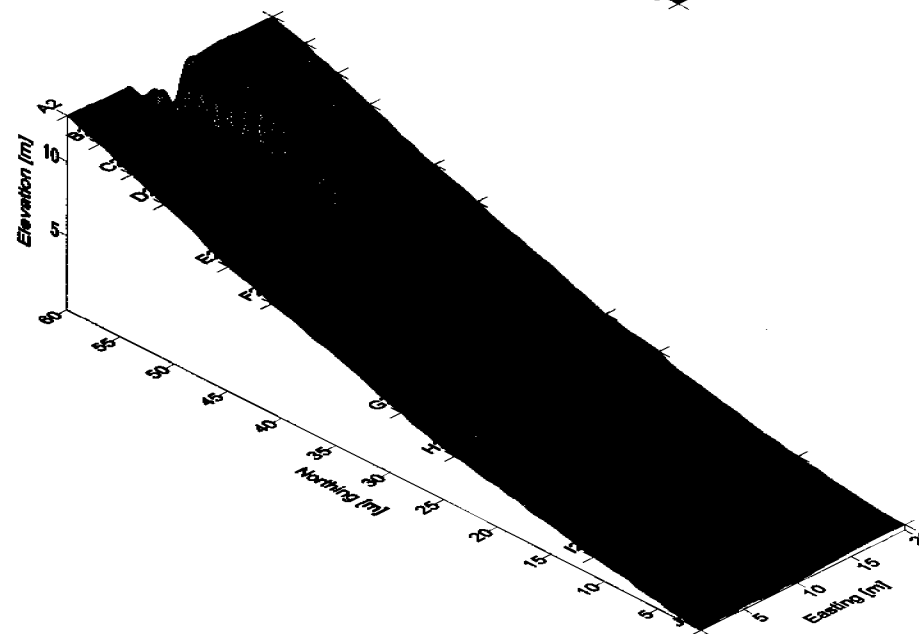
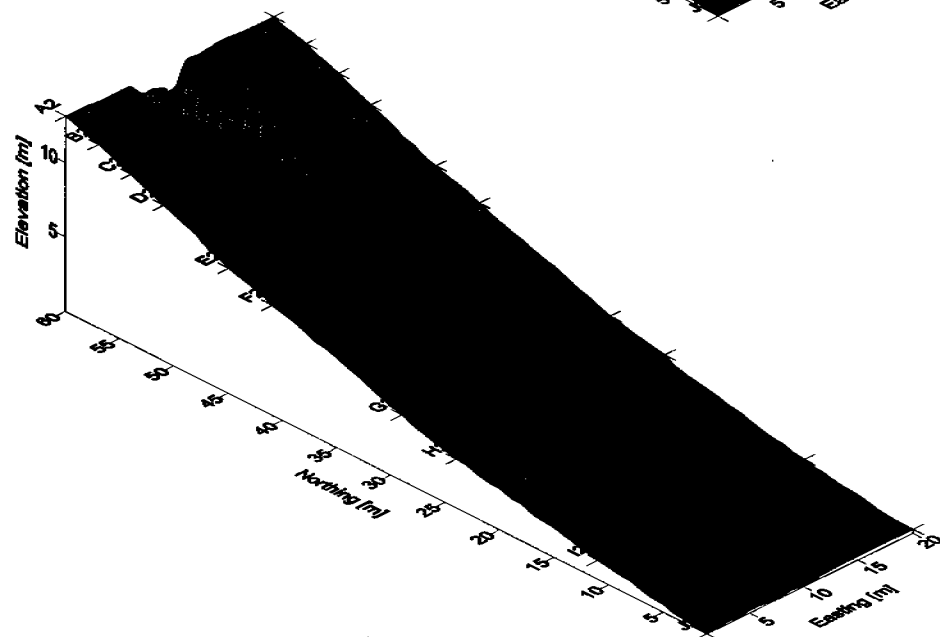
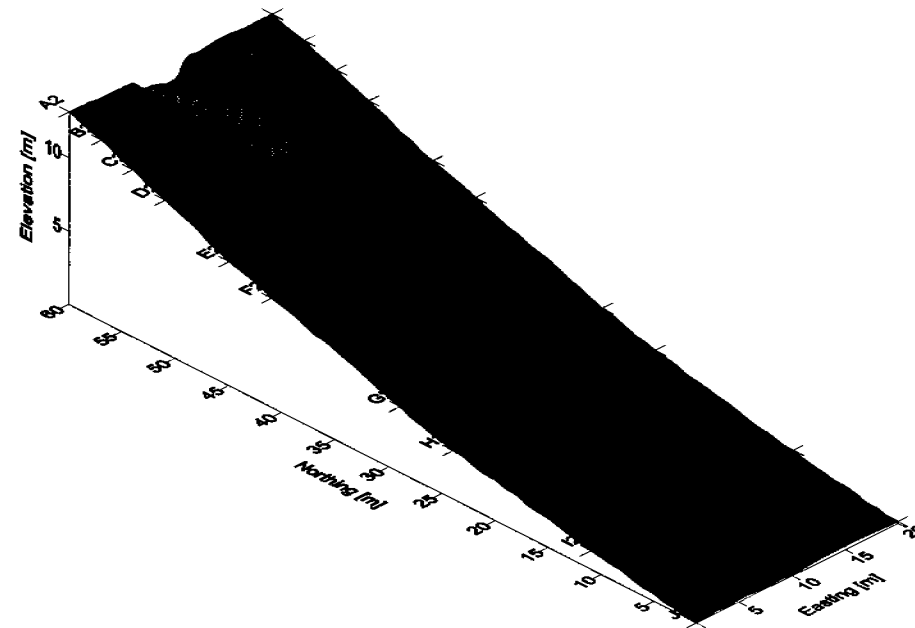
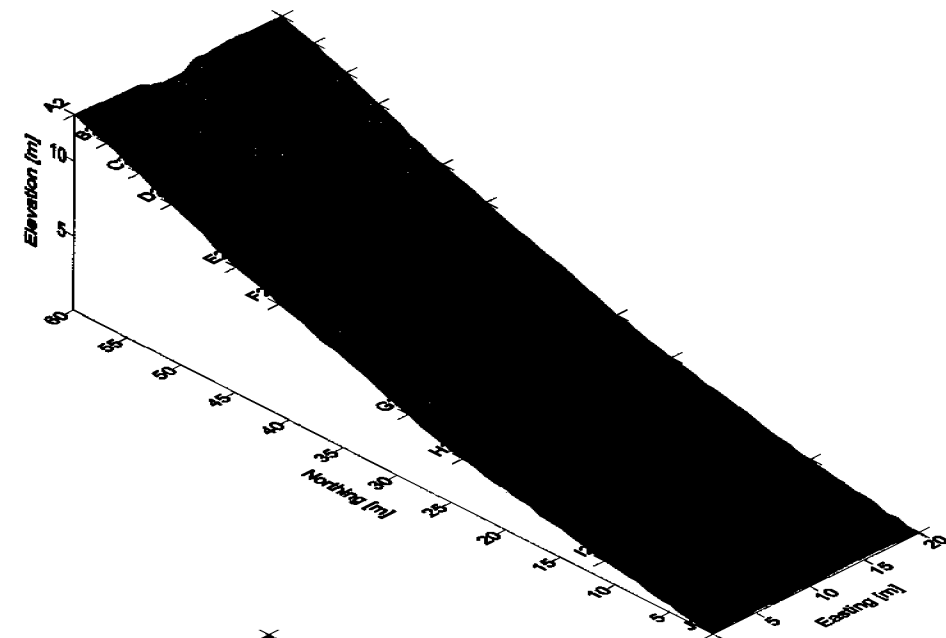


Figure 5.4.7: Simulations for standard batter slope profile with increased width inlet point to four points instead of only two, combined with randomised erodibility, a) 10 minutes, b) 20 minutes, c) 30 minutes, and d) 1 hour.

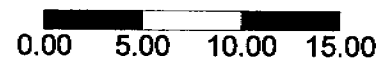
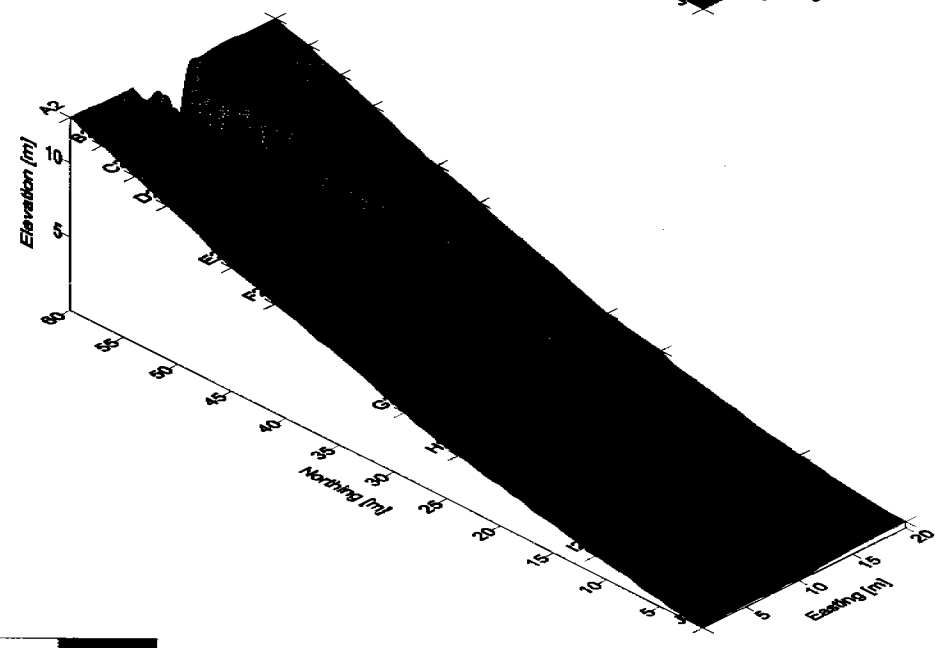
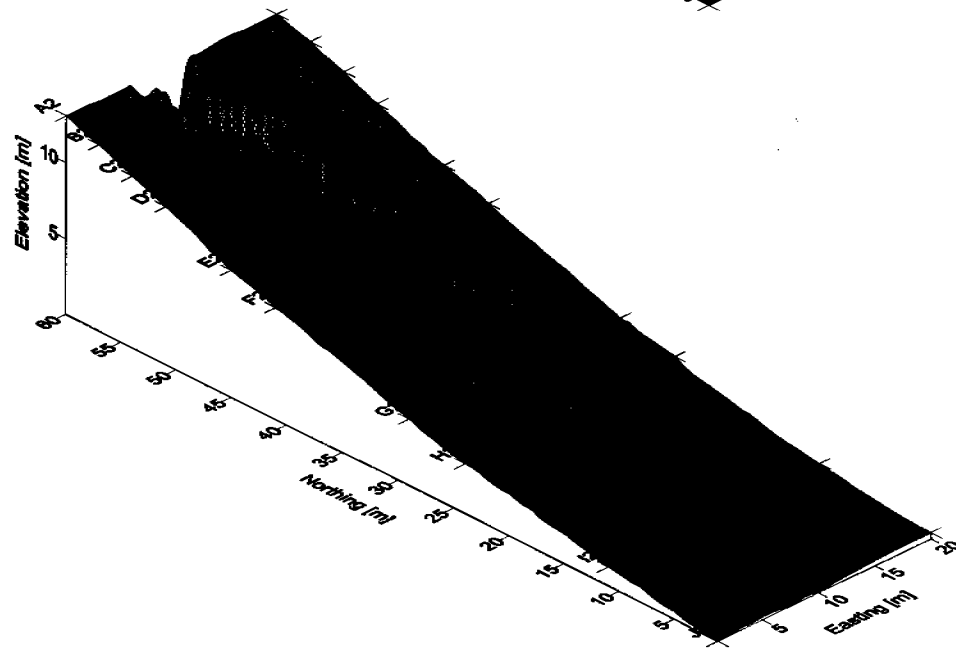
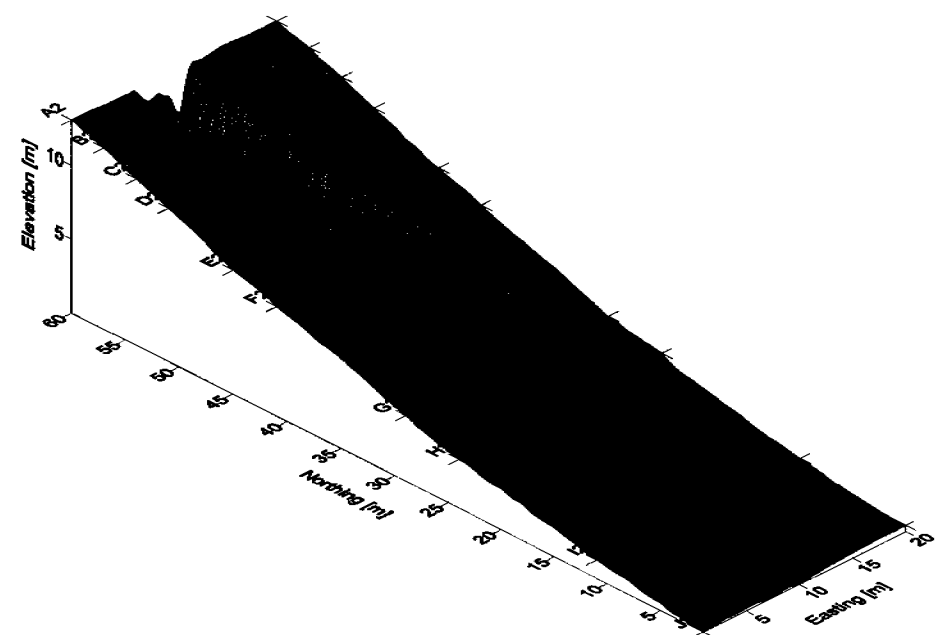
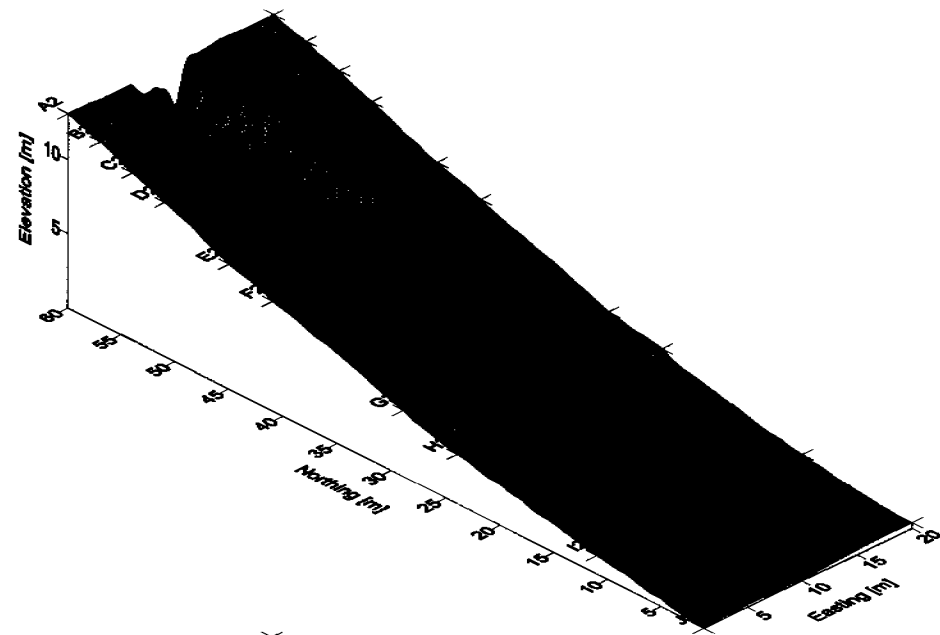


Figure 5.4.8: Simulations for standard batter slope profile with increased width inlet point to four points instead of only two, combined with randomised erodibility, at a) 1.5 hours, b) 2 hours this represents the second storm event, and c) 2.5 hours and d) 3 hours representing the final storm event.

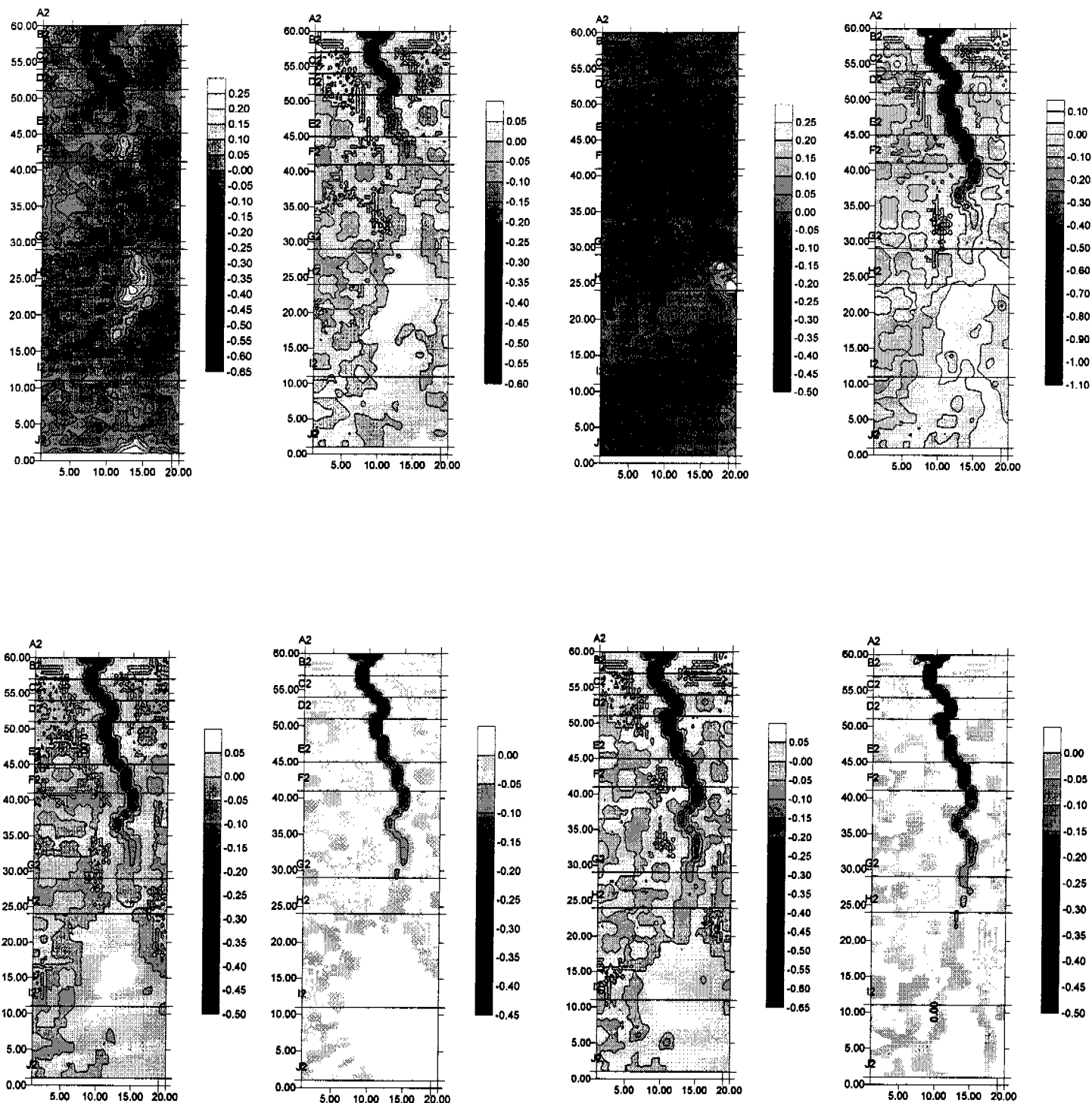
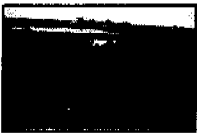


Figure 5.4.9: The morphology contour plots a) initial profile and 10 minutes, b) 10 minutes and 20 minutes, c) 20 minutes and 30 minutes, d) 30 minutes and 1 hour. The difference in elevations are also calculated from the remainder of the simulations with e) difference between 1 hours and 1.5 hours, f) 1.5 and 2 hours, g) 2 and 2.5 hours, and h) 2.5 and 3 hours.



5.5 Differential Erodibility with Depth

The next component of this investigation involved alteration of the nature of surface material from randomised erodibility (somewhat heterogeneous) to include differential erodibility with depth function.

By approximating erodibility using mean grain diameter basis, an increase in d_{50} from 2mm to 20mm over 2m depth equated to a reduction in erodibility of 30 fold. This represents a conservative estimate, as illustrated in Figure 4.3.5, with these ratios considered very conservative over a differential depth of only 20cm. However, as noted once the armouring rock layer was breached and the soft earthen material extracted from above the mined ore is exposed and this erodibility factor will change dramatically. Further work currently being conducted into dynamism in sediment size profile, with development over the dry season also considered important given the rate of geochemical weathering noted on the waste rock dumps.

The preliminary investigation would also involve an assessment of the impact of a change in the magnitude of this reduction factor, with modelling simulations used to evaluate the impact of decreasing this factor to 1/10, with depth coefficient set at $C \sim 2$, instead of $C \sim 15$.

Figure 5.5.1, and Figure 5.5.2 illustrate simulations using only the depth coefficient of $C = 2$. The comparison between Figure 5.1.1, and Figure 5.1.2 with these runs suggest that depth coefficient chosen reduces depth of erosion in all sections uniformly, with maximum erosion depth of 5 to 6m compared to about 4m for these predictions.

Equation 4.3.1 highlights the mechanism by which this armouring component functions. The change of elevation is calculated for each node point during a iteration and then this result is multiplied by the depth-erodibility relationship to reduce this depth by a factor of 1/10 for Figure 5.5.1_a, to Figure_d. However for the next iteration representative of the consequent storm event, the same scenario is repeated, as equation is reapplied and depth of erosion is reduced by a factor of 1/10 again. This can be observed as a jump in erosion depth between Figure 5.5.1_d and 5.5.2_a.

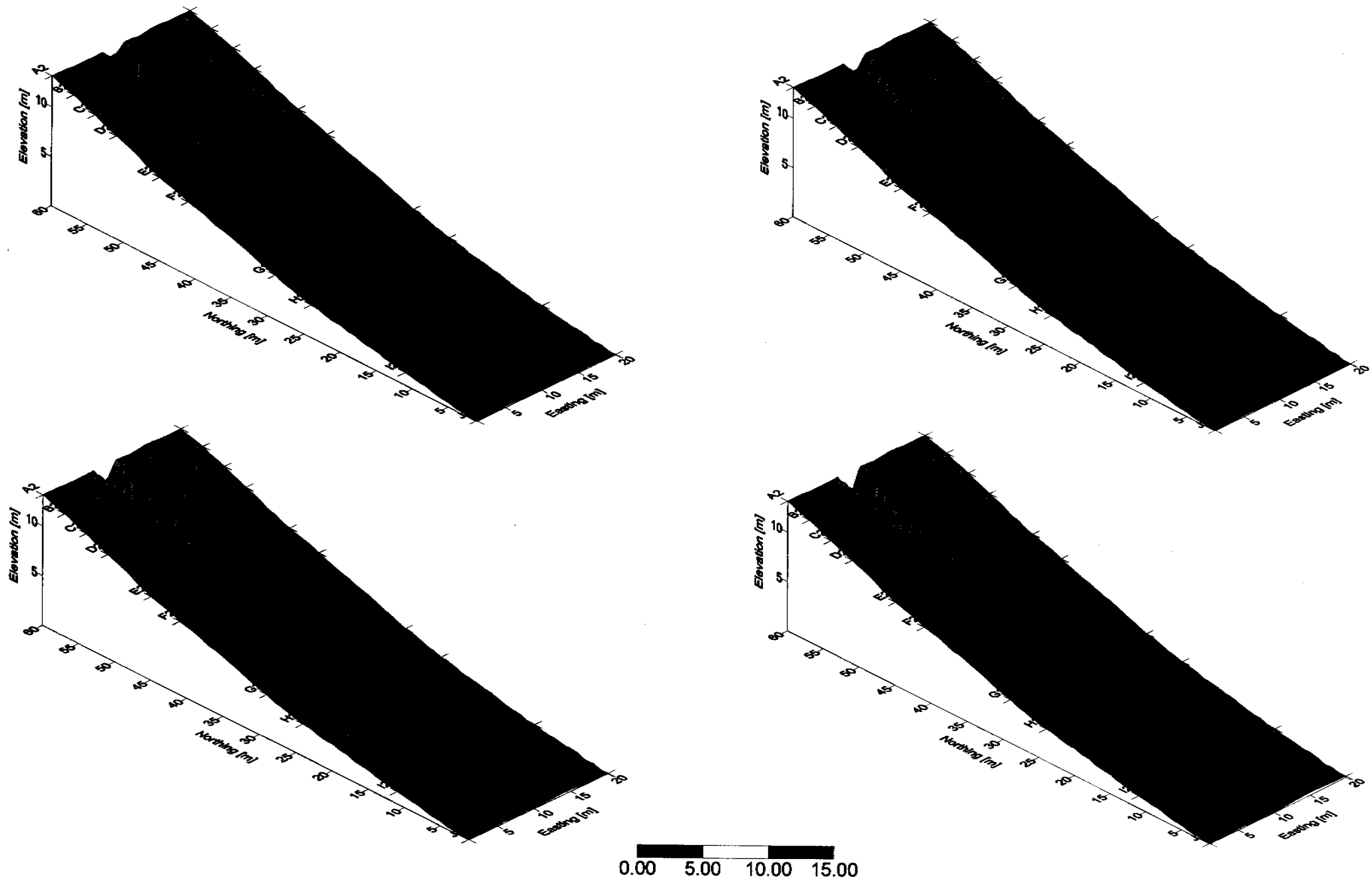


Figure 5.5.1: Simulations for standard batter slope profile with differential erodibility with depth function set at depth coefficient of 2, at a) 10 minutes, b) 20 minutes, c) 30 minutes, and d) 1 hour.

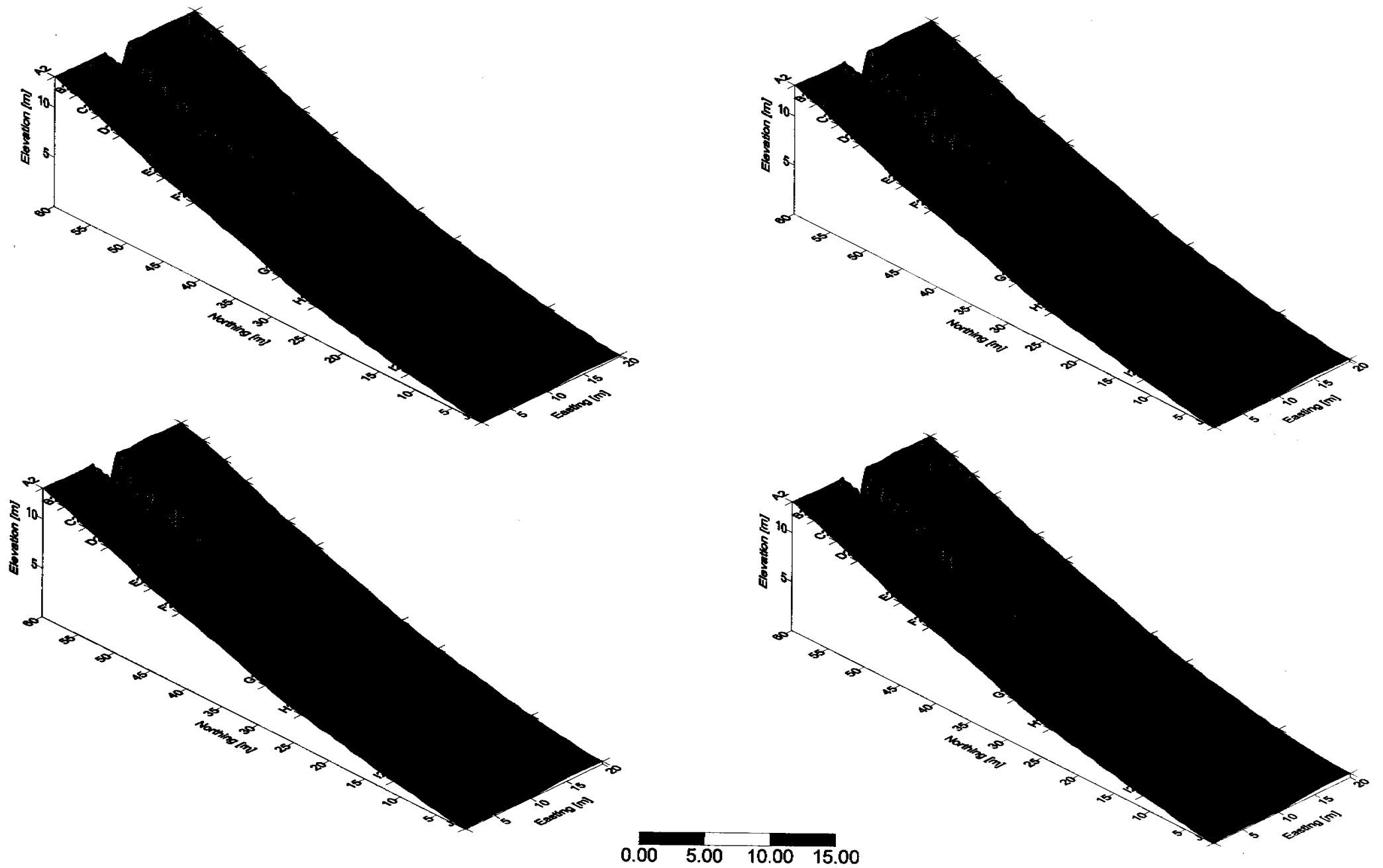


Figure 5.5.2: Simulations for standard batter slope profile with differential erodibility with depth function set at depth coefficient of 2, at a) 1.5 hours, b) 2 hours this represents the second storm event, and c) 2.5 hours and d) 3 hours representing the final storm event.

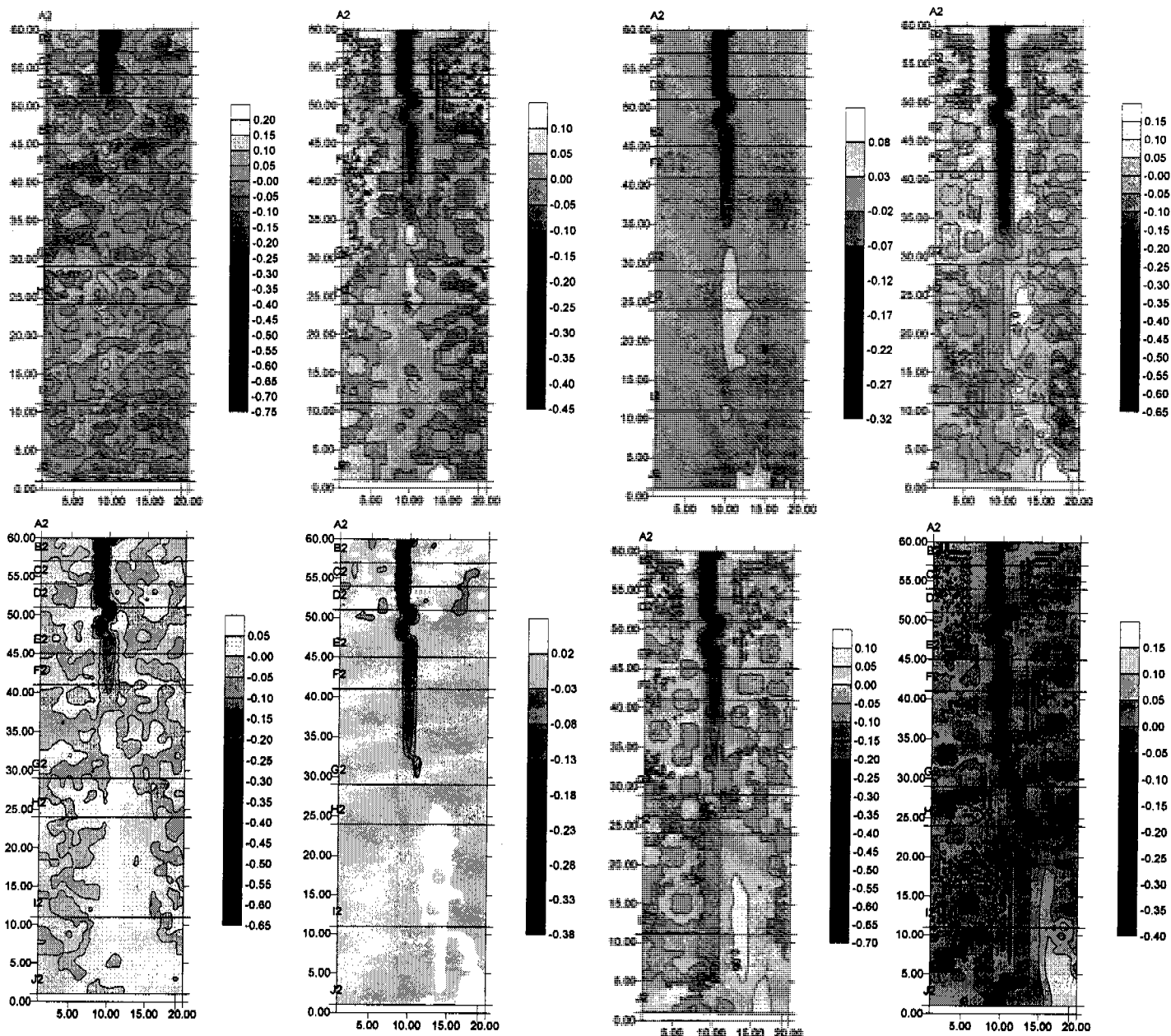


Figure 5.5.3: The morphology contour plots a) initial profile and 10 minutes, b) 10 minutes and 20 minutes, c) 20 minutes and 30 minutes, d) 30 minutes and 1 hour. The difference in elevations are also calculated from the remainder of the simulations with e) difference between 1 hours and 1.5 hours, f) 1.5 and 2 hours, g) 2 and 2.5 hours, and h) 2.5 and 3 hours.



Monitoring Gully Formation

The implementation of a series of three initial surfaces is not considered the usual adaptation for this model, and as such this application would represent an over-prediction of erosion depth for these simulations.

The implementation of the armouring component can be considered at the developmental stage, with a more realistic approximation devised when a depth coefficient of $C \sim 15$, equating to a reduction factor of $1/30$ when adopted. Figure 5.5.4, and Figure 5.5.5 illustrate these simulations, with Figure 5.5.6 highlighting the change in elevations between simulation time periods.

Maximum erosion depth, in this case reaches to only about 2 to 3m, approximately half of that observed in simulations observed in Section 5.1.

The development of the gully is similar between the lower erodibility coefficient and high erodibility coefficient, with more deposition of material with increased erosion associated with reduction factor of $1/10$.

This is also verified when compared to the standard scenario Figure 5.1.1, and Figure 5.1.2, where the change in curvature at Row H to Row G is associated with accumulation of material and change in the path of the gully. Once again this behaviour is representative of an alteration in only one component, with the combination of these simulations with inclusion of randomised erodibility considered an even more realistic approximation.

Figure 5.5.7, and Figure 5.5.8 illustrate the effect of reduction of erodibility with depth on the extended batter site (Figure 5.1.4, and Figure 5.1.5). Similarities in development can be observed between these figures, however it is noted that from Figure 5.1.4_d compared to Figure 5.5.7_d, that the gully can be seen to have developed to reach Row G, whereas it has reached only Row E in the earlier simulation. A similar comparison using Figure 5.5.4_d and Figure 5.1.1_d that although the gully depth of only about 10cm, the formation has reach almost Row I (at 60 minutes). Two explanations for this phenomenon, with reduction in transported sediment equating to a reduction in material deposited at the outlet of the gully resulting in drainage direction at these outlet points not being altered.

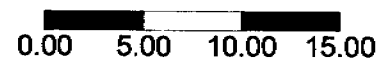
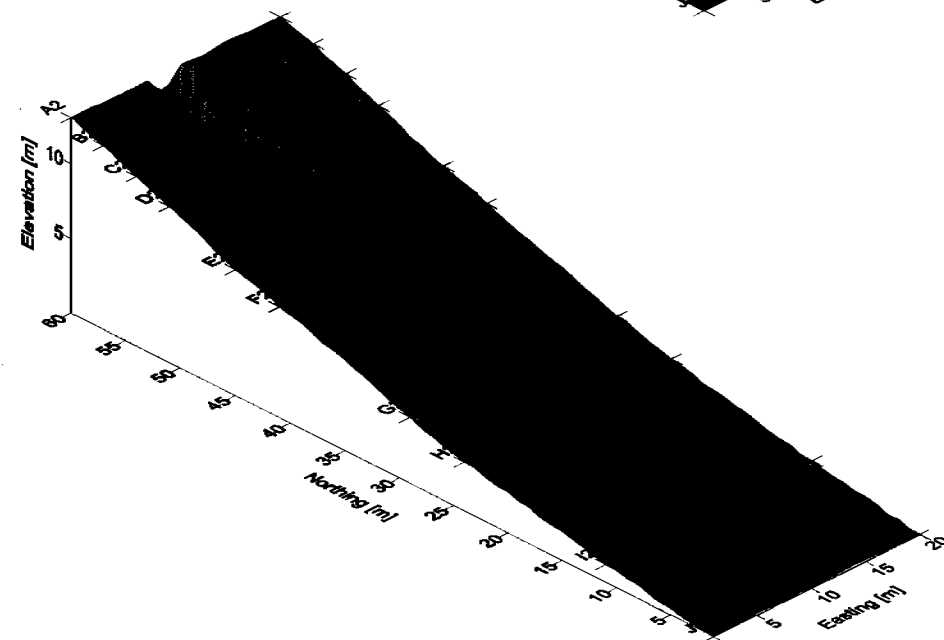
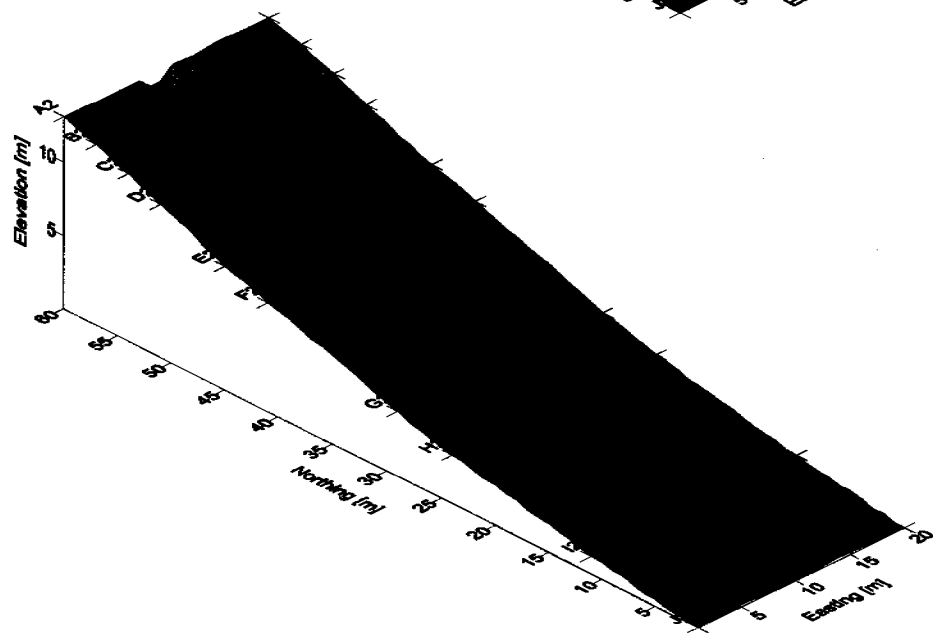
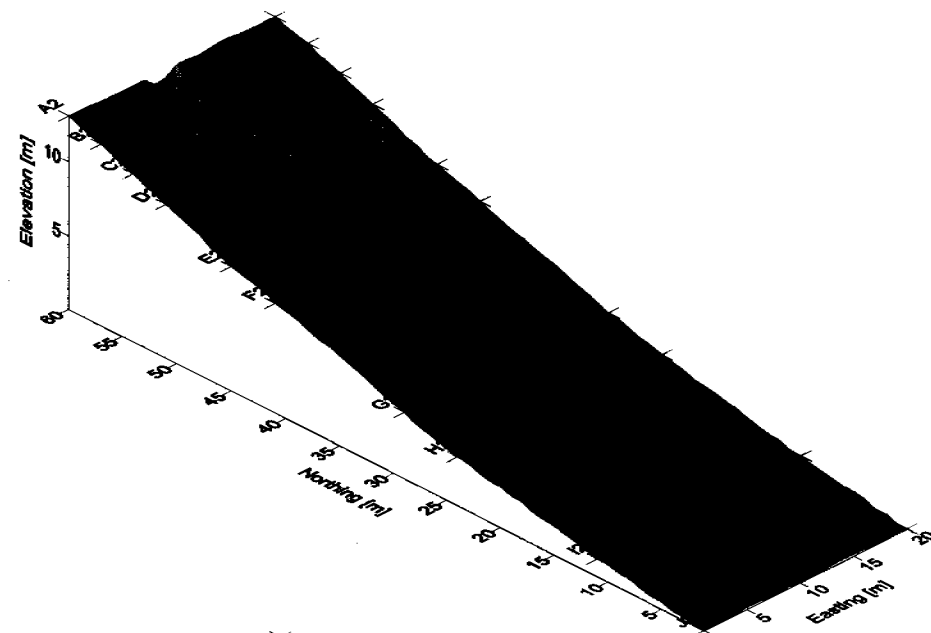
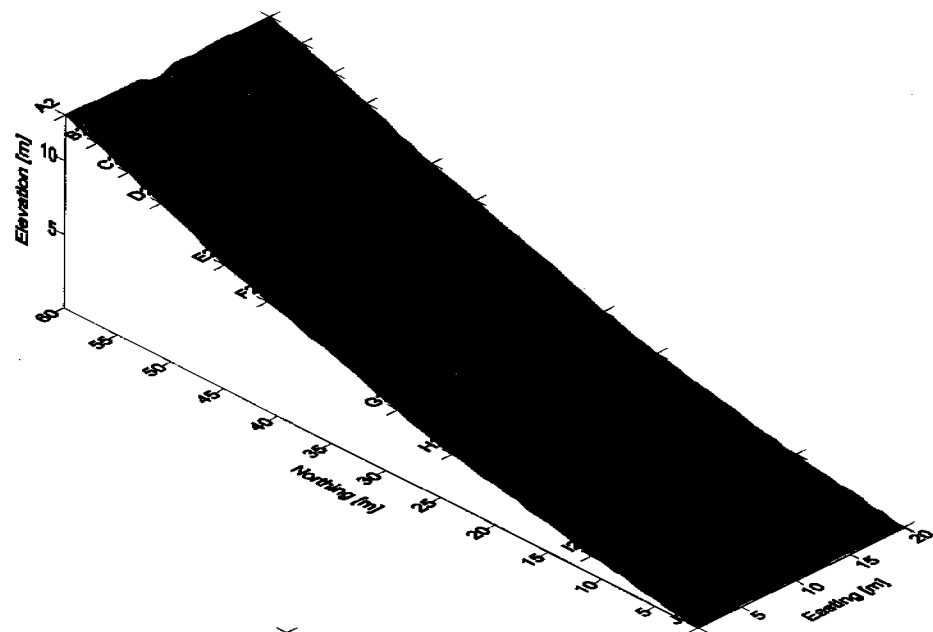


Figure 5.5.4: Simulations for standard batter slope profile with differential erodibility with depth function set at depth coefficient of 15, at a) 10 minutes, b) 20 minutes, c) 30 minutes, and d) 1 hour.

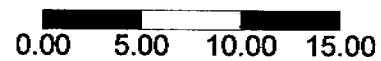
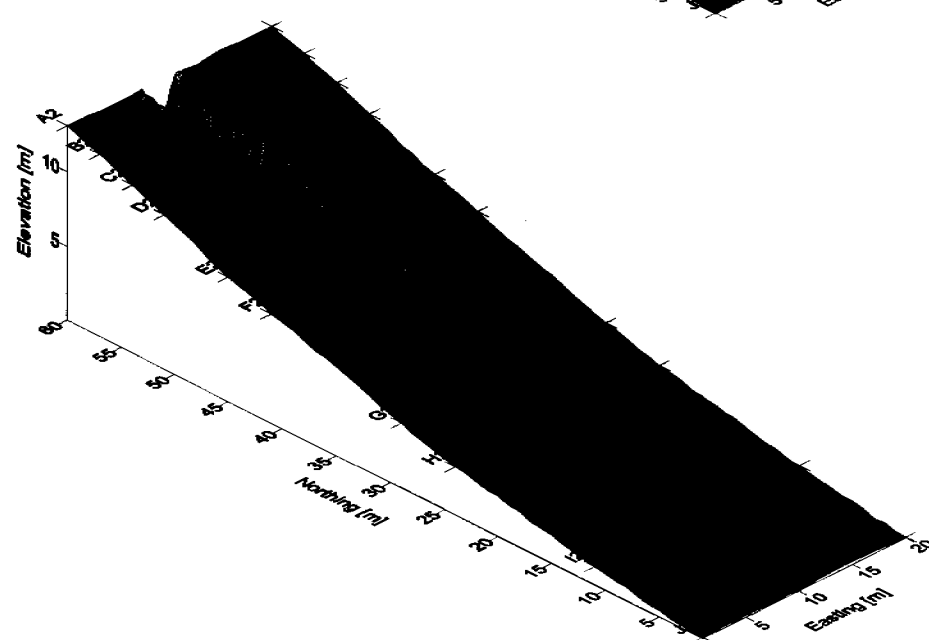
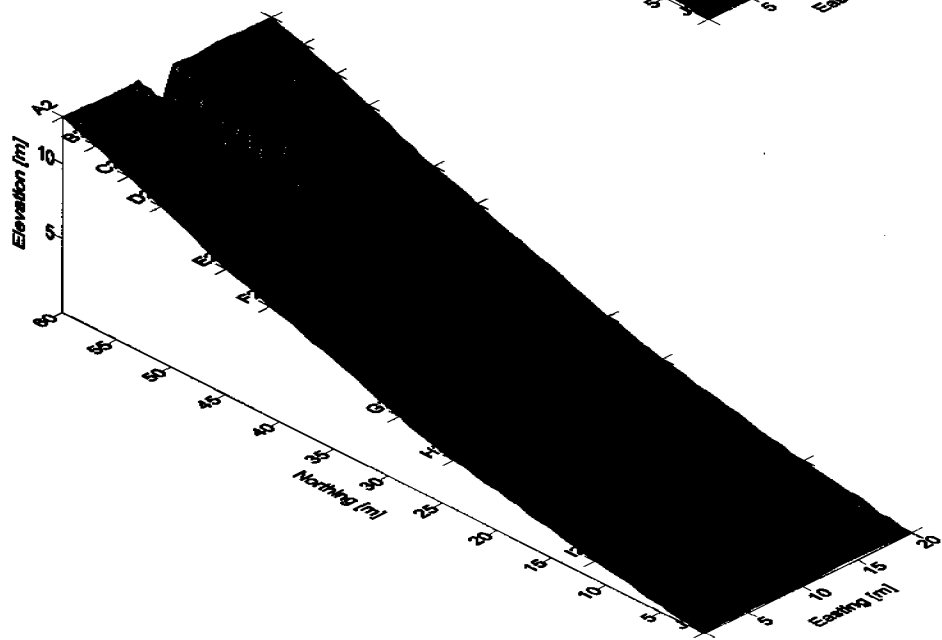
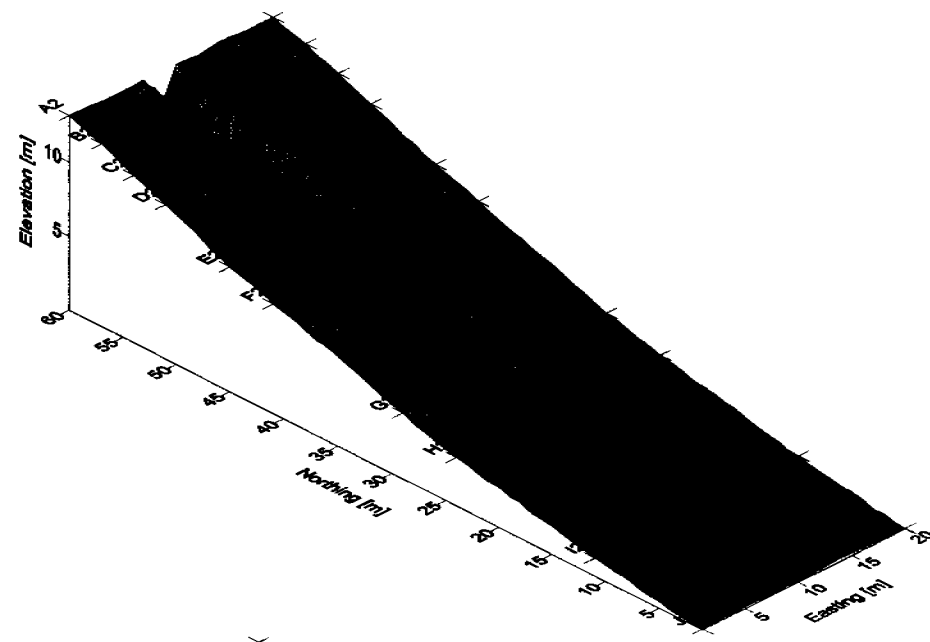
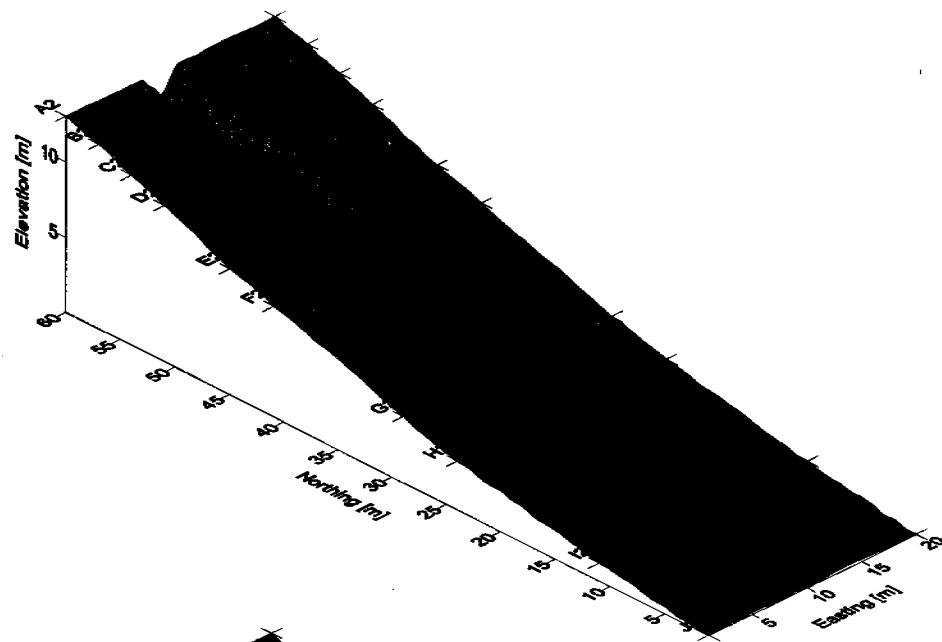


Figure 5.5.5: Simulations for standard batter slope profile with differential erodibility with depth function set at depth coefficient of 15, at a) 1.5 hours, b) 2 hours this represents the second storm event, and c) 2.5 hours and d) 3 hours representing the final storm event.

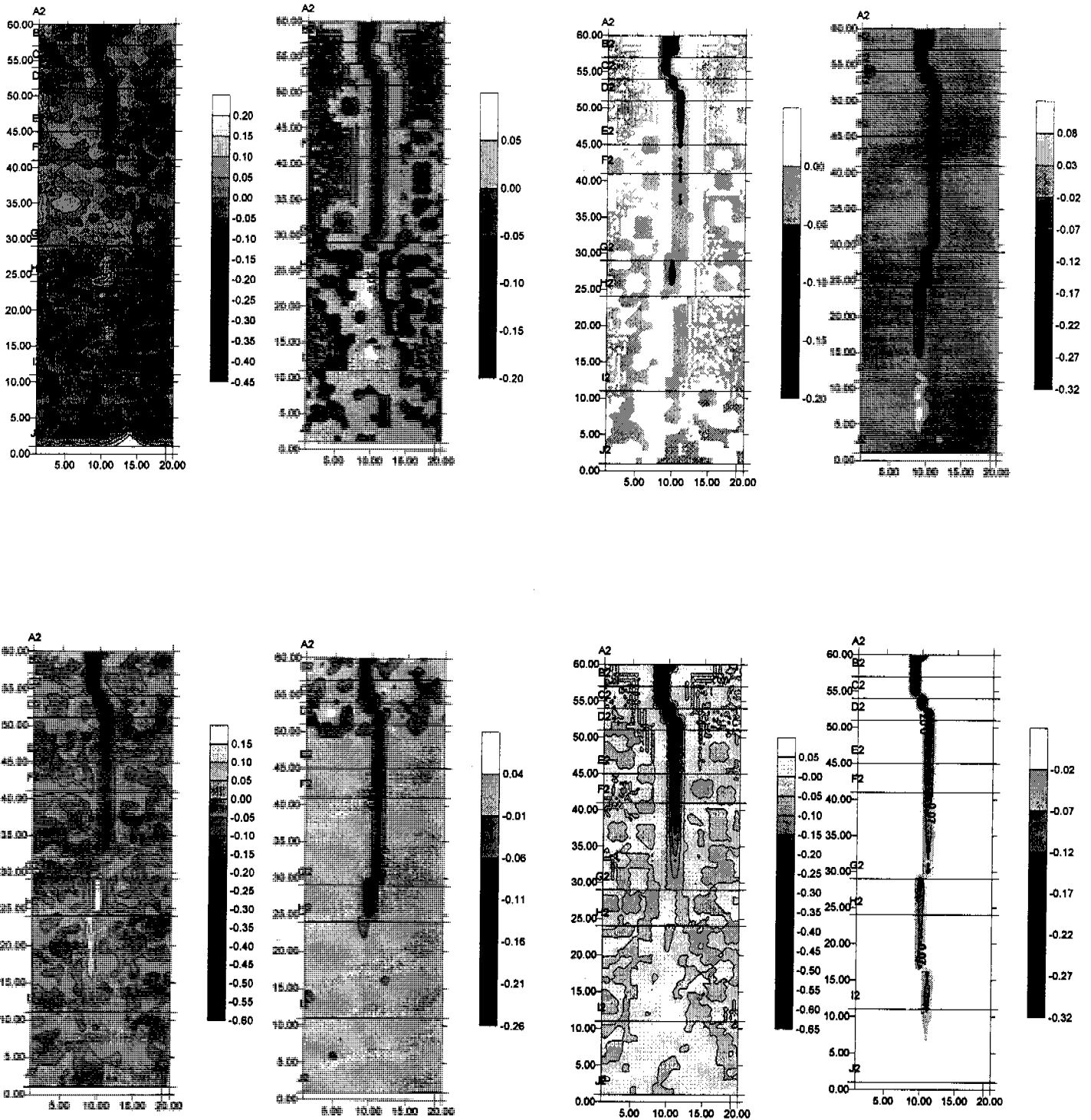


Figure 5.5.6: The morphology contour plots a) initial profile and 10 minutes, b) 10 minutes and 20 minutes, c) 20 minutes and 30 minutes, d) 30 minutes and 1 hour. The difference in elevations are also calculated from the remainder of the simulations with e) difference between 1 hours and 1.5 hours, f) 1.5 and 2 hours, g) 2 and 2.5 hours, and h) 2.5 and 3 hours.

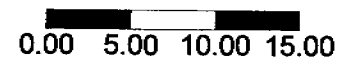
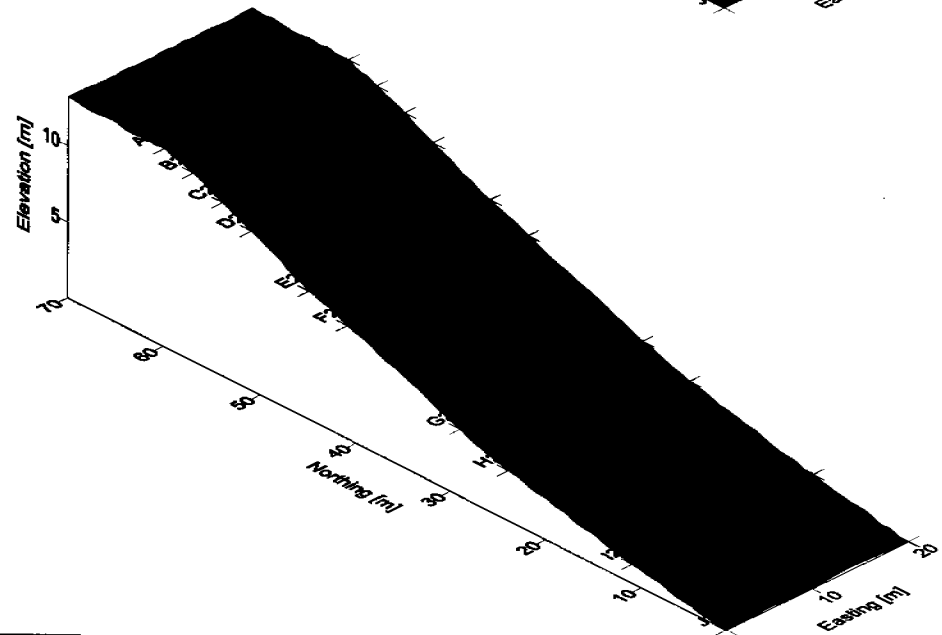
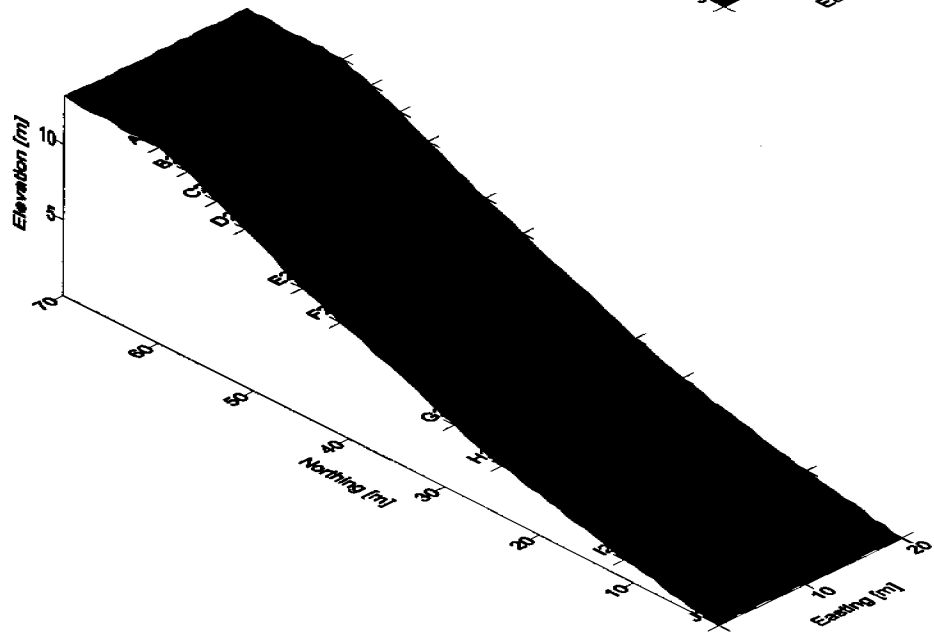
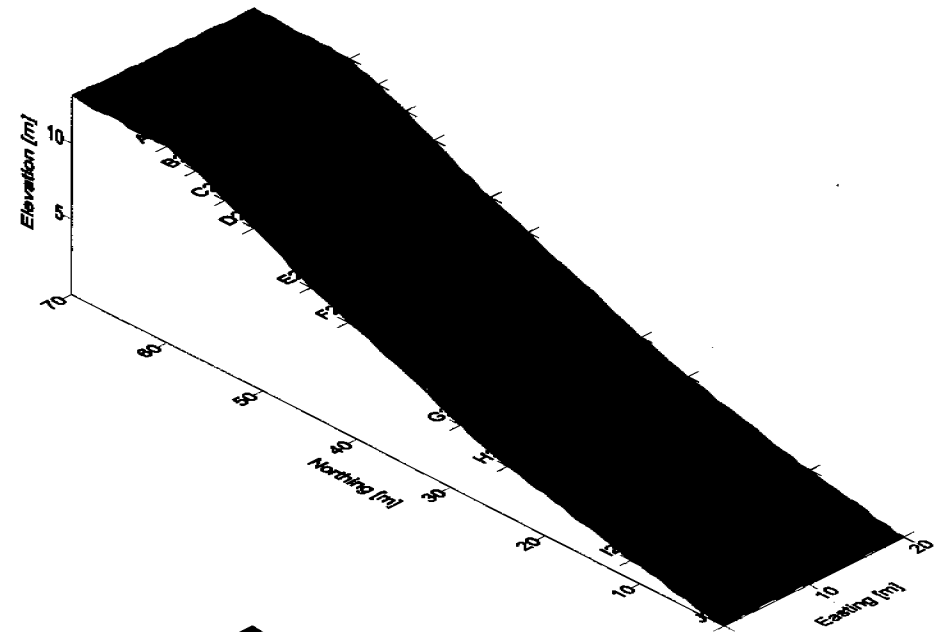
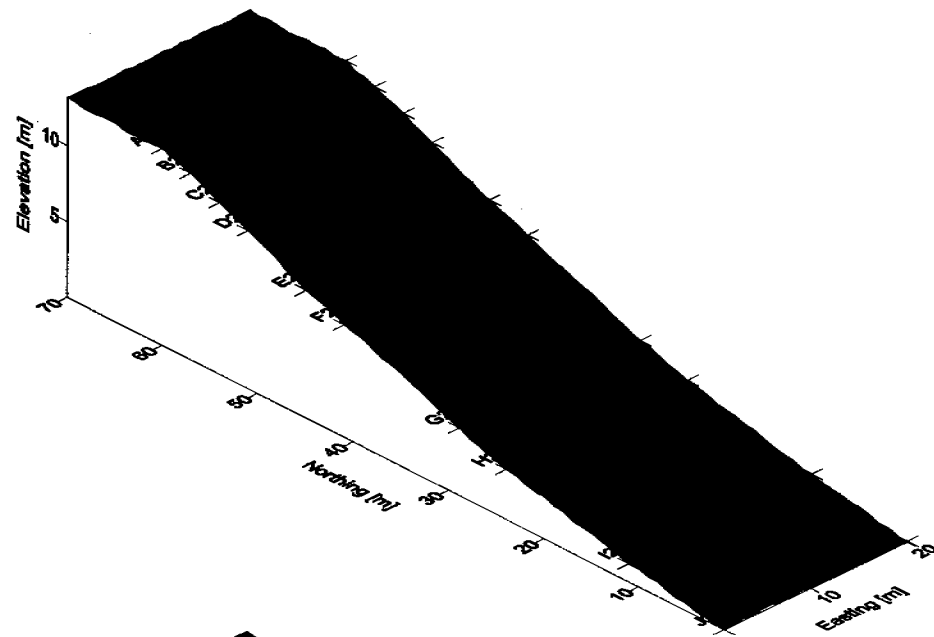


Figure 5.5.7: Simulations for extended batter slope profile with differential erodibility with depth, at a) 10 minutes, b) 20 minutes, c) 30 minutes, and d) 1 hour.

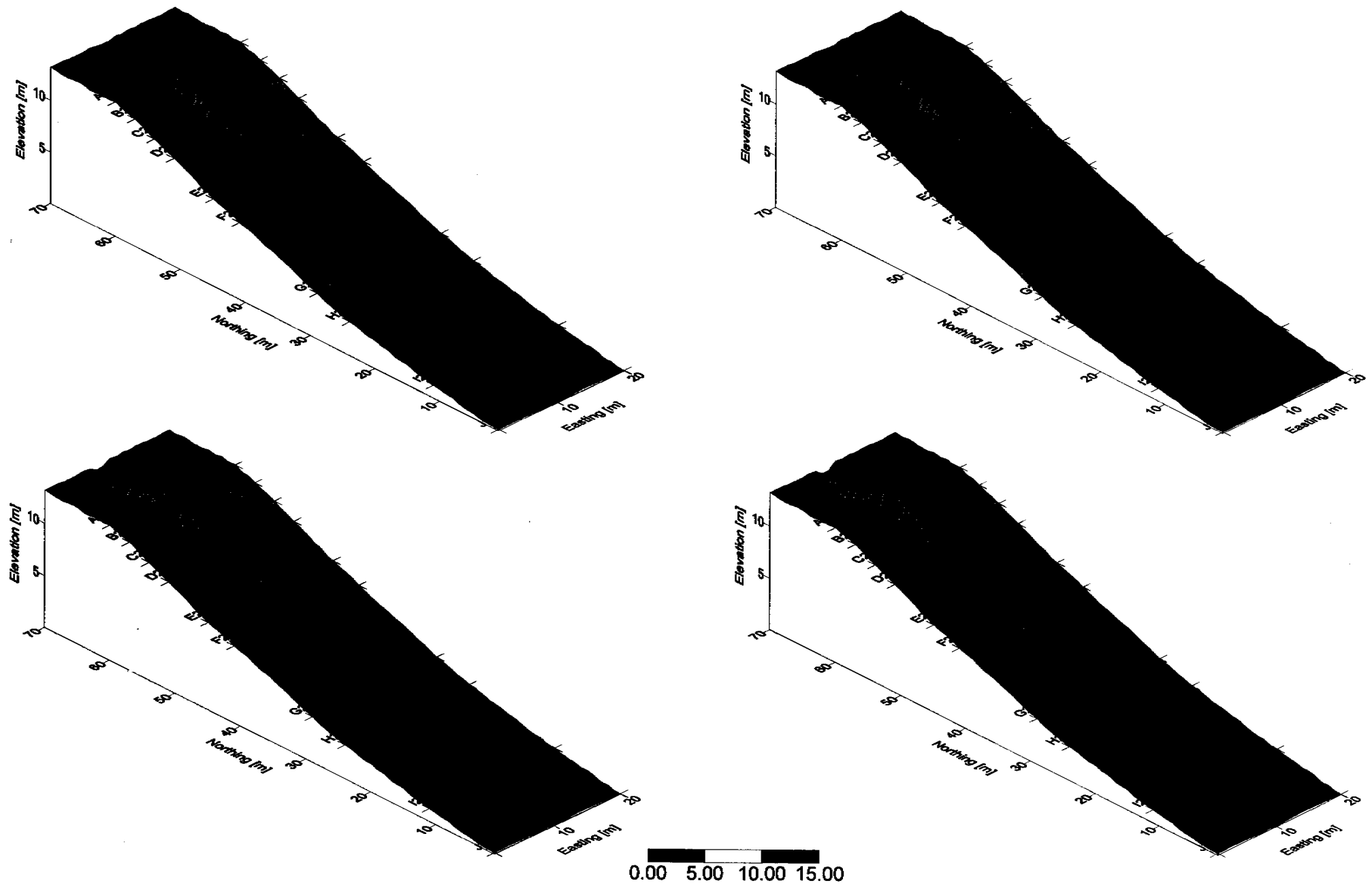


Figure 5.5.8: Simulations for extended batter slope profile with differential erodibility with depth function, at a) 1.5 hours, b) 2 hours this represents the second storm event, and c) 2.5 hours and d) 3 hours representing the final storm event.

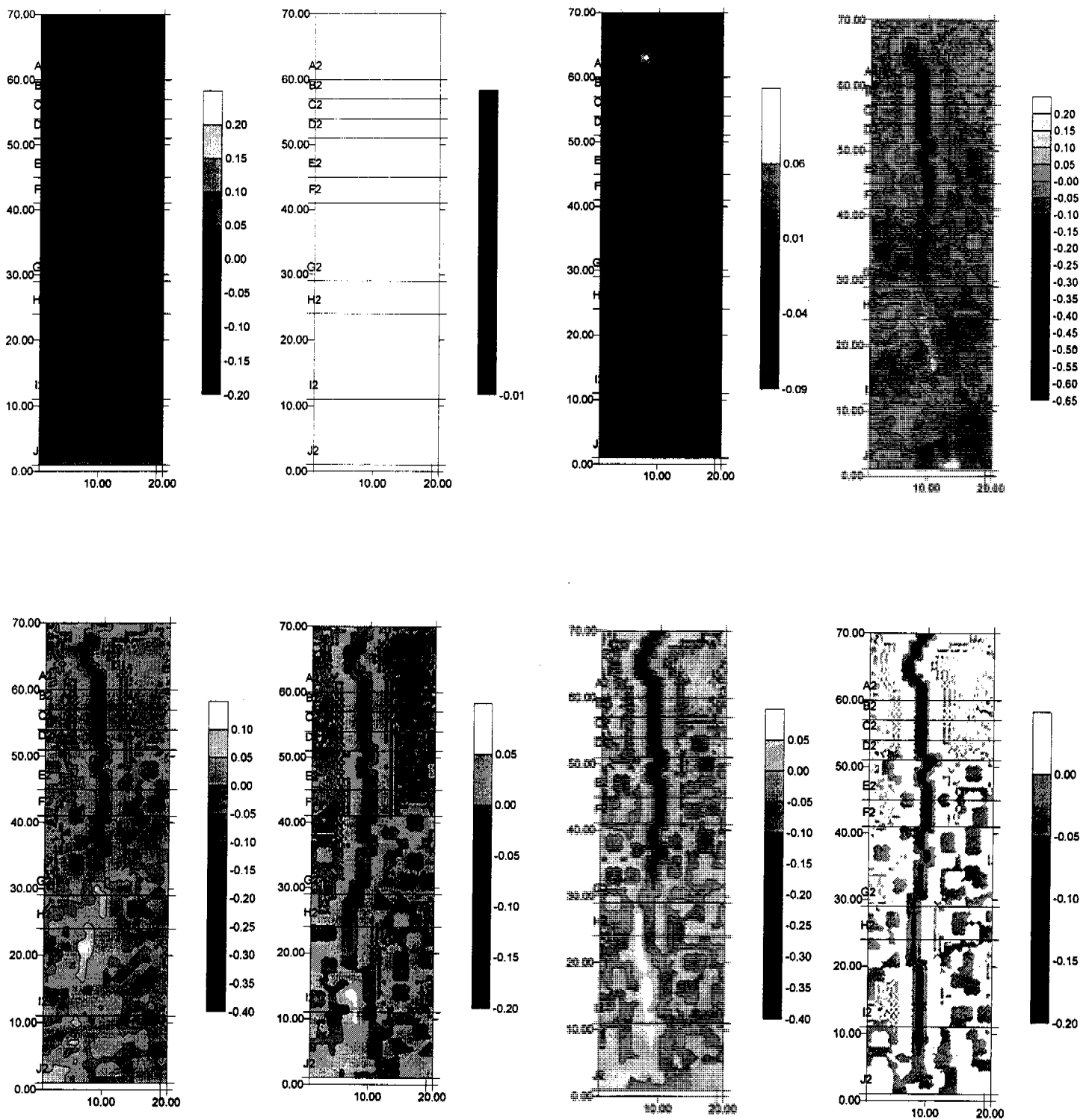


Figure 5.5.9: The morphology contour plots a) initial profile and 10 minutes, b) 10 minutes and 20 minutes, c) 20 minutes and 30 minutes, d) 30 minutes and 1 hour. The difference in elevations are also calculated from the remainder of the simulations with e) difference between 1 hours and 1.5 hours, f) 1.5 and 2 hours, g) 2 and 2.5 hours, and h) 2.5 and 3 hours.



Monitoring Gully Formation

This is observed in Figure 5.1.1_d where the gully has developed to beyond Row F, and has incised about 0.5 to 0.8m at this point, whilst the gully in Figure 5.5.4_d has developed to Row H with depths of about 40cm at Row F and 10cm noticeable due to the uniform nature of the material. Material deposited at the outlet of the gully in Figure 5.1.1_d is not apparent in Figure 5.5.4_d.

The other observation is made by the comparison between Figure 5.5.4_d and 5.5.5_d at 60 minutes and 1.5 hours respectively, where material from increased incision of the gully in the upper section smothers the 10cm pathway revealed at the 60 minute time period. This is illustrated in Figure 5.5.6 where about 10 to 15cm of material is deposited over the gully at Row H to Row I. This suggests a change in the overall discharge relationship β_3 from 0.00272 to 0.00199 has an impact on the nature of erosion at these points, with the same observation made comparing Figure 5.5.7_a and Figure 5.5.8_a with shallow formation at the bottom end of slope smothered by introduction of consequent storm event.

The next considerations were the combination of randomised erodibility and the depth-erodibility coefficient for both the usual cases including increased inlet width, whilst similarities between simulations without inclusion of wide inlet verify previous observations.

The first scenario is illustrated Figure 5.5.10, with Figure 5.5.11 representing the second and third storm events with narrow inlet feed and the combination of characteristics from randomised erodibility and armouring erosion module. Figure 5.5.12 exhibits an obvious combination of characteristics from investigations above. The depth of erosion is similar to that observed in Figure 5.5.4 and Figure 5.5.5, with the nature of pathway being altered due to the randomised erodibility as expected.

The maximum depth of erosion for simulations incorporating the wide inlet point can be considered similar to Figure 5.5.4, and Figure 5.5.5. Below the inlet zone of influence at Row C in Figure 5.5.13, and Figure 5.5.14, the gully congregates into a single flowpath once again with depth of erosion observed to replicate that of comparative figures.

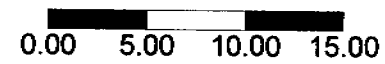
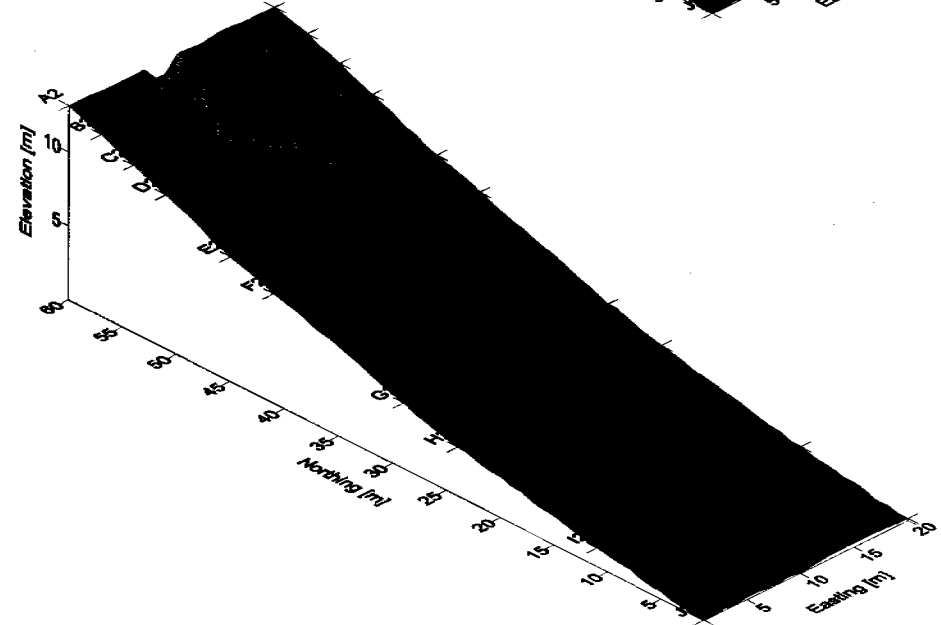
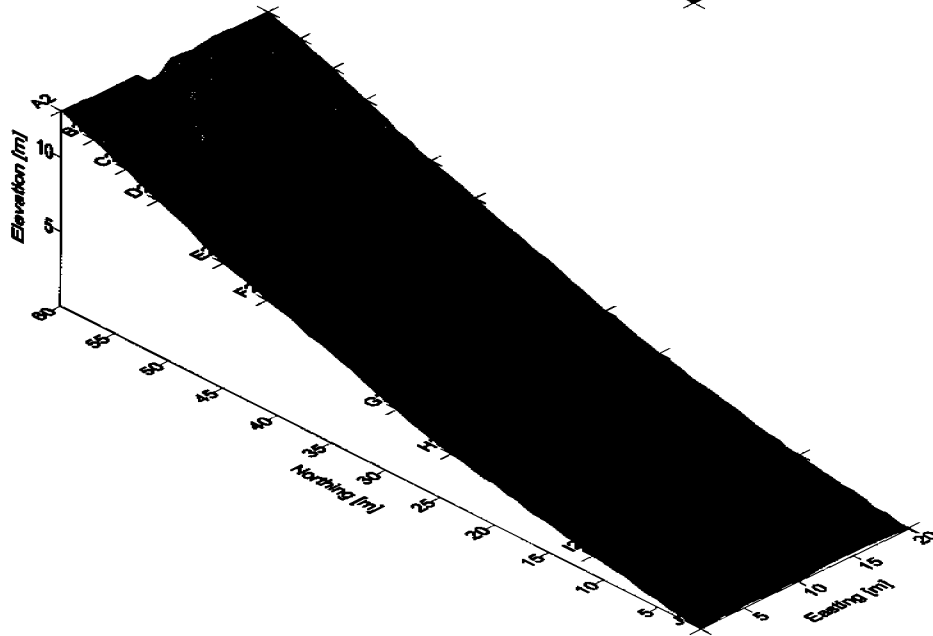
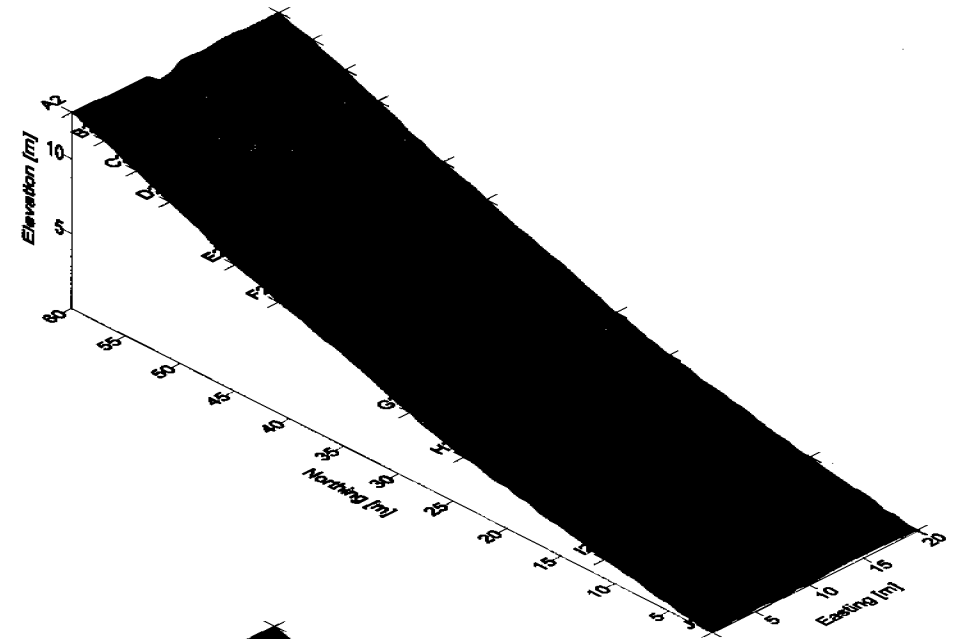
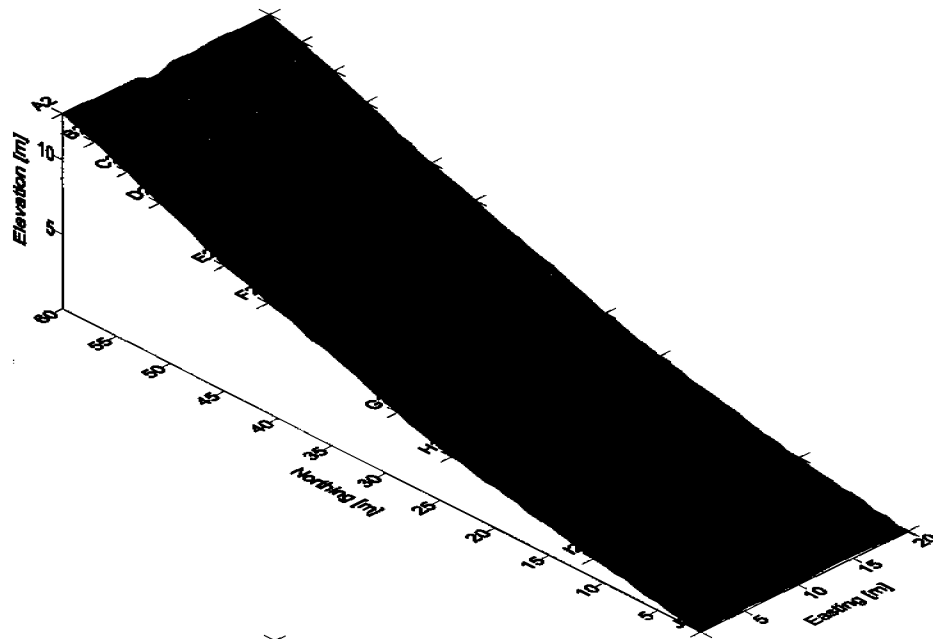


Figure 5.5.10: Simulations for standard batter slope profile with differential erodibility with depth, and randomised erodibility function, at a) 10 minutes, b) 20 minutes, c) 30 minutes, and d) 1 hour.

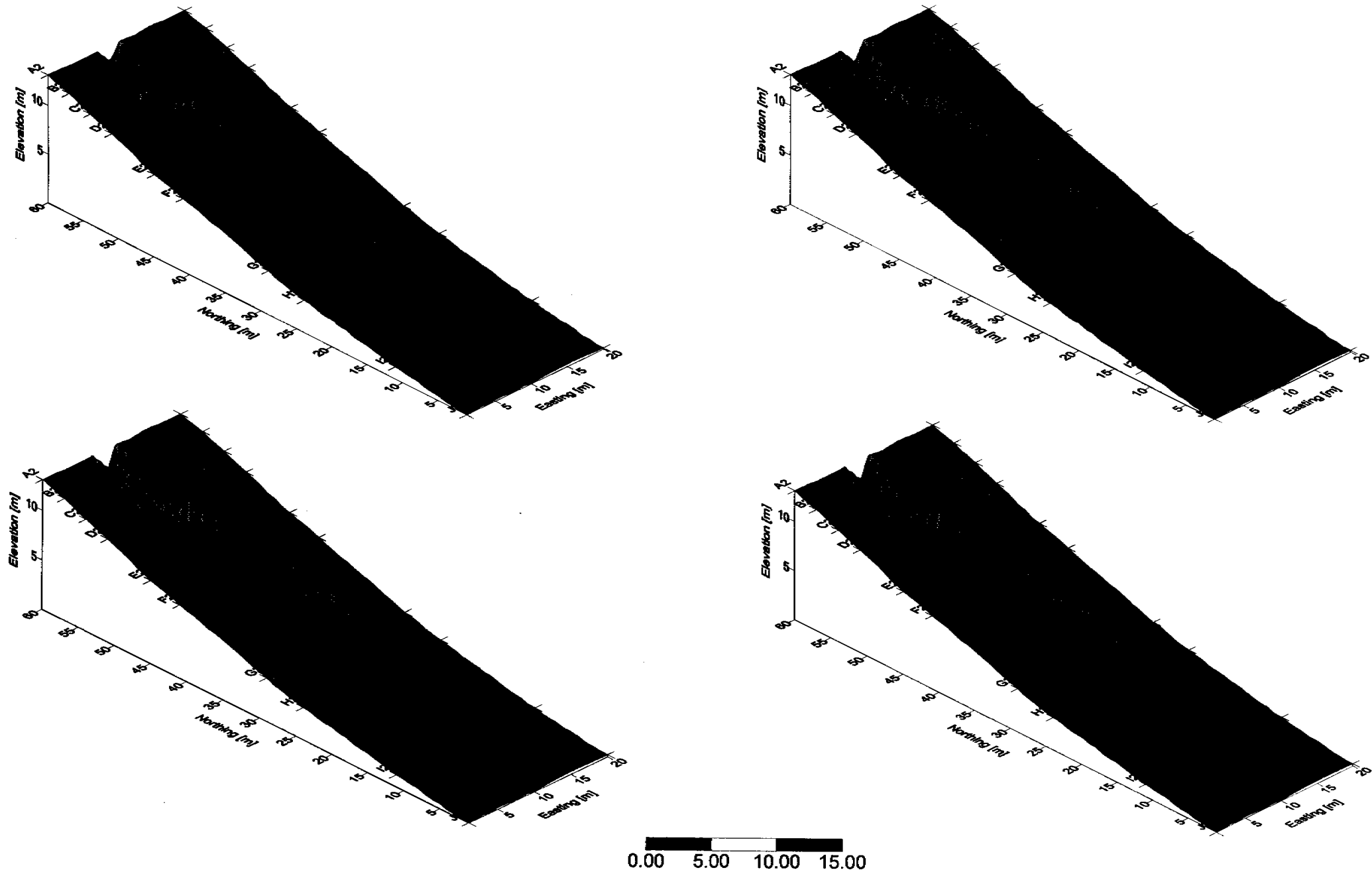


Figure 5.5.11: Simulations standard batter slope profile with differential erodibility with depth, and randomised erodibility function, at a) 1.5 hours, b) 2 hours this represents the second storm event, and c) 2.5 hours and d) 3 hours representing the final storm event.

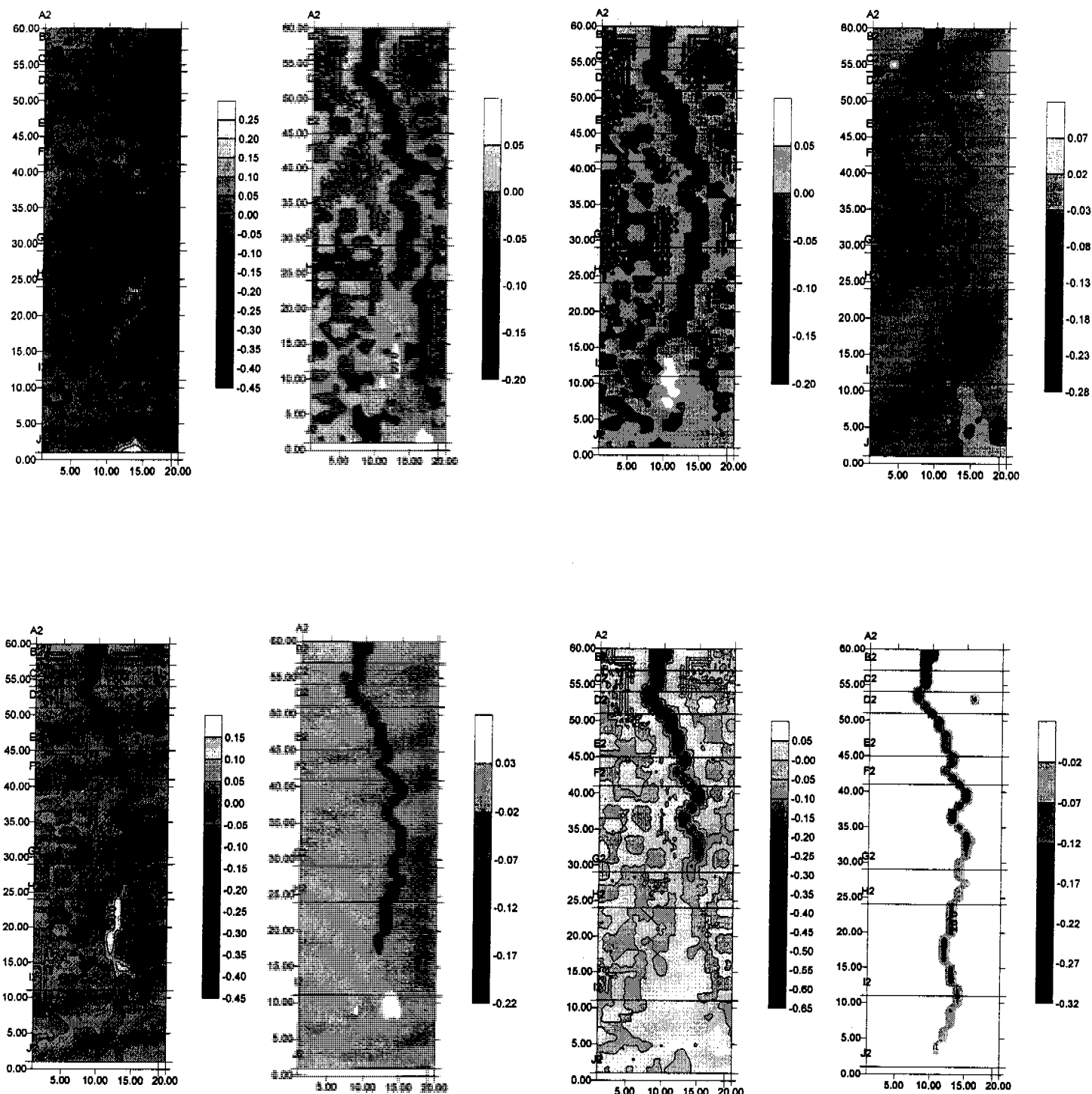


Figure 5.5.12: The morphology contour plots a) initial profile and 10 minutes, b) 10 minutes and 20 minutes, c) 20 minutes and 30 minutes, d) 30 minutes and 1 hour. The difference in elevations are also calculated from the remainder of the simulations with e) difference between 1 hours and 1.5 hours, f) 1.5 and 2 hours, g) 2 and 2.5 hours, and h) 2.5 and 3 hours.

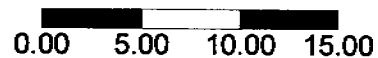
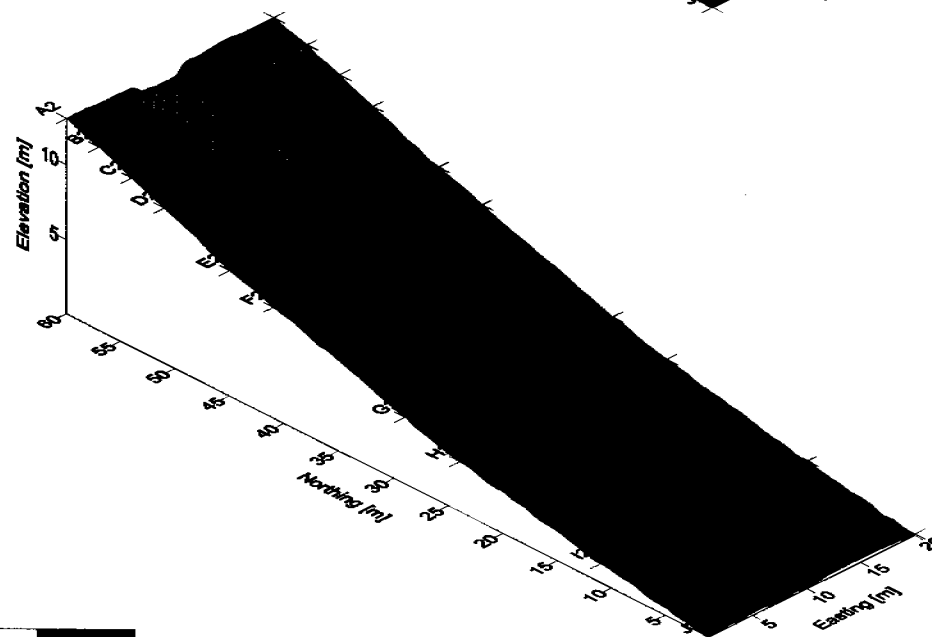
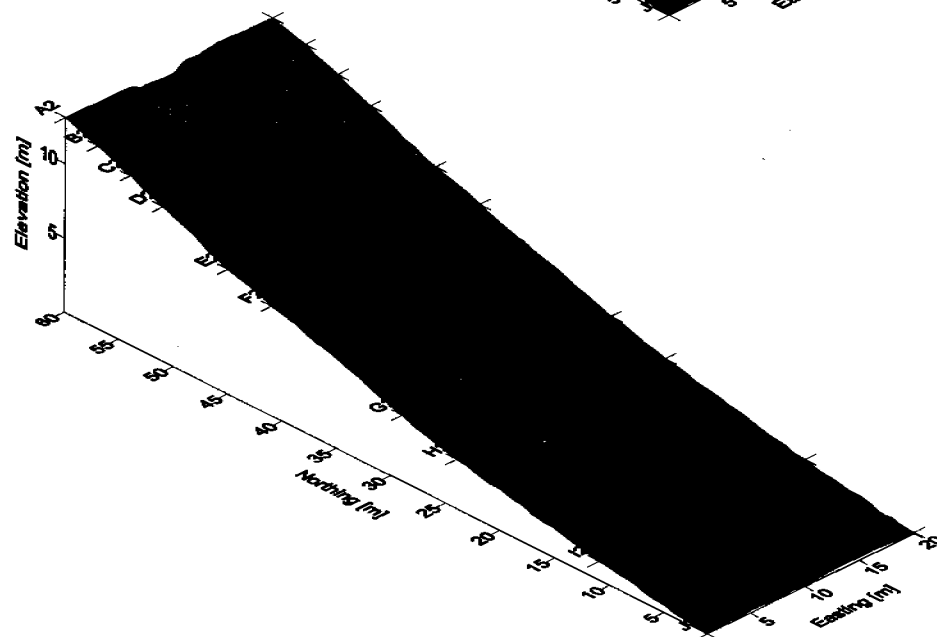
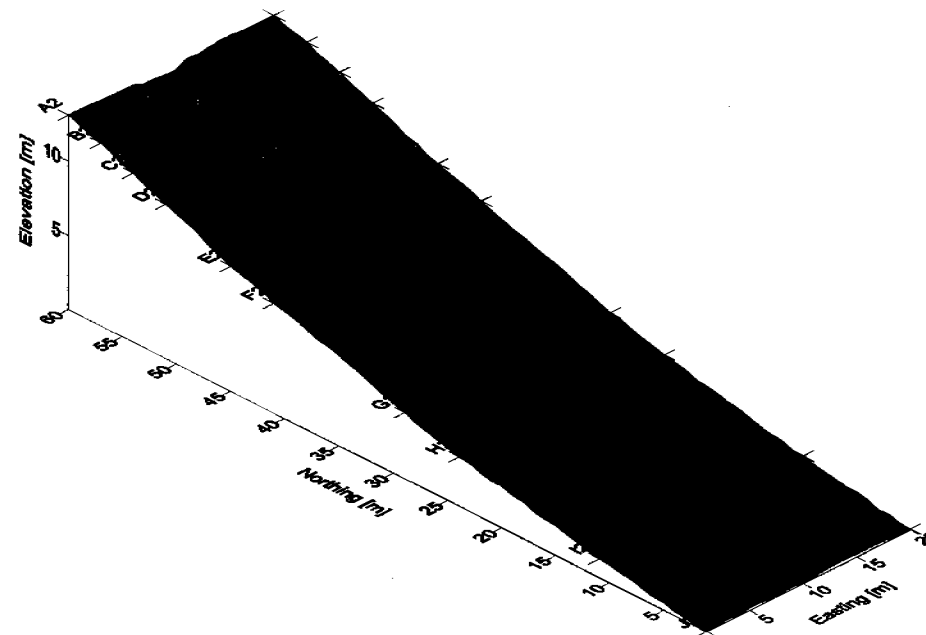
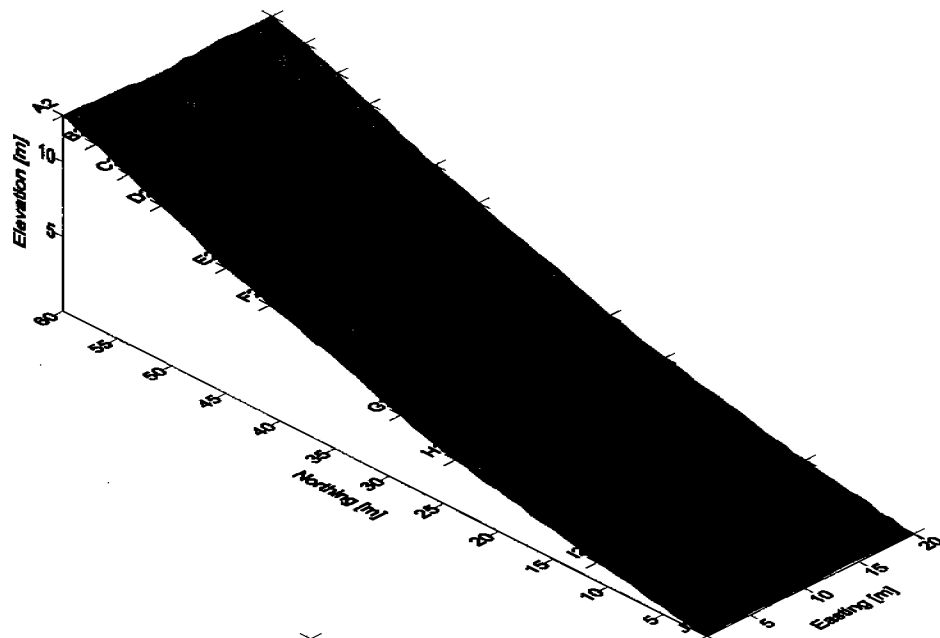


Figure 5.5.13: Simulations for standard batter slope profile with differential erodibility with depth, and randomised erodibility function, as well as wide inlet point, at a) 10 minutes, b) 20 minutes, c) 30 minutes, and d) 1 hour.

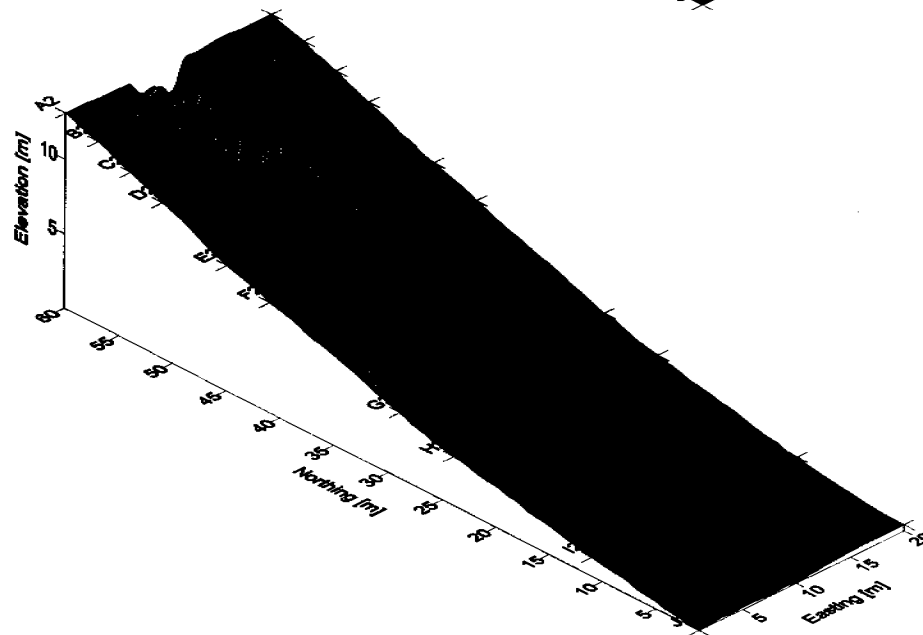
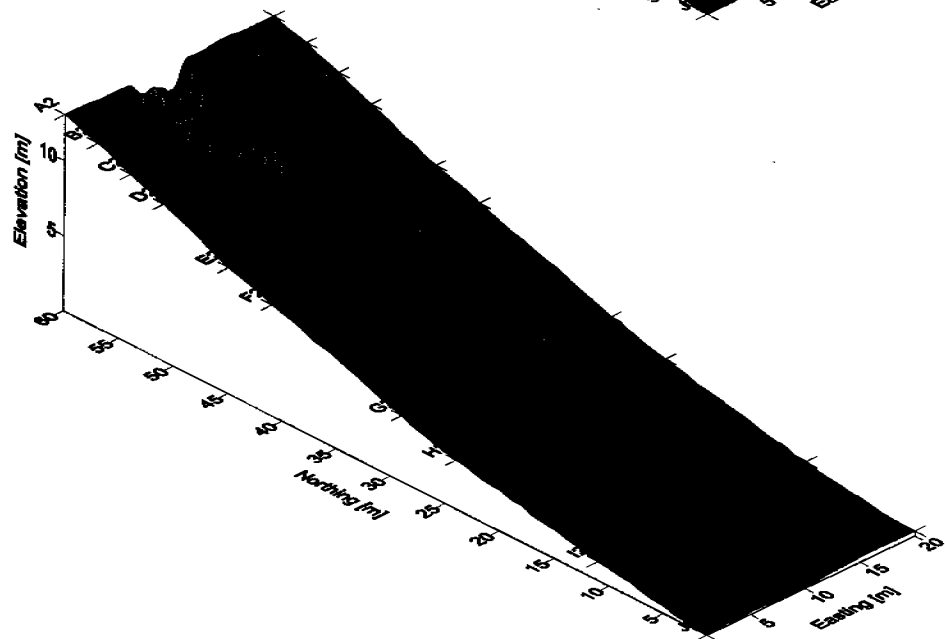
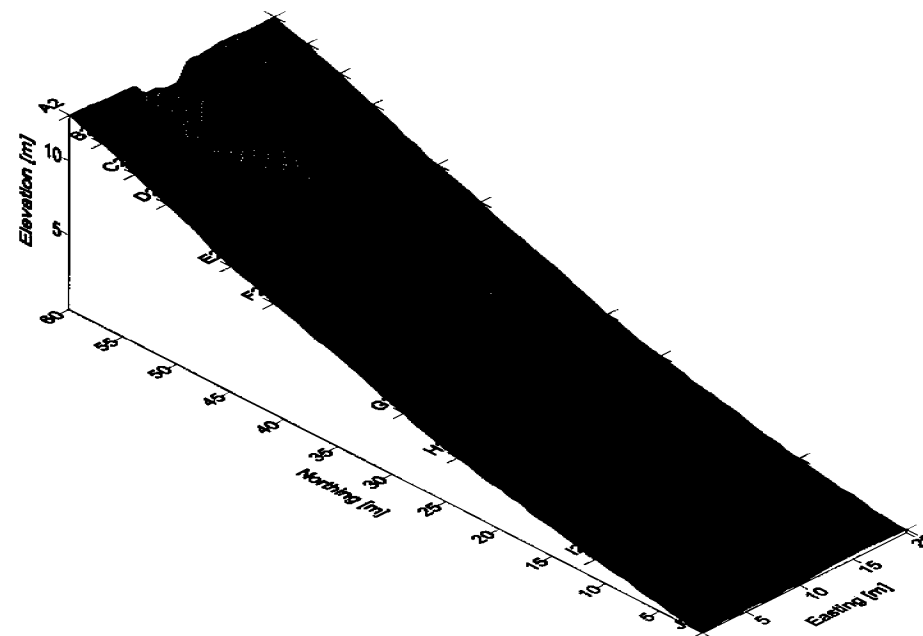
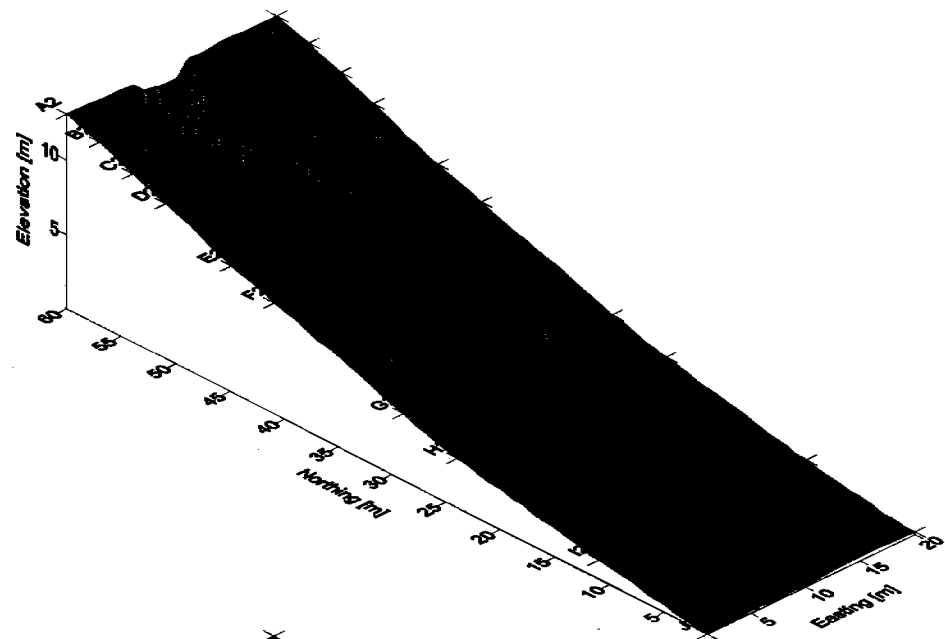


Figure 5.5.14: Simulations standard batter slope profile with differential erodibility with depth, and randomised erodibility function, as well as a wide deep point, a) 1.5 hours, b) 2 hours this represents the second storm event, and c) 2.5 hours and d) 3 hours representing the final storm event.

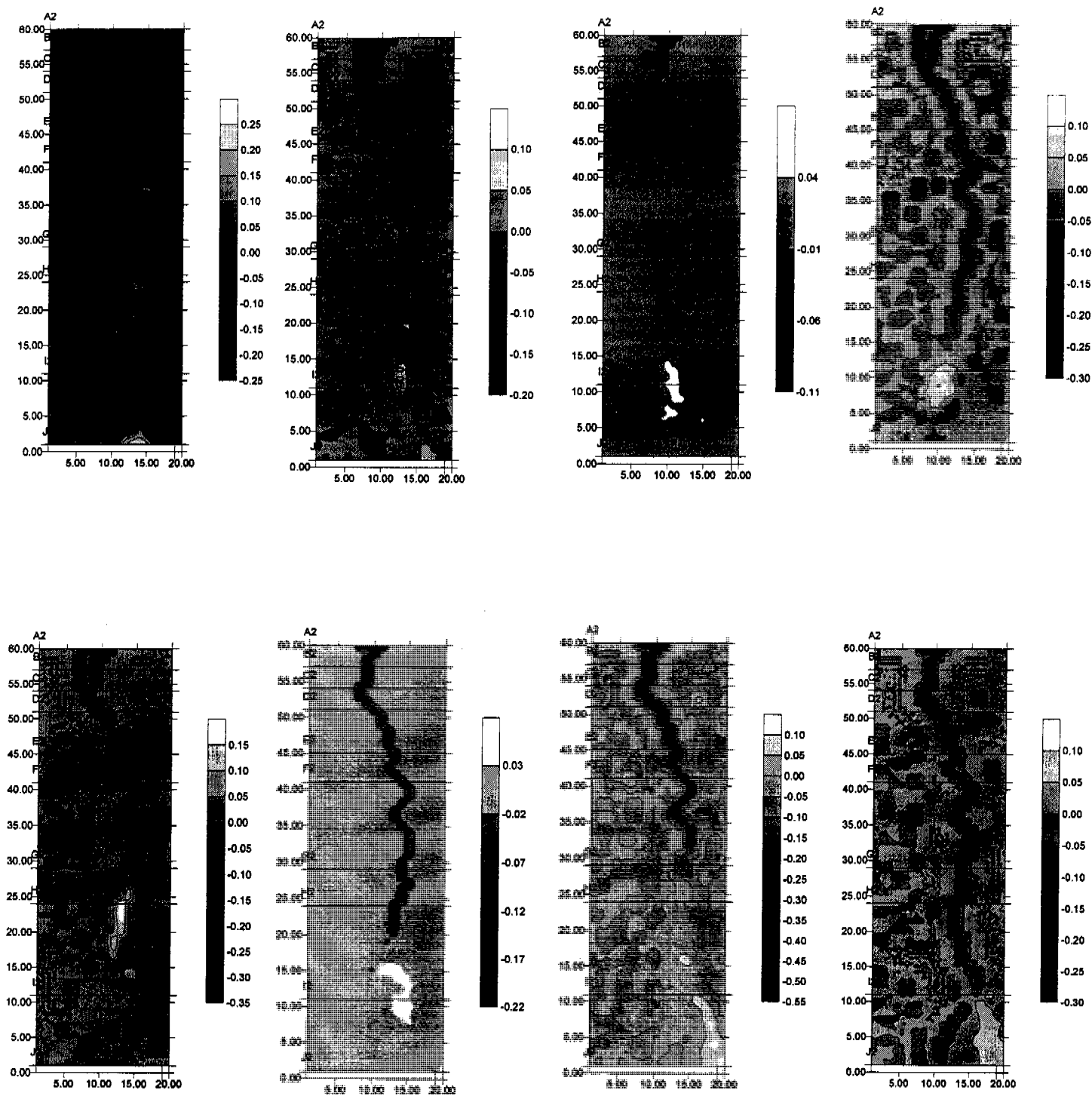


Figure 5.5.15: The morphology contour plots a) initial profile and 10 minutes, b) 10 minutes and 20 minutes, c) 20 minutes and 30 minutes, d) 30 minutes and 1 hour. The difference in elevations are also calculated from the remainder of the simulations with e) difference between 1 hours and 1.5 hours, f) 1.5 and 2 hours, g) 2 and 2.5 hours, and h) 2.5 and 3 hours.



Monitoring Gully Formation

Further investigations consider the same scenarios with the extended batter slope profile, where similar behaviour is exhibited in Figure 5.5.16, Figure 5.5.17 for narrow inlet point, and Figure 5.5.19, and Figure 5.5.20 for wide inlet point respectively.

The gully formation at 60 minutes duration is compared to observations on site in Figure 3.2.6 above, with results of first storm event excavating material between Row B and Row D and gully extending down to Row G. Approximately 40 to 50cm depth of material was transported between Row C to Row D whereas from Figure 5.5.15, a total depth of 60 to 70cm was predicted. It is noted that the initial delay in gully development observed in earlier simulations is repeated in Figure 5.5.19 and Figure 5.5.20 even though final landscapes are of similar extent and magnitude.

The maximum depth of erosion at the head of the gully was 2.2m for the standard case, and 1.9m overall for the extended profile scenario (Figure 5.5.18_d and Figure 5.5.20_d respectively). This represents an over-prediction with maximum depth observed on site at Row A in the order of 20 to 25cm, however as noted, this transition was considered to be heavily armoured and buffered due to the reservoir.

The formation of shallow tributaries ahead of the main gully was also observed on site, with 10 to 20cm depth seen in Figure 5.5.17d) of comparable magnitude to that seen in Figure 3.2.4, Figure 3.2.5, Figure 3.2.6.

The final landform pictured in Figure 5.5.18_d illustrates a few noteworthy characteristics, with depth of gully increasing uniformly in the upper sections of the slope, and movement of the formation down the hillslope, combined with deposition of material observed between Row H to Row I. The development observed on site is comparable, with deposition of material observed between Row H and Row I and excavation of material to a maximum depth of 60 to 70cm at Row G.

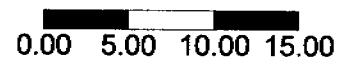
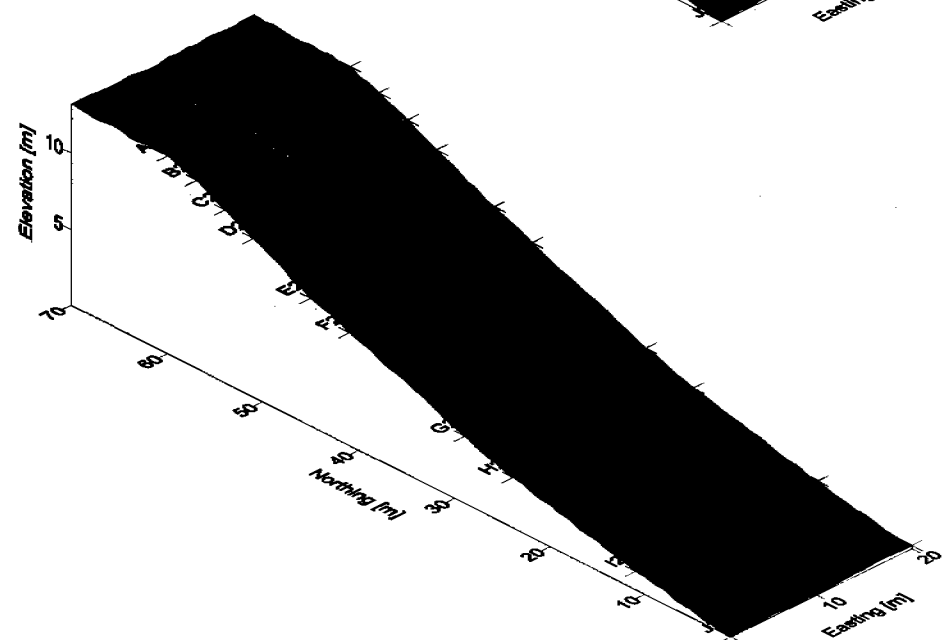
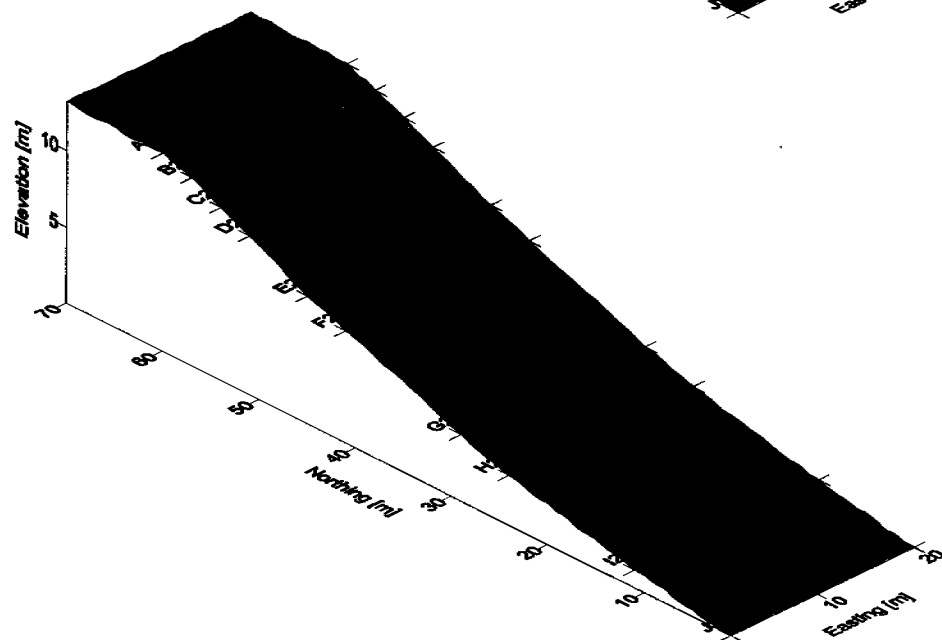
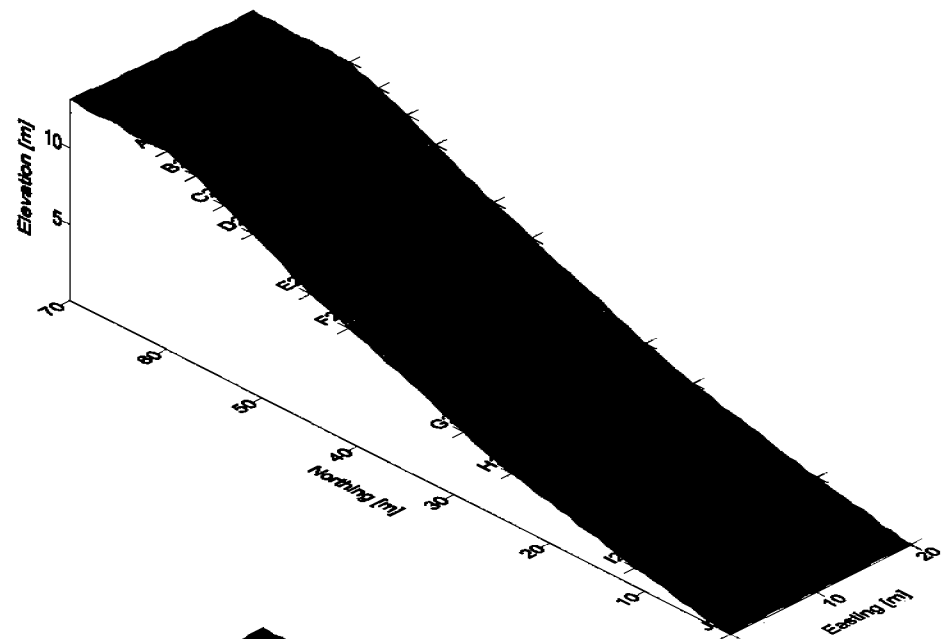
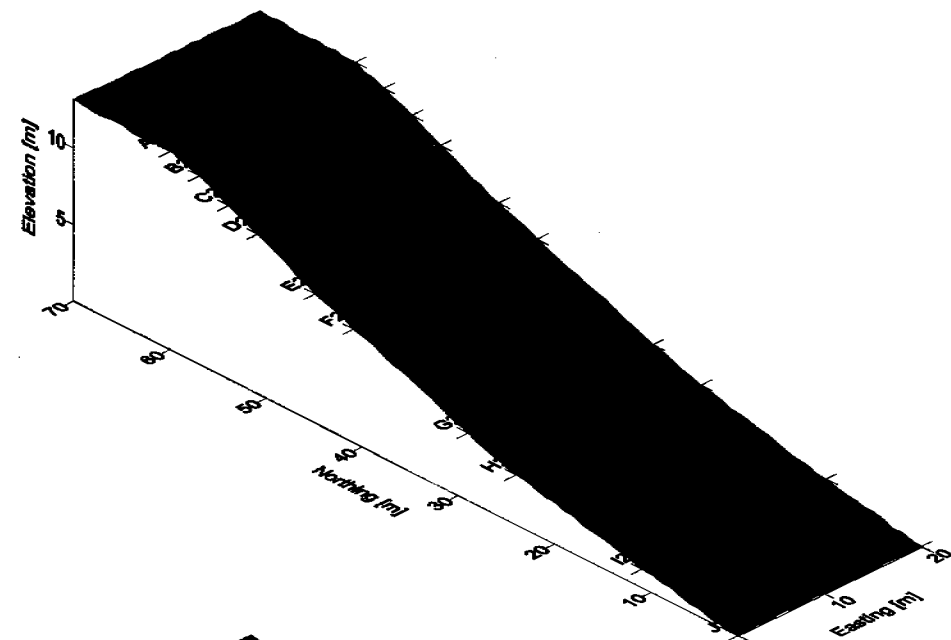
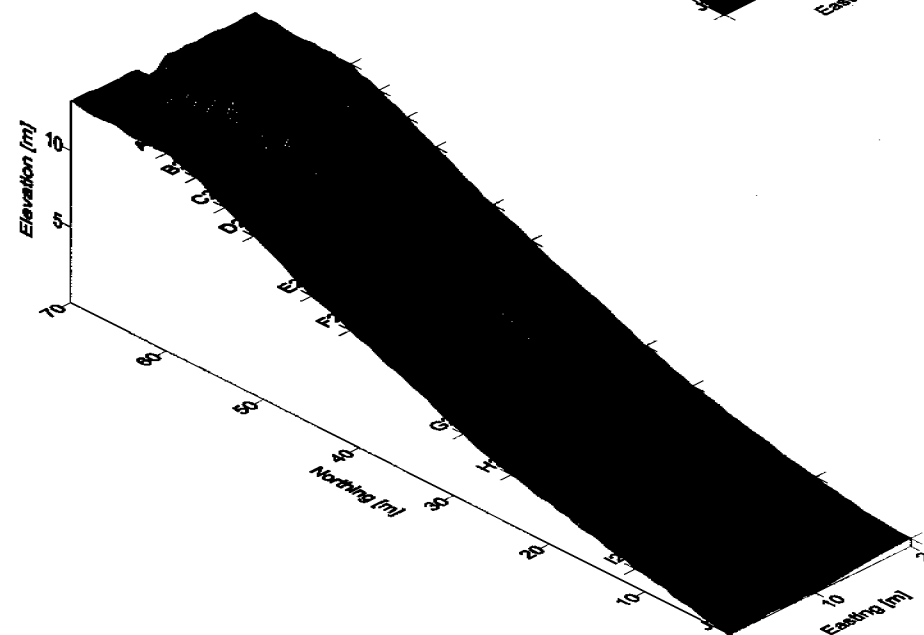
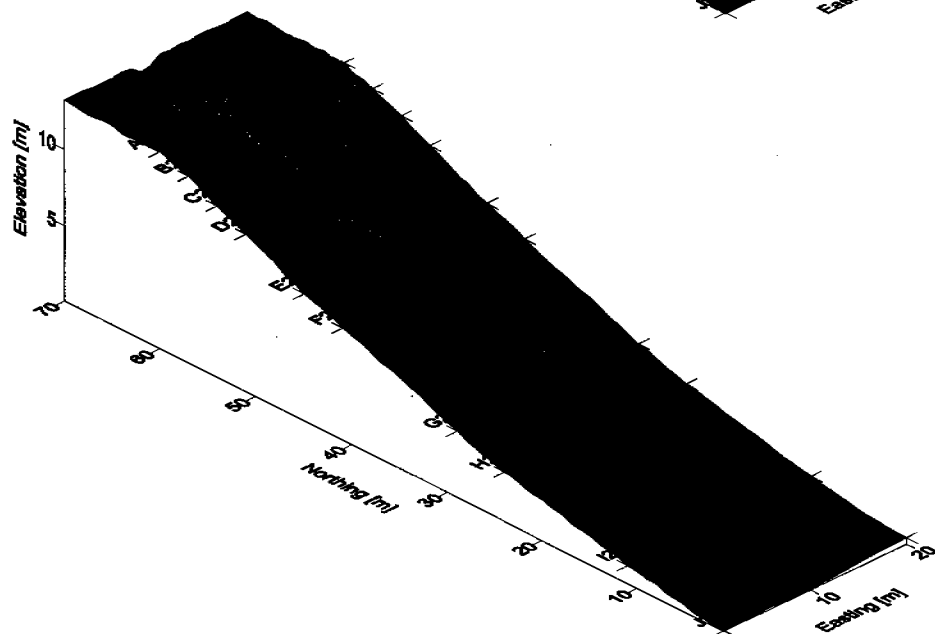
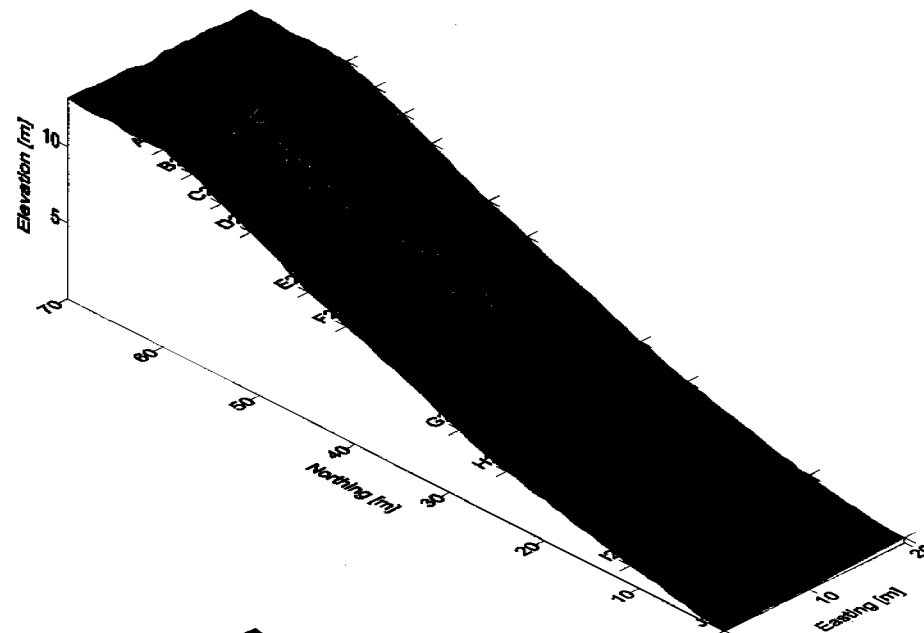
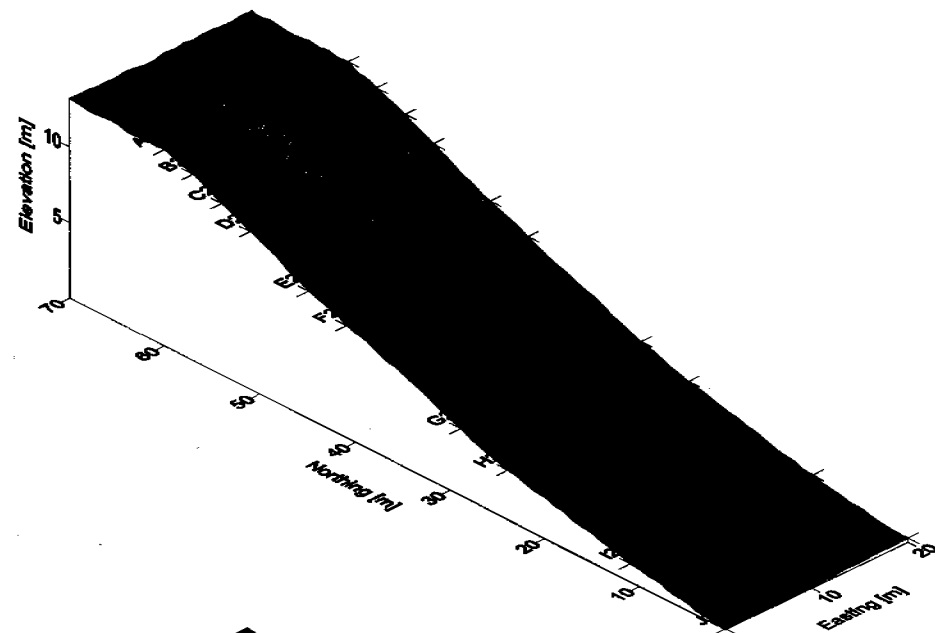


Figure 5.5.16: Simulations for extended batter slope profile with differential erodibility with depth, and randomised erodibility function, at a) 10 minutes, b) 20 minutes, c) 30 minutes, and d) 1 hour.



0.00 5.00 10.00 15.00

Figure 5.5.17: Simulations extended batter slope profile with differential erodibility with depth, and randomised erodibility function, at a) 1.5 hours, b) 2 hours this represents the second storm event, and c) 2.5 hours and d) 3 hours representing the final storm event.

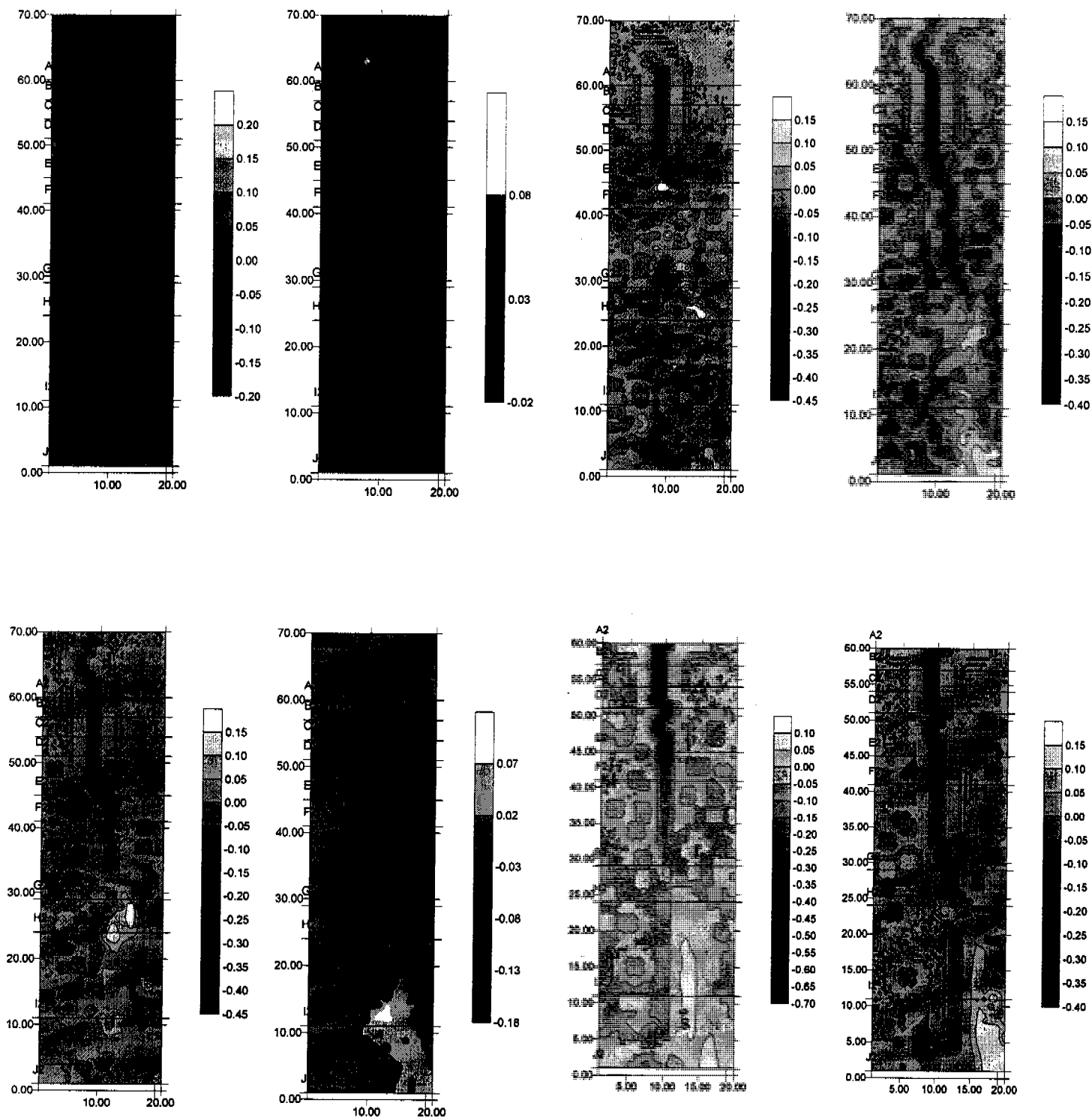


Figure 5.5.18: The morphology contour plots a) initial profile and 10 minutes, b) 10 minutes and 20 minutes, c) 20 minutes and 30 minutes, d) 30 minutes and 1 hour. The difference in elevations are also calculated from the remainder of the simulations with e) difference between 1 hours and 1.5 hours, f) 1.5 and 2 hours, g) 2 and 2.5 hours, and h) 2.5 and 3 hours.

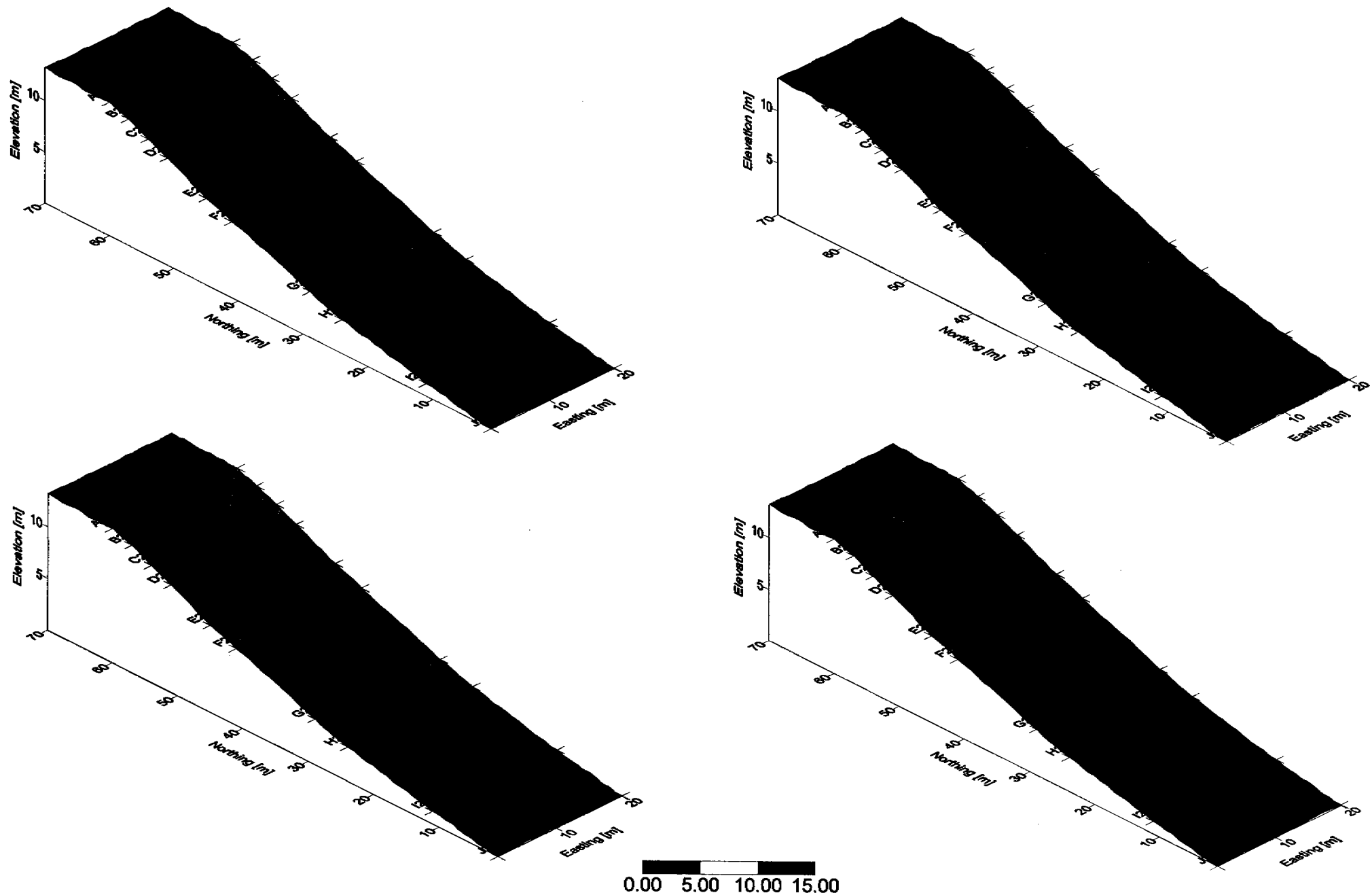


Figure 5.5.19: Simulations for extended batter slope profile with differential erodibility with depth, and randomised erodibility function, as well as wide inlet point, at a) 10 minutes, b) 20 minutes, c) 30 minutes, and d) 1 hour.

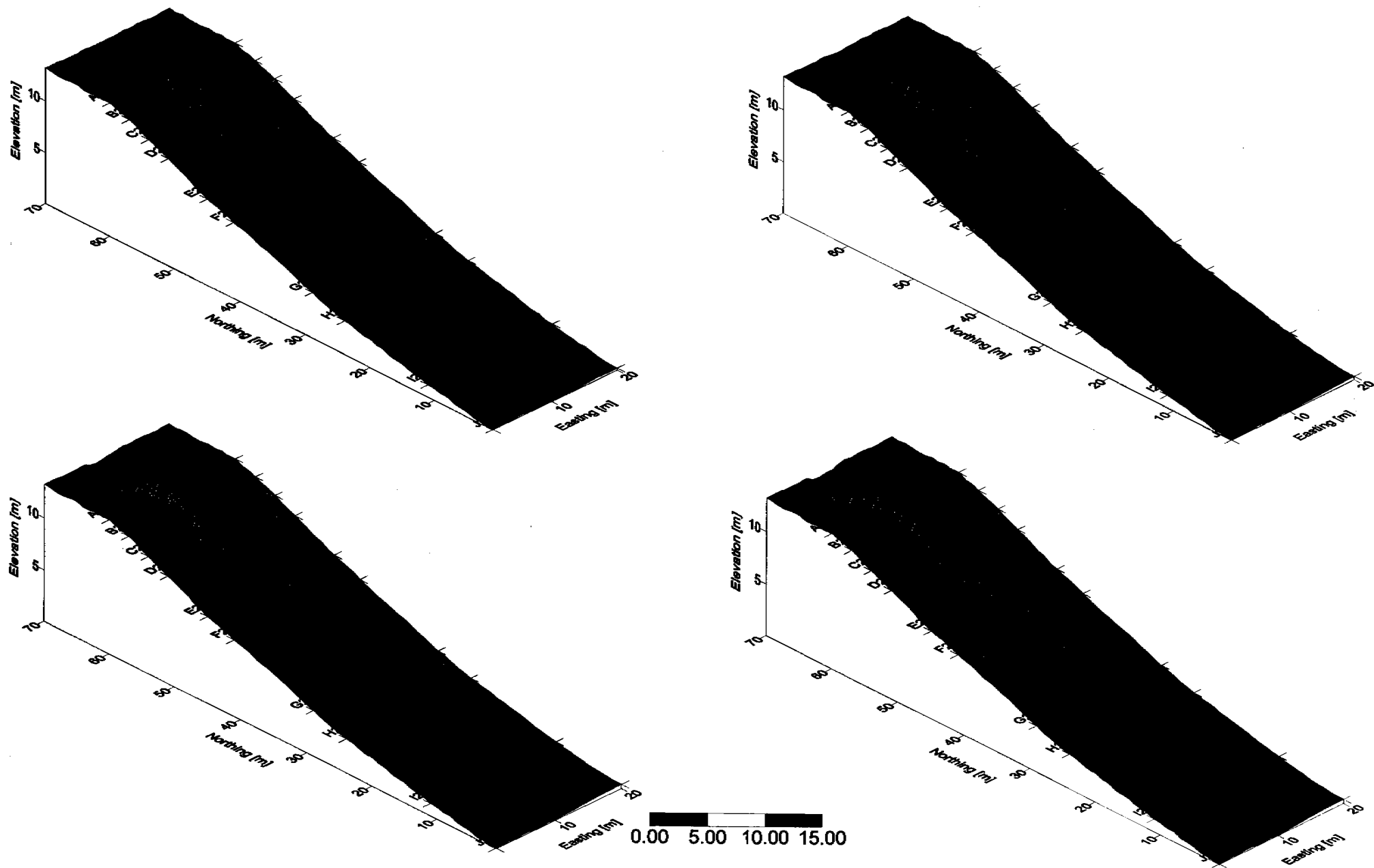


Figure 5.5.20: Simulations extended batter slope profile with differential erodibility with depth, and randomised erodibility function, as well as wide inlet point, at a) 1.5 hours, b) 2 hours this represents the second storm event, and c) 2.5 hours and d) 3 hours representing the final storm event.

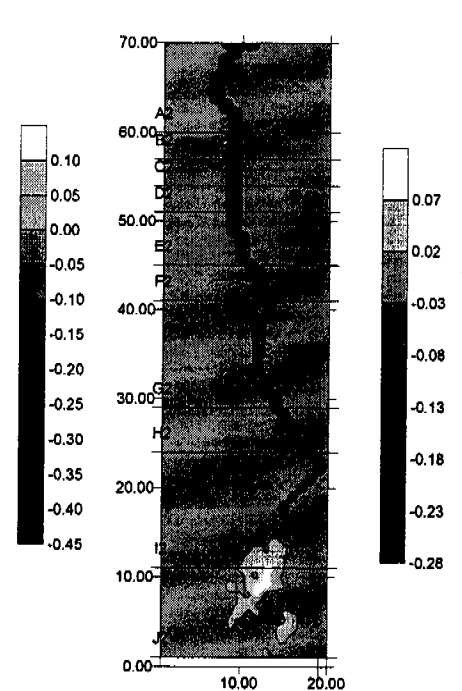
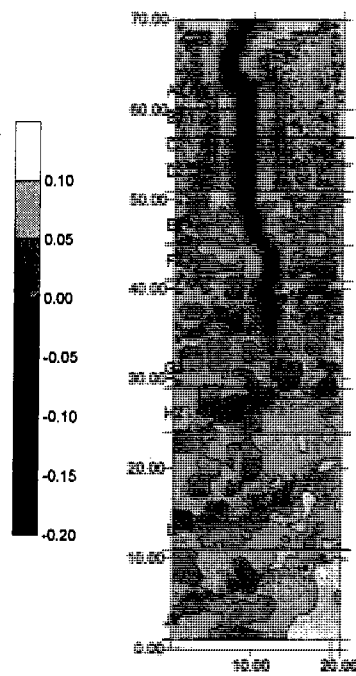
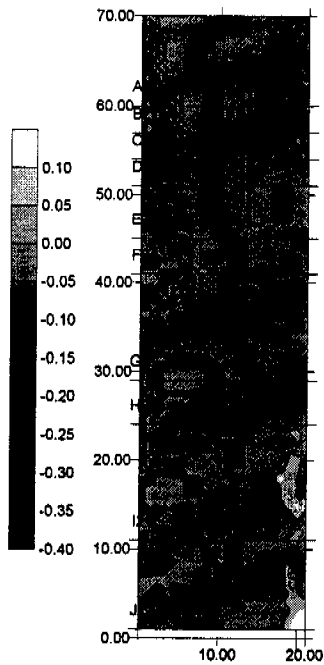
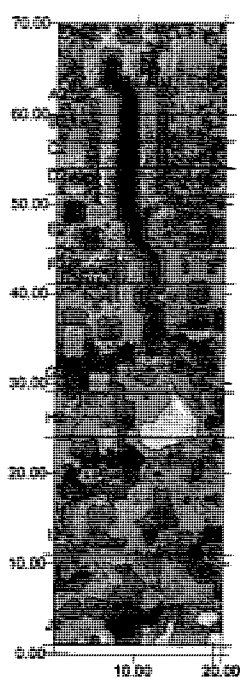
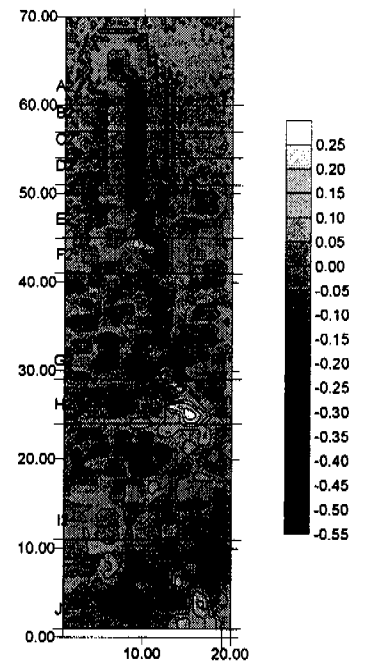


Figure 5.5.21: The morphology contour plots a) initial profile and 10 minutes, b) 10 minutes and 20 minutes, c) 20 minutes and 30 minutes, d) 30 minutes and 1 hour. The difference in elevations are also calculated from the remainder of the simulations with e) difference between 1 hours and 1.5 hours, f) 1.5 and 2 hours, g) 2 and 2.5 hours, and h) 2.5 and 3 hours.



Monitoring Gully Formation

The incision at Row A in Figure 5.5.19, reaches a maximum depth of 1.8m with depth at 60 minutes reaching 60cm. Development of the gully at this point has begun to extend back into the catchment, whilst 20cm shallow tributaries extend down to Row F. Although these figures represent 2 different development scenarios, the overall depth of erosion and extent are similar (Figure 5.5.18, and Figure 5.5.20).

The depth of incision into the catchment reaches 1.5m just before the transition point back to 50cm adjacent to the inlet point, and reflects a similar observation to that seen in Figure 5.1.4 at 60 minute mark. In this figure the pathway adopted is identical, confirming that development follows the same process by extending backward from the incision point. The depth of incision at 60 minutes was only 60cm as stated above, whereas 1.8m was predicted with the standard profile.

These landforms perhaps represent the closest approximation devised from the modelling process, and can be considered a reasonable estimate. Depth within the gully of either of the two important simulations of Figures 5.5.18, or Figure 5.5.20 between 1.8 m and 0.6m for Rows A to Row C with 0.6m gully representing the depth of the secondary tributary observed in Figure 5.5.18.



5.6 Slope Final

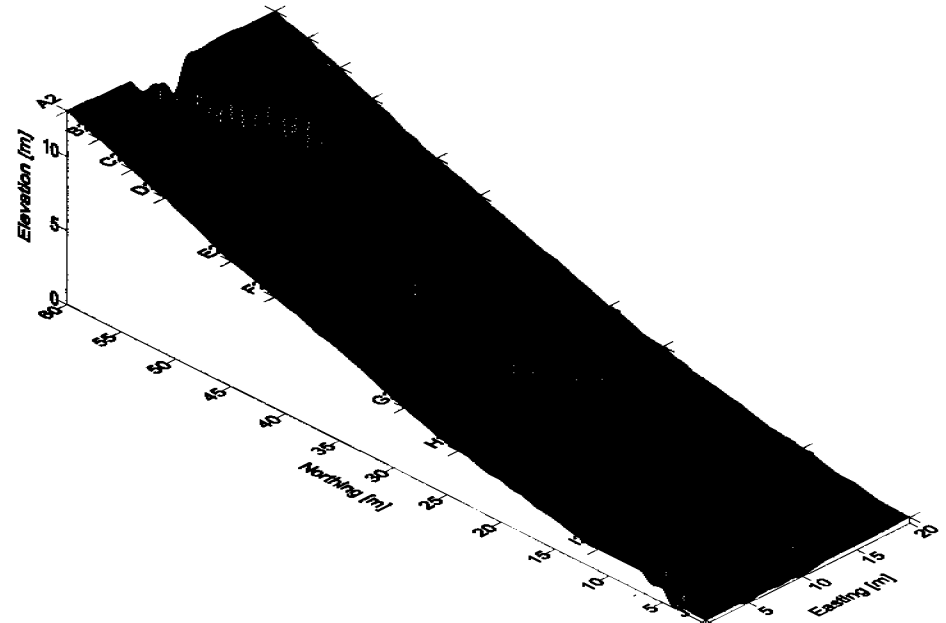
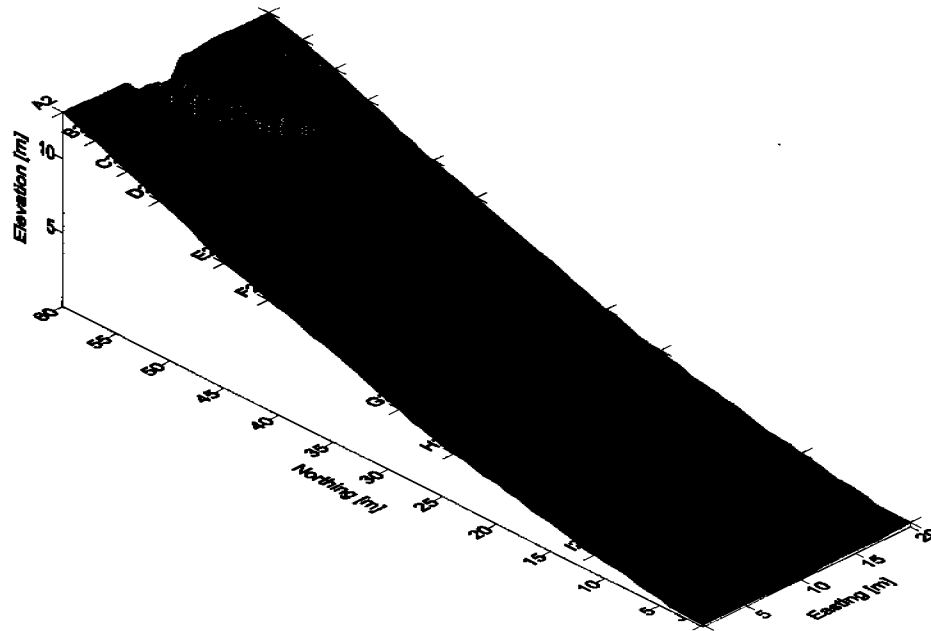
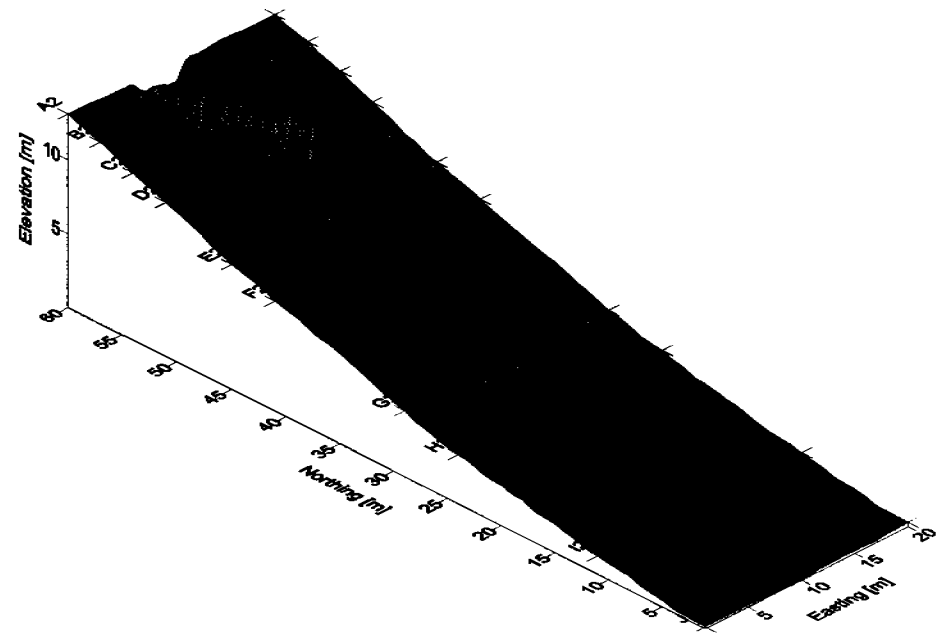
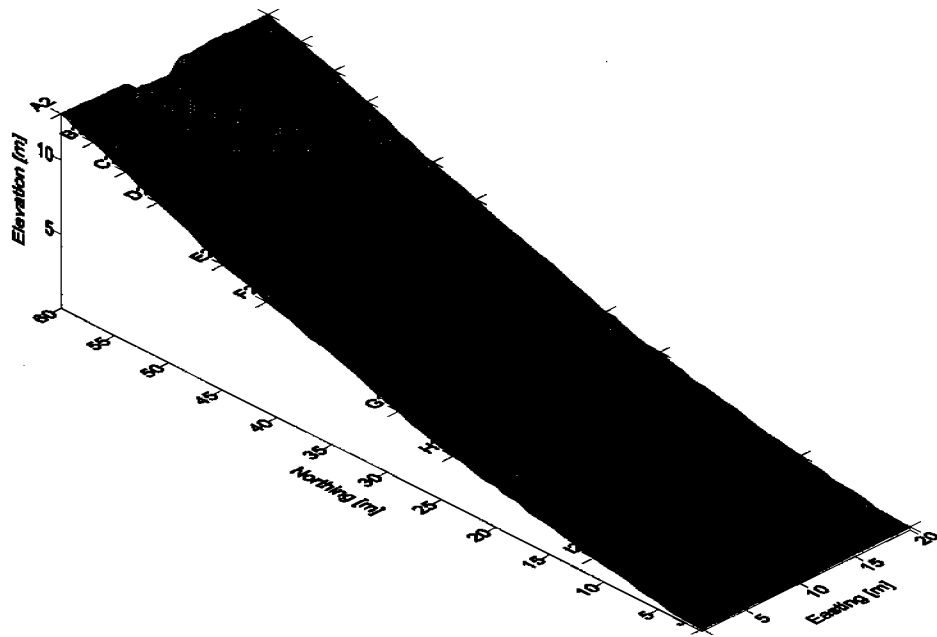
The final modelling regime considered was the modification of the exponent on the slope term in the sediment transport equation, n_1 . This investigation generated surfaces illustrated in Section 5.2, with none of the additional erosion modules enabled. As noted, the results seen in these figures were considered dramatic with maximum depths of erosion about 11m by end of the monitoring period, with a maximum depth of 5m observed in the extended profile case.

The final model scenarios investigated included all of the erosional modules, with slope exponent n_1 altered from 2.1 to 0.69. The slope exponent n_1 was considered the most sensitive parameter, with field observations indicating a significant change in erodibility with depth. The batter slope profile and extended profile were both investigated, with depths of erosion at the head of the gully reaching 4m, for the standard profile case.

The extended profile, however does not erode significantly, with gully development considerably slower than that observed in previous simulations with inclusion of wide inlet. Maximum depth of erosion, and development behaviour is sporadic, with comparisons favourable between these simulations and observed depths.

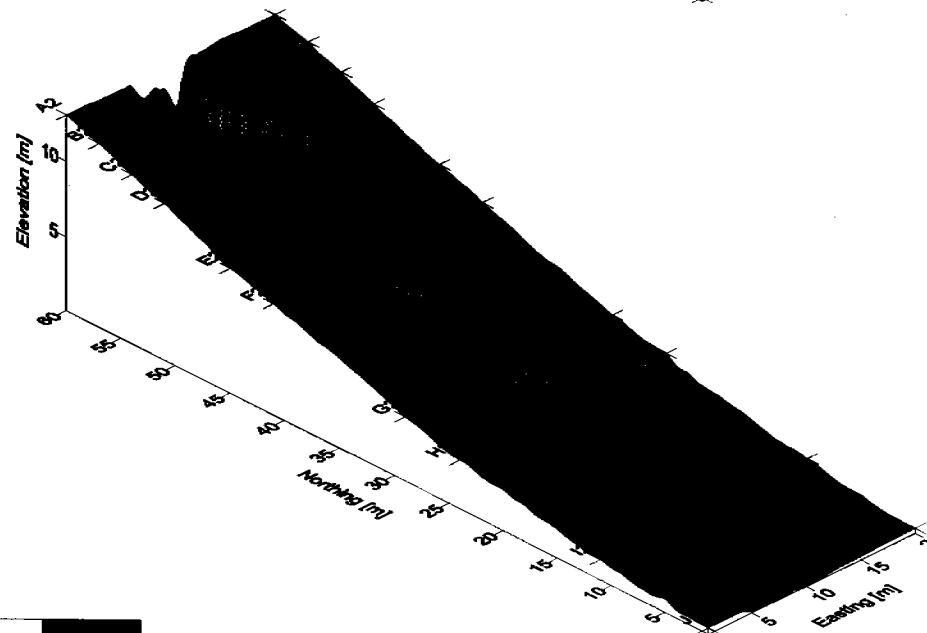
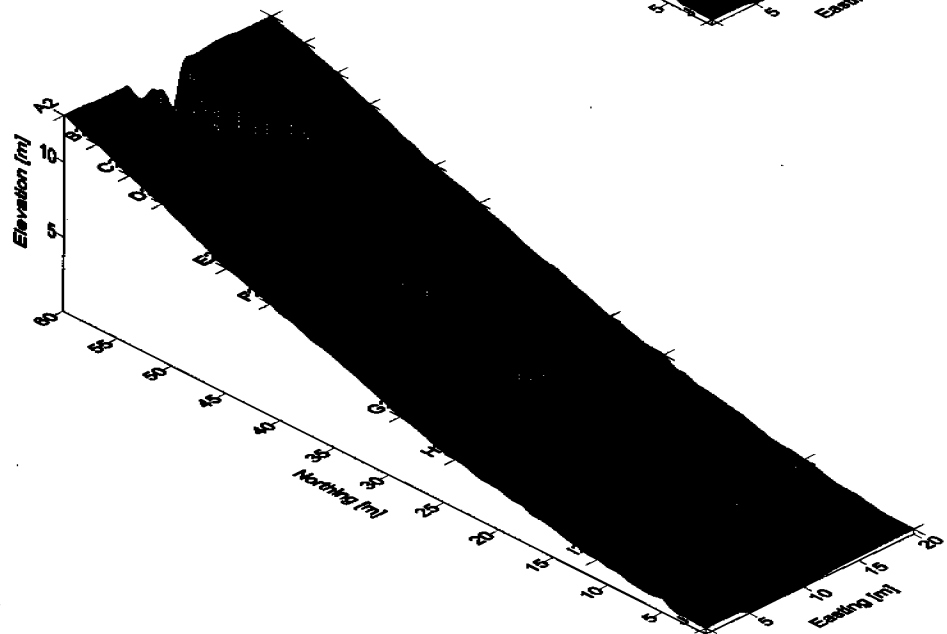
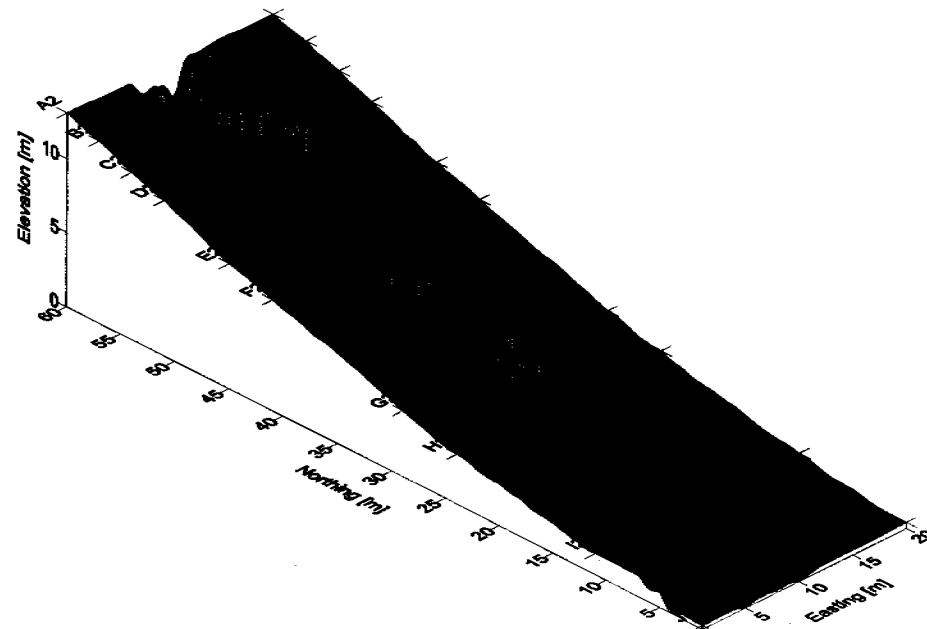
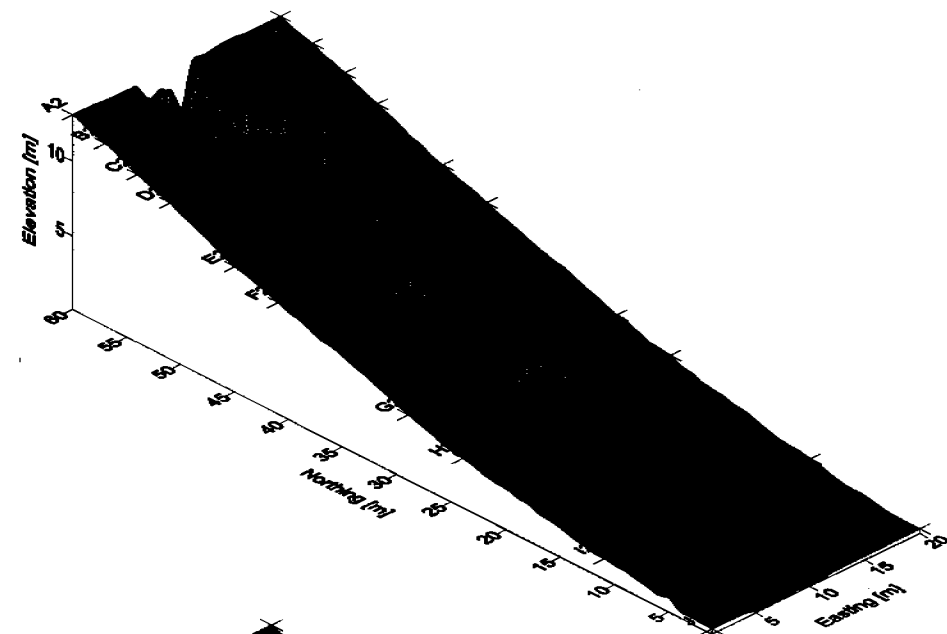
Also noted that the gully does not extend from the transition point (Row A) back into the cap site with this simulation, and it is suggested that this is a product of the combination of the armouring component and similar observations in Section 5.3.

As noted, the derivation of this exponent is dependent on mean particle diameter and hence considered subjective. The maximum depth of erosion at the head of the gully was 3 to 4 m, with this prediction greater than that observed in Figure 5.5.14 at about 2 m. However the depths of erosion below this initial inlet zone, Row C, are comparable, although the rate of development of the gully is much more rapid, with the gully extending to the bottom of the slope within the first storm event. The simulation also exhibits some indication of numerical instability, although for the extended profile, similar behaviour to that observed in Figure 5.2.4, and 5.2.5 where the wide inlet point given the fitted value of n_1 at 0.69 resulted in the gully not developing, as incision at transition point did not occur.



0.00 5.00 10.00 15.00

Figure 5.6.1: Simulations for standard batter slope profile with differential erodibility with depth, and randomised erodibility function, together with wide inlet point and n_1 slope exponent at 0.69 instead of 2.1, at a) 10 minutes, b) 20 minutes, c) 30 minutes, and d) 1 hour.



0.00 5.00 10.00 15.00

Figure 5.6.2: Simulations standard batter slope profile with differential erodibility with depth, and randomised erodibility function, together with wide inlet point and n_1 slope exponent at 0.69 instead of 2.1, at a) 1.5 hours, b) 2 hours this represents the second storm event, and c) 2.5 hours and d) 3 hours representing the final storm event.

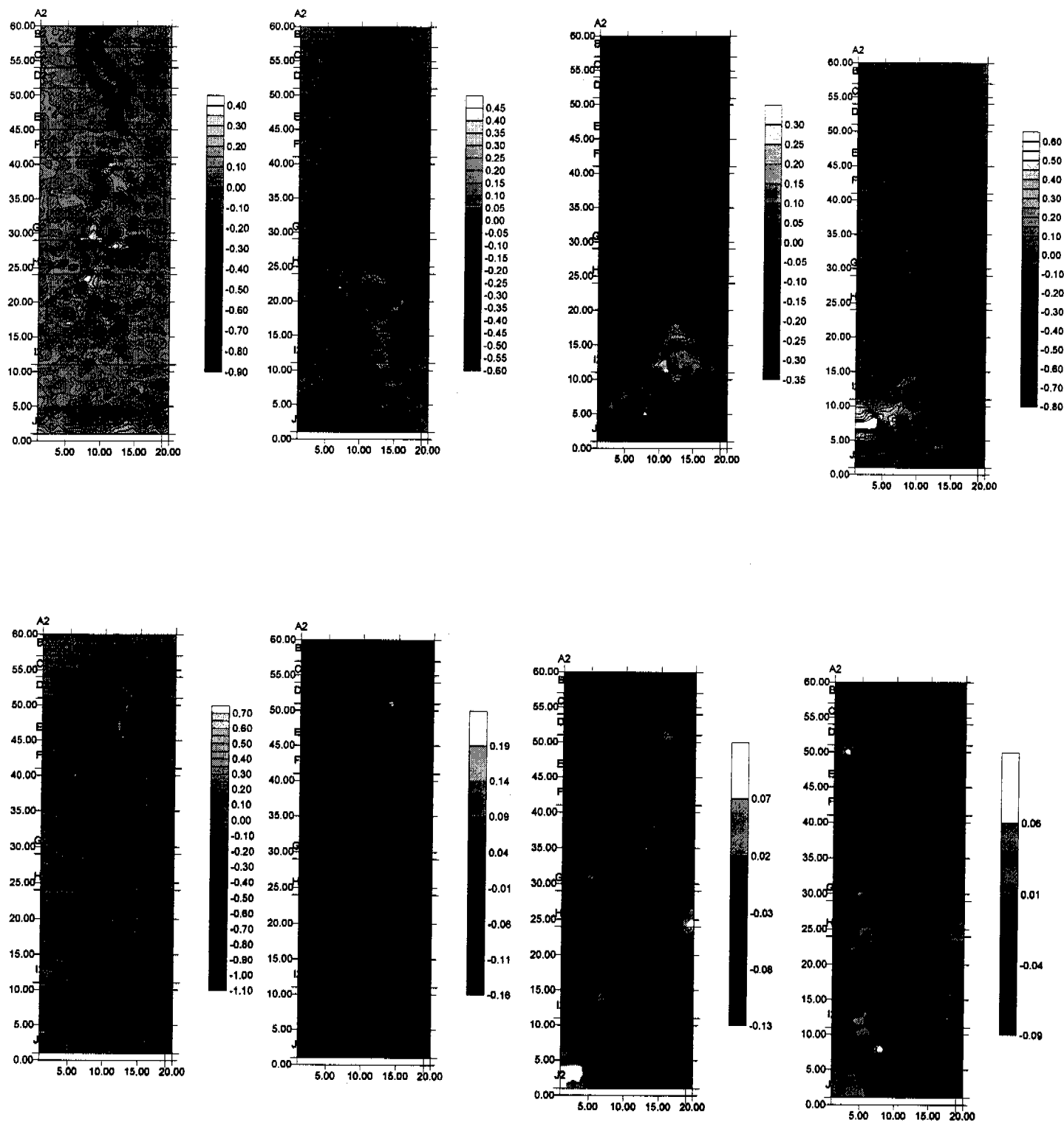


Figure 5.6.3: The morphology contour plots a) initial profile and 10 minutes, b) 10 minutes and 20 minutes, c) 20 minutes and 30 minutes, d) 30 minutes and 1 hour. The difference in elevations are also calculated from the remainder of the simulations with e) difference between 1 hours and 1.5 hours, f) 1.5 and 2 hours, g) 2 and 2.5 hours, and h) 2.5 and 3 hours.

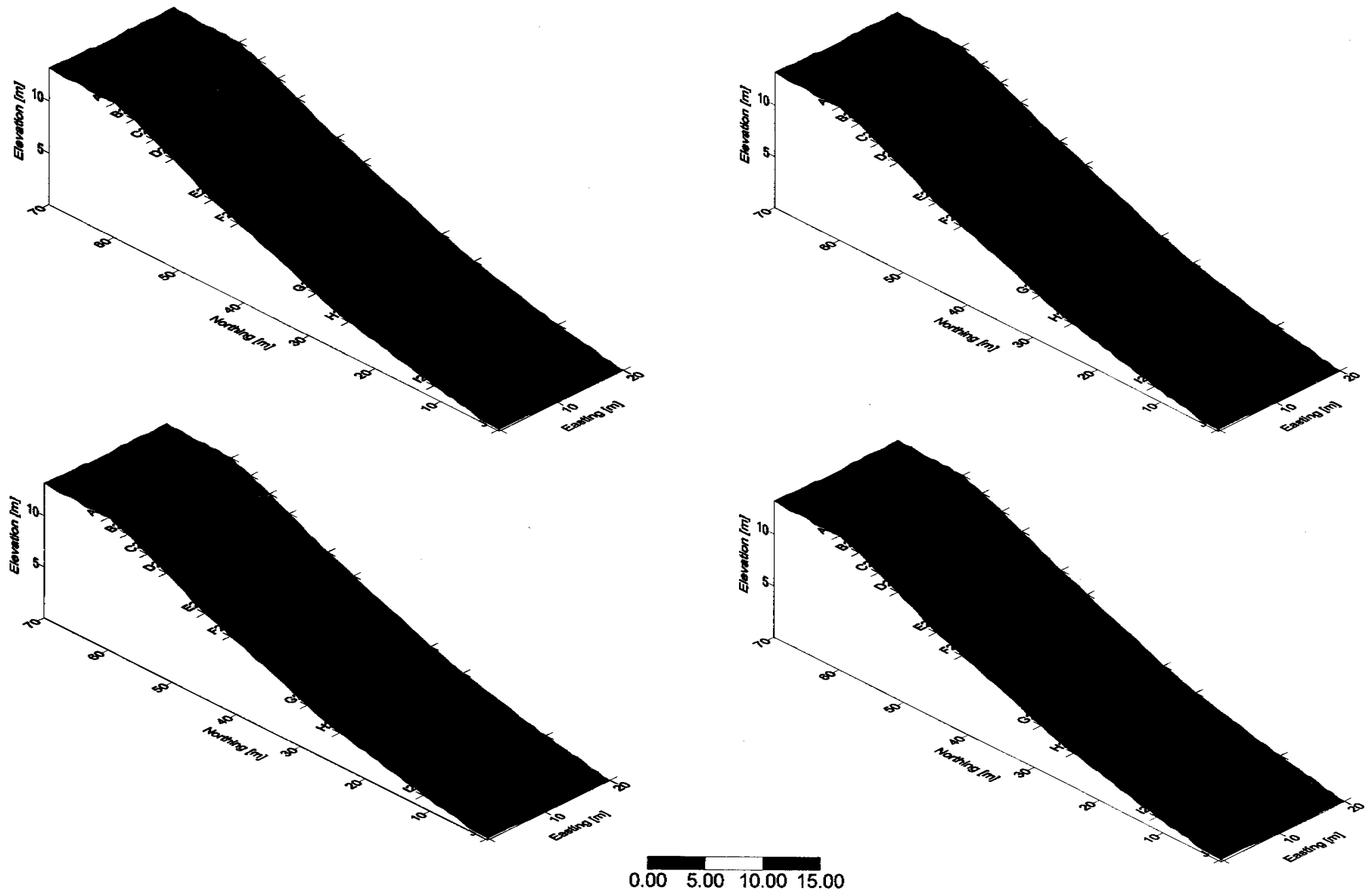
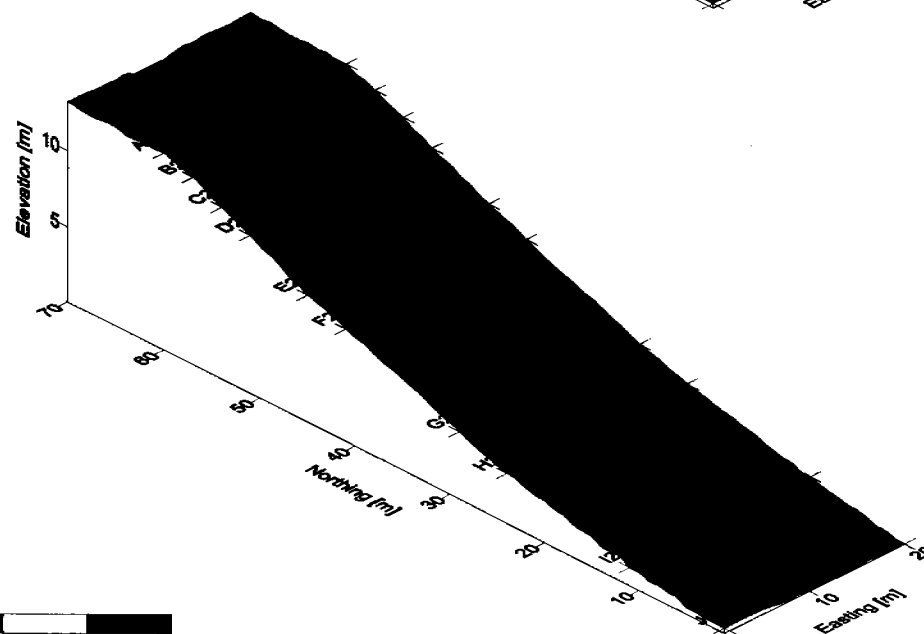
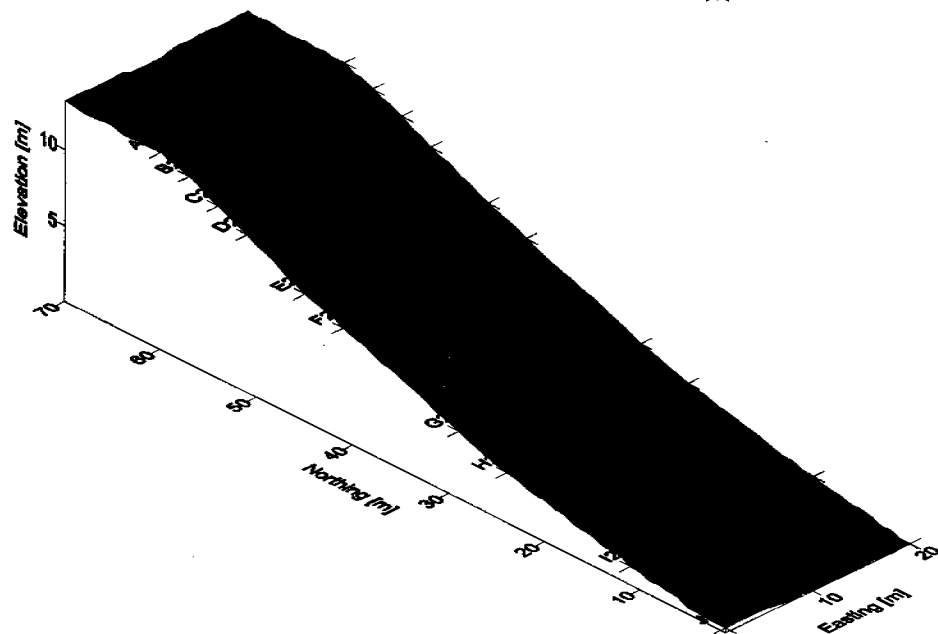
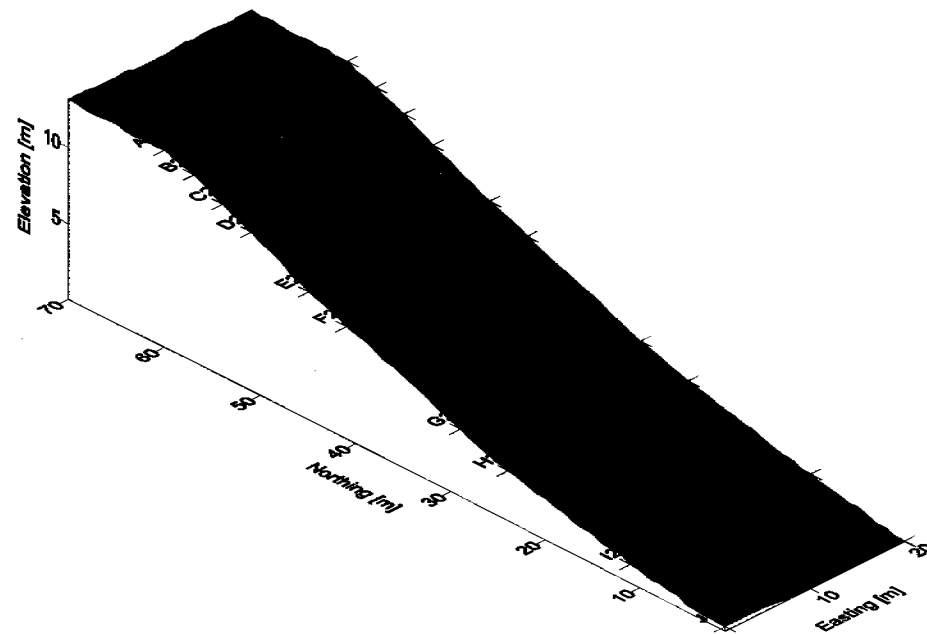
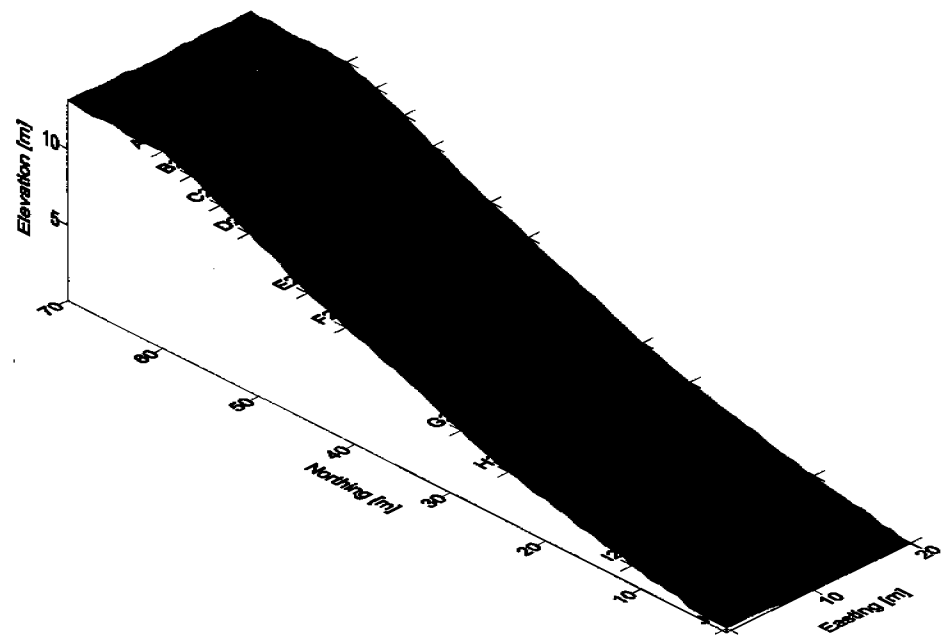


Figure 5.6.4: Simulations for extended batter slope profile with differential erodibility with depth, and randomised erodibility function, together with wide inlet point and n_1 slope exponent at 0.69 instead of 2.1, at a) 10 minutes, b) 20 minutes, c) 30 minutes, and d) 1 hour.



0.00 5.00 10.00 15.00

Figure 5.6.5: Simulations extended batter slope profile with differential erodibility with depth, and randomised erodibility function, together with wide inlet point and n_1 slope exponent at 0.69 instead of 2.1, at a) 1.5 hours, b) 2 hours this represents the second storm event, and c) 2.5 hours and d) 3 hours representing the final storm event.

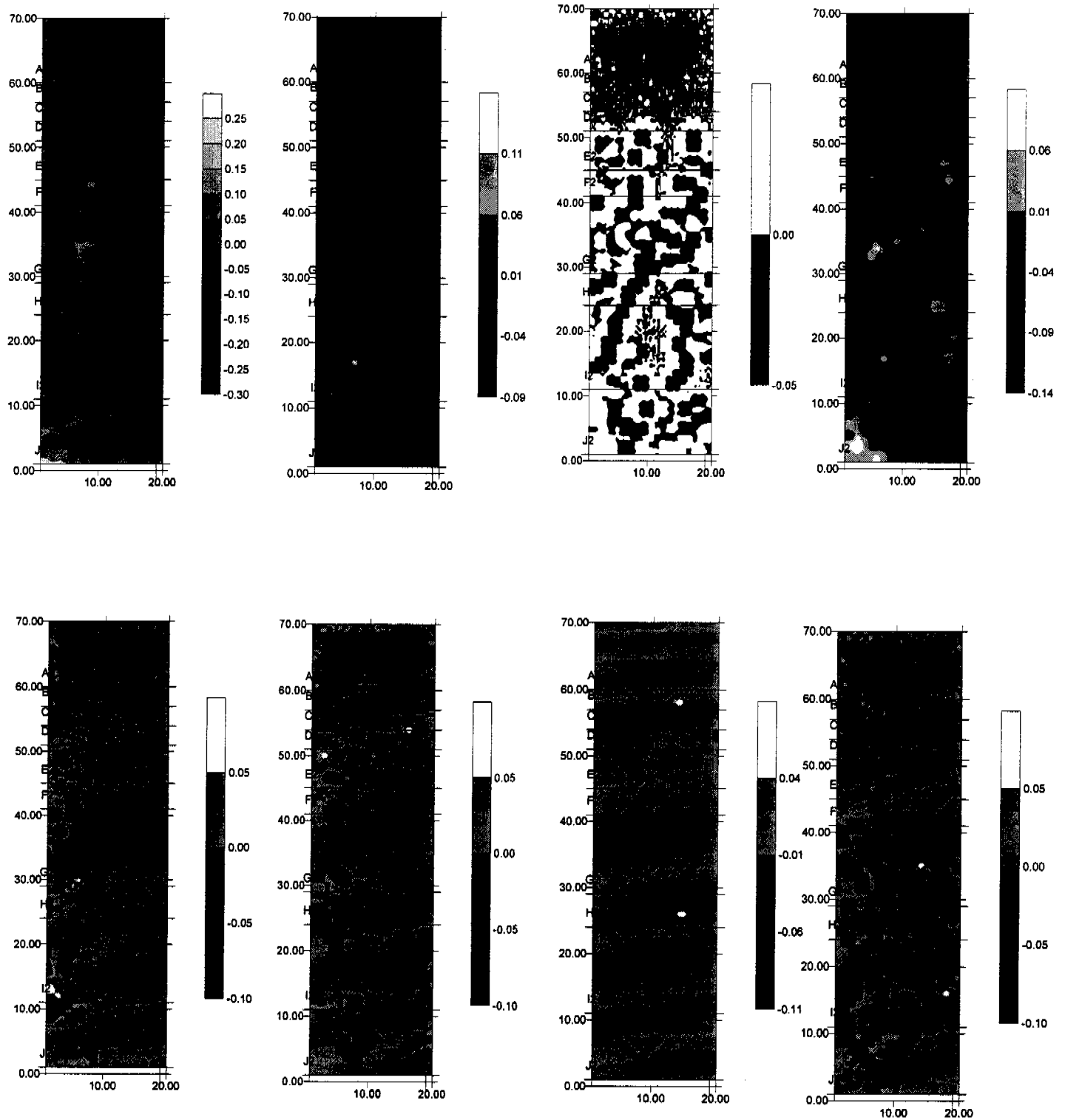


Figure 5.6.6: The morphology contour plots a) initial profile and 10 minutes, b) 10 minutes and 20 minutes, c) 20 minutes and 30 minutes, d) 30 minutes and 1 hour. The difference in elevations are also calculated from the remainder of the simulations with e) difference between 1 hours and 1.5 hours, f) 1.5 and 2 hours, g) 2 and 2.5 hours, and h) 2.5 and 3 hours.

6.0 Discussion

The simulations have indicated regions likely to suffer significant erosion, and these have compared favourably with observations of actual gully formation. The development of a gully has been characterised by significant movement of material onto the lower sections whilst maximum depths range between 1.0m and 1.8m for upper sections.

The location of the gully in model simulations is dependent on the development process dictated by which erosion modules were implemented. Gully formation typically reaches between Row H and Row I in almost all approximations.

The depth of erosion is typically 40 to 70cm, ranging along the observed active sections of Row E through to Row G, whereas the depth of gully in upper section Row A to Row D ranges between 1 to 2m. These details are best described schematically, such as in Figure 6.1, Figure 6.2, and Figure 6.3, and Figure 6.4, with erosion depths with differences between simulations on an event by event basis.

Although the model simulations will over-predict the maximum depth of erosion at the top of the batter slope, the upper section activity seems reasonably estimated with overall depth ranging between 50 to 70cm, in Figure 6.2. Incision at this transition point initially and consequent development down the hillslope and back into the catchment are comparable to standard profile observed in Figure 6.1, as expected. The difference in elevations devised between each storm event was estimated by subtracting the upper surface from the newly eroded surface and the volume approximated.

Table 6.1: Volumetric approximation of overall elevation change between consequent storm events. These estimates were conducted for both final simulation scenarios used in Section 5.5, and Section 5.6. Erosion is represented by negative values, whilst deposition is represented by positive values. These calculations appear in Appendix C.

Surface Profile	Randomised, armouring, wide inlet point, with $n_1 = 2.1$.			Randomised erodibility, armouring, and wide inlet point with $n_1 = 0.69$.		
	261296	010197	230197	261296	010197	230197
batter slope	-6.04 m ³	-5.17 m ³	-9.42 m ³	+25.73 m ³	+2.93 m ³	-1.59 m ³
extended profile	+0.58 m ³	-1.04 m ³	-9.04 m ³	-1.11 m ³	-1.28 m ³	-5.07 m ³
experimental	-46.74 m ³	+1.68 m ³	+5.51 m ³			

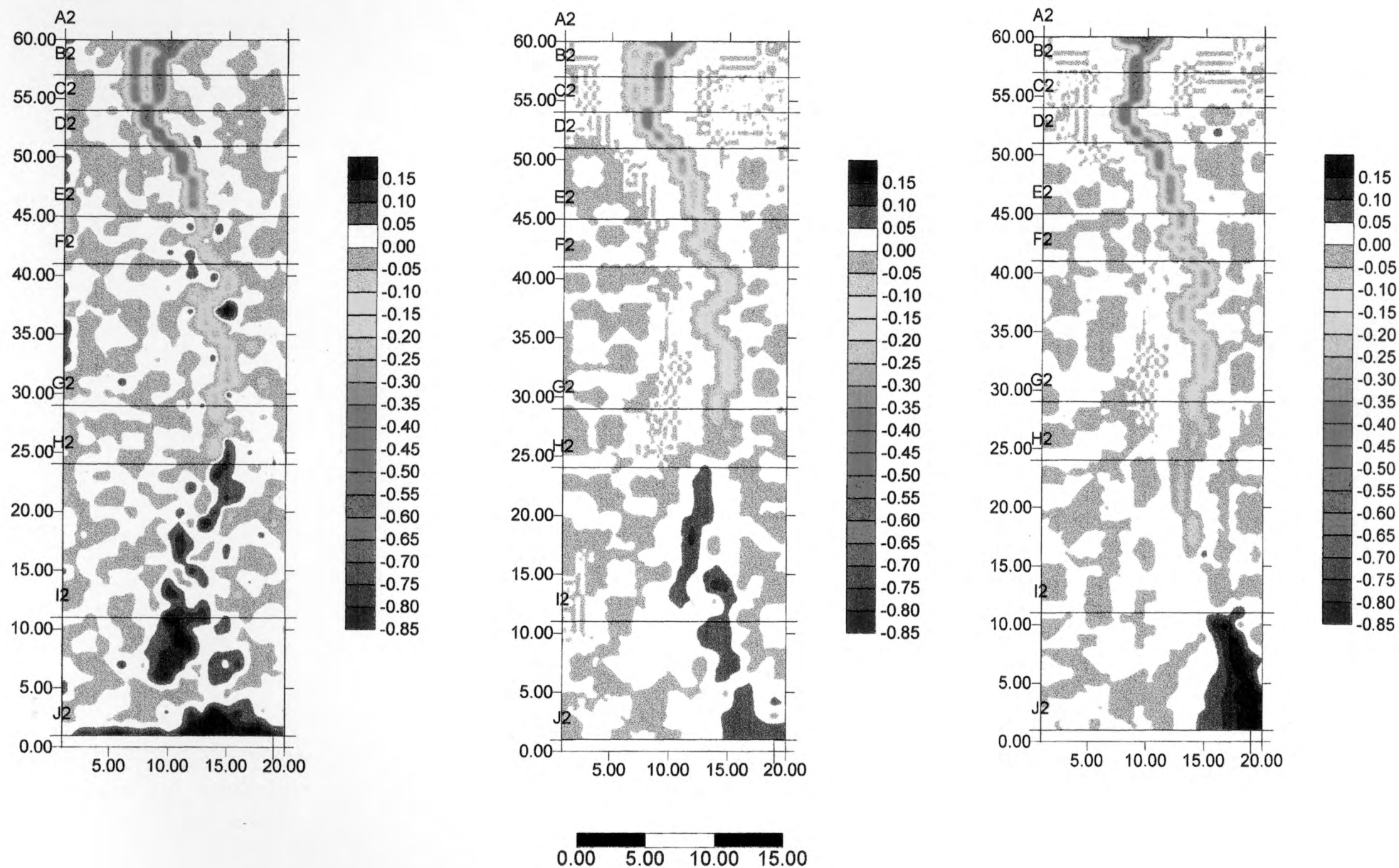
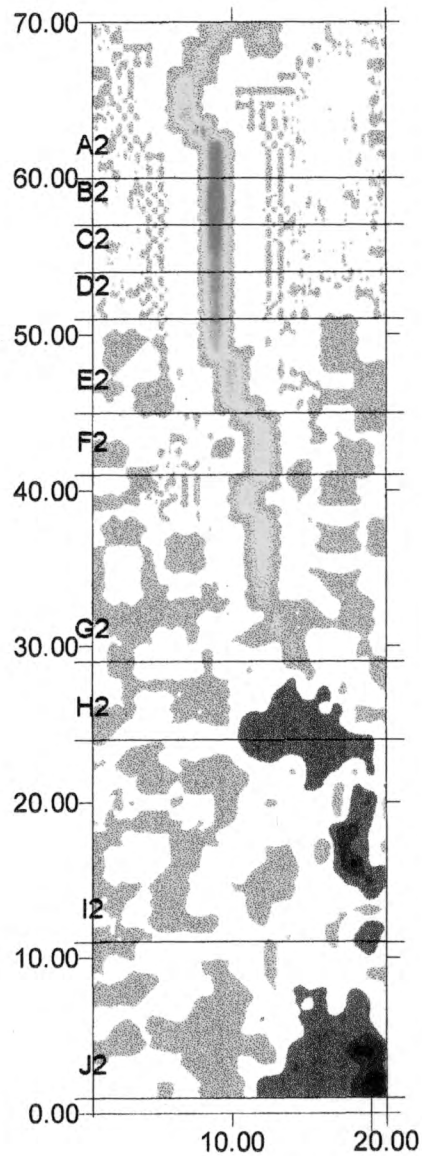
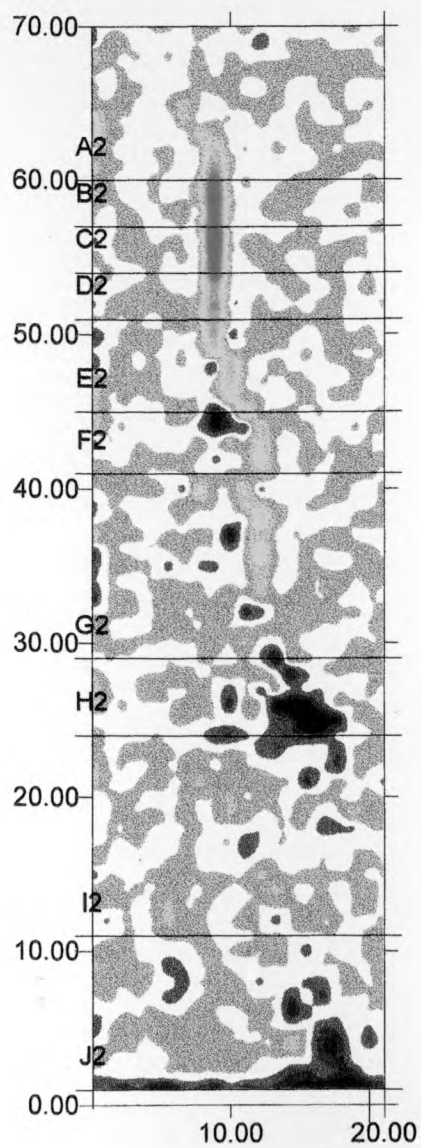


Figure 6.1: The change in elevation from the initial surface is represented by erosion negative, and deposition positive. These simulations are evaluated on a per storm event basis, and include all of the erosion modules as discussed in Section 5.5.



0.00 5.00 10.00 15.00

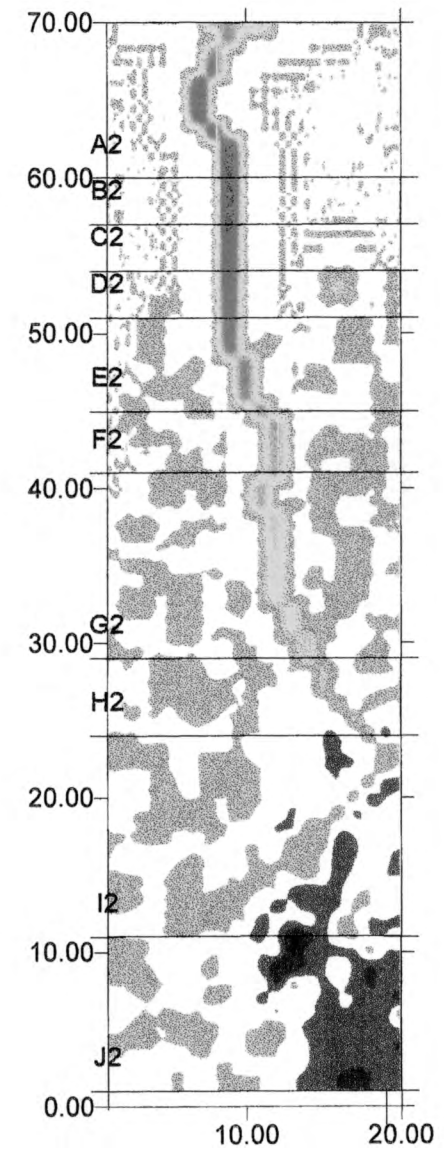


Figure 6.2: The change in elevation between each consequent storm event, is highlighted in this figure, with simulations devised using the erosion modules outlined in Section 5.5. This scenario represents the extended batter slope profile.

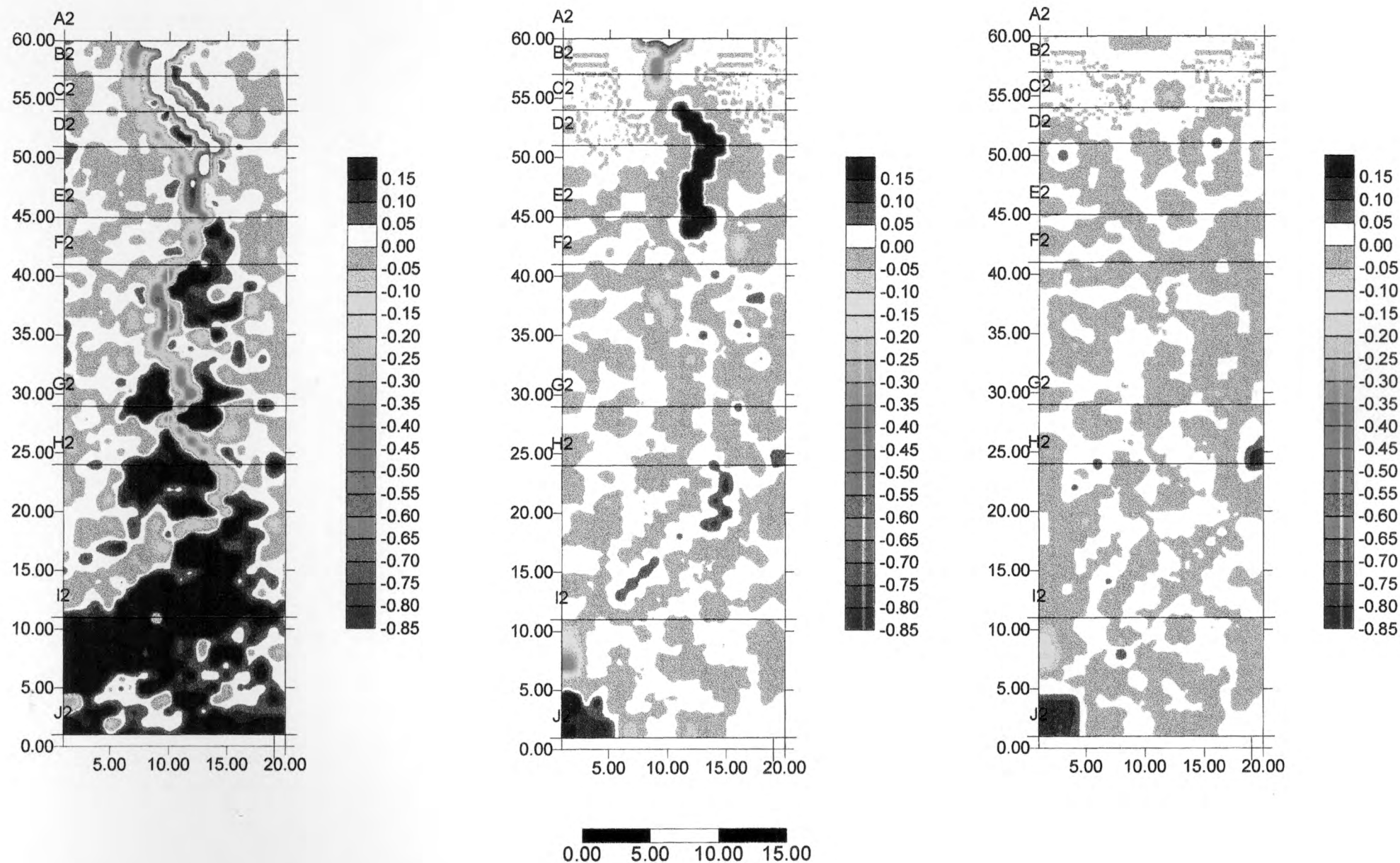


Figure 6.3: The change in elevation between consequent storm events, was evaluated using the simulations from Section 5.6, where this slope is representative of standard batter slope profile.

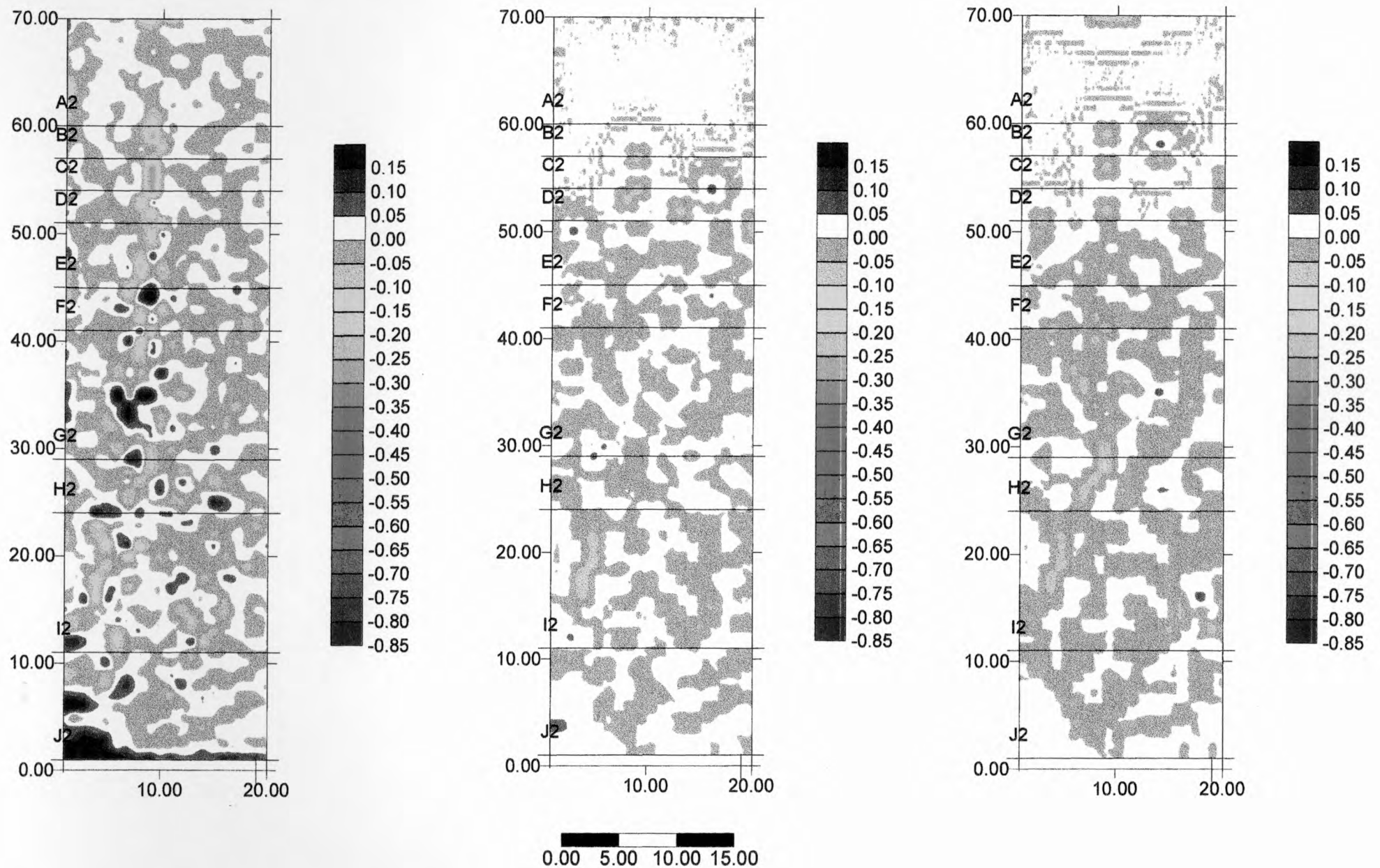


Figure 6.4: The change in elevations between each of the three storm events, are simulated using results from Section 5.6, where the exponent on the slope term in the sediment transport equation is reset to fitted value of 0.69 instead of 2.1.



Monitoring Gully Formation

The comparison of erosional values between experimental results from field trial and model simulations from the two final model scenarios indicate a similar overall result, although development of the gully is considerably different. Given the inherent variability in the surface material and the large scale of the field site, a reasonable comparison between these figures was expected., although the development process in the model simulations was more sequential.

Willgoose and Loch, 1996 notes that the behaviour of the incising erosion model can be quantified by the parameter, α .

$$\alpha = \frac{m_1 m_3 - 1}{n_1} \quad (6.0.1)$$

where

m_1, m_3 = physical parameter exponents in the sediment transport model.

For the erosion studies previous conducted parameter values obtained of m_1, n_1 and m_3 of 1.68, 0.69 and 0.9 equated to an α of 0.65. These adapted results were used in this study with m_3 taken to be 1, and $m_1 = 1.68$, whilst the slope parameter n_1 was examined using two cases $n_1 = 0.69$, and $n_1 = 2.1$, with model simulations in Section 5.5 having equivalent value of alpha at 0.32 ($n_1 = 2.1$).

The rate of incision is highly dependent on the armouring of the WRD site, with large boulders exposed in the upper sections of the gully were of significant size, with other considerations such as the with of the formation dependent on the nature of the inlet point.

The sensitivity of the model to parameter choice for n_1 seems critical, although once the fully developed armouring module is enabled the surface in erosion depths observed in Section 5.6, will be abated, leading to a less incising model.

However detailed examination of particle size profile of the site was not conducted during this time, although this will not present insurmountable difficulties as estimates can be made from exposed side walls such as those appearing in Figure 3.2.19.



Monitoring Gully Formation

As discussed, the development of equilibrium profile of the slope was demonstrated by accumulation of fine material at the very top of the slope, resulting in only several centimetres of erosion before large fragments encountered. Also noted was the dynamic nature of waste rock with geochemical weathering observed during the dry season altering the gully formation significantly.

The dynamic equilibrium between and accumulation of material in the channel beds by weathering may establish a layer of material which is constantly changing, averting maximum erosion depths observed on-site, as well as in model simulations lasting for long periods.

Thus in summary, this investigation has demonstrated that gully development on the steep batter slopes can be feasibly represented by model simulations of SIBERIA without the addition of physically based processes to alter the homogenous initial surface, and allow for the armouring that does occur.

Results for non-armoured surface indicated that depths of the order of 4 to 5m at the top of the slope, although these predictions are highly dependent on slope exponent parameter selection with behaviour of gully development representative of that observed on site. Armouring reduces maximum depth of erosion to 1.8m.

The heterogenous, armoured, and increased width inlet scenario represents the optimal calibration of the model at this stage to the study site. Further investigation into the derivation of the value for the slope component n_1 is warranted, as demonstrated above. However all of the model simulations encapsulate the observed development mechanisms, with the development of a more realistic, less conservative estimate of depth-erodibility relationship, increased grid discretisation and further increasing the accuracy of model predictions.

The combination of aspects such as random erodibility, increased catchment outlet width, and rudimentary armouring module has improved estimate of total erosion depth whilst maintaining the dynamical behaviour observed.

7.0 References

Evans, K.G, Willgoose, G.R, and Riley, S.J, 1995, IR 182, *Preliminary Report on the derivation of sediment transport model parameters using large scale rainfall simulator data from Ranger Uranium Mine*, Office of the Supervising Scientist, Jabiru.

Kirkby, M.J, 1995, *A Role for theoretical models in Geomorphology*, Scientific Nature of Geomorphology, Proceedings of the 27th Binghampton Symposium in Geomorphology, John Wiley and Sons, Chicester.

Moliere, D.R, Evans, K.G, Riley, S.J, and Willgoose, G.R., 1996, IR 237, *Erosion and DISTFW Hydrology Model Paramters for Tin Camp Creek Catchments, Arnhem Land, Northern Territory*, Office of the Supervising Scientist, Jabiru.

Prosser, I., 1996, *Thresholds of Channel Initiation in Historical and Holocene Time, South East Australia*, Advances in Hillslope Processes, John Wiley and Sons, Chicester.

Willgoose, G.R, Bras, R.L, and Rodriguez-Iturbe, I., 1991, *A physically based coupled network growth and hillslope evolution model: 1 Theory*, Water Resources Research, 27(7), pp 1671 - 1684.

Willgoose, G.R, Bras, R.L, and Rodriguez-Iturbe, I., 1991, *A physically based coupled network growth and hillslope evolution model: 2 Applications*, Water Resources Research, 27(7), pp 1685 - 1696.

Willgoose, G.R, Bras, R.L, and Rodriguez-Iturbe, I., 1991, *A physical explanation oa an observed link area-slope relationship*, Water Resources Research, 27(7), pp 1697 - 1702.

Willgoose, G.R, Bras, R.L, and Rodriguez-Iturbe, I., 1991, *Results from a new model of river basin evolution*, Earth Surface Processes and Landforms, 16, pp 237 - 254.



Monitoring Gully Formation

Willgoose, G.R., 1992, *User Manual for SIBERIA Version 7.051*, Department of Civil, Surveying, and Environmental Engineering, University of Newcastle, Callaghan.

Willgoose, G.R., and Loch, R., IR229, *Assessment of Narbalek rehabilitation, Tin Camp Creek, and other mine sites in the Alligator Rivers Region as test sites for examining long term erosion processes and validation of the SIBERIA model*, Office of the Supervising Scientist, Jabiru.

Willgoose, G.R., and Riley, S.J., 1992, *Application of catchment evolution model to the prediction of long term erosion on the spoil heap at Ranger Uranium Mine Stage 1 Report*, Office of the Supervising Scientist, Jabiru.

Willgoose, G.R., and Riley, S.J., 1993, *The assessment of the long term erosional stability of engineered structures of a proposed mine rehabilitation*, Environmental Management, Geo-Water and Engineering Aspects.

Acknowledgements

I wish to acknowledge the following persons who have been of invaluable assistance during this project:

Dr Garry Willgoose for his continuing assistance and grateful supervision,

Mr Dene Moliere, Mr Ken Evans, Mr Bryan Smith, and Mr Michael Saynor, as well as the rest of the team outside the Hydrology and Geomorphology Group at *eriss*.

Mr Peter Woods (ERARM Head Environmental Scientist), Mr Garry Stuart (ERARM), Mr Bill Monaghan (ERARM), Mr Phil Savoury (ERARM), and Mr Jeff Cramb (ERARM - *eriss* liason, who made everything happen), for their collective assistance in construction of study site, and kind permission for time allowed on site.

Mr Lyndon Bell, reciprocating honours project conducted simultaneously.

Mr T House, and T Mount for computer equipment assistance whilst at *eriss*.



Appendix A

During the 96-97 Wet Season numerous storm events were monitored.

Of these events three were considered of significant magnitude and intensity that calibration and prediction hydrographs for the gully catchment were made.

The non-linear regression package NLFIT was used to determine the parameters of the DISTFW model. These parameters were separated into kinematic routing parameters: C_r and e_m (flow geometry, and surface roughness), and infiltration parameters (sorptivity and long term infiltration).

The model was used to fit parameters to each hydrograph from the cap site, and then scaled up from cap site to be representative of gully catchment by a factor of 12.204, as outlined in Section 2.2. The following tables summarise the input files required for operation of the NLFIT DISTFW model, with exact replication of results described in Section 3.0.

The following files are included:

*.fw the two site input data files. As outlined in Figure 2.3, and Figure 2.5, the discretisation of the catchment and cap site into subcatchments is necessary for input into hydrology model.

*.ro, *.rf runoff, and cumulative rainfall respectively for each of the 3 events.

The results of these 'fits' appear in Table A-1. The fitted hydrographs for individual storm events, and multiple fitting of all three events was conducted for both the cap and gully catchment sites.



Monitoring Gully Formation

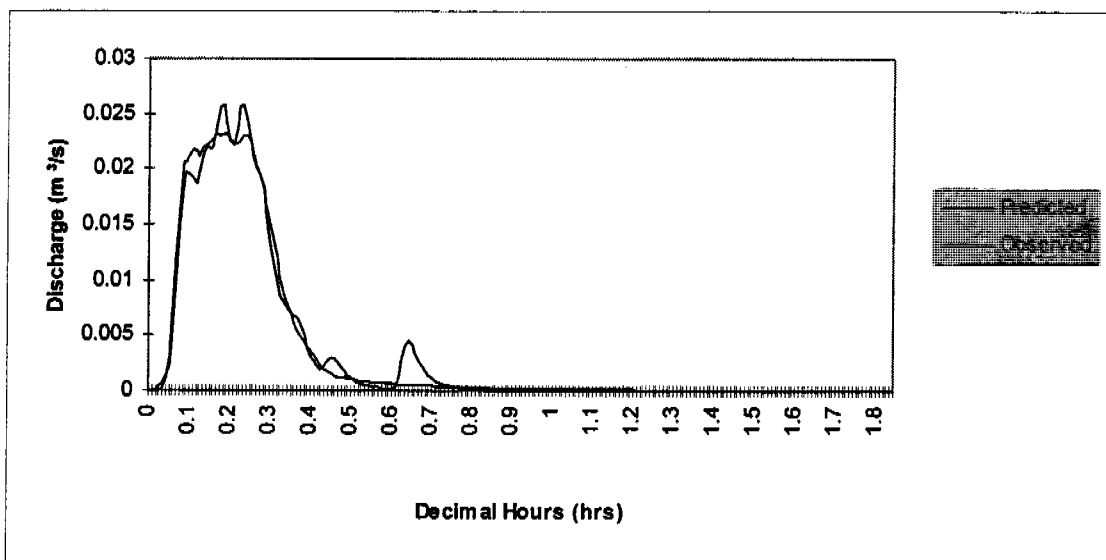
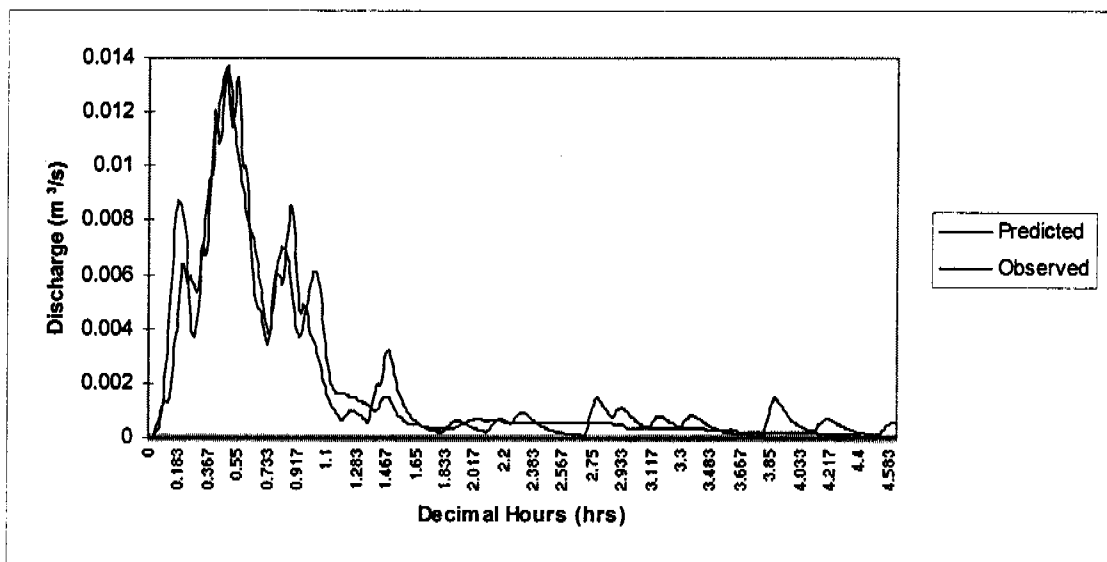
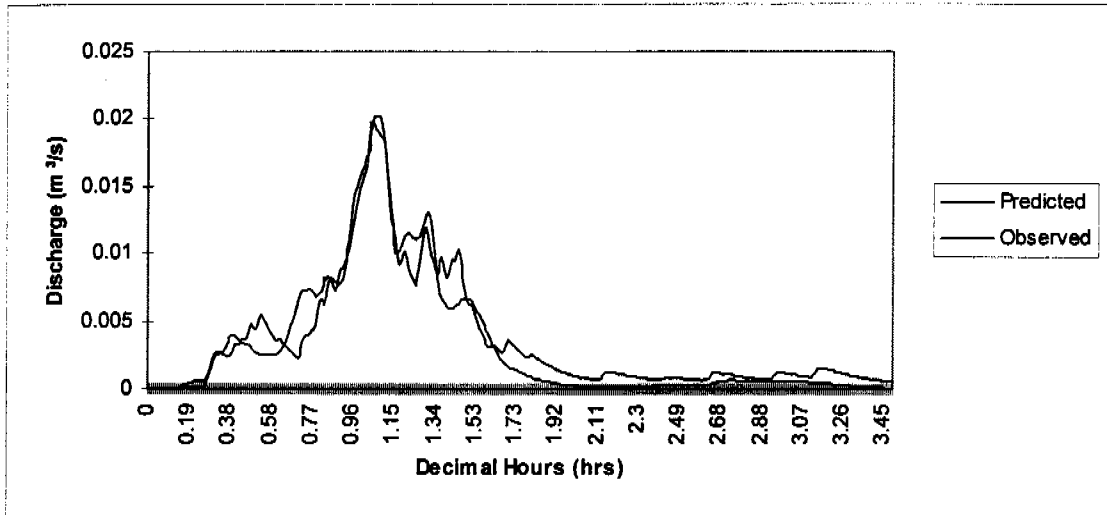


Figure A-1a, b, and c for individually fitted cap site storm events.



Monitoring Gully Formation

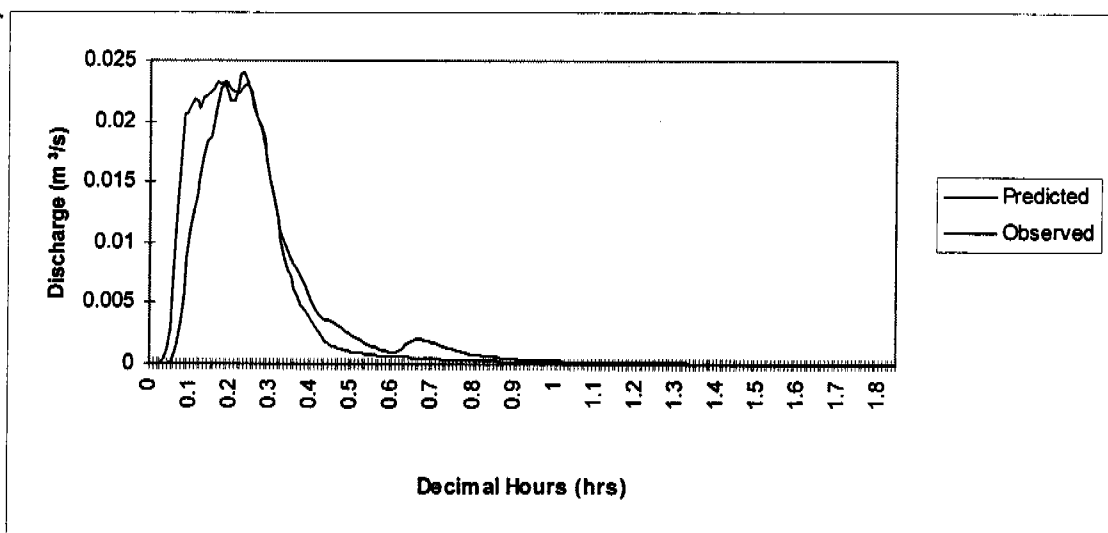
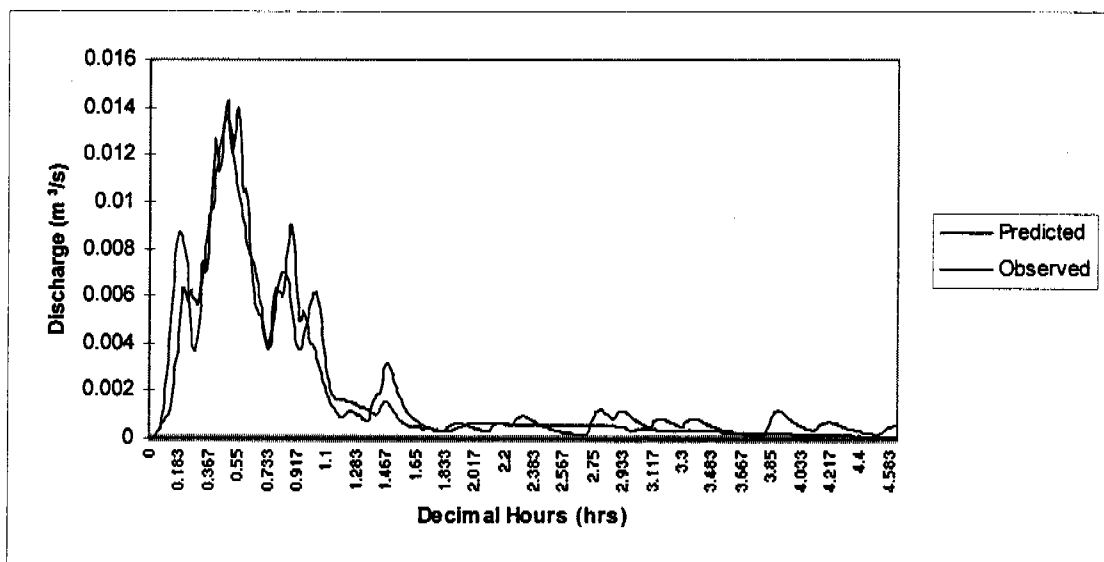
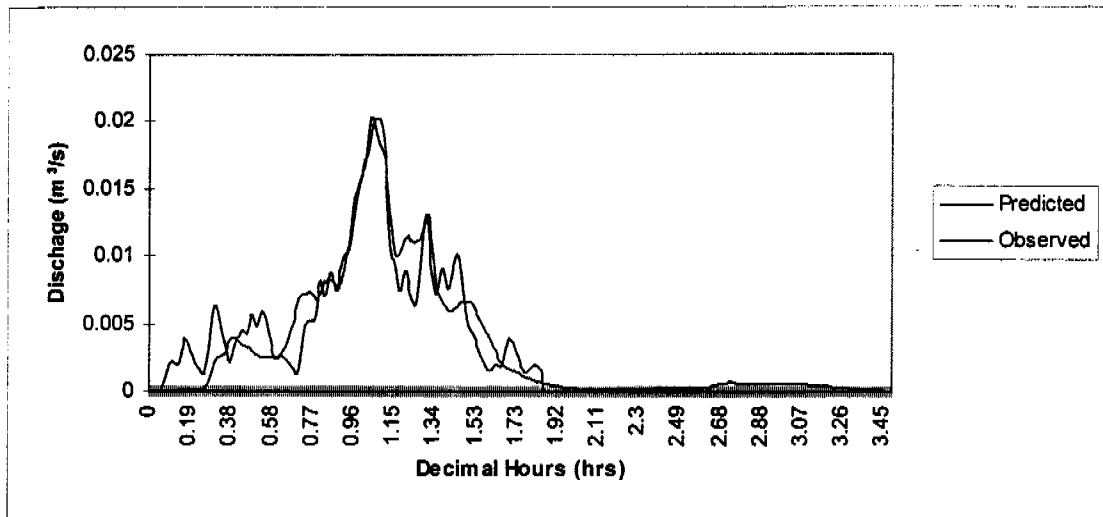


Figure A-2a, b, and c for multiple fitted cap site storm events.

Monitoring Gully Formation

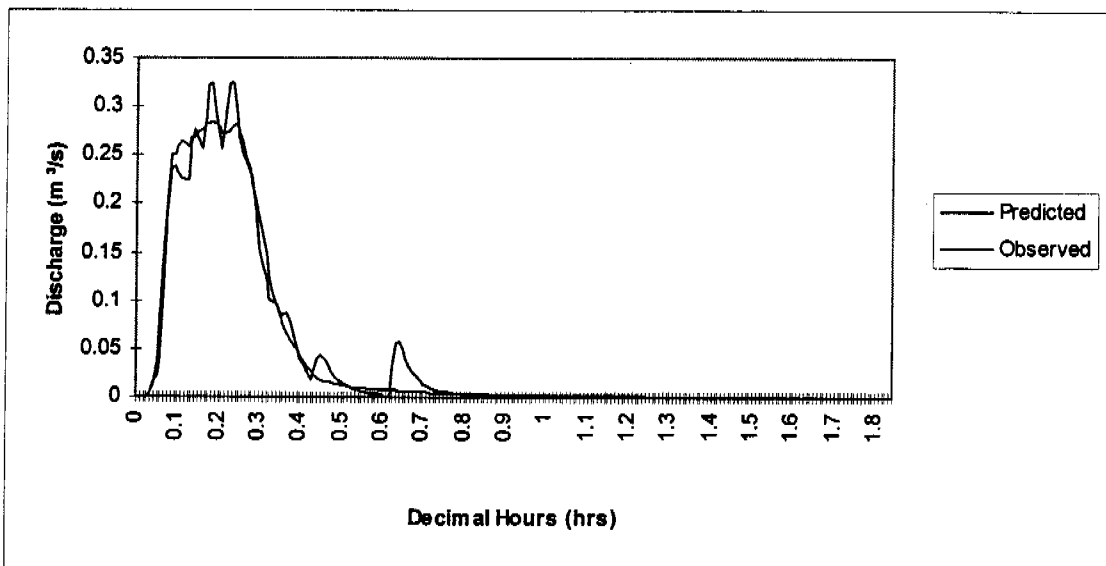
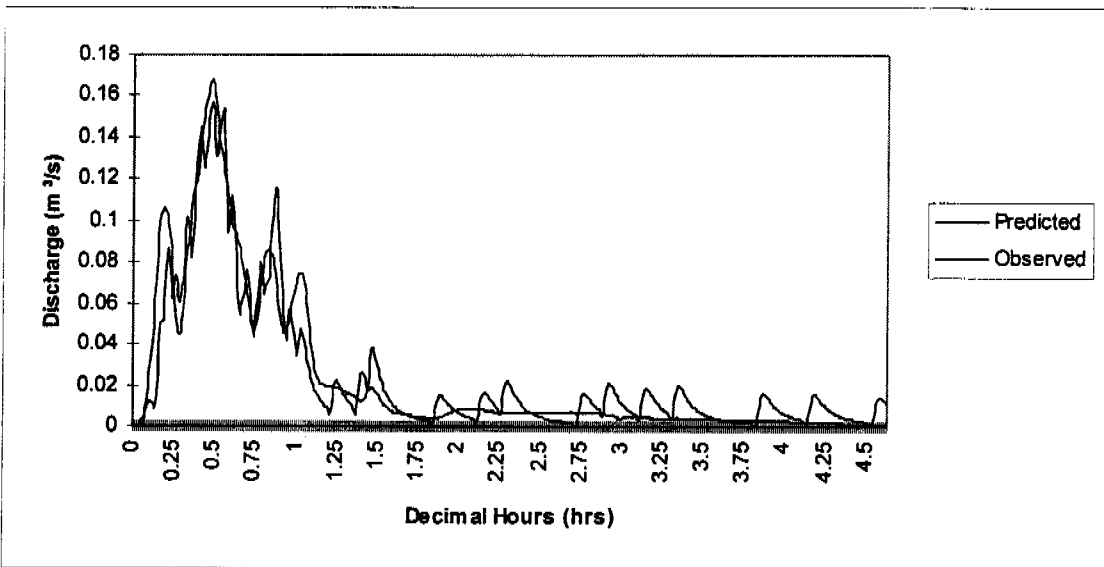
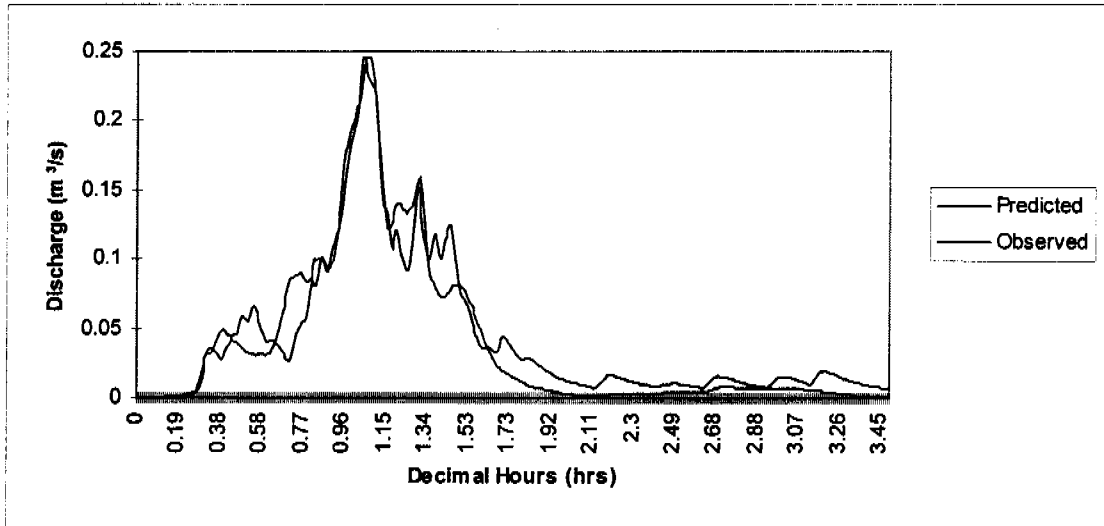


Figure A-3a, b, and c for individually fitted gully catchment events.



Monitoring Gully Formation

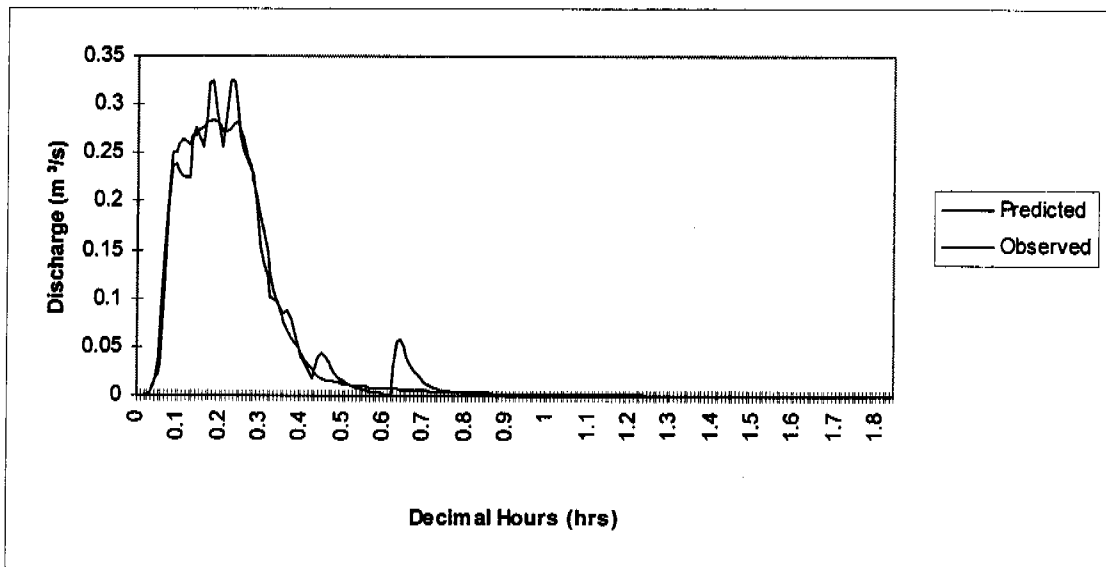
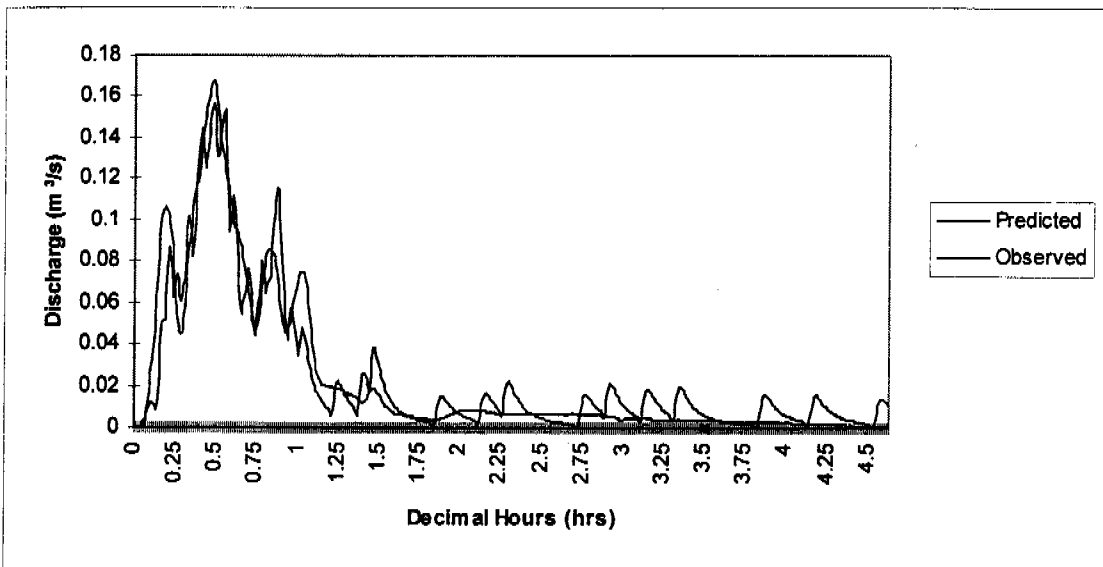
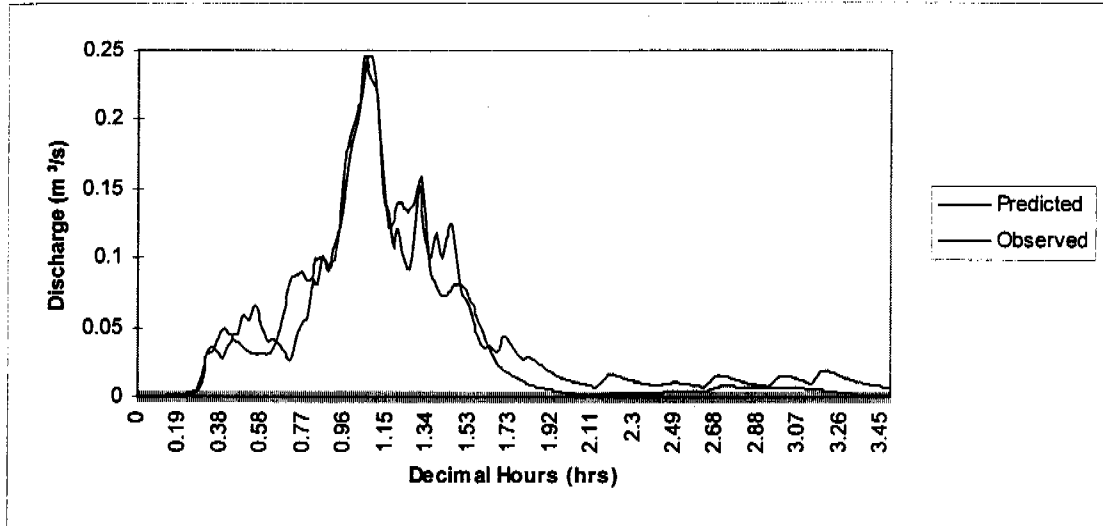


Figure A-4a, b, and c for collectively fitted gully catchment events.

Gully Catchment RUM 96-97 Wet Season
 3 significant events: 26/12, 01/01, and 23/01.

CATCHMENT

No of elements, No of reservoirs, no of u/S elements
 6 0 3

No of U/S element draining into D/S elements

#

zero time (hrs), timestep (minutes), time of duration of storm (hrs)

#

0 0.5 4.633

#

OUTPUT PARAMETERS

#

no of pts for output discharge, psteps

1 1

subareas at which discharge requested

6

maximum discharge on output graph

0.002

#

INCIDENCES

0	0	0	1	0	2
0	0	0	3	0	4
0	0	0	0	0	5

PARAMETERS

Kind of element

0

No Area Length U/S D/S SWSupply Gamma Sorpt Phi

GWsupply

#

Elevation Elevation

#

1	3091.8	112.10	51.36	50.16	1.0	1.0	1.0	1.0	1.0
2	1626.0	78.40	51.36	49.88	1.0	1.0	1.0	1.0	1.0
3	515.7	25.80	50.55	50.16	1.0	1.0	1.0	1.0	1.0
4	299.4	12.10	50.16	50.00	1.0	1.0	1.0	1.0	1.0
5	1163.8	46.80	50.72	49.88	1.0	1.0	1.0	1.0	1.0
6	449.9	21.60	50.00	49.96	1.0	1.0	1.0	1.0	1.0

Hillslope and Channel conveyances

#

1st set are hillslope conveyances

2nd set are channel conveyances

#

Element No, No of conveyances

CR, EM, CONVEY

#

CONVEYANCES

1 2

0.092 1. 0.

0.092 1. 1000.

2 2

0.125 1. 0.

0.125 1. 1000.

3 2

0.138 1. 0.

0.138 1. 1000.

4 2

0.126 1. 0.

0.126 1. 1000.

5 2

0.086 1. 0.

0.086 1. 1000.

6 2

```

0.115      1.      0.
0.115      1.     1000.
#
# Parameter Multipliers
# Ch-CR Ch-EM SWSupply SWGamma Sorptivity Phi GWSupply
timing(sec)
MULTIPLIERS
    7.8    1.33    0.03    0.375  0.00001    6.5    1000.    0.0
1
0.0 0.0
# -----
# No of pluvios
# -----
RAINFALL #1
    1
CUMPLUVIO 2612cc.rf
1.00 1.00 1.00 1.00 1.00 1.00 1.00 1.00 1.00 1.00 1.00 1.00
RAINFALL #2
    1
CUMPLUVIO 0101ccc.rf
1.00 1.00 1.00 1.00 1.00 1.00 1.00 1.00 1.00 1.00 1.00 1.00
RAINFALL #3
    1
CUMPLUVIO 2301cca.rf
1.00 1.00 1.00 1.00 1.00 1.00 1.00 1.00 1.00 1.00 1.00 1.00
# -----
# No of known initial flows at stations
# -----
INITIALQ
title line 1
title line 2
title line 3
    1
# stations at which flows known and initial flow (cumecs)
    6  0.0
# No of stations with known inflows
INFLOWQ NONE
# Hydrograph to calibrate with (no of values)
CALIB #1 gcat2612.ro
CALIB #2 gcat0101.ro
CALIB #3 gcat2301.ro
END

```

Gully Cap Site RUM 96-97 Wet Season
 These are fw files on cap site itself using KE, fw as template.
 01/01/97c 60mm, 38.53mm/hr, 3.49pm to 5.24pm.

CATCHMENT

No of elements, No of reservoirs, no of u/S elements

13 0 4

No of U/S element draining into D/S elements

#

zero time (hrs), timestep (minutes), time of duration of storm (hrs)

#

0.0 0.5 4.633

#

OUTPUT PARAMETERS

#

no of pts for output discharge, psteps

1 1

subareas at which discharge requested

13

maximum discharge on output graph

0.002

#

INCIDENCES

0	1	0	0	4	0	0	0	8	0	10	0	11
0	0	0	0	3	0	0	0	7	0	9	0	2
0	0	0	0	0	0	0	0	6	0	0	0	12
0	0	0	0	0	0	0	0	5	0	0	0	0

PARAMETERS

Kind of element

0

No Area Length U/S D/S SWSupply Gamma Sorpt Phi

GWsupply

#

Elevation Elevation

#

1	73.7	18.00	0.690	0.32	1.0	1.0	1.0	1.0	1.0
2	105.1	17.10	0.320	-0.04	1.0	1.0	1.0	1.0	1.0
3	31.6	12.45	0.700	0.28	1.0	1.0	1.0	1.0	1.0
4	37.3	12.00	0.690	0.28	1.0	1.0	1.0	1.0	1.0
5	5.2	5.25	0.280	0.15	1.0	1.0	1.0	1.0	1.0
6	39.3	16.05	0.730	0.15	1.0	1.0	1.0	1.0	1.0
7	62.4	17.40	0.730	0.15	1.0	1.0	1.0	1.0	1.0
8	30.3	7.50	0.400	0.13	1.0	1.0	1.0	1.0	1.0
9	55.8	3.75	0.150	0.115	1.0	1.0	1.0	1.0	1.0
10	44.5	13.95	0.510	0.115	1.0	1.0	1.0	1.0	1.0
11	61.3	9.75	0.115	-0.08	1.0	1.0	1.0	1.0	1.0
12	42.6	10.05	0.340	-0.12	1.0	1.0	1.0	1.0	1.0
13	2.5	1.50	-0.040	-0.11	1.0	1.0	1.0	1.0	1.0

Hillslope and Channel conveyances

#

1st set are hillslope conveyances

2nd set are channel conveyances

#

Element No, No of conveyances

CR, EM, CONVEY

#

CONVEYANCES

1 2

0.341 1. 0.

0.341 1. 1000.

2 2

0.268 1. 0.

0.268 1. 1000.

3 2

0.484 1. 0.

0.484 1. 1000.

4 2

```

0.412      1.      0.
0.412      1.     1000.
5 2
1.587      1.      0.
1.587      1.     1000.
6 2
0.513      1.      0.
0.513      1.     1000.
7 2
0.388      1.      0.
0.388      1.     1000.
8 2
0.386      1.      0.
0.386      1.     1000.
9 2
0.716      1.      0.
0.716      1.     1000.
10 2
0.428      1.      0.
0.428      1.     1000.
11 2
0.276      1.      0.
0.276      1.     1000.
12 2
0.357      1.      0.
0.357      1.     1000.
13 2
0.481      1.      0.
0.481      1.     1000.
#
# Parameter Multipliers
# Ch-CR Ch-EM SWSupply SWGamma Sorptivity Phi GWSupply
timing(sec)
MULTIPLIERS
  7.8  1.33  0.03  0.375  0.00001  6.5  1000.  0.0
1
0.0 0.0
# -----
# No of pluvios
# -----
RAINFALL #1
  1
CUMPLUVIO 0101ccc.rf
1.00 1.00 1.00 1.00 1.00 1.00 1.00 1.00 1.00 1.00 1.00 1.00 1.00
# -----
# No of known initial flows at stations
# -----
INITIALQ
title line 1
title line 2
title line 3
  1
# stations at which flows known and initial flow (cumecs)
  13 0.0
# No of stations with known inflows
INFLOWQ NONE
# Hydrograph to calibrate with (no of values)
CALIB #1 010197c.ro
END

```



Monitoring Gully Formation

Appendix B



Date 240197.
This is transect information for gully plot.
Graphs drawn in GRAPHER, widths also collated here.
Row Width m(left) Width m(right) Comments

R1-R2 (2.9m)			
1m	10.6	11.4	Width measurements from R1 at 1m and 2m.
	11.6	12.7	distance 2.9m apart.
	13.1	14.6	
2m	10.6	12.8	
	13.3	14.9	
R2-R3 (3.4m)			
1m	11.6	13.4	Width at 1m and 2m.
	14.1	14.5	distance 3.4m apart.
	15.3	16.7	unchanged
2m	11.1	12.6	
	13	14.6	
	15.6	16.7	unchanged
R3-R4 (2.6m)			
1.5m	10.4	11.9	Width at 1.5m,
	12.6	13.7	
	14.1	15.4	
	16.7	18.3	unchanged
R4-EP1(3m) ???			
1.5m	10.5	11.8	Width at 1.5m,
	12.7	14	distance 3m ???
	15.8	16.8	
	17.2	19.6	
EP1-R5 (3.6m).			
2m	6.6	10.5	Assume 2m from EP1, measure from R5.
	11	12.9	Distance 3.6m.
	14.2	17.9	
R5-R6 (3.6m)			
2m	7.9	9.5	At 2m from R5, measure from R5.
	10.8	17.6	Distance 3.6m.
R6-EP2 (7.9m).			
3m	6	7.5	At 3m width measurements from R6.
	7.9	9.9	Distance 7.9m
	11.3	12.2	
	14.3	16.8	
EP2-R7 (3.8m)			
2m	4.8	6.1	Measurement taken from R7, at 2m.
	7.3	9.5	
	9.9	11.7	
	13.9	15.7	
R7-R8 (5.7m)			
2m	5.9	6.7	Measured from R7 at 2m. This interval has changed.
	7.4	8.5	unchanged
	9.5	11.1	
	11.8	13.3	
	13.9	16.2	
R8-EP3 (5.2m)			
2m.	7.6	8.3	Measured from R8 at 2.0 m
	9	9.7	
	10.3	12.1	
	12.7	14.7	
EP3-R9 (7.8m)			
2m	8.7	10.9	Measurements from R9 at 2m. I.e. back up the slope.
	11.4	13.7	both changed, Rest deposited but no gully.
R9-EP4 (6.9m)			
3m	7.6	8.5	Width 3m, Measurements taken from R9. Both of these changed.
	11.2	16	changed
	16.7	17.4	unchanged
EP4-R10(5.7m).			
3m.	7.4	9.2	Measurements taken from R10, at 3m from EP4. Also changed.
	10.4	12.8	changed
	15.95	17.1	changed

33

Date 230197.

This is transect information for gully plot.

Graphs drawn in GRAPHER, widths also collated here.

Row	Width m(left)	Width m(right)	Comments
-----	---------------	----------------	----------

no width measurements taken.

Row 1	230197, no change	Row 2	no change	Row 3	no change	Row 4	no change	Row 5	some change	Row 6	change	Row 7	change	Row 8	change	Row 9	small change	Row 10	no change
Horizontal Height (m) equal change		Horizontal Height (m)		Horizontal Height (m)		Horizontal Height (m)		Horizontal Height (m)		Horizontal Height (m)		Horizontal Height (m)		Horizontal Height (m)		Horizontal Height (m)		Horizontal Height (m)	
1	196 01-1	1	152 03-1	1	229 03-1	1	242 04-1	1	307 05-1	1	367 06-1	1	424 07-1	1	481 08-1	1	538 09-1	1	595 10-1
2	197 10-6 to 12-65m	2	153 03-2	2	230 03-2	2	243 04-2	2	308 05-2	2	368 06-2	2	425 07-2	2	482 08-2	2	539 09-2	2	596 10-2
3	147 03-5	3	106 04-2	3	167 05-2	3	180 06-2	3	231 07-2	3	291 08-2	3	348 09-2	3	405 10-2	3	462 11-2	3	519 12-2
4	117 13-00 to 14-30m	4	61 18-70m to 12-65m	4	90 19-00 to 17-90m	4	115 04-2	4	130 05-2	4	145 06-2	4	160 07-2	4	175 08-2	4	190 09-2	4	205 10-2
5	104 164	5	45 45	5	101 88	5	103 113	5	105 115	5	107 117	5	109 119	5	111 121	5	113 123	5	115 125
6	101 168	6	42 02-3	6	102 89	6	104 114	6	106 116	6	108 118	6	110 120	6	112 122	6	114 124	6	116 126
7	103 190	7	39 12-90 to 14-10m	7	103 124	7	105 126	7	107 128	7	109 130	7	111 132	7	113 134	7	115 136	7	117 138
8	105 192	8	36 13-00 to 14-30m	8	104 125	8	106 127	8	108 129	8	110 131	8	112 133	8	114 135	8	116 137	8	118 139
9	107 194	9	33 14-00 to 15-30m	9	105 126	9	107 128	9	109 130	9	111 132	9	113 134	9	115 136	9	117 138	9	119 140
10	109 196	10	30 15-00 to 16-30m	10	106 127	10	108 129	10	110 131	10	112 133	10	114 135	10	116 137	10	118 139	10	120 141
11	111 198	11	27 16-00 to 17-30m	11	107 128	11	109 130	11	111 132	11	113 134	11	115 136	11	117 138	11	119 140	11	121 142
12	113 200	12	24 17-00 to 18-30m	12	108 129	12	110 131	12	112 133	12	114 135	12	116 137	12	118 139	12	120 141	12	122 143
13	115 202	13	21 18-00 to 19-30m	13	109 130	13	111 132	13	113 134	13	115 136	13	117 138	13	119 140	13	121 142	13	123 144
14	117 204	14	18 19-00 to 20-30m	14	110 131	14	112 133	14	114 135	14	116 137	14	118 139	14	120 141	14	122 143	14	124 145
15	119 206	15	15 20-00 to 21-30m	15	111 132	15	113 134	15	115 136	15	117 138	15	119 140	15	121 142	15	123 144	15	125 146
16	121 208	16	12 21-00 to 22-30m	16	112 133	16	114 135	16	116 137	16	118 139	16	120 141	16	122 143	16	124 145	16	126 147
17	123 210	17	9 22-00 to 23-30m	17	113 134	17	115 136	17	117 138	17	119 140	17	121 142	17	123 144	17	125 146	17	127 148
18	125 212	18	6 23-00 to 24-30m	18	114 135	18	116 137	18	118 139	18	120 141	18	122 143	18	124 145	18	126 147	18	128 149
19	127 214	19	3 24-00 to 25-30m	19	115 136	19	117 138	19	119 140	19	121 142	19	123 144	19	125 146	19	127 148	19	129 150
20	129 216	20	0 25-00 to 26-30m	20	116 137	20	118 139	20	120 141	20	122 143	20	124 145	20	126 147	20	128 149	20	130 151
21	131 218	21	0 26-00 to 27-30m	21	117 138	21	119 140	21	121 142	21	123 144	21	125 146	21	127 148	21	129 150	21	131 152
22	133 220	22	0 27-00 to 28-30m	22	118 139	22	120 141	22	122 143	22	124 145	22	126 147	22	128 149	22	130 151	22	132 153
23	135 222	23	0 28-00 to 29-30m	23	119 140	23	121 142	23	123 144	23	125 146	23	127 148	23	129 150	23	131 152	23	133 154
24	137 224	24	0 29-00 to 30-30m	24	120 141	24	122 143	24	124 145	24	126 147	24	128 149	24	130 151	24	132 153	24	134 155
25	139 226	25	0 30-00 to 31-30m	25	121 142	25	123 144	25	125 146	25	127 148	25	129 150	25	131 152	25	133 154	25	135 156
26	141 228	26	0 31-00 to 32-30m	26	122 143	26	124 145	26	126 147	26	128 149	26	130 151	26	132 153	26	134 155	26	136 157
27	143 230	27	0 32-00 to 33-30m	27	123 144	27	125 146	27	127 148	27	129 150	27	131 152	27	133 154	27	135 156	27	137 158
28	145 232	28	0 33-00 to 34-30m	28	124 145	28	126 147	28	128 149	28	130 151	28	132 153	28	134 155	28	136 157	28	138 159
29	147 234	29	0 34-00 to 35-30m	29	125 146	29	127 148	29	129 150	29	131 152	29	133 154	29	135 156	29	137 158	29	139 160
30	149 236	30	0 35-00 to 36-30m	30	126 147	30	128 149	30	130 151	30	132 153	30	134 155	30	136 157	30	138 159	30	140 161
31	151 238	31	0 36-00 to 37-30m	31	127 148	31	129 150	31	131 152	31	133 154	31	135 156	31	137 158	31	139 160	31	141 162
32	153 240	32	0 37-00 to 38-30m	32	128 149	32	130 151	32	132 153	32	134 155	32	136 157	32	138 159	32	140 161	32	142 163
33	155 242	33	0 38-00 to 39-30m	33	129 150	33	131 152	33	133 154	33	135 156	33	137 158	33	139 160	33	141 162	33	143 164
34	157 244	34	0 39-00 to 40-30m	34	130 151	34	132 153	34	134 155	34	136 157	34	138 159	34	140 161	34	142 163	34	144 165
35	159 246	35	0 40-00 to 41-30m	35	131 152	35	133 154	35	135 156	35	137 158	35	139 160	35	141 162	35	143 164	35	145 166
36	161 248	36	0 41-00 to 42-30m	36	132 153	36	134 155	36	136 157	36	138 159	36	140 161	36	142 163	36	144 165	36	146 167
37	163 250	37	0 42-00 to 43-30m	37	133 154	37	135 156	37	137 158	37	139 160	37	141 162	37	143 164	37	145 166	37	147 168
38	165 252	38	0 43-00 to 44-30m	38	134 155	38	136 157	38	138 159	38	140 161	38	142 163	38	144 165	38	146 167	38	148 169
39	167 254	39	0 44-00 to 45-30m	39	135 156	39	137 158	39	139 160	39	141 162	39	143 164	39	145 166	39	147 168	39	149 170
40	169 256	40	0 45-00 to 46-30m	40	136 157	40	138 159	40	140 161	40	142 163	40	144 165	40	146 167	40	148 169	40	150 171
41	171 258	41	0 46-00 to 47-30m	41	137 158	41	139 160	41	141 162	41	143 164	41	145 166	41	147 168	41	149 170	41	151 172
42	173 260	42	0 47-00 to 48-30m	42	138 159	42	140 161	42	142 163	42	144 165	42	146 167	42	148 169	42	150 171	42	152 173
43	175 262	43	0 48-00 to 49-30m	43	139 160	43	141 162	43	143 164	43	145 166	43	147 168	43	149 170	43	151 172	43	153 174
44	177 264	44	0 49-00 to 50-30m	44	140 161	44	142 163	44	144 165	44	146 167	44	148 169	44	150 171	44	152 173	44	154 175
45	179 266	45	0 50-00 to 51-30m	45	141 162	45	143 164	45	145 166	45	147 168	45	149 170	45	151 172	45	153 174	45	155 176
46	181 268	46	0 51-00 to 52-30m	46	142 163	46	144 165	46	146 167	46	148 169	46	150 171	46	152 173	46	154 175	46	156 177
47	183 270	47	0 52-00 to 53-30m	47	143 164	47	145 166	47	147 168	47	149 170	47	151 172	47	153 174	47	155 176	47	157 178
48	185 272	48	0 53-00 to 54-30m	48	144 165	48	146 167	48	148 169	48	150 171	48	152 173	48	154 175	48	156 177	48	158 179
49	187 274	49	0 54-00 to 55-30m	49	145 166	49	147 168	49	149 170	49	151 172	49	153 174	49	155 176	49	157 178	49	159 180
50	189 276	50	0 55-00 to 56-30m	50	146 167	50	148 169	50	150 171	50	152 173	50	154 175	50	156 177	50	158 179	50	160 181
51	191 278	51	0 56-00 to 57-30m	51	147 168	51	149 170	51	151 172	51	153 174	51	155 176	51	157 178	51	159 180	51	161 182
52	193 280	52	0 57-00 to 58-30m	52	148 169	52	150 171	52	152 173	52	154 175	52	156 177	52	158 179	52	160 181	52	162 183
53	195 282	53	0 58-00 to 59-30m	53	149 170	53	151 172	53	153 174	53	155 176	53	157 178	53	159 180	53	161 182	53	163 184
54	197 284	54	0 59-00 to 60-30m	54	150 171	54	152 173	54	154 175	54	156 177	54	158 179	54	160 181	54	162 183	54	164 185
55	199 286	55	0 60-00 to 61-30m	55	151 172	55	153 174	55	155 176	55	157 178	55	159 180	55	161 182	55	163 184	55	165 186
56	201 288	56	0 61-00 to 62-30m	56	152 173	56	154 175	56	156 177	56	158 179	56	160 181	56	162 183	56	164 185	56	166 187
57	203 290	57	0 62-00 to 63-30m	57	153 174	57	155 176	57	157 178	57	159 180	57	161 182	57	163 184	57	165 186	57	167 188
58	205 292	58	0 63-00 to 64-30m	58	154 175	58	156 177	58	158 179	58	160 181	58	162 183	58	164 185	58	166 187	58	168 189
59	207 294	59	0 64-00 to 65-30m	59	155 176	59	157 178	59	159 180	59	161 182	59	163 184	59	165 186	59	167 188	59	169 190
60	209 296	60	0 65-00 to 66-30m	60	156 177	60	1												

Date 130197

This is transect information for gully plot.

Graphs drawn in GRAPHER, widths also collated here.

Row	Width m(left)	Width m(right)	Comments
-----	---------------	----------------	----------

no width measurements were taken.

Row 1	change	Row 2	change	Row 3	change	Row 4	change	Row 5	change	Row 6	change	Row 7	change	Row 8	change	Row 9	change	Row 10	change
Horizontal Height (m)	Horizontal Height (m)	Horizontal Height (m)	Horizontal Height (m)	Horizontal Height (m)	Horizontal Height (m)	Horizontal Height (m)	Horizontal Height (m)	Horizontal Height (m)	Horizontal Height (m)	Horizontal Height (m)	Horizontal Height (m)	Horizontal Height (m)	Horizontal Height (m)	Horizontal Height (m)	Horizontal Height (m)	Horizontal Height (m)	Horizontal Height (m)	Horizontal Height (m)	Horizontal Height (m)
5	156 01-1	5	152 02-1	5	152 03-1	5	152 04-1	5	152 05-1	5	152 06-1	5	152 07-1	5	152 08-1	5	152 09-1	5	152 10-1
6	137 10.50 to 12.50m	6	95 9.75m to 10.30m	6	214 10.20m to 10.10m	6	196 10.4m to 10.10m	6	230 9.20m to 7.50m	6	307 8.50m to 8.30m	6	241 4.95 to 6.15m	6	223 8.50m to 9.15m	6	241 11.20m to 10.30m	6	214 8.00m to 7.20m
7	143 unchanged width	7	101 unchanged	7	101 unchanged	7	118 unchanged	7	208 new gully	7	302	7	222 unchanged	7	181 05-2	7	81 unchanged	7	154 unchanged
8	147 01-2	8	66 02-2	8	187 03-2	8	115 04-2	8	117 05-2	8	247 06-2	8	230 07-2	8	247 08-2	8	55 13.00m to 11.70m	8	200 10.50m to 12.50m
9	117 13.00 to 14.30m	9	61 10.70m to 12.50m	9	85 13.70m to 17.90m	9	85 13.70m to 17.90m	9	152 16.95m to 19.00m	9	202 8.20 to 10.60m	9	249 10.3 to 13.0m	9	122 change	9	153 unchanged	9	249 changed
10	144 no change in here at	10	45	10	56	10	56	10	232 unchanged	10	64 202 unchanged	10	340	10	182 09-2	10	116 unchanged	10	263 016.3
10.1	149	10.1	57 02-3	10.1	60	10.1	60	10.1	113 11.5m to 19.55m	10.1	64 202 unchanged	10.1	340	10.1	182 09-2	10.1	116 unchanged	10.1	263 016.3
10.2	153	10.2	79 12.90 to 14.10m	10.2	49	10.2	49	10.2	115	10.2	227 11.15m to 15.10m	10.2	340	10.2	182 09-2	10.2	116 unchanged	10.2	263 016.3
10.3	159	10.3	124 unchanged	10.3	181	10.3	181	10.3	181	10.3	258 unchanged	10.3	494	10.3	182 09-2	10.3	116 unchanged	10.3	263 016.3
10.4	169	10.4	134	10.4	134	10.4	134	10.4	134	10.4	258 unchanged	10.4	494	10.4	182 09-2	10.4	116 unchanged	10.4	263 016.3
10.5	190	10.5	160	10.5	160	10.5	160	10.5	160	10.5	217 15.35m to 17.75m	10.5	494	10.5	182 09-2	10.5	116 unchanged	10.5	263 016.3
10.6	192	10.6	131	10.6	131	10.6	131	10.6	131	10.6	178 unchanged	10.6	494	10.6	182 09-2	10.6	116 unchanged	10.6	263 016.3
10.7	176	10.7	131	10.7	131	10.7	131	10.7	131	10.7	178 unchanged	10.7	494	10.7	182 09-2	10.7	116 unchanged	10.7	263 016.3
10.8	180	10.8	122	10.8	122	10.8	122	10.8	122	10.8	178 unchanged	10.8	494	10.8	182 09-2	10.8	116 unchanged	10.8	263 016.3
10.9	186	10.9	145	10.9	145	10.9	145	10.9	145	10.9	178 unchanged	10.9	494	10.9	182 09-2	10.9	116 unchanged	10.9	263 016.3
11	172	11	19	11	19	11	19	11	19	11	178 unchanged	11	494	11	182 09-2	11	116 unchanged	11	263 016.3
11.1	146	11.1	9	11.1	361 change	11.1	361 change	11.1	361 change	11.1	361 change	11.1	361 change	11.1	361 change	11.1	361 change	11.1	361 change
11.2	156	11.2	9	11.2	361 change	11.2	361 change	11.2	361 change	11.2	361 change	11.2	361 change	11.2	361 change	11.2	361 change	11.2	361 change
11.3	186	11.3	131	11.3	327 change	11.3	327 change	11.3	327 change	11.3	327 change	11.3	327 change	11.3	327 change	11.3	327 change	11.3	327 change
11.4	239	11.4	189	11.4	327 change	11.4	327 change	11.4	327 change	11.4	327 change	11.4	327 change	11.4	327 change	11.4	327 change	11.4	327 change
11.5	263	11.5	189	11.5	327 change	11.5	327 change	11.5	327 change	11.5	327 change	11.5	327 change	11.5	327 change	11.5	327 change	11.5	327 change
11.6	274	11.6	260	11.6	345 change	11.6	345 change	11.6	345 change	11.6	345 change	11.6	345 change	11.6	345 change	11.6	345 change	11.6	345 change
11.7	221 changed	11.7	251	11.7	219	11.7	219	11.7	219	11.7	219	11.7	219	11.7	219	11.7	219	11.7	219
11.8	216 changed	11.8	229	11.8	189	11.8	189	11.8	189	11.8	189	11.8	189	11.8	189	11.8	189	11.8	189
11.9	232 changed	11.9	229	11.9	229	11.9	229	11.9	229	11.9	229	11.9	229	11.9	229	11.9	229	11.9	229
12	272 changed	12	229	12	227	12	227	12	227	12	227	12	227	12	227	12	227	12	227
12.1	282 changed	12.1	418	12.1	340	12.1	340	12.1	340	12.1	340	12.1	340	12.1	340	12.1	340	12.1	340
12.2	302 changed	12.2	512	12.2	452	12.2	452	12.2	452	12.2	452	12.2	452	12.2	452	12.2	452	12.2	452
12.3	224 changed	12.3	585	12.3	439	12.3	439	12.3	439	12.3	439	12.3	439	12.3	439	12.3	439	12.3	439
12.4	127 change	12.4	419	12.4	429	12.4	429	12.4	429	12.4	429	12.4	429	12.4	429	12.4	429	12.4	429
12.5	140 change	12.5	419	12.5	429	12.5	429	12.5	429	12.5	429	12.5	429	12.5	429	12.5	429	12.5	429
12.6	122 change	12.6	419	12.6	429	12.6	429	12.6	429	12.6	429	12.6	429	12.6	429	12.6	429	12.6	429
12.7	211 change	12.7	419	12.7	429	12.7	429	12.7	429	12.7	429	12.7	429	12.7	429	12.7	429	12.7	429
12.8	221	12.8	402	12.8	245	12.8	245	12.8	245	12.8	245	12.8	245	12.8	245	12.8	245	12.8	245
12.9	217	12.9	264	12.9	264	12.9	264	12.9	264	12.9	264	12.9	264	12.9	264	12.9	264	12.9	264
13	257	13	16	13	373 change	13	373 change	13	373 change	13	373 change	13	373 change	13	373 change	13	373 change	13	373 change
13.1	257	13.1	16	13.1	373 change	13.1	373 change	13.1	373 change	13.1	373 change	13.1	373 change	13.1	373 change	13.1	373 change	13.1	373 change
13.2	250	13.2	78	13.2	373 change	13.2	373 change	13.2	373 change	13.2	373 change	13.2	373 change	13.2	373 change	13.2	373 change	13.2	373 change
13.3	296	13.3	78	13.3	373 change	13.3	373 change	13.3	373 change	13.3	373 change	13.3	373 change	13.3	373 change	13.3	373 change	13.3	373 change
13.4	280	13.4	79	13.4	373 change	13.4	373 change	13.4	373 change	13.4	373 change	13.4	373 change	13.4	373 change	13.4	373 change	13.4	373 change
13.5	257	13.5	267	13.5	481 change	13.5	481 change	13.5	481 change	13.5	481 change	13.5	481 change	13.5	481 change	13.5	481 change	13.5	481 change
13.6	284	13.6	264	13.6	447 change	13.6	447 change	13.6	447 change	13.6	447 change	13.6	447 change	13.6	447 change	13.6	447 change	13.6	447 change
13.7	296	13.7	264	13.7	447 change	13.7	447 change	13.7	447 change	13.7	447 change	13.7	447 change	13.7	447 change	13.7	447 change	13.7	447 change
13.8	276	13.8	264	13.8	447 change	13.8	447 change	13.8	447 change	13.8	447 change	13.8	447 change	13.8	447 change	13.8	447 change	13.8	447 change
13.9	269	13.9	264	13.9	447 change	13.9	447 change	13.9	447 change	13.9	447 change	13.9	447 change	13.9	447 change	13.9	447 change	13.9	447 change
14	292	14	264	14	423 change	14	423 change	14	423 change	14	423 change	14	423 change	14	423 change	14	423 change	14	423 change
14.1	295	14.1	264	14.1	423 change	14.1	423 change	14.1	423 change	14.1	423 change	14.1	423 change	14.1	423 change	14.1	423 change	14.1	423 change
14.2	224	14.2	264	14.2	312	14.2	312	14.2	312	14.2	312	14.2	312	14.2	312	14.2	312	14.2	312
14.3	223	14.3	219	14.3	312	14.3	312	14.3	312	14.3	312	14.3	312	14.3	312	14.3	312	14.3	312
14.4	210	14.4	211	14.4	312	14.4	312	14.4	312	14.4	312	14.4	312	14.4	312	14.4	312	14.4	312
14.5	199	14.5	196	14.5	232 change	14.5	232 change	14.5	232 change	14.5	232 change	14.5	232 change	14.5	232 change	14.5	232 change	14.5	232 change
14.6	200	14.6	167	14.6	248	14.6	248	14.6	248	14.6	248	14.6	248	14.6	248	14.6	248	14.6	248
14.7	195	14.7	171	14.7	235	14.7	235	14.7	235	14.7	235	14.7	235	14.7	235	14.7	235	14.7	235
14.8	203	14.8	156	14.8	235	14.8	235	14.8	235	14.8	235	14.8	235	14.8	235	14.8	235	14.8	235
14.9	221	14.9	220	14.9	189	14.9	189	14.9	189	14.9	189	14.9	189	14.9	189	14.9	189	14.9	189
15	224	15	220	15	227	15	227	15	227	15	227	15	227	15	227	15	227	15	227
15.1	280	15.1	86	15.1	240	15.1	240	15.1	240	15.1	240	15.1	240	15.1	240	15.1	240	15.1	240
15.2	239	15.2	188	15.2	332	15.2	332	15.2	332	15.2	332	15.2	332	15.2	332	15.2	332	15.2	332
15.3	232	15.3	261	15.3	264	15.3	264	15.3	264	15.3	264	15.3	264	15.3	264	15.3	264	15.3	264
15.4	246	15.4	222	15.4	272	15.4	272	15.4	272	15.4	272	15.4	272	15.4	272	15.4	272	15.4	272
15.5	246	15.5	300	15.5	272	15.5	272	15.5	272	15.5	272	15.5	272	15.5	272	15.5	272	15.5	272
15.6	278	15.6	296	15.6	272	15.6	272	15.6	272	15.6	272	15.6	272	15.6	272	15.6	272	15.6	272
15.7	291	15.7	291	15.7	249	15.7	249	15.7	249	15.7	249	15.7	249	15.7	249	15.7	249	15.7	249
15.8	323 change	15.8	267 change	15.8	267 change	15.8	267 change	15.8	267 change	15.8	267 change	15.8	267 change	15.8	267 change	15.8	267 change	15.8	267 change
15.9	323 change	15.9	321 change	15.9	321 change	15.9	321 change	15.9	321 change	15.9	321 change	15.9	321 change	15.9	321 change	15.9	321 change	15.9	321 change
16	280	16	280	16	280	16	280	16											

Gully Measurements: 070197.

Date 070197.

This is transect information for gully plot.

Graphs drawn in GRAPHER, widths also collated here.

Row Width m(left) Width m(right) Comments

R1-R2 (2.9m)

1m	10.65	12.7	Width measurements from R1 at 1m and 2m.
	13	14.6	distance 2.9m apart.
2m	10.65	12.7	
	13	15.3	

R2-R3 (3.4m)

1m	11.3	13.75	Width at 1m and 2m.
	15.37	16.5	distance 3.4m apart.
2m	10.9	14.25	10.90m unchanged.
	15.25	17.1	

R3-R4 (2.6m)

1m			no change.
----	--	--	------------

R4-EP1(3m) ???

1.5m	10.15	15.54	Width at 1.5m, sound good.
	16.6	18.25	distance 3m ???

EP1-R5 (3.6m).

2m	8.7	10.8	Width measurements made at 2m from EPin 1, measmt taken from Row 5.
	11.2	16.9	Distance 3.6m.

R5-R6 (3.6m)

2m			no change.
----	--	--	------------

R7-R8 (5.7m)

2m	5.8	6.55	Measured from R7 at 2m.
	7.25	8.55	
	13.85	16.1	

R8-EP3 (5.2m)

2.5m.	7.45	8.15	Measured from R8 at 2.5m
	8.9	11.75	
	13.6	15.7	

EP3-R9 (7.8m)

3m.	9.2	10.9	Measurements from R9 at 3m. i.e. back up the slope.
	15.65	16.85	

R9-EP4 (6.9m)

3m	7.55	8.1	
	11.2	13.05	
	15.05	15.75	
	15.5	16.15	Check this out ??

EP4-R10(5.7m).

3m.	7.35	8.6	Measurements taken from R10, at 3m from EP4.
	11.35	12.35	
	14.65	17.4	

R10-EP5 (9.2m).

No change.

Date 020197.

This is transect information for gully plot.

Graphs drawn in GRAPHER, widths also collated here.

Row	Width m(left)	Width m(right)	Comments
-----	---------------	----------------	----------

no width measurements taken.

Date 271296

This is transect information for gully plot.

Graphs drawn in GRAPHER, widths also collated here.

Row Width m(left) Width m(right) Comments

R1-R2 (2.9m)			
1m	10.55	12.6	Width measurements from R1 at 1m and 2m.
	13.2	14.8	distance 2.9m apart.
2m	10.6	12.55	
	13.15	15.1	
R2-R3 (3.4m)			
1m	10	10.55	Width at 1m and 2m.
	11.35	13.72	distance 3.4m apart.
	15.3	16.6	
2m	10	10.35	
	10.9	12.3	
	12.7	13.7	
	15.2	17	
R3-R4 (2.6m)			
1m	10.55	15	Width at 1m.
	16.1	17.8	distance 2.6m.
R4-EP1(3m) ???			
1.5m	11.65	12.8	Width at 1.5m ??
	13.7	15.25	distance 3m ???
	15.65	17.4	
	18	20.7	
EP1-R5 (3.6)			
2m	8.75	10.6	Width measurements made at 2m from EP in 1, measnt taken from Row 5.
	11.2	12	Distance 3.6m.
	13.3	16.7	
R5-R6 (3.6m)			
2m	8	9.1	At 2m from R5, measure from R5.
	11.7	13	Distance 3.6m.
	13.3	15	
	15.4	17.6	
R6-EP2 (7.9m).			
3m	6.6	8	At 3m and 6m width measurements from R6.
	8.3	9	Distance 7.9m
	10.2	12.1	
6m	14.65	17.2	
	6.8	7.55	
	8.45	10.3	
	10.8	13	
	14.1	17.3	
EP2-R7 (3.8m)			
2m	5	6.1	Measurent taken from R7, at 2m.
	7.2	8.65	
	14.1	15.2	
R7-R8 (5.7m)			
3m	7.35	8.5	Measured from R7 at 3m.
	11.6	13	
	14	16	
R8-EP3 (5.2m)			
3m	7.5	8.5	Measured from R8 at 3m
	9.2	10.9	
	11.7	14.3	
EP3-R9 (7.8m)			
No significant deposits from below.			
R9-EP4 (6.9m)			
EP4-R10(5.7m).			
R10-EP5 (9.2m).			

201264	Row 1	Horizontal Height (m)	Row 2	Horizontal Height (m)	Row 3	Horizontal Height (m)	Row 4	Horizontal Height (m)	Row 5	Horizontal Height (m)	Row 6	Horizontal Height (m)	Row 7	Horizontal Height (m)	Row 8	Horizontal Height (m)	Row 9	Horizontal Height (m)	Row 10	Horizontal Height (m)
1	196	01-1	5	152	02-1	7	229	03-1	9	262	04-1	5	302	05-1	5	415	06-1	3	284	07-1
2	107	10.65 to 12.70	6	95	9.75m to 10.20m	8	274	10.2 to 15.0m	10	196	10.6m to 16.0m	6	230	9.20 to 10.50m	4	387	6.50m to 9.30m	2	282	08-1
3	143		7	106		9	197	03-2	11	718		7	187		4	291	4.9 to 8.10m	2	257	5.95m to 8.10m
4	117	13.00 to 14.30	2	66	02-2	7	201		8	119	04-2	7	229	05-2	4	343	06-2	3	272	08-2
5	144		9	81	10.70m to 12.45m	9	193	15.1m to 17.85m	10	110	11.1m to 19.6m	8	87	11.10m to 14.90m	5	349	10.3 to 13.3m	3	271	10.9m to 11.7m
6	104		8	45		10	56		10	232		8	71		6	350	06-3	4	251	11.10.65 to 12.85m
7	101		8.6	52	03-3	10	11		10	103		8.2	113	05-3	5	146		3	222	08-3
8	102		8.6	76	12.90 to 14.20m	10	11		10	104		8.1	119	15.40m to 17.75m	6	375	14.3 to 17.7m	5	225	13.3m to 12.15m
9	104		8.6	134		10	11		10	105		8.1	119		6	375		5	225	
10	104		8.6	160		10	11		10	106		8.1	119		6	375		5	225	
11	104		8.6	180		10	11		10	107		8.1	119		6	375		5	225	
12	104		8.6	200		10	11		10	108		8.1	119		6	375		5	225	
13	104		8.6	220		10	11		10	109		8.1	119		6	375		5	225	
14	104		8.6	240		10	11		10	110		8.1	119		6	375		5	225	
15	104		8.6	260		10	11		10	111		8.1	119		6	375		5	225	
16	104		8.6	280		10	11		10	112		8.1	119		6	375		5	225	
17	104		8.6	300		10	11		10	113		8.1	119		6	375		5	225	
18	104		8.6	320		10	11		10	114		8.1	119		6	375		5	225	
19	104		8.6	340		10	11		10	115		8.1	119		6	375		5	225	
20	104		8.6	360		10	11		10	116		8.1	119		6	375		5	225	
21	104		8.6	380		10	11		10	117		8.1	119		6	375		5	225	
22	104		8.6	400		10	11		10	118		8.1	119		6	375		5	225	
23	104		8.6	420		10	11		10	119		8.1	119		6	375		5	225	
24	104		8.6	440		10	11		10	120		8.1	119		6	375		5	225	
25	104		8.6	460		10	11		10	121		8.1	119		6	375		5	225	
26	104		8.6	480		10	11		10	122		8.1	119		6	375		5	225	
27	104																			

Row 1 Horizontal	191286 (m)	Little DATA Horiz	Row 2 Horizontal	(m)	Row 3 Horizontal	(m)	Row 4 Horizontal	Height (m)	Row 5 Horizontal	Height (m)	Row 6 Horizontal	Height (m)	Row 7 Horizontal	Height (m)	Row 8 Horizontal	Height (m)	Row 9 Horizontal	Height (m)	Row 10 Horizontal	Height (m)
12.25	30	12.20m to 12.4	11.1	90	G2-1	11.1	130	13.1	154	G4-1	10.3	320								
12.3	130		11.2	105	11.20m to 12.00m	11.1	130	13.2	168	13.10m to 15.00m	10.4	320								
12.35	100	Gully G1-2	11.3	150	G2-2	11.2	140	13.3	120		10.5	370								
12.4	80	13.20m to 14.4	11.4	175	13.00m to 13.90m	11.3	40	13.4	81	G4-2	10.6	370								
13.2	120		11.5	70		11.4	110	13.5	89	16.40m to 17.60m	10.7	350								
13.3	145		11.6	105	G2-3	11.5	120	13.6	54		10.8	390								
13.4	204		11.7	150	14.70m to 15.60m	11.6	70	13.7	75		10.9	400								
13.5	210		11.8	11		11.7	20	13.8	130		11	260								
13.6	205		12	95		11.8	25	13.9	158		11.1	250								
13.7	154		13	70		12	0	14	145		11.2	260								
13.8	175		13.1	110		12.1	20	14.1	198		11.3	250								
13.9	172		13.2	220		12.2	5	14.2	285		11.4	230								
14	158		13.3	250		12.3	50	14.3	380		11.5	230								
14.1	155		13.4	170		12.4	40	14.4	360		11.6	230								
14.2	128		13.5	230		12.5	115	14.5	300		11.7	180								
14.3	118		13.6	205		12.6	120	14.6	278		11.8	180								
14.4	111		13.7	200		12.7	25	14.7	233		11.9	210								
			13.8	190		12.8	80	14.8	155		12	190								
			13.9	80		12.9	10	14.9	176		12.1	260								
			14	80		13	15	15	145		12.2	260								
			14.1	85		13.1	55	16.1	270		12.3	230								
			14.2	200		13.2	70	16.2	345		12.4	240								
			14.3	290		13.3	80	16.3	355		12.5	200								
			15	310		13.4	110	16.4	393		12.6	200								
			15.1	220		13.5	100	16.5	378		12.7	220								
			15.2	250		13.6	100	16.6	314		12.8	180								
			15.3	270		13.7	130	16.7	310		12.9	170								
			15.4	245		13.8	230	17	305		13	170								
			15.5	210		13.9	190	17.1	318		13.1	170								
			15.6	160		14	180	17.2	308		13.2	240								
						14.1	170	17.3	321		13.3	230								
						14.2	170	17.4	371		13.4	200								
						14.3	210	17.5	317		13.5	200								
						14.4	200	17.6	345		13.6	190								
						14.5	175	17.7	345		13.7	280								
						14.6	140				13.8	195								
						14.7	100				13.9	260								
						14.8	100				14	270								
						14.9	50				14.1	340								
						15	20				14.2	280								
						15.1	20				14.3	280								
						15.2	20				14.4	320								
						15.3	160				14.5	340								
						15.4	160				14.6	320								
						15.5	50				14.7	250								
						15.6	70				14.8	250								
						15.7	50				14.9	340								
						15.8	10				15	300								
						15.9	20				15.1	270								
						16	80				15.2	580								
						16.1	80				15.3	350								
						16.2	140				15.4	350								
						16.3	170				15.5	420								
						16.4	180				15.6	400								
						16.5	220				15.7	230								
						16.6	280				15.8	120								
						16.7	230				15.9	250								
						16.8	130				16	295								
											16.1	350								

Rows 5,7,8,9 and 10 were installed on Christmas EVE.

191296.wb1 191296

Date 191296.

This is transect information for gully plot.

Graphs drawn in GRAPHER, widths also collated here.

Row Width m(left) Width m(right) Comments

no width measurements taken before the 281296.



Monitoring Gully Formation

Appendix C



VOLUME COMPUTATIONS

UPPER SURFACE

Grid File: C:/SURFER6/FINAL 1310/GREUWN11-60.GRD
Grid size as read: 148 cols by 448 rows
Delta X: 0.129252
Delta Y: 0.154362
X-Range: 1 to 20
Y-Range: 1 to 70
Z-Range: 0.0742561 to 13.2

LOWER SURFACE

Grid File: C:/SURFER6/FINAL 1310/GREUWN12-60.GRD
Grid size as read: 148 cols by 448 rows
Delta X: 0.129252
Delta Y: 0.154362
X-Range: 1 to 20
Y-Range: 1 to 70
Z-Range: 0.0741444 to 13.2

VOLUMES

Approximated Volume by
Trapezoidal Rule: 5.0696
Simpson's Rule: 5.06872
Simpson's 3/8 Rule: 5.06876

CUT & FILL VOLUMES

Positive Volume [Cut]: 7.36498
Negative Volume [Fill]: 2.29538
Cut minus Fill: 5.0696

AREAS

Positive Planar Area
(Upper above Lower): 683.027
Negative Planar Area
(Lower above Upper): 627.973
Blanked Planar Area: 0
Total Planar Area: 1311

Positive Surface Area
(Upper above Lower): 683.421
Negative Surface Area
(Lower above Upper): 628.061

VOLUME COMPUTATIONS

UPPER SURFACE

Grid File: C:/SURFER6/FINAL 1310/GREUWN1-60.GRD
Grid size as read: 148 cols by 448 rows
Delta X: 0.129252
Delta Y: 0.154362
X-Range: 1 to 20
Y-Range: 1 to 70
Z-Range: 0.0744283 to 13.2

LOWER SURFACE

Grid File: C:/SURFER6/FINAL 1310/GREUWN11-60.GRD
Grid size as read: 148 cols by 448 rows
Delta X: 0.129252
Delta Y: 0.154362
X-Range: 1 to 20
Y-Range: 1 to 70
Z-Range: 0.0742561 to 13.2

VOLUMES

Approximated Volume by
Trapezoidal Rule: 1.28752
Simpson's Rule: 1.28733
Simpson's 3/8 Rule: 1.28735

CUT & FILL VOLUMES

Positive Volume [Cut]: 4.33231
Negative Volume [Fill]: 3.04472
Cut minus Fill: 1.28759

AREAS

Positive Planar Area
(Upper above Lower): 583.369
Negative Planar Area
(Lower above Upper): 727.631
Blanked Planar Area: 0
Total Planar Area: 1311

Positive Surface Area
(Upper above Lower): 583.584
Negative Surface Area
(Lower above Upper): 727.729

VOLUME COMPUTATIONS

UPPER SURFACE

Grid File: C:/SURFER6/FINAL 1310/GULLYUP.GRD
Grid size as read: 148 cols by 448 rows
Delta X: 0.129252
Delta Y: 0.154362
X-Range: 1 to 20
Y-Range: 1 to 70
Z-Range: -0.00718905 to 13.1849

LOWER SURFACE

Grid File: C:/SURFER6/FINAL 1310/GREUWN1-60.GRD
Grid size as read: 148 cols by 448 rows
Delta X: 0.129252
Delta Y: 0.154362
X-Range: 1 to 20
Y-Range: 1 to 70
Z-Range: 0.0744283 to 13.2

VOLUMES

Approximated Volume by
Trapezoidal Rule: 1.1089
Simpson's Rule: 1.1123
Simpson's 3/8 Rule: 1.1125

CUT & FILL VOLUMES

Positive Volume [Cut]: 16.6359
Negative Volume [Fill]: 15.5266
Cut minus Fill: 1.10924

AREAS

Positive Planar Area
(Upper above Lower): 710.62
Negative Planar Area
(Lower above Upper): 600.38
Blanked Planar Area: 0
Total Planar Area: 1311

Positive Surface Area
(Upper above Lower): 712.77
Negative Surface Area
(Lower above Upper): 602.112

VOLUME COMPUTATIONS

UPPER SURFACE

Grid File: C:/SURFER6/FINAL 1310/GREWN11-60.GRD
Grid size as read: 148 cols by 448 rows
Delta X: 0.129252
Delta Y: 0.131991
X-Range: 1 to 20
Y-Range: 1 to 60
Z-Range: 0.072109 to 13.1

LOWER SURFACE

Grid File: C:/SURFER6/FINAL 1310/GREWN12-60.GRD
Grid size as read: 148 cols by 448 rows
Delta X: 0.129252
Delta Y: 0.131991
X-Range: 1 to 20
Y-Range: 1 to 60
Z-Range: 0.0727892 to 13.1

VOLUMES

Approximated Volume by
Trapezoidal Rule: 1.59113
Simpson's Rule: 1.59089
Simpson's 3/8 Rule: 1.59094

CUT & FILL VOLUMES

Positive Volume [Cut]: 5.11929
Negative Volume [Fill]: 3.52803
Cut minus Fill: 1.59127

AREAS

Positive Planar Area
(Upper above Lower): 617.891
Negative Planar Area
(Lower above Upper): 503.109
Blanked Planar Area: 0
Total Planar Area: 1121

Positive Surface Area
(Upper above Lower): 618.092
Negative Surface Area
(Lower above Upper): 503.274

VOLUME COMPUTATIONS

UPPER SURFACE

Grid File: C:/SURFER6/FINAL 1310/GREWN1-60.GRD
Grid size as read: 148 cols by 448 rows
Delta X: 0.129252
Delta Y: 0.131991
X-Range: 1 to 20
Y-Range: 1 to 60
Z-Range: -0.0053389 to 13.1

LOWER SURFACE

Grid File: C:/SURFER6/FINAL 1310/GREWN11-60.GRD
Grid size as read: 148 cols by 448 rows
Delta X: 0.129252
Delta Y: 0.131991
X-Range: 1 to 20
Y-Range: 1 to 60
Z-Range: 0.072109 to 13.1

VOLUMES

Approximated Volume by
Trapezoidal Rule: -2.93096
Simpson's Rule: -2.93613
Simpson's 3/8 Rule: -2.93599

CUT & FILL VOLUMES

Positive Volume [Cut]: 10.3875
Negative Volume [Fill]: 13.3183
Cut minus Fill: -2.93076

AREAS

Positive Planar Area
(Upper above Lower): 562.34
Negative Planar Area
(Lower above Upper): 558.66
Blanked Planar Area: 0
Total Planar Area: 1121

Positive Surface Area
(Upper above Lower): 565.196
Negative Surface Area
(Lower above Upper): 562.677

VOLUME COMPUTATIONS

UPPER SURFACE

Grid File: C:/SURFER6/FINAL 1310/GULLY.GRD
Grid size as read: 148 cols by 448 rows
Delta X: 0.129252
Delta Y: 0.131991
X-Range: 1 to 20
Y-Range: 1 to 60
Z-Range: -0.00718805 to 13.091

LOWER SURFACE

Grid File: C:/SURFER6/FINAL 1310/GREWN1-60.GRD
Grid size as read: 148 cols by 448 rows
Delta X: 0.129252
Delta Y: 0.131991
X-Range: 1 to 20
Y-Range: 1 to 60
Z-Range: -0.0053389 to 13.1

VOLUMES

Approximated Volume by
Trapezoidal Rule: -25.7291
Simpson's Rule: -25.7336
Simpson's 3/8 Rule: -25.7344

CUT & FILL VOLUMES

Positive Volume [Cut]: 49.0484
Negative Volume [Fill]: 74.7779
Cut minus Fill: -25.7295

AREAS

Positive Planar Area
(Upper above Lower): 434.924
Negative Planar Area
(Lower above Upper): 686.076
Blanked Planar Area: 0
Total Planar Area: 1121

Positive Surface Area
(Upper above Lower): 471.65
Negative Surface Area
(Lower above Upper): 695.702

VOLUME COMPUTATIONS

UPPER SURFACE

Grid File: C:/SURFER6/FINAL 1310/GREUPW1-60.GRD
Grid size as read: 148 cols by 448 rows
Delta X: 0.129252
Delta Y: 0.154362
X-Range: 1 to 20
Y-Range: 1 to 70
Z-Range: 0.0725886 to 13.2

LOWER SURFACE

Grid File: C:/SURFER6/FINAL 1310/GREUPW2-60.GRD
Grid size as read: 148 cols by 448 rows
Delta X: 0.129252
Delta Y: 0.154362
X-Range: 1 to 20
Y-Range: 1 to 70
Z-Range: 0.071882 to 13.2

VOLUMES

Approximated Volume by
Trapezoidal Rule: 9.04404
Simpson's Rule: 9.04275
Simpson's 3/8 Rule: 9.04265

CUT & FILL VOLUMES

Positive Volume [Cut]: 20.6759
Negative Volume [Fill]: 11.632
Cut minus Fill: 9.04393

AREAS

Positive Planar Area
(Upper above Lower): 504.476
Negative Planar Area
(Lower above Upper): 806.524
Blanked Planar Area: 0
Total Planar Area: 1311

Positive Surface Area
(Upper above Lower): 511.321
Negative Surface Area
(Lower above Upper): 806.854

VOLUME COMPUTATIONS

UPPER SURFACE

Grid File: C:/SURFER6/FINAL 1310/GREUPW-60.GRD
Grid size as read: 148 cols by 448 rows
Delta X: 0.129252
Delta Y: 0.154362
X-Range: 1 to 20
Y-Range: 1 to 70
Z-Range: 0.073895 to 13.2

LOWER SURFACE

Grid File: C:/SURFER6/FINAL 1310/GREUPW1-60.GRD
Grid size as read: 148 cols by 448 rows
Delta X: 0.129252
Delta Y: 0.154362
X-Range: 1 to 20
Y-Range: 1 to 70
Z-Range: 0.0725886 to 13.2

VOLUMES

Approximated Volume by
Trapezoidal Rule: 1.04362
Simpson's Rule: 1.04256
Simpson's 3/8 Rule: 1.04237

CUT & FILL VOLUMES

Positive Volume [Cut]: 12.1965
Negative Volume [Fill]: 11.1532
Cut minus Fill: 1.04326

AREAS

Positive Planar Area
(Upper above Lower): 467.003
Negative Planar Area
(Lower above Upper): 843.997
Blanked Planar Area: 0
Total Planar Area: 1311

Positive Surface Area
(Upper above Lower): 469.957
Negative Surface Area
(Lower above Upper): 844.313

VOLUME COMPUTATIONS

UPPER SURFACE

Grid File: C:/SURFER6/FINAL 1310/GULLYUP.GRD
Grid size as read: 148 cols by 448 rows
Delta X: 0.129252
Delta Y: 0.154362
X-Range: 1 to 20
Y-Range: 1 to 70
Z-Range: -0.00718905 to 13.1849

LOWER SURFACE

Grid File: C:/SURFER6/FINAL 1310/GREUPW-60.GRD
Grid size as read: 148 cols by 448 rows
Delta X: 0.129252
Delta Y: 0.154362
X-Range: 1 to 20
Y-Range: 1 to 70
Z-Range: 0.073895 to 13.2

VOLUMES

Approximated Volume by
Trapezoidal Rule: -0.582538
Simpson's Rule: -0.578776
Simpson's 3/8 Rule: -0.578766

CUT & FILL VOLUMES

Positive Volume [Cut]: 15.4438
Negative Volume [Fill]: 16.0265
Cut minus Fill: -0.582666

AREAS

Positive Planar Area
(Upper above Lower): 638.639
Negative Planar Area
(Lower above Upper): 672.361
Blanked Planar Area: 0
Total Planar Area: 1311

Positive Surface Area
(Upper above Lower): 641.556
Negative Surface Area
(Lower above Upper): 673.715

VOLUME COMPUTATIONS

UPPER SURFACE

Grid File: C:/SURFER6/FINAL 1310/GRERODW1-60.GRD
Grid size as read: 148 cols by 448 rows
Delta X: 0.129252
Delta Y: 0.131991
X-Range: 1 to 20
Y-Range: 1 to 60
Z-Range: 0.0386643 to 13.1

LOWER SURFACE

Grid File: C:/SURFER6/FINAL 1310/GRERODW2-60.GRD
Grid size as read: 148 cols by 448 rows
Delta X: 0.129252
Delta Y: 0.131991
X-Range: 1 to 20
Y-Range: 1 to 60
Z-Range: 0.0391576 to 13.1

VOLUMES

Approximated Volume by
Trapezoidal Rule: 9.41993
Simpson's Rule: 9.41612
Simpson's 3/8 Rule: 9.41618

CUT & FILL VOLUMES

Positive Volume [Cut]: 17.0696
Negative Volume [Fill]: 7.65
Cut minus Fill: 9.41964

AREAS

Positive Planar Area
(Upper above Lower): 491.6
Negative Planar Area
(Lower above Upper): 629.4
Blanked Planar Area: 0
Total Planar Area: 1121

Positive Surface Area
(Upper above Lower): 497.12
Negative Surface Area
(Lower above Upper): 629.652

VOLUME COMPUTATIONS

UPPER SURFACE

Grid File: C:/SURFER6/FINAL 1310/GRERODW-60.GRD
Grid size as read: 148 cols by 448 rows
Delta X: 0.129252
Delta Y: 0.131991
X-Range: 1 to 20
Y-Range: 1 to 60
Z-Range: 0.0387761 to 13.1

LOWER SURFACE

Grid File: C:/SURFER6/FINAL 1310/GRERODW1-60.GRD
Grid size as read: 148 cols by 448 rows
Delta X: 0.129252
Delta Y: 0.131991
X-Range: 1 to 20
Y-Range: 1 to 60
Z-Range: 0.0386643 to 13.1

VOLUMES

Approximated Volume by
Trapezoidal Rule: 5.17578
Simpson's Rule: 5.17419
Simpson's 3/8 Rule: 5.17424

CUT & FILL VOLUMES

Positive Volume [Cut]: 12.263
Negative Volume [Fill]: 7.08735
Cut minus Fill: 5.17563

AREAS

Positive Planar Area
(Upper above Lower): 481.085
Negative Planar Area
(Lower above Upper): 639.915
Blanked Planar Area: 0
Total Planar Area: 1121

Positive Surface Area
(Upper above Lower): 483.911
Negative Surface Area
(Lower above Upper): 640.104

VOLUME COMPUTATIONS

UPPER SURFACE

Grid File: C:/SURFER6/FINAL 1310/GULLY.GRD
Grid size as read: 148 cols by 448 rows
Delta X: 0.129252
Delta Y: 0.131991
X-Range: 1 to 20
Y-Range: 1 to 60
Z-Range: -0.00718805 to 13.091

LOWER SURFACE

Grid File: C:/SURFER6/FINAL 1310/GRERODW-60.GRD
Grid size as read: 148 cols by 448 rows
Delta X: 0.129252
Delta Y: 0.131991
X-Range: 1 to 20
Y-Range: 1 to 60
Z-Range: 0.0387761 to 13.1

VOLUMES

Approximated Volume by
Trapezoidal Rule: 6.04445
Simpson's Rule: 6.04578
Simpson's 3/8 Rule: 6.04592

CUT & FILL VOLUMES

Positive Volume [Cut]: 21.8192
Negative Volume [Fill]: 15.775
Cut minus Fill: 6.04417

AREAS

Positive Planar Area
(Upper above Lower): 524.06
Negative Planar Area
(Lower above Upper): 596.94
Blanked Planar Area: 0
Total Planar Area: 1121

Positive Surface Area
(Upper above Lower): 530.518
Negative Surface Area
(Lower above Upper): 598.255

Appendix D

Consequently to the cessation of monitoring period, during the dry season (June), field samples were taken to gauge some of the characteristics of waste rock material from the batter site.

Three sites were investigated by the geomorphology group at *eriss*, and moisture content and bulk density determined.

Bulk density defined as weight of rock sample divided by total volume, including porosity. Moisture content for this purpose refers to a difference between dry and wet weight of the sample.

The total weight of wet soil sample and the volume occupied as determined using standard techniques.

On each of the 3 sites, 3 samples were taken and examined.

Average bulk Density was determined to be 1.93 g/cm^3 .

Table D-1: Bulk Density determination series 3 samples taken at 3 locations.

Sample	Soil Mass (Wet)	Soil Mass (Dry)	Volume (cc)	Bulk Density	Moisture Content (%)
1A	481.55	479.94	286.67	1.67	0.38
1B	678.44	674.37	377.65	1.79	0.60
1C	536.05	533.09	294.83	1.81	0.55
2A	484.99	482.43	226.51	2.13	0.53
2B	526.94	524.77	275.73	1.90	0.41
2C	513.70	512.10	273.91	1.87	0.31
3A	345.32	342.50	180.61	1.89	0.82
3B	299.21	296.84	140.43	2.11	0.79
3C	249.96	247.98	111.25	2.23	0.79